博士論文

Study on

Early Forecasting of Flood through Historical Hydrologic Data Analysis and Numerical Simulation in Kelantan Watershed, Malaysia

（歴年水文データ解析と数値シミュレーションによる
マレーシア・ケランタン川流域の早期洪水予測に関する研究）

Che Ros Faizah

チェ　ロス　ファイザ

This thesis is dedicated to my parents,
Che Ros and Fatimah for their endless love,
encouragement and support.

ACKNOWLEDGMENTS

The present thesis is the final output of my three year study. This PhD research was sponsored by the Japanese International Cooperation Agency (JICA). I am sincerely grateful to JICA for their financial support in the form of a scholarship to undertake this study.

This thesis would not have been possible without the continuous encouragement of my supervisor, Professor Dr. Tosaka Hiroyuki. I am very grateful to him not only for directing my research, but also invaluable moral support and remarkable guidance I received throughout this PhD journey. He has won my everlasting gratitude for his time, energy, patience and insights in guiding this research into its finished form.

I am also profoundly grateful to my senior, Dr. Sasaki Kenji and all members of Tosaka Laboratory, Department of Systems Innovation in University of Tokyo (UT) for their invaluable assistance during my study. My gratitude also goes to Professor Ir. Dr. Lariyah, Ms. Hidayah from Universiti Tenaga Nasional (UNITEN), Mr. Azad, Ms. Livia and Mr. Hafiz from Department of Irrigation and Drainage Malaysia (DID) for their ideas, provision of relevant materials during preparation and development, and providing me with necessary data to complete this research.

To my great circle of friend in UT, Liana, Lee, Iza, Soraya, Lela, Nadia, and Ralph, each of you has always been there for me, given me support; mentally and physically. To my brother Mohamad Izham and my friends in Malaysia, Badariah, Dalia, Ayuniez and Fixx, thank you for your help and support. To my neighbours, Ayumi Tsunoda, Nobuko Herrle and Klaus Herrle, thank you very much for your moral support.

Last, but most important, I am indebted to my husband Farhan Faiz, my son Faeq Farhan and my family who always encourage, support and give me the opportunity to complete my PhD work. I shall never forget and will make it up to you through the rest of my life.

Thank you.

Faizah Che Ros

August 2015

ABSTRACT

In Malaysia, flood is the most serious natural disaster in terms of frequency, areal extent and the number of population affected. The east coast of Peninsular Malaysia, northern part of Sabah and southern part of Sarawak experience heavy floods/inundations almost every year during the north east monsoon season from November to January.

The Kelantan river watershed, located in the north east of Peninsular Malaysia, is one of the biggest watersheds in Malaysia spreading over 12,000 km^2, and has been damaged seriously by monsoon floods/inundations in many places along the river and its tributaries in midstream to downstream areas. Thus, constructing a reliable system for early warning and evacuation, as well as making countermeasures for reducing the magnitude of damages, is a crucial requirement here.

To address this problem, the author took three main steps; 1) historical data collection and consistency/trend check, 2) development of observation-based statistical models to predict the water level at downstream point from the data of upstream multiple gauge points, 3) construction of physically based, distributed numerical model and determination method of rainfall distribution. Followings are the contents and major results covered in this thesis.

1) <u>Collection of Historical observation data, consistency check and trend analysis</u>
   - Historical hydrologic data such as rainfall records at distributed gauge stations from 1948 through 2013, water level observations, etc. were collected, arranged and stored with continuous time stamp in the database.
   - To provide a reliable database for further hydrologic analyses, the quality of long-term records were checked by using four statistical homogeneity tests. Among fifty rainfall stations, four stations were finally determined as inhomogeneous, then omitted from further analysis.
   - Three types of Mann-Kendall Test (MK) were devised and applied to trend analysis. The MK test using 30-year sampling period showed decreasing rainfall trend in the first half 30 years (1957-1987) and increasing trend in the latter (1981-2011). The MK test using 10-year sampling period successfully extracted very definite trend from the fluctuating observation data, which were corresponded to the historical cycles of El Nino and La Nina. The effects of both cycles were different for

upstream inland area and downstream area near the coast of South China Sea. By extending the MK test of 10-year sampling plot, rainfall fluctuation in several years was estimated.

2) Observation-based statistical model for early flood prediction.

- To realize quick and reliable early flood prediction, two statistical models that estimate the water level at downstream forecasting point were developed. The first model utilized only the information coming to the forecasting point from various upstream gauge stations in hourly scale, while in the second model, most recent observed data at forecasting point was considered to improve predictability.
- The basic form of model consists of a linear combination of the time-series data of multiple upstream stations considering the time lags and its ranges for respective stations. Cross-correlation analyses were conducted to find suitable time lags and lag ranges for respective pairs of gauge stations through monsoon season of the year. In determining coefficients of the linear system, the least square method was used for the summated data sampled over the period from the beginning of monsoon season in November to the end in next January.
- The method was applied for the prediction of water level at Kuala Krai (C) using the observed data at two upstream stations, Galas (A) and Lebir (B), while for the prediction of water level at Guillemard Bridge (D), upstream data at A, B and C were used. It was found that a combination of station A and B with average delay time gave more reliable prediction at C than using a single station. Similarly, at station D, the case by utilizing all upstream point A, B and C provided higher predictability. In most of the cases, the water level predicted from the model has the Absolute Mean Error (MAE) within 1 m from the starting time of flood up to the peak of flood event. However, the predictability of the model deteriorates when the downstream area received rainfall earlier than the upstream area.
- To improve the predictability, in the second model, most recent observation data at forecasting station was included. It successfully attained good prediction up to average lag time for station C and D, respectively, with MAE of 0.3 meter for all events in year 2011, 2013 and 2014. This improved method could produce a

continuous reliable prediction by updating hourly the coefficients of time-series data, assuming the upstream telemetry data is updated in monitoring system.

3) Numerical-based approach for early flood prediction.

- A basic 3-D numerical model for the Kelantan watershed was constructed using topographic data (SRTM 90m resolution), river network and land-use information. Two-stage initialization was done to make initial distribution of pressure and surface/subsurface water saturation by setting basic parameters such as permeability, porosity, surface manning's roughness factor, etc. Basic performance of the model was checked by comparing the calculated with the observed flow rate at Guillemard Bridge.
- Detailed investigation on grid-wise rainfall distribution on daily basis was conducted by using the Inverse Distance Weight (IDW) family methods. It was found that the simplest IDW method was appropriate for the vast Kelantan watershed since the differences among the family methods were insignificantly small in terms of cumulative amounts and the performance of hydrographs obtained by the numerical simulator under the same simple condition neglecting unclear canopy interception and evapotranspiration effects.
- Considering the necessity of quick timely estimation of rainfall distribution for the numerical prediction, reliability of the estimated distributions by using only telemetry stations sparsely distributed in the watershed was discussed. It was found that the same IDW parameter used for the case of all available stations could be applied to telemetry-based estimation, and difference between two distributions was not significant in terms of cumulative amount over watershed. The simulated hydrographs using two distributions for year 2010 to 2013 gave relatively small difference and it was concluded that telemetry-based estimation might work for the input of numerical model for early prediction purpose.
- The numerical model was run for checking data adaptability using basic parameters and estimated rainfall distributions for years 2007-2013 on daily scale. Simulation results showed that calculated hydrographs were generally in good agreement with the observed flow rate during high peak in monsoon, while they showed significant

difference from the observed during low-flood season. Results of trial runs considering evapotranspiration effect gave the difference much smaller. It suggested that in tuning model parameters to attain good matching in the future, the hydrologic treatment of canopy interception, evapotranspiration, as well as basic hydraulic parameters should be properly assembled.

The trend analysis might provide information about regional meteorological background to be considered in administrative policy. The proposed observation-based model might be introduced easily into practical use, and the numerical model, if satisfactory calibration is done, will provide us information what flow is occurring in the surface and subsurface of the whole watershed and help us planning countermeasures to minimize flood/inundation damages in this watershed.

Table of contents

ABSTRACT ..... **i**

List of Figure ..... **viii**

List of Tables ..... **xvii**

1 Introduction **1**

1.1 Objective 1
1.2 Motivation and background 1
1.3 Thesis overview 4

2 Study Area and Data **6**

2.1 Location of Study Area 6
2.2 Hydrological and Climate 7
2.3 Topography, Geology and Soil 9
2.4 Land use 12
2.5 Historical Flood 15
2.6 Data availability 16
2.6.1 Geographic information system data 16
2.6.2 Hydro-meteorological data 16
2.6.3 Database-development 17

3 Homogeneity and Trend Analysis **19**

3.1 Introduction 19
3.2 Absolute Homogeneity Test 21
3.2.1 Buishand Range Test 23
3.2.2 Standard Normal Homogeneity Test 24
3.2.3 Pettitt Test 25
3.2.4 Von Neumann Ratio Test 25
3.3 Trend Analysis 26
3.4 Result and Discussion 28
3.4.1 Homogeneity Test 28
3.4.2 Trend Analysis 32
3.5 Conclusion 37

4 Observation-based Approach for Early Flood Prediction **39**

4.1 Introduction 39
4.2 Review of Observation-based Models 39
4.2.1 ARMA/ARIMA 39
4.2.2 Artificial Neural Network (ANNs) & Fuzzy Logic 41
4.3 Development of an Upstream-Observation-based Model 42
4.3.1 Objective 42
4.3.2 Basic Assumptions 43
4.3.3 The Mathematical Model 44
4.4 Analysis of Average Delay Time 47
4.4.1 Conventional Graphical Approach 47
4.4.2 Cross-correlation by mean value 48
4.4.3 Cross-correlation by derivative 48

4.4.4 Cross-correlation by double derivative 48
4.4.5 Delay analysis from Galas (A) and Lebir (B) to Kuala Krai (C) 49
4.4.6 Delay analysis from Galas(A), Lebir (B) and Kuala Krai (C) to Guillemard Bridge (D) 58
4.5 Sensitivity analysis of lag range 58
4.6 Early Flood Prediction 61
4.6.1 Early Flood Prediction at Kuala Krai (C) 61
4.6.1.1. Prediction at C by constant A coefficients 61
4.6.1.2. Prediction at C by updated A coefficient at selected flood level 63
4.6.1.3. Prediction at C by updated A coefficient - hourly 64
4.6.2 Early Flood Prediction at Guillemard Bridge (D) 66
4.6.2.1. Prediction at D by constant A coefficients 66
4.6.2.2. Prediction at D by updated A coefficients at selected flood level 68
4.6.2.3. Prediction at D by updated A coefficient – hourly 70
4.7 Improved Linear Observation-based Model. 71
4.7.1 Auto-correlation of Kuala Krai (C) and Guillemard Bridge (D) 71
4.7.2 The Mathematical Model using forecasting point data 73
4.7.3 Improved Early Flood Prediction at Kuala Krai (C) 75
4.7.3.1. Prediction at C at selected flood level 75
4.7.3.2. Prediction at C by updated A coefficient hourly 83
4.7.4 Improved Early Flood Prediction at Guillemard Bridge (D) 90
4.7.4.1. Prediction at D at selected flood level 90
4.7.4.2. Prediction at D by updated A coefficient hourly 98
4.7.5 Performance of A Coefficients for Different Flood Event 106
4.8 Discussion 110
4.8.1 Predictability of New Linear Observation-based Model 110
4.8.2 Predictability of New Improved Linear Observation-based Model 110
4.8.3 Highlights of Observation-based Modelling 111
4.9 Conclusion 112

5 Numerical Approach for Early Flood Prediction 114

5.1 Introduction 114
5.2 Summary of Numerical Simulator 114
5.3 Basic Modelling Procedure 118
5.3.1 Grid Construction 118
5.3.2 Model Initialization 119
5.4 Analysis of Rainfall Distribution 121
5.4.1 Review 121
5.4.2 Objective 124
5.4.3 Estimation Methods 124
5.4.3.1. Average Areal Rainfall 124
5.4.3.2. Inverse Distance Weighting Method (IDW) 126
5.4.3.3. Inverse Distance and Elevation Weighting Method (IDEW) 127
5.4.4 Cross-Validation Assessment 128
5.4.5 Sensitivity Analysis of Rainfall Distribution Parameter – All Stations 130
5.4.6 Sensitivity Analysis of Rainfall Distribution Variation – All Stations 132
5.4.7 Sensitivity Analysis of Rainfall Distribution Parameter - Telemetry Stations 135
5.5 Discussion on Rainfall Distribution by Numerical Simulation 140

5.5.1 Assumption of Simulation 140
5.5.2 Comparison Among Rainfall Distribution Estimation Methods 140
5.5.3 Estimation by Telemetry Stations 141
5.6 Reproducibility of Guillemard Bridge Runoff Hydrograph 141
5.6.1 Proto-type Model Performance 141
5.6.2 Improved Model Performance 143
5.6.3 Future Work to Improve Calibration 147
5.7 Conclusion 147

6 Conclusion and Future Work 149

6.1 Conclusion 149
6.2 Limitations and Future Works 152

References 153

Appendix 163

List of Figure

Figure 1.1. Flooding at Kuala Krai on 23rd December 2014 (source: Utusan Malaysia online). 3

Figure 2.1. Location of Kelantan watershed (source: OpenStreetMap). 6

Figure 2.2. Average monthly rainfall in Kelantan for years 2007 – 2013. 7

Figure 2.3. River network of Kelantan watershed (DID, 2013). 8

Figure 2.4. Daily rainfall pattern on Isohyet Map from 14th to 17th December 2014 (DID, 2014) 10

Figure 2.5. Daily rainfall pattern on Isohyet Map from 22th to 25th December 2014 (DID, 2014) 11

Figure 2.6. Topography map of Kelantan watershed from a digital elevation map (Department of Minerals and Geoscience Malaysia, 2012) 12

Figure 2.7. General geology map of Kelantan by Department of Minerals and Geoscience Malaysia (2003). 13

Figure 2.8. Land use map of Kelantan watershed by Department of Minerals and Geoscience Malaysia (2010). 14

Figure 2.9. Telemetry system in Kelantan watershed (DID, 2003) 17

Figure 2.10. Water level database in gregorian time format.....18

Figure 3.1. Location of 50 long-term rainfall stations used in this analysis 22

Figure 3.2. Three different sampling period methods for the Mann-Kendall (MK) test. 27

Figure 3.3. Location of homogenous, suspect and doubtful rainfall stations based on absolute homogeneity test 29

Figure 3.4. Inhomogeneous rainfall stations from the four absolute homogeneity test 30

Figure 3.5(a)-(h). Comparison between inhomogeneous rainfall stations with homogenous surrounding /nearby rainfall stations 31

Figure 3.6. Mean annual rainfall for 1948-2011. 32

Figure 3.7. Performance of MK-S value for different rainfall patterns 34

Figure 3.8. Upstream and midstream trends of Kelantan watershed (Ref. of ENSO: National Weather Service, 2015). 35

Figure 3.9. Downstream trends of Kelantan watershed (Ref. of ENSO: National Weather Service, 2015). 36

Figure 4.1. Schematic diagram of ANNs (Abrahart and See, 2000) 42

Figure 4.2. Location of water level and rainfall stations used in observation based approach 43

Figure 4.3. Schematic diagram of Kelantan River network in which the information passed at station A, B, C flows towards station D 44

Figure 4.4. Schematic diagram of water level stations used in this method. 46

Figure 4.5. Observed water level and rainfall for station A, B C and D during the north east monsoon season in 2008. 50

Figure 4.6. Observed water level and rainfall for station A, B, C and D during the north east monsoon season in 2011. 51

Figure 4.7. Observed water level and rainfall for station A, B and C during the north east monsoon season in 2013. 52

Figure 4.8. Cross correlation of three methods between A and C. 53

Figure 4.9. Cross correlation of three methods between B and C 53

Figure 4.10. Cross correlation of three methods between A and D. 54

Figure 4.11. Cross correlation of three methods between B and D. 54

Figure 4.12. Cross correlation of three methods between C and D 55

Figure 4.13. Starting time of hydrograph rising limb for station A, B and C in 2011 and 2013. 56

Figure 4.14. Kelantan watershed rainfall distribution in daily scale for year 2011. 57

Figure 4.15. Kelantan watershed rainfall distribution in daily scale for year 2013. 57

Figure 4.16. Schematic diagram of how the average delay time 58

Figure 4.17. Sensitivity analysis of lag range at station C 59

Figure 4.18. Sensitivity analysis of lag range at station D 60

Figure 4.19. Observed water level at A, B and C and flood prediction at C by constant A coefficients for year 2011 and 2013 62

Figure 4.20. Flood prediction at C by constant A coefficients for year 2011 and 2013. 62

Figure 4.21. Flood prediction at C by updated A coefficients at certain flood level, peak 1 2011 63

Figure 4.22. Flood prediction at C by updated A coefficients at certain flood level, peak 2 2011 63

Figure 4.23. Flood prediction at C by updated A coefficients at certain flood level, peak 3 2011 64

Figure 4.24. Flood prediction at C by updated A coefficients at certain flood level, peak 1 2013 64

Figure 4.25. Flood prediction at C by updated A coefficients at certain flood level, peak 2 2013. 64

Figure 4.26. Flood prediction at C by updated A coefficients - hourly, 2011 65

Figure 4.27. Flood prediction at C by updated A coefficients - hourly, 2013 66

Figure 4.28. Observed water level at A, B, C and D and flood prediction at D by constant A coefficients for year 2011 and 2013 67

Figure 4.29. Flood prediction at D for year 2011 and 2013 by constant A coefficients for year 2011 and 2013 67

Figure 4.30. Flood prediction at D by updated A coefficients at certain flood level, peak 1 2011 68

Figure 4.31. Flood prediction at D by updated A coefficients at certain flood level, peak 2 2011 68

Figure 4.32. Flood prediction at D by updated A coefficients at certain flood level, peak 3 2011 69

Figure 4.33. Flood prediction at D by updated A coefficients at certain flood level, peak 1 2013 69

Figure 4.34. Flood prediction at D by updated A coefficients at certain flood level, peak 2 2013.....69

Figure 4.35. Flood prediction at D by updated A coefficients - hourly, 2011.....70

Figure 4.36. Flood prediction at D by updated A coefficients - hourly, 2013.....71

Figure 4.37. Auto-correlation and variogram of C and D for year 2008, 2011 and 2013. 72

Figure 4.38. Illustration of correction 1 and 2 method. 74

Figure 4.39. Improved flood prediction at C at certain flood level, peak 1 2011.....76

Figure 4.40. Improved flood prediction at C at certain flood level, peak 2 2011.....77

Figure 4.41. Improved flood prediction at C at certain flood level, peak 3 2011.....78

Figure 4.42. Improved flood prediction at C at certain flood level, peak 1 2013.....79

Figure 4.43. Improved flood prediction at C at certain flood level, peak 2 2013.....80

Figure 4.44. Improved flood prediction at C at certain flood level, peak 1 2014.....81

Figure 4.45. Improved flood prediction at C at certain flood level, peak 2 2014.....82

Figure 4.46. Improved flood prediction at C, peak 1 by updated A coefficients - hourly, 2011 83

Figure 4.47. Improved flood prediction at C, peak 2 by updated A coefficients - hourly, 2011 84

Figure 4.48. Improved flood prediction at C, peak 3 by updated A coefficients - hourly, 2011 85

Figure 4.49. Improved flood prediction at C, peak 1 by updated A coefficients - hourly, 2013 86

Figure 4.50. Improved flood prediction at C, peak 2 by updated A coefficients - hourly, 2013 87

Figure 4.51. Improved flood prediction at C, peak 1 by updated A coefficients - hourly, 2014 88

Figure 4.52. Improved flood prediction at C, peak 1 by updated A coefficients - hourly, 2014 89

Figure 4.53. Improved flood prediction at D at certain flood level, peak 1 2011.....91

Figure 4.54. Improved flood prediction at D at certain flood level, peak 2 2011.....92

Figure 4.55. Improved flood prediction at D at certain flood level, peak 3 2011.....93

Figure 4.56. Improved flood prediction at D at certain flood level, peak 1 2013.....94

Figure 4.57. Improved flood prediction at D at certain flood level, peak 2 2013.....95

Figure 4.58. Improved flood prediction at D at certain flood level, peak 1 2014.....96

Figure 4.59. Improved flood prediction at D at certain flood level, peak 2 2014.....97

Figure 4.60. Improved flood prediction at D, peak 1 by updated A coefficients - hourly, 2011 99

Figure 4.61. Improved flood prediction at D, peak 2 by updated A coefficients - hourly, 2011 100

Figure 4.62. Improved flood prediction at D, peak 3 by updated A coefficients - hourly, 2011 101

Figure 4.63. Improved flood prediction at D, peak 1 by updated A coefficients - hourly, 2013 102

Figure 4.64. Improved flood prediction at D, peak 2 by updated A coefficients - hourly, 2013 103

Figure 4.65. Improved flood prediction at D, peak 1 by updated A coefficients - hourly, 2014 104

Figure 4.66. Improved flood prediction at D, peak 2 by updated A coefficients - hourly, 2014 105

Figure 4.67. Comparison of A coefficients value for peak 1, 2011 108

Figure 4.68. Comparison of A coefficients value for peak 2, 2013 109

Figure 4.69. Comparison of ARMA and models in this study. 111

Figure 5.1. Schematic of terrestrial water flow (GETFLOWS's manual) 115

Figure 5.2. Steps of Kelantan watershed's grid constructions. 118

Figure 5.3. Three-dimensional view of Kelantan watershed, 115 x 263 x 13grids. 119

(Elevation in meter) 119

Figure 5.4: Saturation distribution of top soil after 1st stage initialization. 120

(Saturation fraction is from 0 to 1) 120

Figure 5.5. View of surface river networks appeared on the surface after the 2nd stage initialization. (Saturation fraction is from 0 to 1) 121

Figure 5.6. Kelantan watershed divided into 8 sub-watersheds.....125

Figure 5.7. RMSE clouds from 1st January to 31st December 2007. 129

Figure 5.8. NSE clouds from 1st January to 31st December 2007.....130

Figure 5.9. Sensitivity Analysis of IDW parameter α.....131

Figure 5.10. Sensitivity Analysis of IDEW parameter z_{min} (α = 2 and z_{max} = 1800m) 131

Figure 5.11. Sensitivity analysis of rainfall distribution types. (α = 2, z_{min} = 200 and z_{max} = 1800m) 132

Figure 5.12. Cumulative rainfall by the four rainfall estimation methods.....133

Figure 5.13. Hydrograph of Kelantan River at Guillemard Bridge in 2007. 133

Figure 5.14. Hydrograph of Kelantan River at Guillemard Bridge for day 1-100 in 2007. ..134

Figure 5.15. Hydrograph of Kelantan River at Guillemard Bridge for day 100-300 in 2007. 134

Figure 5.16. Hydrograph of Kelantan River at Guillemard Bridge for day 300-360 in 2007135

Figure 5.17. Comparison of rainfall distribution with various α, day 325 2011. 136

Figure 5.18. Comparison of rainfall distribution with various α, day 326 2011. 136

Figure 5.19. Comparison of rainfall distribution with various α, day 327 2011. 137

Figure 5.20. Comparison of rainfall distribution with various α, day 328 2011. 137

Figure 5.21. Comparison of rainfall distribution with various α, day 329 2011. 138

Figure 5.22. Cumulative rainfall by telemetry stations (α = 0.5, 1, 2, 3) and all-stations (α =2) for year 2011. 138

Figure 5.23. Cumulative rainfall by telemetry stations (α = 0.5, 1, 2, 3) and all-stations (α =2) for year 2011. 139

Figure 5.24. Cumulative rainfall by telemetry stations (α = 0.5, 1, 2, 3) and all-stations (α =2) for year 2012. 139

Figure 5.25. Cumulative rainfall by telemetry stations (α = 0.5, 1, 2, 3) and all-stations (α =2) for year 2013. 140

Figure 5.26. Hydrograph of Kelantan river at Guillemard Bridge by proto-type model for year 2007 to 2013.....142

Figure 5.27. Hydrograph of Kelantan River at Guillemard Bridge in 2007 of improved model. 143

Figure 5.28. Hydrograph of Kelantan River at Guillemard Bridge in 2008 of improved model. 144

Figure 5.29. Hydrograph of Kelantan River at Guillemard Bridge in 2009 of improved model. 144

Figure 5.30. Hydrograph of Kelantan River at Guillemard Bridge in 2010 of improved model. 145

Figure 5.31. Hydrograph of Kelantan River at Guillemard Bridge in 2011 of improved model. 145

Figure 5.32. Hydrograph of Kelantan River at Guillemard Bridge in 2012 of improved model. 146

Figure 5.33. Hydrograph of Kelantan River at Guillemard Bridge in 2013 of improved model. 146

List of Tables

Table 2.1. Type of topographic units based (Raj, 2009).....9

Table 2.2. Summary of Kelantan State Land Use (2010).....15

Table 2.3. Annual historical floods and its impact in Kelantan (2004-2014).....16

Table 3.1. Geographical coordinates and elevations of rainfall gauges in Kelantan watershed (DID, 2012).....23

Table 3.2. Critical values (1%) for homogeneity test statistics 26

Table 3.3. Inhomogeneous stations based on four absolute homogeneity tests 30

Table 3.4. Result of Mann-Kendall tests (MK) using 30-year sampling.....33

Table 3.5. El Niño and La Niña events from 1950 to 2012[a].....37

Table 4.1. Distance between each water level station used. 46

Table 4.2. Delay time, τ by comparing peak and starting time of the hydrograph.....47

Table 4.3. Delay time using three cross-correlation method 55

Table 4.4: Kuala Krai Variables 106

Table 4.5: Guillemard Bridge Variables.....106

Table 5.1. Functional comparison of GETFLOWS and other simulators (www.getc.co.jp) 117

Table 5.2. Sensitive input parameters introduced to GETFLOWS simulator 119

Table 5.3. Cross-validation assessment performance and ranking of different interpolation methods based on root mean square error (RMSE) and Nash-Sutcliffe efficiency (NSE). 129

1 Introduction

1.1 *Objective*

This study aims to develop reliable early flood prediction models in Kelantan watershed based upon observation-based and numerical-based approach, and discuss their possible implementation as a forecasting tool for the future flood warning system. This includes

1) Field data acquisition and database construction.
2) Reliability test and trend analysis of the historical rainfall data.
3) Development of observation-based model for early flood prediction
4) Construction of numerical (physically-distributed) based approach for early flood prediction using a physically-based, distributed parameter runoff model.

1.2 *Motivation and background*

Flooding happens when water overtops the river banks due to an excess rainfall that cannot be absorbed by the soils or discharged fast enough by the river network. Contrary to present view, flood was once seen as great benefits. The Egyptian relied on its agricultural wealth, taking advantage of the Nile River that annually covered their lands bringing in silt-laden waters that when the flood receded, the fertilizing silts would stay behind, until the completion of Aswan Dam in 1970. However, current flood event is rather seen as a natural disaster since agriculture is no longer the primary industry in our civil society. Moreover, urbanization tends to concentrate population and economic activity around the cities which most of them have historically been built along the river. This growth often takes advantage of floodplains to expand and thus enhances the risk of flooding. Therefore, damage resulting by floods has become more vital than its benefits.

Throughout history, floods throughout four continents in the world have taken a heavy toll on properties and lives. Whether modern or developing country, the world has witnessed that floods have devastated both economically and environmentally more than any kind of natural disaster. In Europe, the 1928 Thames flood was a disastrous flood that affected riverside of London due to the unusually heavy rain and sudden thaw of snow in the upstream area.

However, especially in tropical regions are observed to be getting more severe floods now, than in the past (Mohamed Desa et. al, 2010). The World Bank has estimated US $45.7 billion in economic damages and losses due to flooding in 2011 Thailand flooding where most of this damage was due to the manufacturing industry (World Bank, 2012). The cause of flood is heavy rain during summer monsoon contributed to a rainfall anomaly.

In case of Malaysia, the east coast of Peninsular Malaysia, northern part of Sabah and southern part of Sarawak experience heavy flood almost annually due to the influenced of northeast monsoon that brings heavy rainfall. Since 1920, Malaysia has been experiencing several severe flood events in the year of 1926, 1931, 1947, 1954, 1957, 1963, 1965, 1967, 1969, 1971, 1973, 1983, 1988, 2001, 2007, 2009, 2011, 2012 (DID, 2013). From these occurrences, the pattern of heavy rainfall and flood event is getting more frequent. It has been estimated that 9% of the total land area of the country is flood prone affecting 15% of Malaysia's population. The average annual flood damage was estimated around RM 100 million in 1980's and has escalated to RM 915 million as estimated in National Registry of River Basin study (DID, 2003).

There have been immense uses of technology to mitigate measures of flood disaster i.e. structural and non-structural. The Government of Malaysia has spent more than RM 3 billion on structural measures to mitigate flooding since 1970's until now. However, this figure is still insufficient and this amount will keep on accumulate due to the increasing project cost and flooded areas. Moreover, structural measures are time consuming which involves physical works such as construction of dams, channel improvement, river diversion, embankment and levee to keep floods away from people. Thus, the non-structural measure such as flood-forecasting and warning systems is preferred to reduce the future flood effects as it can help a responsible authority to plan an effective emergency response towards flood disaster.

Kelantan state, located in the north east of Peninsular Malaysia is subjected to flood during the northeast monsoon that prevails from November to February every year. The recent floods in 2014 have caused severe inundation to Kelantan affecting more than 37,500 people where 18 people dead compared with previous year in 2012 where 12,650 were affected and 3 people drown due to flood. Thus, prompt measures in response to potential floods warnings are crucial to reduce flood risk as when issued early in advance, the people can considerably mitigate the negative impact of floods. Flood warning proves to be very useful if it can be made within sufficient time and reliable. This is where flood forecasting plays an essential role.

Flooding can be considered as most predictable natural disasters. It is driven by two main factors; rainfall and watershed characteristics. Knowing how much water will fall on the

watershed is the first step of prediction process of flood events. By knowing the amount of rain, we can assess how it will be drained to the river network; take into consideration the characteristics of watershed. Hydrological and hydraulic models are often used in flood forecasting and warning systems. These model can be an effective tool in providing early flood prediction and mitigating flood damages through non-structural approach if they are optimally calibrated and validated. With recent development, increasing computational power and availability, distributed hydrologic models with the capability to incorporate a variety of spatially-varying land characteristics such as digital elevation models (DEM), and geographic information system (GIS), are thought to give more accuracy and potential as a tool in improving flood forecasting (Theresa and Konstantine, 2006). Some physically based distributed models have obtained worldwide recognition as for instance Topmodel (Beven, 1991) and SHE model (Abbot et. al., 1986). GETFLOWS simulator is a general purpose terrestrial fluid-flow simulator which has been developed for comprehensive modelling by computing surface and subsurface coupled fluid flows including contaminant and heat transport, developed by Tosaka (2000).

Figure 1.1. Flooding at Kuala Krai on 23rd December 2014 (source: Utusan Malaysia online).

However, despite recent advance in technology, water level or river discharge forecasts performed by conceptual models may still prone to errors. There are many reasons that lead to inaccuracy of this conceptual reproduction such as lack of information which leads to failure in understanding the physical phenomena in the watershed itself. This research introduces a

novel observation-based flood prediction approach by utilizing the time sequence of flood information that is observed at upstream and flowing into the prediction point.

The current flood forecasting model in Kelantan state managed by Department of Drainage and Irrigation Malaysia (DID) was developed using Sugawara's Tank Model, a type of lumped model in the early 1980 (Hoong, 2007). After more than 35 years in operation, the performance of Kelantan Tank Model has deteriorated, due to the inaccessible source code and restricted model re-calibration. Currently, the water engineers uses a traditional flood forecasting and operation based on manual calculations.

The importance of early flood prediction is particularly evident in the north east of Malaysia where the density of population is high and urban infrastructures will possibly receive serious damage by inundation, especially during the north east monsoon season. Hence, early flood prediction in Kelantan watershed is the focus of this thesis.

1.3 *Thesis overview*

This thesis comprises 6 chapters, which are briefly outlined below.

Chapter 1: Introduction

This chapter discusses the motivation, background and problem statement, objectives of the study, expected outcome and their importance in the region.

Chapter 2: Study area and Data

Descriptions of the study area are presented including the geographical, topographic, climatic, geologic conditions, and availability of various data historically observed in this watershed.

Chapter 3: Homogeneity and Trend Analysis

In this chapter, consistency of rainfall data series is checked using four types of the absolute homogeneity tests, and rainfall trend is analysed by means of the Mann-Kendall test for annual scale.

Chapter 4: Observation-based Approach for Early Flood Prediction

Development of a statistical model for forecasting water level at downstream point by using the observation data at multiple upstream points is presented. A review of flood forecasting

methods available is presented, followed by a description of the main concepts of the observation based approach method and procedures to obtain controlling parameter such as the delay time and lag range. Model calibration results for two flood seasons in 2011 and 2013 based on hourly rainfall data for Kelantan watershed are presented. 2014 flood event was also used to validate the model.

Chapter 5: Numerical-based Approach for Early Flood Prediction

This chapter mainly discusses on comprehensive Kelantan watershed numerical model for early flood prediction. Introducing the basic model construction procedures, the estimation methods of rainfall distribution over the watershed, which is the most important input to the simulator, are discussed. Discussion on the reliability of estimation by using only telemetry stations are made. Finally, model calibration results for year 2007 to 2013 based on daily rainfall data are presented.

Chapter 6: Conclusion and Future Work

This chapter summarizes the contents and overall conclusions of the thesis, followed by the statement of limitations and further studies.

2 Study Area and Data

2.1 *Location of Study Area*

Kelantan is one of the largest states in Malaysia, situated in the north east of Peninsular Malaysia, which lies between latitudes 4.40° and 6.12° north and between longitudes 101.20° and 102.20° east, facing the South China Sea. The total area of the watershed is 13,100 km^2 or 85 percent of the Kelantan state land area. The maximum length and width of the watershed is 150 x 140 km respectively. The floodplain of Kelantan watershed consists of several districts namely Kota Bharu, Pasir Mas, Tumpat, Tanah Merah, Machang, Kuala Krai, Jeli and Gua Musang. About 68.5 percent of the Kelantan population live in the Kelantan watershed.

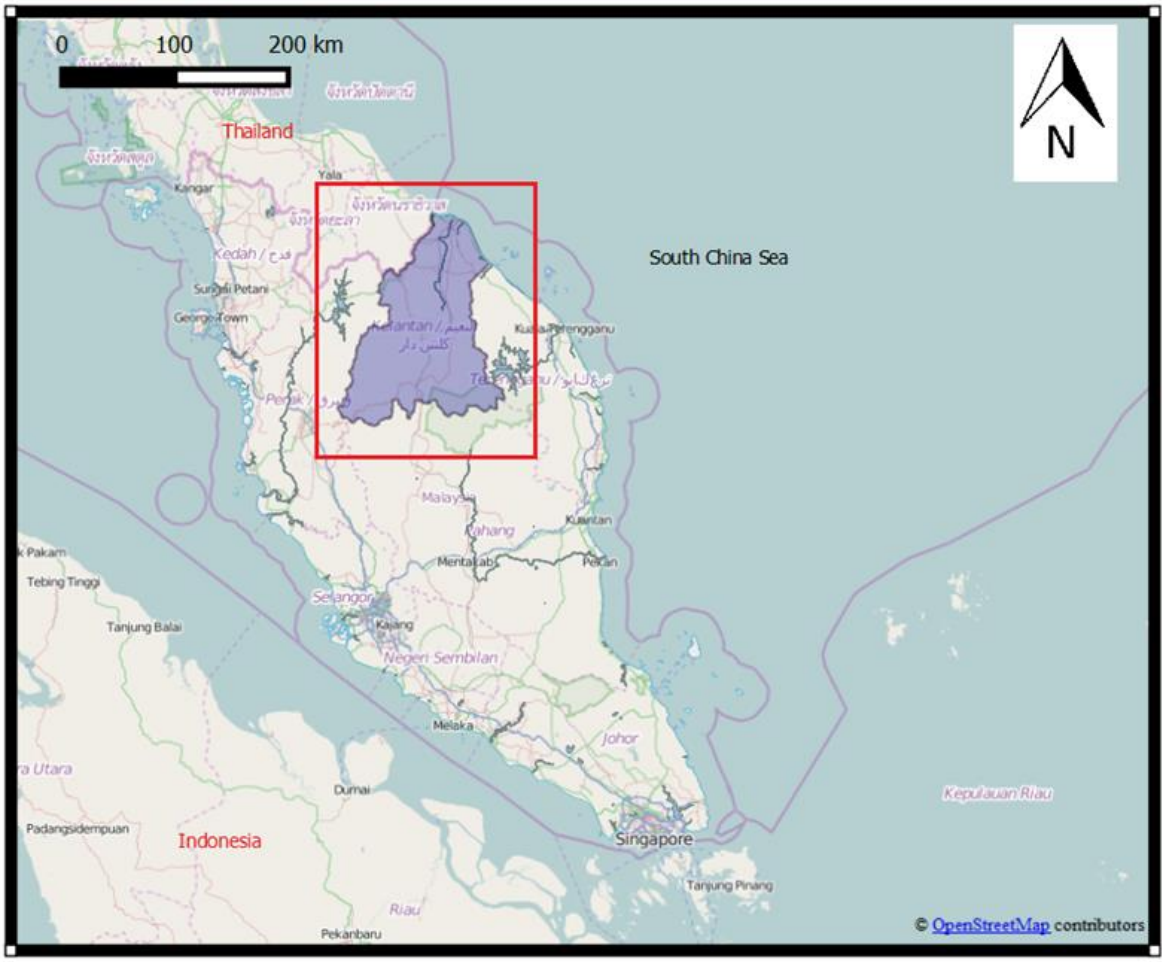

Figure 2.1. Location of Kelantan watershed (source: OpenStreetMap).

2.2 *Hydrological and Climate*

As located near the equator, Malaysia's climate is categorized as tropical, being hot and humid with temperatures ranging from 21 to 32° C throughout the year. The Kelantan watershed has an annual rainfall around 2,700 mm, of which more than 50% of rainfall occurs during the north east monsoon season from November to January every year. After monsoon season, days are typically warm and dry from early February through April. Figure 2.2 shows the average monthly rainfall in Kelantan.

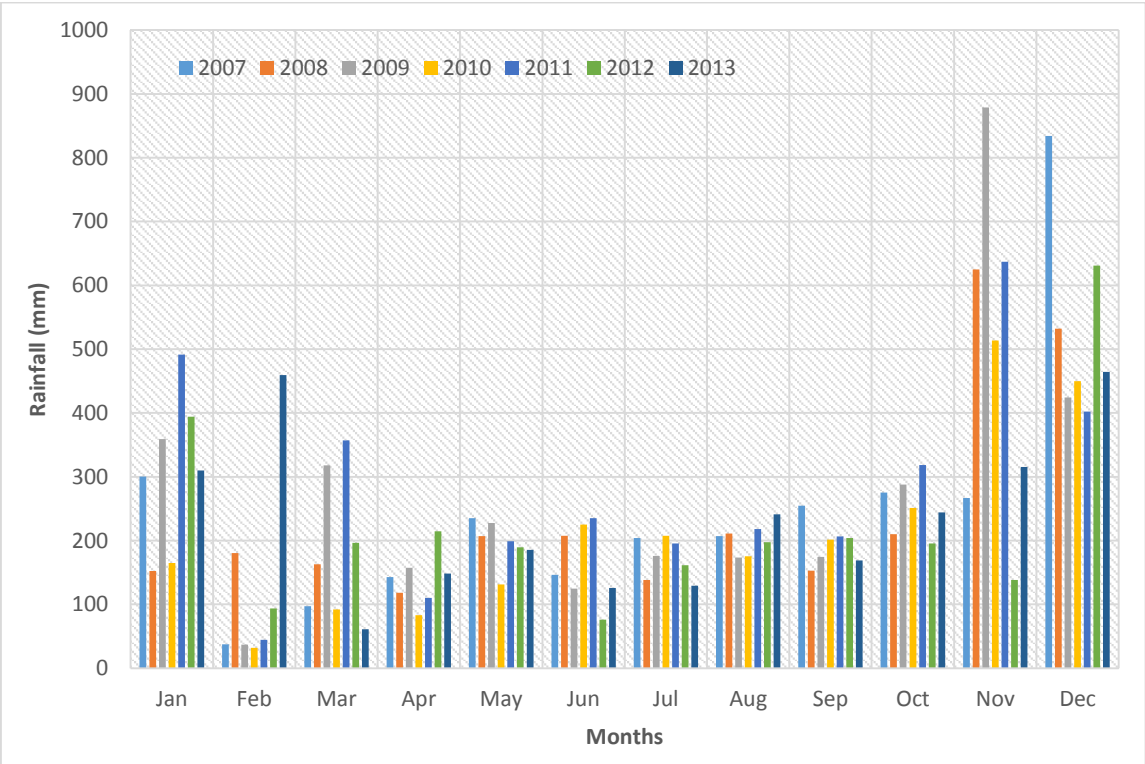

Figure 2.2. Average monthly rainfall in Kelantan for years 2007 – 2013.

Kelantan River is the major river in Kelantan. Another watershed is Golok River situated in between Malaysian and Thailand border area and Semerak watershed located at the east side, downstream of Kelantan. The Kelantan River has four main tributaries namely Nenggiri, Pergau, Galas and Lebir. The total length of Kelantan River and its longest tributary is 388 km (DID, 2013). The watershed has contrasted topography ranges from 0 in coastal area to 1750 meter in inland mountainous area. The main river, Kelantan River with length about 105 km, is named for the river after the confluence of Lebir River and Galas River at Kuala Krai. The Kelantan River flows through several populated area such as Kuala Krai, Tanah Merah and

main city of Kota Bharu before discharging to South China Sea. Figure 2.3 illustrates the river network in Kelantan state.

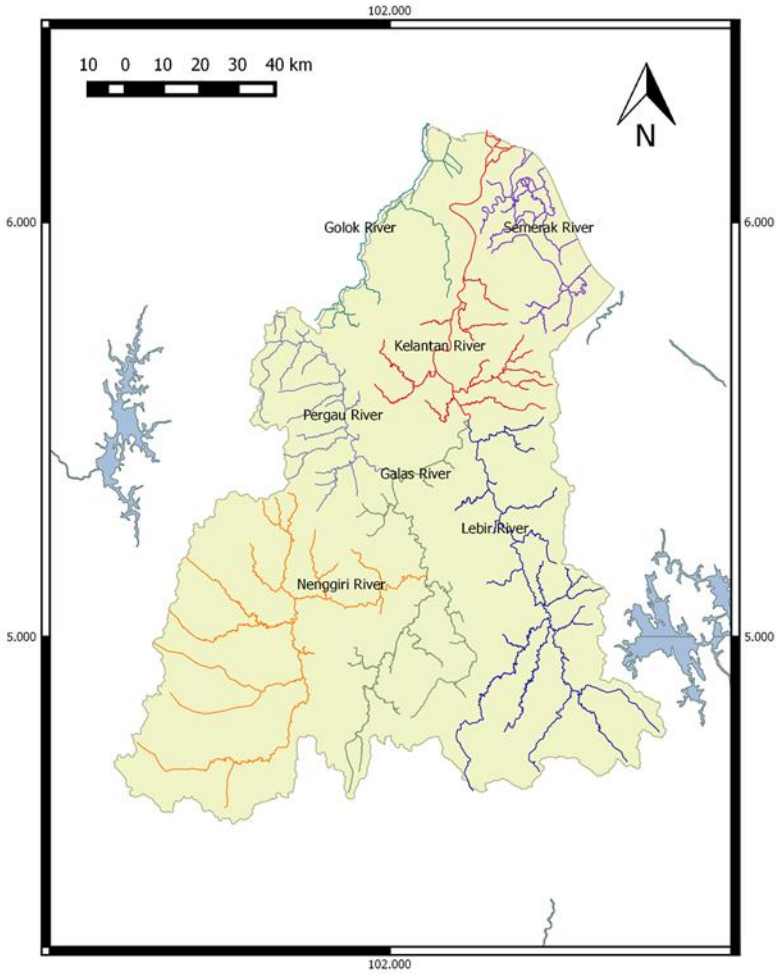

Figure 2.3. River network of Kelantan watershed (DID, 2013).

As reported by JICA in 1982, the difficulties of flood mitigation in Kelantan are in the vast coastal plain and relatively lower flow capacity in river channel. This scenario can be illustrated in recent monsoon season in 2014 as shown in Figures 2.4 and 2.5. The first heavy rainfall strikes downstream of Kelantan starting from 14th to 18th December 2014.The second rainfall event occurred on the 21st until 24th of December and the rainfall was mostly concentrated in upstream of Kelantan. Noted that the surface soil at downstream of Kelantan during the second events was fully saturated due to the first event, hence this might have caused huge flooding especially in the valley of Kuala Krai.

2.3 *Topography, Geology and Soil*

The topographic features of Kelantan watershed are characterized by geological strata running from the south to north direction as shown in Figures 2.6 and 2.7. High mountain ranges located at the eastern, western and southern sides of the watershed make a border with the states of Terengganu, Perak and Thailand, respectively. There are five broad topographic unit that can be distinguished based on differences in mean elevations (Raj, 2009) as shown in Table 2.1:

Table 2.1. Type of topographic units based (Raj, 2009)

Type of Topography	**Elevations (m)**
Low lying	< 15 above sea level
Rolling	16 – 30
Undulating	31 – 75
Hilly	76 – 300
Mountainous	> 301

Geologic structure in Kelantan watershed is comprised of 25% granite and intermediate intrusive rocks (Zakaria, 1975). The remainder consist of sedimentary rocks as shown in Figure 2.7. Most of the downstream area of Kelantan state is covered by Quaternary alluvium and topographically is dominated by the coastal plain with elevation less than 50 m above mean sea level. While the eastern and western granitic masses consist of various rock such as shales, sandstones, conglomerate, quartzite, limestone, siltstone/mudstone and metamorphic rocks of the Paleozoic age (Awaldalla and Nor, 1991). Its depth seldom exceeds a few meters. In the steep land area, particularly in the mountainous area, acid igneous rock formations exist and also soils such as alluvium, clay-loam-sand soil which support the growth of thick tropical forest. The upstream parts of the watershed consist of Triassic and Permian granite. The upstream of Kelantan watershed until Kusial streamflow gauge station consist of soil from lithosil types on high slopes area. The low slope areas are dominated by podzoil red-yellow mixed with podzoil yellow-grey soil (granite rock formation) and also sediment rocks and laterite soil (DID, 2000).

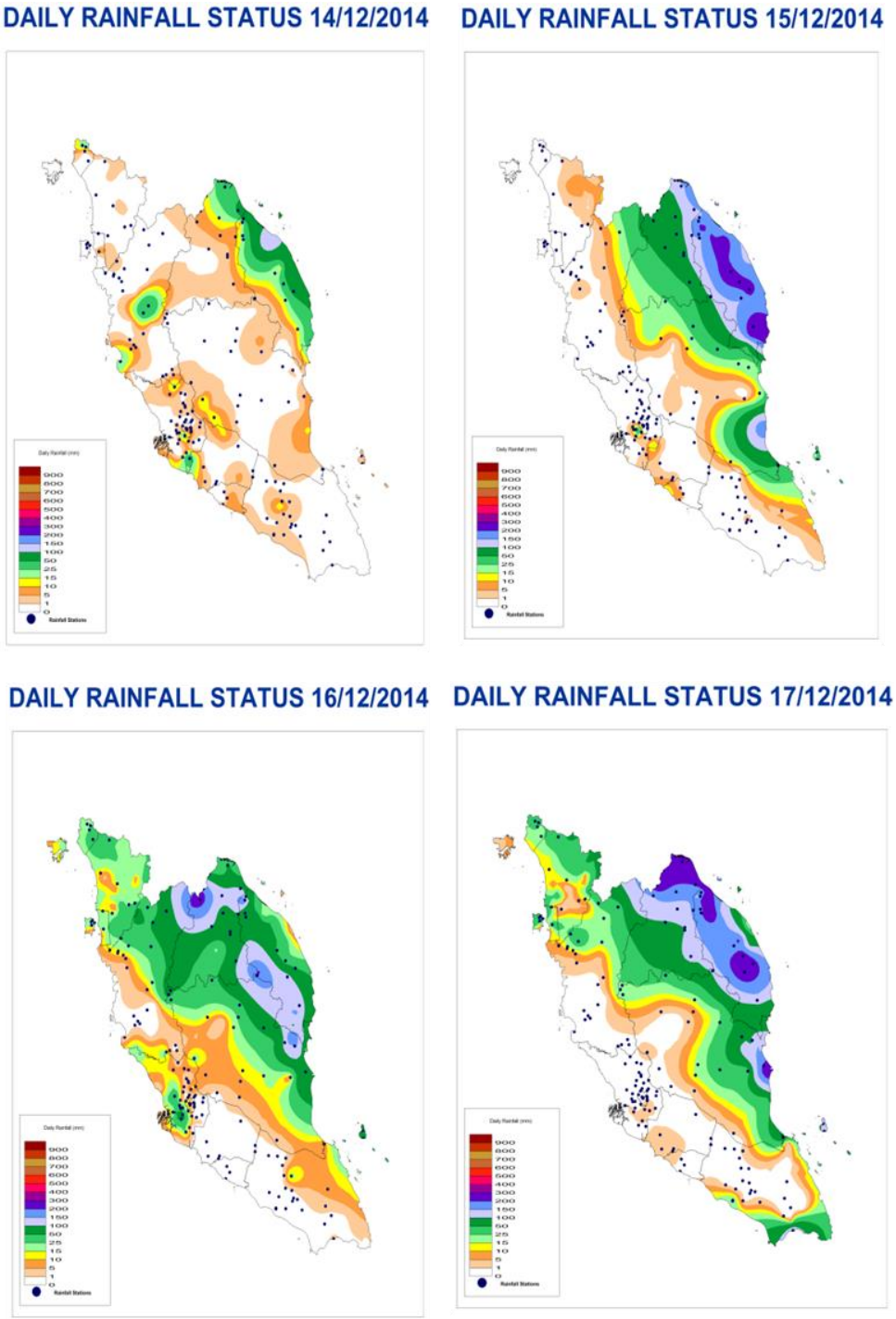

Figure 2.4. Daily rainfall pattern on Isohyet Map from 14th to 17th December 2014 (DID, 2014)

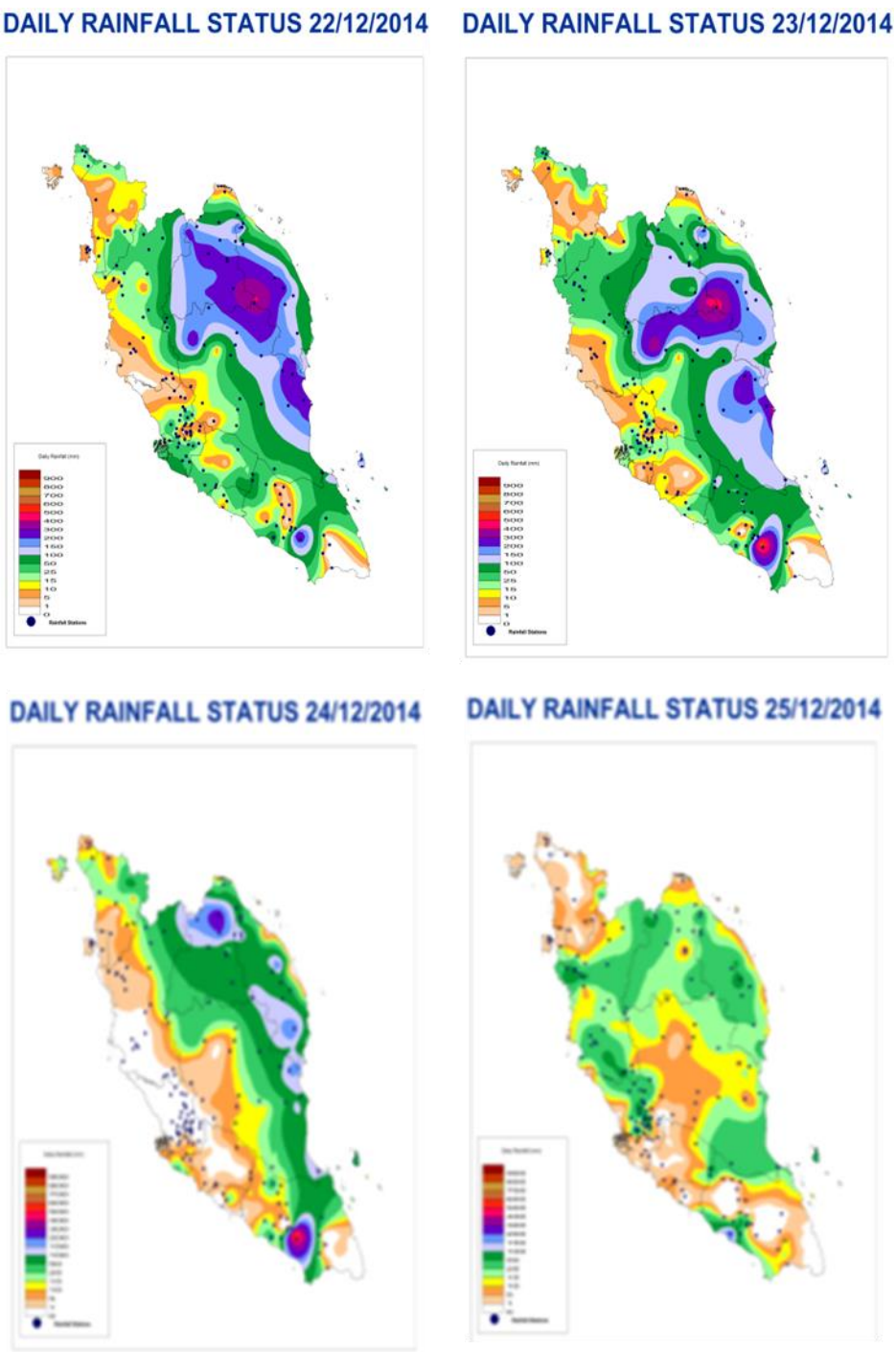

Figure 2.5. Daily rainfall pattern on Isohyet Map from 22th to 25th December 2014 (DID, 2014)

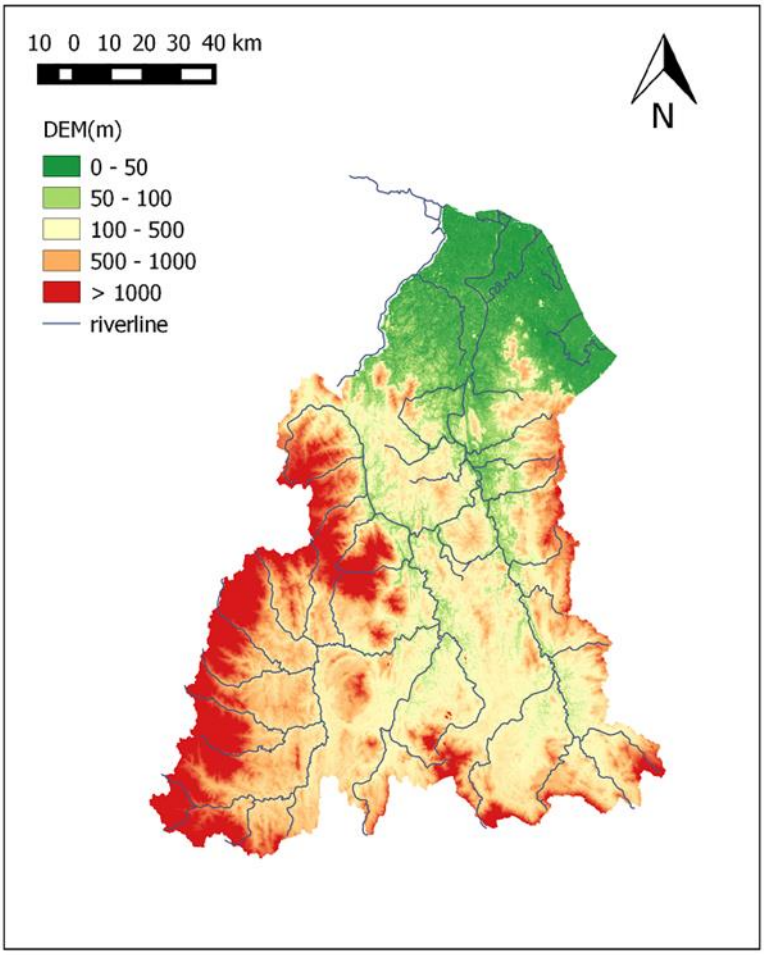

Figure 2.6. Topography map of Kelantan watershed from a digital elevation map (Department of Minerals and Geoscience Malaysia, 2012)

2.4 *Land use*

Figure 2.8 shows land use distribution of Kelantan state as of 2010. The largest land use component by far at present is forest which covers 64% of the surface area. The second largest component of the current land use is agricultural purposed area such as rubber, palm and paddy. Rubber and palm are widely grown in the upstream and middle stream of watershed whereas for paddy in the downstream area. Listed in Table 2.2 is the summary of land use distribution in Kelantan.

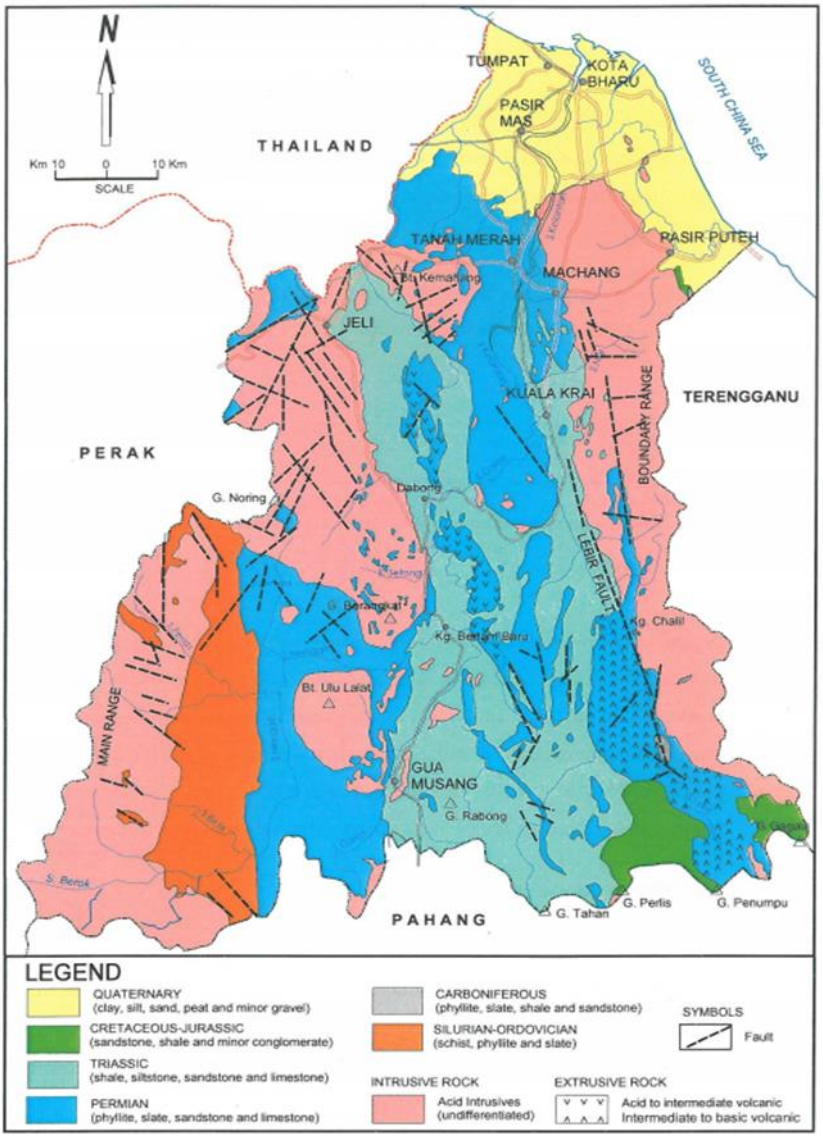

Figure 2.7. General geology map of Kelantan by Department of Minerals and Geoscience Malaysia (2003).

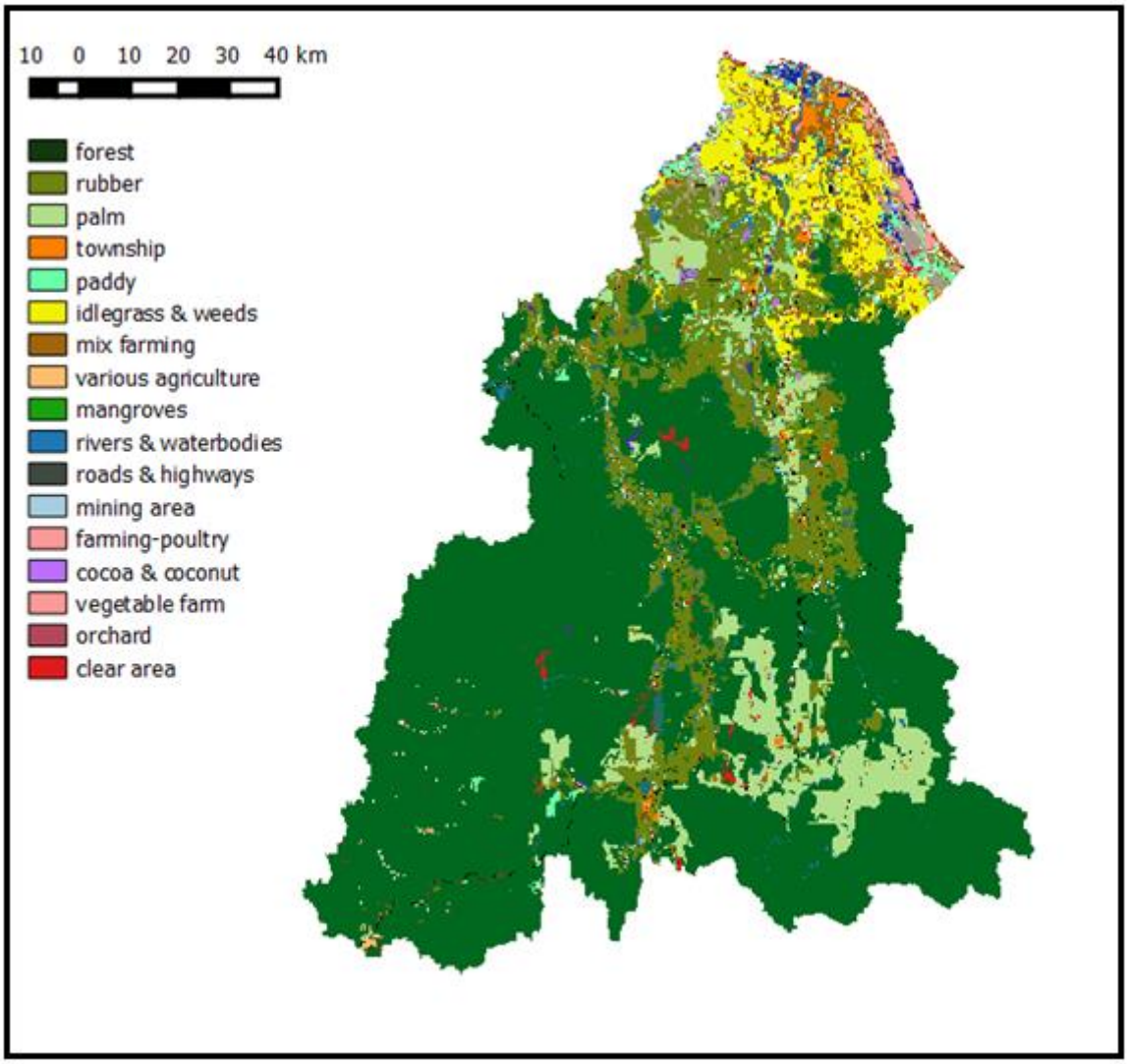

Figure 2.8. Land use map of Kelantan watershed by Department of Minerals and Geoscience Malaysia (2010).

Table 2.2. Summary of Kelantan State Land Use (2010)

Type	Area (km^2)	Percentage (%)
Forest	9,622.2	63.63
Rubber	2,167.2	14.33
Palm	1,104.4	7.30
Paddy	646.8	4.28
Mix farming	526.1	3.48
Idle grass & weeds	232.69	1.54
Mangroves	164.75	1.09
Waterbodies	148.46	0.98
Township	108.1	0.71
Orchard	102.9	0.68
Clear area	75.9	0.50
Various agriculture	67.3	0.45
Roads & highways	66.2	0.43
Cocoa & coconut	47.2	0.31
Farming poultry	19.5	0.13
Mining area	13.7	0.09
Vegetable farm	9.2	0.06
Total Area	**15,122.6**	**100**

2.5 *Historical Flood*

Flooding in Malaysia has been reported as early in 1800s with specific attention to monsoon and flash floods. The first reported severe flood event took place in 1886 in Kelantan that caused extensive damage (Chan and Parker, 1996). In 1926, flooding affected most of Peninsular Malaysia damaging property, road systems and agricultural (Malaysia National Committee, 1976). In 1967, disastrous floods surged across the Kelantan, Terengganu and Peak state. The almost same magnitude of flood as that occurred in 1971 swept across many parts of the country (Chan, 2002). As for Kelantan watershed, it has been always become a main subject to the most severe monsoon flooding in Malaysia apart from Terengganu and Pahang. Flooding appears to be increasing in Kelantan in terms of frequency as well as magnitude (MMD, 2007). Table 2.3 shows the historical flood and its impact from 2004 to 2014.

Table 2.3. Annual historical floods and its impact in Kelantan (2004-2014)

Year	Evacuees	Death	Estimation Damages (RM)
2004	10,400	12	14,320,000
2005	7,800	3	12,100,000
2006	No record	No record	No record
2007	12,000	5	63,310,000
2008	No record	No record	No record
2009	No record	No record	No record
2010	6,062	3	133,233,000
2011	2,812	6	22,648,500
2012	12,650	3	11,374,100
2013	No record	No record	No record
2014	22,225	18	200,100,000

2.6 *Data availability*

2.6.1 *Geographic information system data*

DEM derived from SRTM was obtained from Department of Drainage and Irrigation Malaysia (DID). Kelantan land use map was obtained from the Department of Minerals and Geoscience Malaysia in shapefile format. Land use information was processed using QGIS.

2.6.2 *Hydro-meteorological data*

The hydro-meteorological data of Kelantan watershed are obtained from DID. These are daily, hourly, and 5 minutes data of rainfall, daily and hourly streamflow and water level data. For rainfall data, there are two systems, one under *Rangkaian Hidrologi Nasional* (RHN) system and another under telemetry system. For RHN, the data transmitted from observation station to the main hydrology office by global system for mobile communications (GSM). For remote area, the data is obtained every three months via helicopter. Figure 2.9 shows how the data transmitted for telemetry system.

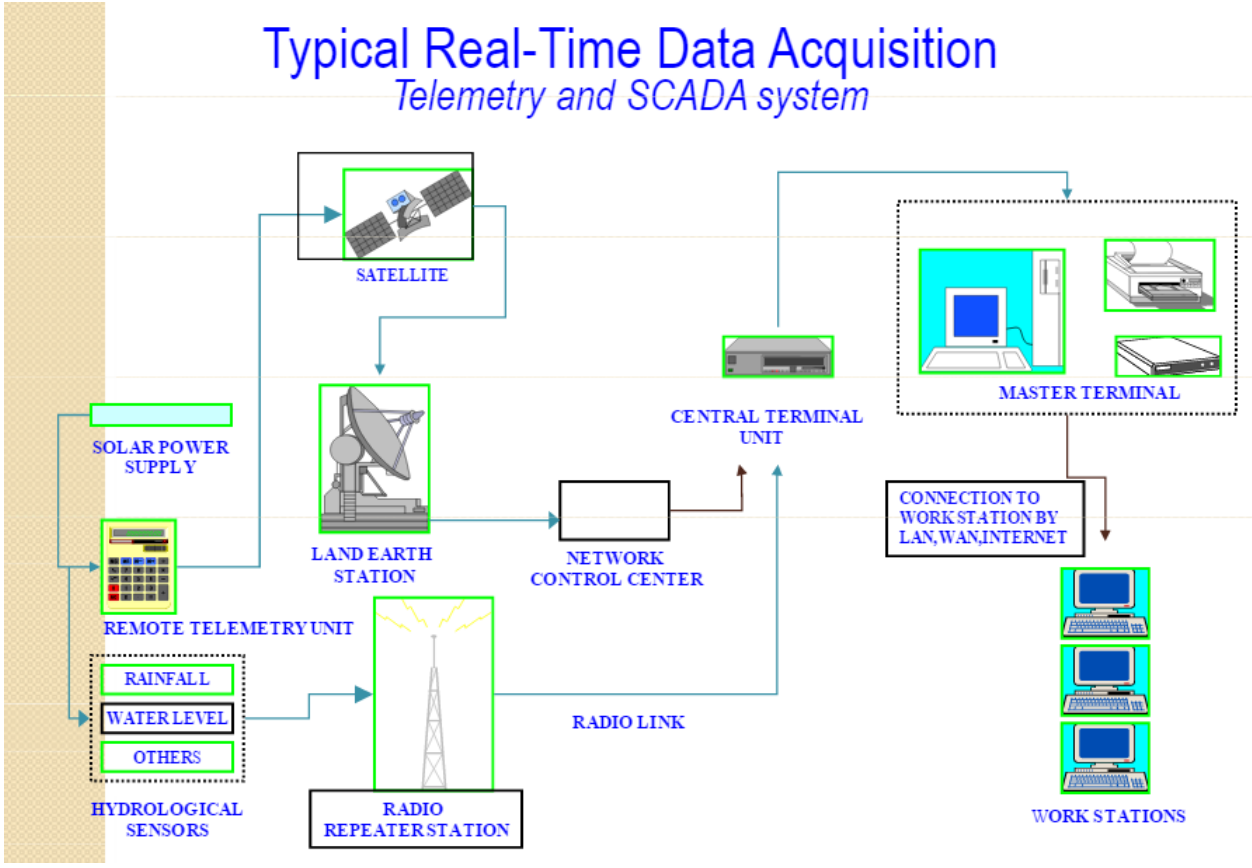

Figure 2.9. Telemetry system in Kelantan watershed (DID, 2003)

2.6.3 *Database-development*

To standardize the format in terms of arrangement of date, time and data information, a new database system is developed. All processing were done by making C programs. The data volume of all historical observation is around 6.5 GB, up to May 2015. Figure 2.10 shows an example of water level database developed in this study.

Year, month, date, hour, min, sec | Gregorian date | Water-level

wl_loc.txt | greg.c | gtime-kusial_6721442.txt

```
1,2001, 7, 3,21, 0, 0,18811.875000,8.500000
2,2001, 7, 3,22, 0, 0,18811.916667,8.500000
3,2001, 7, 3,23, 0, 0,18811.958333,8.500000
4,2001, 7, 4, 0, 0, 0,18812.000000,8.500000
5,2001, 7, 4, 1, 0, 0,18812.041667,8.500000
6,2001, 7, 4, 2, 0, 0,18812.083333,8.500000
7,2001, 7, 4, 3, 0, 0,18812.125000,8.500000
8,2001, 7, 4, 4, 0, 0,18812.166667,8.500000
9,2001, 7, 4, 5, 0, 0,18812.208333,8.500000
10,2001, 7, 4, 6, 0, 0,18812.250000,8.500000
11,2001, 7, 4, 7, 0, 0,18812.291667,8.500000
12,2001, 7, 4, 8, 0, 0,18812.333333,8.490000
13,2001, 7, 4, 9, 0, 0,18812.375000,8.490000
14,2001, 7, 4,10, 0, 0,18812.416667,8.490000
15,2001, 7, 4,11, 0, 0,18812.458333,8.490000
16,2001, 7, 4,12, 0, 0,18812.500000,8.490000
17,2001, 7, 4,13, 0, 0,18812.541667,8.490000
18,2001, 7, 4,14, 0, 0,18812.583333,8.490000
19,2001, 7, 4,15, 0, 0,18812.625000,8.490000
20,2001, 7, 4,16, 0, 0,18812.666667,8.500000
21,2001, 7, 4,17, 0, 0,18812.708333,8.500000
22,2001, 7, 4,18, 0, 0,18812.750000,8.500000
23,2001, 7, 4,19, 0, 0,18812.791667,8.510000
24,2001, 7, 4,20, 0, 0,18812.833333,8.510000
25,2001, 7, 4,21, 0, 0,18812.875000,8.510000
26,2001, 7, 4,22, 0, 0,18812.916667,8.520000
27,2001, 7, 4,23, 0, 0,18812.958333,8.520000
28,2001, 7, 5, 0, 0, 0,18813.000000,8.520000
29,2001, 7, 5, 1, 0, 0,18813.041667,8.530000
30,2001, 7, 5, 2, 0, 0,18813.083333,8.530000
31,2001, 7, 5, 3, 0, 0,18813.125000,8.530000
32,2001, 7, 5, 4, 0, 0,18813.166667,8.530000
33,2001, 7, 5, 5, 0, 0,18813.208333,8.530000
```

Figure 2.10. Water level database in gregorian time format

3 Homogeneity and Trend Analysis

3.1 *Introduction*

Climate in a narrow sense is defined as the average weather, or more rigorously as the statistical description in terms of the mean and variability of significant quantities over a period ranging from months to thousands or millions of years (Cubasch et. al., 2013). There are many indicators of climate change; these include changes in surface temperature, atmospheric water vapour, precipitation such as rainfall and snow, frequency of severe events, continental/oceanic glaciers, and sea level. Rainfall trends on spatial and temporal scales have been a great concern during the past century. The Intergovernmental Panel on Climate Change (IPCC) indicates that there are positive global trends by suggesting rainfall over tropical land areas (30ºS to 30ºN) has increased over the last decade, reversing the drying trend that occurred from mid-1970s to mid-1990s (Hartmann et. al., 2013).There are many different ways in which climate change may affect watershed behaviour, such as changes in total rainfall, location, seasonality and intensity, effects on temperature, radiation and evaporation (Roberts, 1998).

Time-series rainfall records observed at distributed rainfall stations within a given river basin represent the most basic data for hydrologic analyses, for example, water resource evaluation, flood/inundation prediction, and modeling environmental problems. Long-term meteorological times-series records provide vital information about climate variability, and the trends and cycles related to disputed global meteorological changes. In the Kelantan watershed, Malaysia, modern rainfall observations started in 1948, and extensive time-series data have been accumulated by the Department of Irrigation and Drainage Malaysia (DID) over the past 70 years. Currently, an international cooperative project is working to reduce damage by flood/inundation and landslides, disasters that the river basin has historically experienced. In this study, we aimed to provide a reliable database for hydrologic analyses by reviewing the quality of the long-term records, and secondly, to analyze meteorological variability in the Kelantan watershed.

Long time-series rainfall data are often inconsistent or inhomogeneous, a situation caused by a number of non-climatic factors that result in unrealistic trends, shifts, and jumps (Peterson et al., 1998, Mestre et al., 2013, Philbert et al., 2014). For example, unreliable shifts are often related to station relocations, modifications in observation schedules, routines, and/or practices, or variations in the methods of preliminary data handling, instrument disclosure, or abrupt changes in the nearby environment (Heino, 1994, Tuomenvirta, 2002, Cao et al., 2012). These

inhomogeneities are more common in older data, but are still sometimes observed in more recent data. Furthermore, for developing countries in particular, rainfall observation systems before the 1980s were not well distributed or equipped; therefore, data processing was not standardized, as it is today, leading to additional potential errors. Removing such inhomogeneity from databases is essential for more reliable hydrologic analyses.

The simplest approach to identifying and correcting inhomogeneous times-series data is by visual analysis, preferably by experienced meteorologists (Peterson et al., 1998). However, this method, which is laborious and time consuming, is not practical given the huge quantities of time-series data. Thus, the use of digital processing and statistical methods is first required for the extraction of potentially problematic data sequences, after which the graphical method conducted by those with expertise can be employed to evaluate the appropriateness of the results.

To date, several statistical methods, known as 'homogeneity tests', have been developed to identify inhomogeneity. These tests can be performed in two ways: relative tests (i.e., testing with respect to neighboring stations that are considered homogenous), and absolute tests (i.e., used if the two data series are not sufficiently correlated; Wijngaard et al., 2003, Sahin and Cigizoglu, 2010). Peterson (1998) suggested that the relative method more easily detects inhomogeneity because of climate variations. However, for rainfall in Malaysia, relative testing may not be suitable since rainfall stations are randomly distributed, with localities spread across mountainous, rural, urban, and coastal areas; therefore, each station represents a unique geographical position and climatic environment. Due to this factor, Suhaila et al. (2008) described the difficulties in identifying homogenous reference stations. Furthermore, in the Kelantan watershed specifically, the extent of missing data at certain rainfall stations also makes it difficult to find homogenous neighboring stations. As a result, absolute homogeneity tests were used in this study. In this study, all rainfall stations were carefully evaluated and used in homogeneity tests before trend analysis were conducted.

A number of studies have dealt with trend analysis for rainfall data in Malaysia (Suhaila et al., 2008, Suhaila et al., 2010, Kang and Fadhilah, 2012). The results of these studies varied depending on the number of rainfall stations used, the length of the time-series, and the statistical tests used. In this study, we used a Mann-Kendall test, commonly employed in hydrology, and considered three different sampling methods to detect long- and short-term trends in rainfall within the Kelantan watershed.

A total of 50 daily rainfall data series of Kelantan watershed having data ranging from 1948-2011 has been used in this homogeneity analysis. Monthly total rainfall values were obtained

by summing up daily rainfall data detected by the observation gauges. Similarly, for annual total rainfall data were calculated by adding monthly total rainfall data after filling in the missing values. Correlation-regression method and inverse distance method were used in filling up the missing values in monthly scales. For trend analysis, homogenous rainfall time-series data at selected 14 rainfall stations were used to elucidate the historical variability and trends.

3.2 *Absolute Homogeneity Test*

Four absolute homogeneity tests were applied to rainfall time-series data to detect breaks. They are Buishand range test, standard normal homogeneity test (SNHT), Pettitt test and Von Neumann ratio test. The first three tests give information about the possible year of such breaks, whereas the last test allows one to estimate only the presence of breaks in the time-series (Wijngaard et. al., 2003). There are some differences between the first three tests above. Pettitt test and Buishand test detect breaks in the middle series, whereas SNHT is sensitive in detecting breaks near the beginning and the end of the time-series (Hawkins, 1977; Costa and Soares, 2009; Kang and Fadhilah, 2012).

A rainfall stations will be marked as ‘homogenous’ when one or zero tests reject the homogeneity. If two tests reject the homogeneity, the rainfall stations will be marked as ‘suspect’. ‘Doubtful’ is given to at three or all tests reject the homogeneity; hence the rainfall stations are considered as inhomogeneous. This evaluation has been used by Wijngaard et. al. (2003).

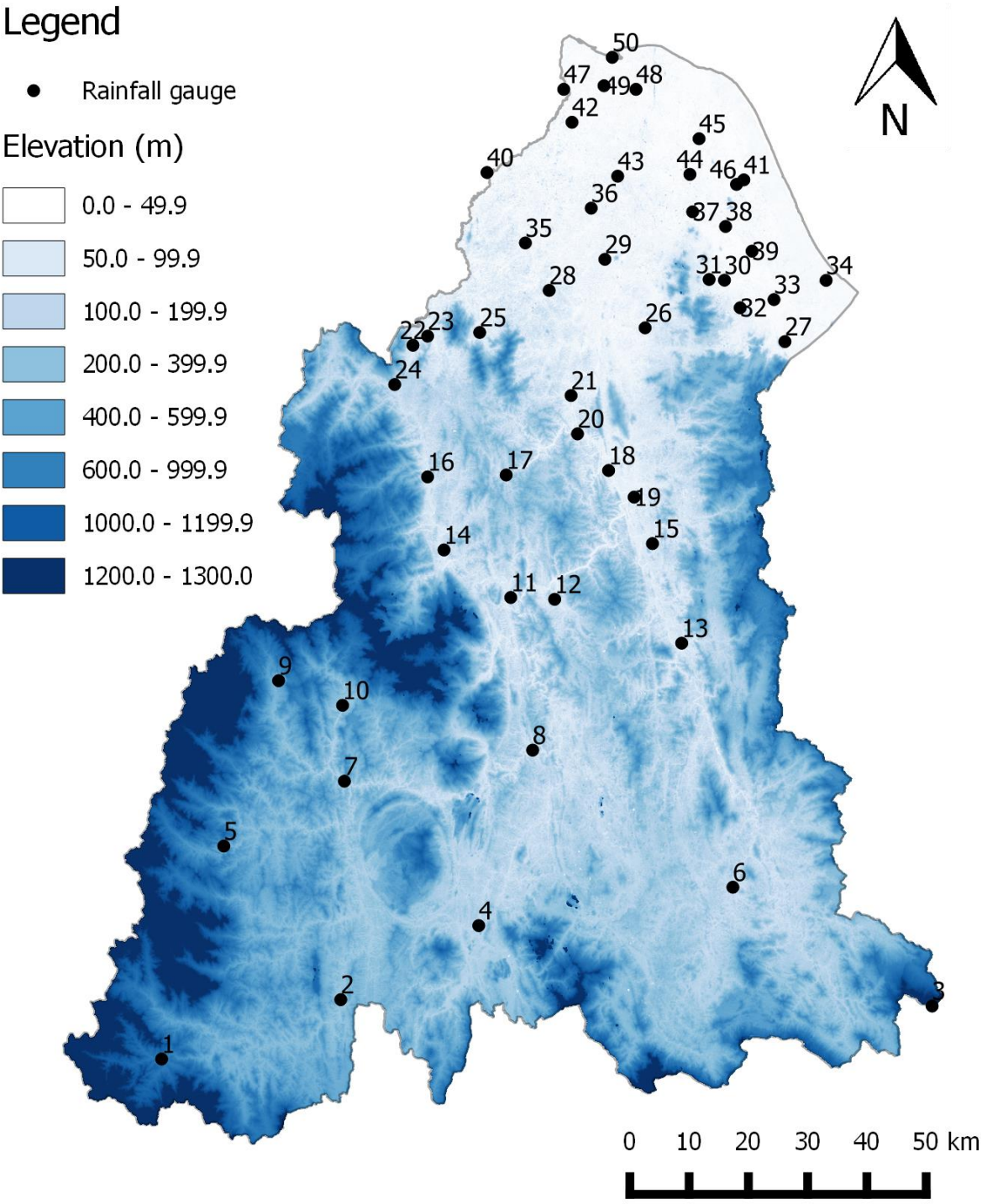

Figure 3.1. Location of 50 long-term rainfall stations used in this analysis

Table 3.1. Geographical coordinates and elevations of rainfall gauges in Kelantan watershed (DID, 2012).

No	Station	Years of Data	Elev. (m)	Long.	Lat.	No	Station	Years of Data	Elev .(m)	Long	Lat
1	Brook	1984-2011	153	101.48	4.67	26	Jps Machang	1991-2011	30.5	102.22	5.79
2	Blau	1984-2010	165	101.72	4.77	27	Kg. Wakaf Raja	1971-2011	13.4	102.43	5.77
3	Gng Gagau	1985-2011	1067	102.66	4.76	28	Bdg Nyior	1981-2012	20	102.07	5.84
4	Gua Musang	1972-2011	93	101.97	4.88	29	Stn. Bkt Panau	1949-2011	15	102.16	5.89
5	Chabai	1989-2010	305	101.58	5.00	30	Ibu Bekalan Tiga Daerah	1979-2012	16	102.34	5.86
6	Kg Aring	1975-2011	73	102.35	4.94	31	Bkt Abal	1948-2012	22	102.32	5.86
7	Gemala	1984-2010	91	101.76	5.10	32	Ldg. Cherang Tuli	1948-2012	15	102.36	5.82
8	Balai Polis Bertam	1952-2010	71	102.05	5.15	33	Sg. Petai	1957-2012	3	102.42	5.83
9	Gob	1985-2010	270	101.66	5.25	34	Cherang Ruku	1948-2012	9	102.49	5.86
10	Pasik	1989-2010	310	101.76	5.21	35	Kg Tandak	1991-2012	10	102.04	5.92
11	Dabong	1972-2005	82	102.02	5.38	36	Ibu Bekalan Tok Uban	1949-2012	12	102.14	5.97
12	Ldg Kuala Gris	1971-2012	43	102.08	5.38	37	Stn Melor	1966-2012	8	102.29	5.96
13	Kg Laloh.	1972-2011	48	102.28	5.31	38	Serdang	1981-2012	5	102.34	5.94
14	Ldg. Kuala Balah	1953-2011	50	101.91	5.45	39	Tok Ajam	1966-2012	3	102.38	5.90
15	Ldg. Lepan Kabu	1953-2011	50	102.23	5.46	40	Rumah Kastam Rantau Pjg	1948-2012	6	101.98	6.02
16	Sek. Keb. Lubok Bungor	1962-2012	111	101.89	5.56	41	Rumah Pam Repek	1947-2012	9	102.10	6.01
17	Ulu Sekor	1983-2011	91	102.01	5.56	42	Kuarters DID Meranti	1966-2011	4	102.11	6.10
18	Ldg Kuala Nal	1948-2011	12	102.16	5.57	43	Rumah Pam Salor	1952-2011	10	102.18	6.02
19	SMT Kuala Krai	1949-2011	29	102.20	5.53	44	Kg Peringat	1979-2011	7	102.29	6.02
20	Ldg Kenneth	1957-2011	30	102.12	5.63	45	Kg Binjai	1981-2011	5	102.30	6.08
21	Ldg Kerilla	1957-2011	24	102.11	5.68	46	Trtk Pulai	1960-2011	6	102.36	6.01
22	Kg. Gemang Bahru	1957-2011	47	101.87	5.76	47	Kuala Jambu	1961-2011	3	102.10	6.15
23	Air Lanas	1981-2011	74	101.89	5.78	48	Kg Kebakat	1981-2011	3	102.21	6.15
24	Kg Jeli	1972-2011	101	101.84	5.70	49	Cbg Ampat	1967-2011	11	102.16	6.16
25	Durian Daun	1980-2011	38	101.97	5.78	50	Stn Tumpat	1949-2011	3	102.17	6.20

3.2.1 *Buishand Range Test*

This parametric test assumes that tested values are independent and identically normally distributed (null hypothesis). The alternative hypothesis assumes that the series has a jump-like shift (break). The test statistics which are the adjusted partial sum, S^*_k (Buishand, 1982) of the first year, k until n years is defined as:

$$S*_k = \frac{n\sum_{i=1}^{k}(Y_i - \bar{Y})}{\sum_{i=1}^{n}(Y_i - \overline{Y})^2}\ , k = 1,2 \ldots n \tag{3.1}$$

$$RS*_0 = 0 \tag{3.2}$$

Hereafter, for each test descriptions, Y_i is i-th element of the time series and $\bar{Y}$ is the mean value of the time series. When time-series is homogenous, the values of $S*_k$ will fluctuate around zero because no systematic deviations of the Y_i values with respect to their mean will appear

The significance of the shift can be tested with rescaled adjusted range, R (range statistics) which is the difference between the maximum and the minimum of the $S*_k$:

$$R = \max_{0 \le k \le n} S*_k - \min_{0 \le k \le n} S*_k \tag{3.3}$$

The 1% critical values for $R/\sqrt{n}$ Buishand range test (Buishand, 1982) for different length of time series can be found in Table 3.2.

3.2.2 *Standard Normal Homogeneity Test*

The likelihood ratio SNHT can be classified as one of the well-known homogeneity test as it can spots break both in the beginning and end of the time-series. The null and alternative hypothesis in this test are the same as in the Buishand range test. Alexandersson and Moberg (1997) proposed a statistic $T(k)$ to compare the mean of the first k years of the record with that of the last $(n-k)$ years:

$$T(k) = k\bar{z}_1^2 + (n-k)\bar{z}_2^2, k = 1,2 \dots n \tag{3.4}$$

where

$$\bar{z}_1 = \frac{1}{k}\sum_{i=1}^{n}\frac{(Y_i - \bar{Y})}{s} \tag{3.5}$$

and

$$\bar{z}_2 = \frac{1}{n-k}\sum_{i=k+1}^{n}\frac{(Y_i - \bar{Y})}{s} \tag{3.6}$$

and

$$s = \frac{1}{n}\sum_{i=1}^{n}(Y_i - \bar{Y})^2 \tag{3.7}$$

If a break occurs at the year K, then $T(k)$ reaches a maximum near the year $k = K$. The test T_o is defined as:

$$T_o = \max_{1 \le k \le n} T(k) \tag{3.8}$$

The null hypothesis is rejected if T_o is above a certain level, which is dependent on the sample size. The 1% critical values for the statistic T_o of single shift SNHT as a function of n (Jarušková, 1996) can be obtain in Table 3.2.

3.2.3 *Pettitt Test*

The null hypothesis in this non-parametric rank test is the same as in the Buishand range test. The ranks $r_1 \dots r_n$ of the $Y_i \dots Y_n$ are used to calculate the statistics (Pettitt, 1979):

$$X_k = 2\sum_{i=1}^{k} r_i - k(n+1), \qquad k = 1,2 \dots\dots n \tag{3.9}$$

If a break occurs in year K, then the statistic is maximal or minimal near the year $k = K$:

$$X_k = \max_{1 \le k \le n} |X_k| \tag{3.10}$$

1% critical values for X_k in different data sets length (Pettitt, 1979) can be obtain in Table 3.2.

3.2.4 *Von Neumann Ratio Test*

This non-parametric test consists of null hypothesis that the data is independent and identically distributed random values. The alternative hypothesis is the values in the series are not randomly distributed. The Von Neumann ratio N is defined as follows (Von Neumann, 1941).

$$N = \frac{\sum_{i=1}^{n-1}(Y_i - Y_{i+1})^2}{\sum_{i=1}^{n}(Y_i - \bar{Y})^2} \tag{3.11}$$

If the time series contains a break, the value of N tends to be lower than the critical value provided in Table 2. If the sample has rapid variations in the mean, then the values of N may rise above 2 (Bingham and Nelson, 1981; Klein Tank, 2007).

Table 3.2. Critical values (1%) for homogeneity test statistics

Test[a]	Time-series length, n					
	20	30	40	50	70	100
Buishand ($R/\sqrt{n}$)	1.60	1.70	1.74	1.78	1.81	1.86
SNHT (T_o)	9.56	10.45	11.01	11.38	11.89	12.32
Pettitt (X_k)	71	133	208	293	488	841
von Neumann (N)	1.04	1.20	1.29	1.36	1.45	1.54

[a] Buishand range test = $R/\sqrt{n}$ (Buishand, 1982); T_o of SNHT (Jarušková, 1996); X_k (Pettitt, 1979); N of the Von Neumann test (Buishand, 1982)

3.3 *Trend Analysis*

The non-parametric Mann-Kendall (MK) trend test (Mann, 1945, Kendall, 1975) is widely used because it is less sensitive to outliers than alternative methods, and because it can be adopted in cases where data are not normally distributed, and for data containing outliers and nonlinear trends (Helsel and Hirsch, 2002, Birsan et al., 2005). Therefore, this technique is the most robust for detecting trends in rainfall time-series data due to the influence of extremes and the fit of applications with skewed variables (Gilbert, 1987, Yue et al., 2002, Hamed, 2008). The MK test of rainfall times-series can be written as

$$S = \sum_{i=1}^{n-1} \sum_{j=i+1}^{n} sgn(x_j - x_i) \tag{3.12}$$

where

$$sgn(x_j - x_i) = \begin{cases} +1 \; if(x_j - x_i) > 0 \\ 0 \; if(x_j - x_i) = 0 \\ -1 \; if(x_j - x_i) < 0 \end{cases} \tag{3.13}$$

where x_j and x_i are the annual rainfall values for years j and i (j > i) respectively and n is the number of data points. Normalized S of MK (i.e., MK-S divided by the number of data summated) is an indicator between -1 and 1, for which an increasing trend will give positive values and a decreasing trend will give negative values. The variance is computed as

$$Var(S) = \frac{n(n-1)(2n+5) - \sum_{i=1}^{P} t_i(t_i - 1)(2t_i + 5)}{18} \tag{3.14}$$

where n is the number of data points, P is the number of tied groups, t_i denotes the number of ties to extent i in the Pth group. The summation term in the numerator is used only if the data series contains tied values (Kisi and Ay, 2014). The standard test statistics, $Z_{(var)}$is calculated as

$$Z_{(var)} = \begin{cases} \dfrac{S-1}{\sqrt{Var(S)}} \; for\; S > 0 \\ 0 \;\; for\; S = 0 \\ \dfrac{S+1}{\sqrt{Var(S)}} \; for\; S < 0 \end{cases} \tag{3.15}$$

Positive values of $Z_{(var)}$ indicate increasing trends while negative $Z_{(var)}$ values show decreasing trends. Testing is done at the specific α significance level. However in this study, only Normalized S of MK is used to investigate trends in Kelantan watershed. The MK test can be considered a type of smearing method for the irregular time-series of real values by using "sign bit". In this study, we use three different sampling methods for detecting trends in different time scales: MK-1, MK-2, and MK-3 as follows. Figure 3.2 explains the methods schematically.

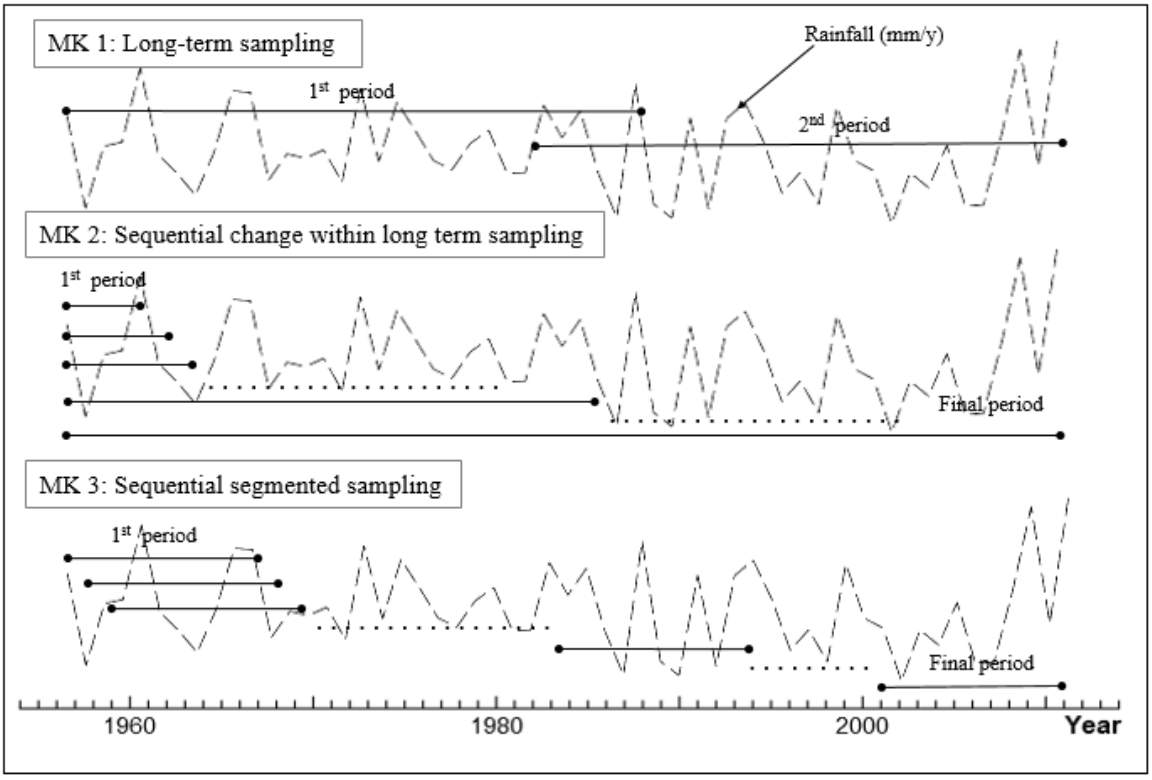

Figure 3.2. Three different sampling period methods for the Mann-Kendall (MK) test.

MK-1

MK method is applied to long time series of data to detect long-term averaged trend.

MK-2

To detect sequential change of trends within a long period, the starting year as the first year of the observation (Ys) is fixed, the ending year (Ye) is set, and MK-S value, S(Ye), is calculated for (Ye-Ys+1) points. Ye is increased one by one, up to the most recent year, so that finally we have sequential MK-S values, which represent the averaged trend from Ys to Ye, as shown in Figure 3.2.

MK-3

To detect trends for a relatively short period, an arbitrary constant period (dY), a starting point (Ys) and an ending point (Ye = Ys + dY) are set, and MK-S value is calculated and stored as S(Ye). Ys is moved according to Ys + 1, Ys + 2, …, until Ye reaches the ending year of the data. The sequence of S (Ye) might express the averaged trend for dY years preceding Ye.

3.4 *Result and Discussion*

3.4.1 *Homogeneity Test*

The homogeneity of the annual total rainfall time series at 50 stations in Kelantan watershed were tested by using Buishand range test, SNHT, Pettitt test and von Neumann ratio test. The results of each method were evaluated at 99% significance level. From the four absolute test results, using the Wijngaard (2003) evaluation, 41 stations are homogenous, 6 are suspects and another 3 stations are inhomogeneous or heterogeneous. Figure 3.3 shows the spatial position of suspects, doubtful and homogenous stations based from the four absolute homogeneity tests. Table 3.3 shows the list of stations listed under ‘suspects’ and ‘doubtful’ containing critical values in brackets and year break. Results shown in Figure 3.4 Table 3.3 indicates that inhomogeneity is generally detected mostly in 1992 in six stations followed by 1957 in two stations. The rest is in 1966, 1975, 1983, 1990 and 1997. To check that the inhomogeneity might be related to the variations of natural meteorological conditions, the heterogeneous rainfall time series focusing on year break period were plotted as in Figure 3.5(a)-(h). By referring to figures stated previously, some of the break year detected by the absolute homogeneity test can be said due to the natural behaviour of climate and rainfall hence the year break will not be considered as inhomogeneous. For example in Figure 3.5(a), (d) and (h)

represent the break year in 1992 at the upstream, midstream and downstream. When compared with homogenous surrounding stations, we can see the same pattern occurred. The same situation occurred in Ladang Kuala Nal (Figure 3.5(c) and (d)) for year 1957 and 1997 where the same behavior can be seen in the plots. However, for Brook in 1992, Ladang Kenneth in 1975, Kg. Gemang Bahru in 1983 and Rumah Kastam Rantau Panjang in 1966 remains inhomogeneous since the plots are slightly different with surrounding stations. Hence we can conclude that the number of homogenous long time series in Kelantan after correction are 46 whereas 4 stations are inhomogeneous where two tests reject the null hypothesis at 99% confidence level.

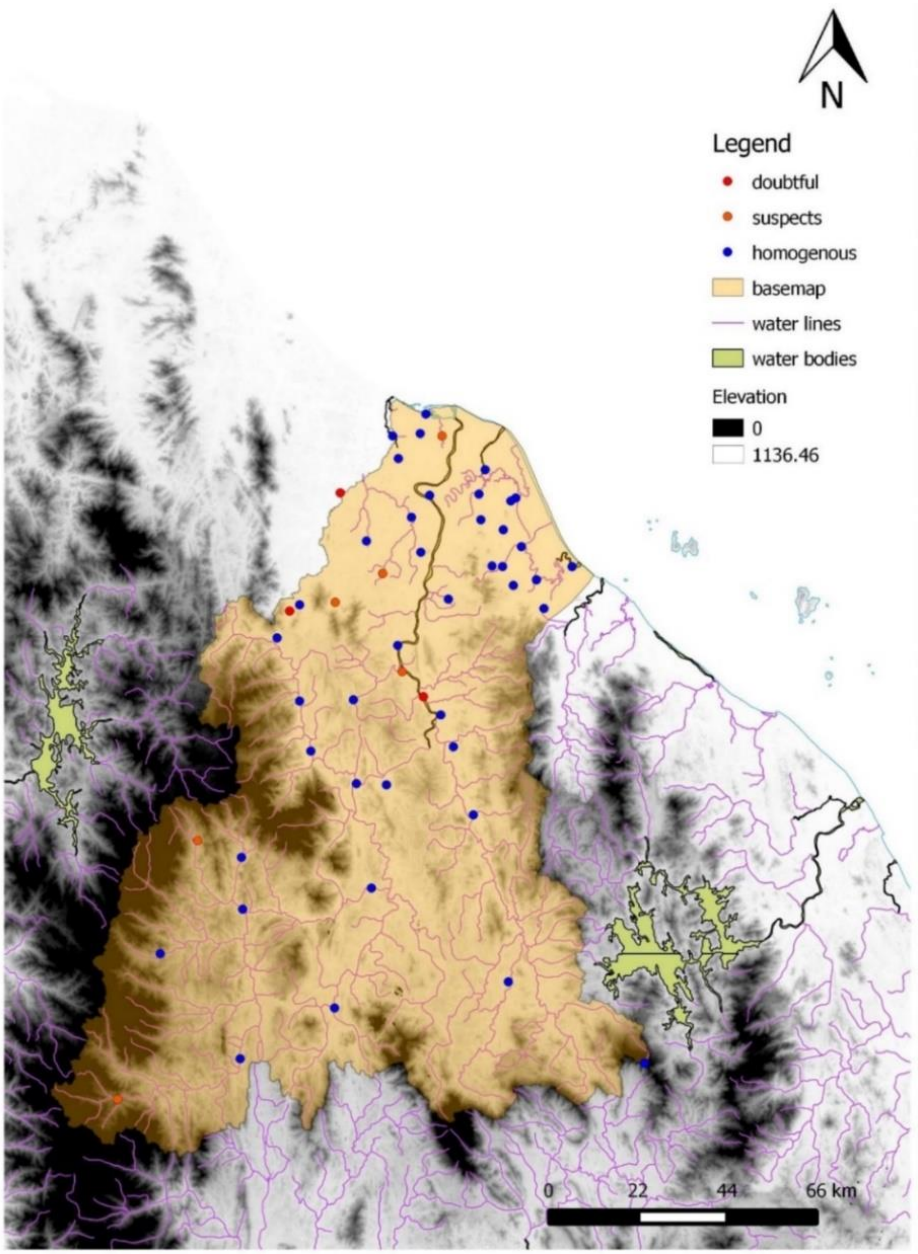

Figure 3.3. Location of homogenous, suspect and doubtful rainfall stations based on absolute homogeneity test

Table 3.3. Inhomogeneous stations based on four absolute homogeneity tests

No	Stations	Buishand ($R/\sqrt{n}$)	SNHT (T_o)	Pettitt (X_k)	von Neumann (N)	Status	After Corrections
1	Brook	-	-	123.0 > (120.6) -1990-	1.01 < (1.17)	Suspect	Suspect
9	Gob	-	12.40 > (10.09) -1992-	124.0 > (108.2) -1992-	-	Suspect	Homogenous
18	Ldg Kuala Nal	2.48 > (1.80) -1957-	20.88 > (11.74) -1997-	559.0 > (429.5) -1992-	1.07 < (1.42)	Doubtful	Homogenous
20	Ldg Kenneth	2.22 > (1.79) -1975-	-	-	1.24 < (1.38)	Suspect	Suspect
22	Kg Gemang Bahru	2.17 > (1.79) -1957-	16.73 > (11.51) -1983-	504.0 > (341.8) -1983-	1.28 < (1.38)	Doubtful	Suspect
22	Durian Daun	-	12.75 > (10.56) -1992-	187.0 > (148.0) -1992-	-	Suspect	Homogenous
28	Bendang Nyior	-	-	158.0 > (140.5) -1992-	1.03 < (1.21)	Suspect	Homogenous
40	Rumah Kastam Rantau Pjg.	2.05 > (1.80) -1966-	11.83 > (11.76) -1992-	512.0 > (439.2) -1992-	1.40 < (1.43)	Doubtful	Suspect
48	Kg Kebakat	-	-	154.0 > (140.5) -1992-	1.10 < (1.21)	Suspect	Homogenous

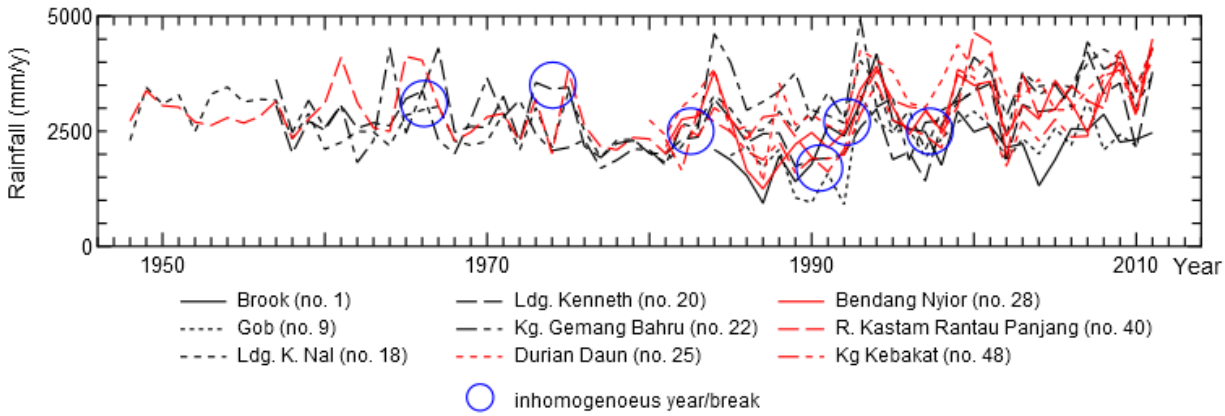

Figure 3.4. Inhomogeneous rainfall stations from the four absolute homogeneity test

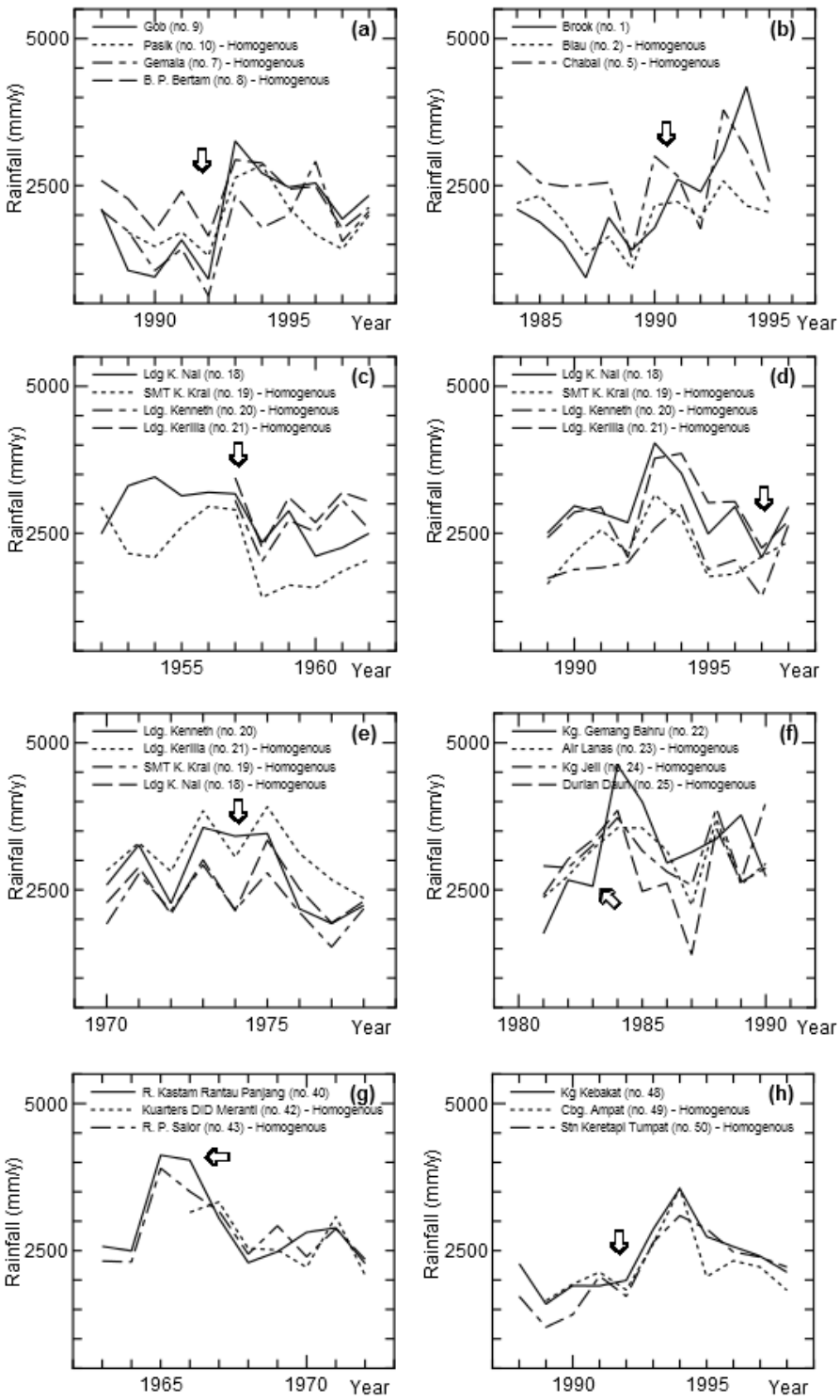

Figure 3.5(a)-(h). Comparison between inhomogeneous rainfall stations with homogenous surrounding /nearby rainfall stations

3.4.2 *Trend Analysis*

Figure 3.6 shows the annual rainfall time-series averaged over all homogenous rainfall stations, together with the number of rainfall stations. By graphical analysis, weakly decreasing or mostly constant periods were observed from 1948 to ~1980–1983, while increasing trends became dominant in the latter half of the record, particularly in the 5-year period before 2011. The trends for the latter period somehow consistent with Suhaila et. al. (2010), indicating the total amount of rainfalls in the east coast of Peninsular Malaysia showed an increased pattern from 1975 to 2004. The same trends were also found in the United Kingdom (Met Office, 2015) and Japan (JMA, 2015) in the period of 1950s-2015. Using the Sen Slope estimator, the slope of the averaged time-series (Figure 3.6) was ~1.8 mm per year, giving an estimated increase of 108 mm in the period 1948–2011, which corresponds to ~4% of the annual value.

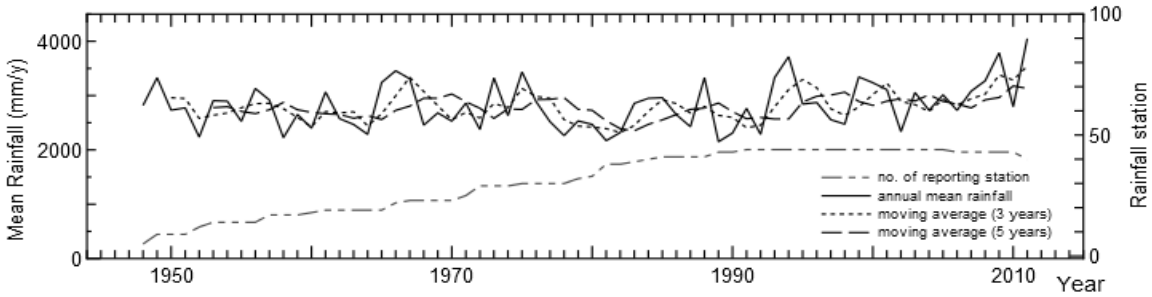

Figure 3.6. Mean annual rainfall for 1948-2011.

The results of trend analysis using MK-1 are shown in Table 3.4. They indicated that the trend was mostly decreasing between 1948 and 1983, but mostly increasing from 1980 to 2011. To identify shorter-term trends within these period, we applied the MK-2 and MK-3 trend tests, with the results shown in Figure 3.7. We tested the methods using four simple patterns: monoclines (pattern 1), sine curves with two cycle types (pattern 2), sine curves with two increasing cycle types (pattern 3), and sine curves with a decreasing baseline (pattern 4). From the results, the basic behaviors of MK-2 and MK-3 can be summarized as follows:

1) The method MK-2 reflects both long-term history trend and temporal change. It becomes nearly constant as the sampling period becomes longer, but at the point of change in trend, the corresponding change appears, although not as sensitive as MK-3.
2) The MK-3 value with short sampling period shows rapid change between negative and positive at the turning point of given patterns. If the real cycle is longer than the sampling period, the MK-3 values become relatively flat, but at every turning point of

given data, a corresponding change is observed. This method appears to be incapable of detecting the constant change in baseline trend, as shown in Figure 3.7(c) and 3.7(d).

3) The MK-3 values will be 0 if the numbers of combinations judged as -1 and 1 are almost the same. The total number of combinationd for is 45 for 10 years from Equation 3.12. If the peak value of MK-3 is around 0.5 as shown in Figure 3.8, the number of combinations judged as 1 is around 2/3, and -1 around 1/3 of all combinations.

Table 3.4. Result of Mann-Kendall tests (MK) using 30-year sampling

No.	Rainfall Station	Normalized MK-S	
		1957–1987	1981–2011
8	B. P. Bertam	−0.058	−0.025
14	Kuala Balah	−0.041	0.252
15	Lepan Kabu	0.178	0.114
16	Lubok Bungor	0.178	0.112
19	SMT K. Krai	0.113	0.110
21	Ldg. Kerilla	−0.084	0.153
29	Bk. Panau.	−0.148	0.316
31	Bkt. Abal	−0.170	0.299
32	Cherang Tuli	−0.071	0.019
33	Sg Petai	−0.080	0.213
34	Cherang Ruku	−0.075	0.351
36	I. B. Tok Uban	−0.006	0.006
41	R. P. Repek	−0.183	0.209
43	R.P. Salor	−0.062	−0.028

Figure 3.8 shows historical rainfall data for six rainfall stations located in the upper to midstream (upper), with data presented as MK-2 values (second), MK-3 values (third) and ENSO strength (bottom). Figure 3.9 shows historical rainfall data for eight downstream stations (upper), with data presented as MK-2 values (second), MK-3 values (third) and ENSO strength (bottom).

In Figure 3.8, a very clear trends of historical rainfall change is shown. The turning points recognized by MK-3 at around 1982, 1988, the mid 1990s', around 2000, 2002–2004, and around 2009 (Figure 3.8) most likely related to the global oceanic environmental changes known as El Niño and La Niña. Hsu et al., (2013) summarized the occurrences of El Niño and La Niña during the period of 1950–2012 (Table 3.5). Our results suggest that the strong El Niño event in ~1982 resulted in low rainfall. However, within 5 years, a strong La Niña event

resulted in increased rainfall. After 15 years, another strong El Niño event occurred and resulted in low rainfall. However, by comparing the up/midstream and downstream areas, we identified difference in ~2000, where up/midstream were only lighted influenced by the La Niña event, while strong effects were felt in downstream areas near the South China Sea.

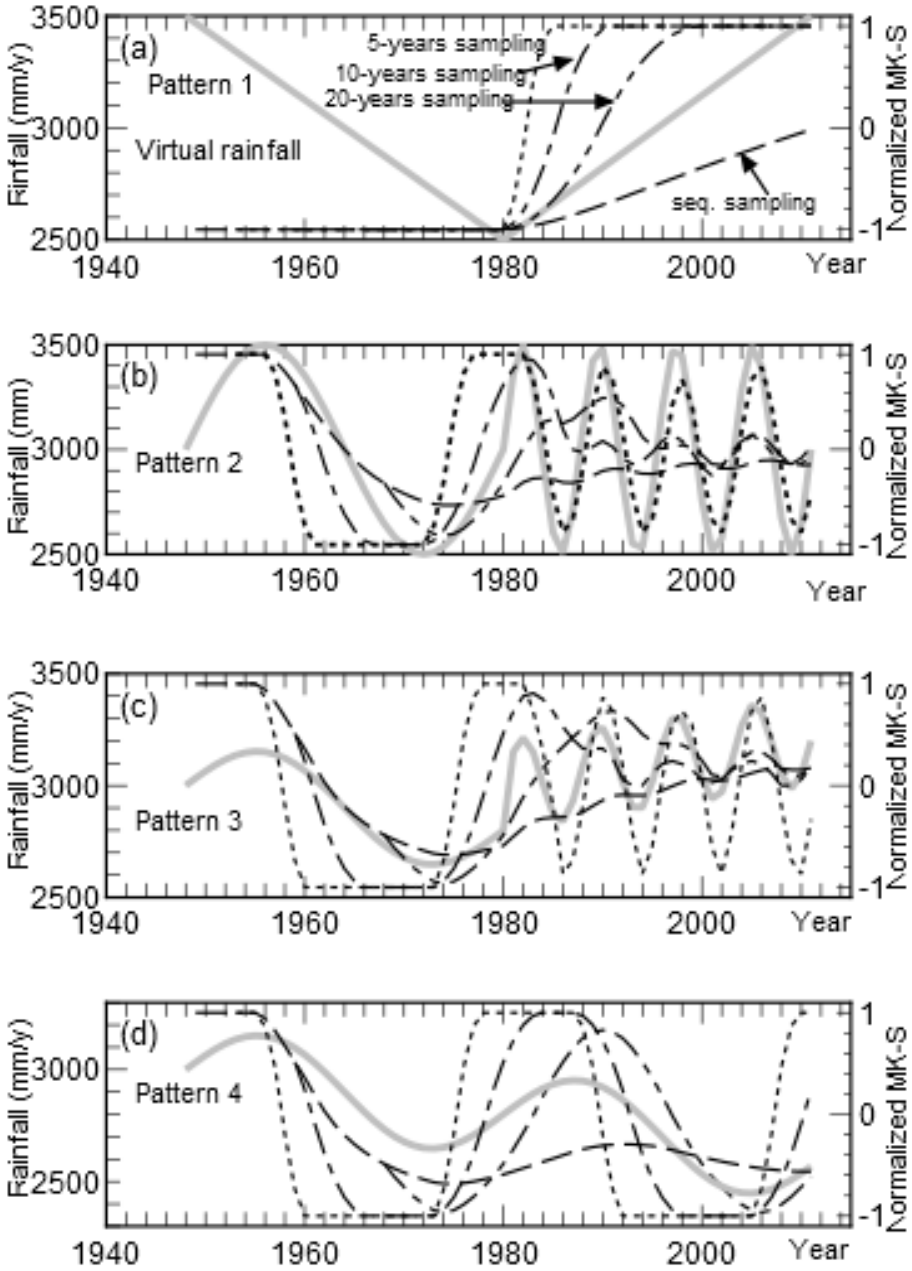

Figure 3.7. Performance of MK-S value for different rainfall patterns

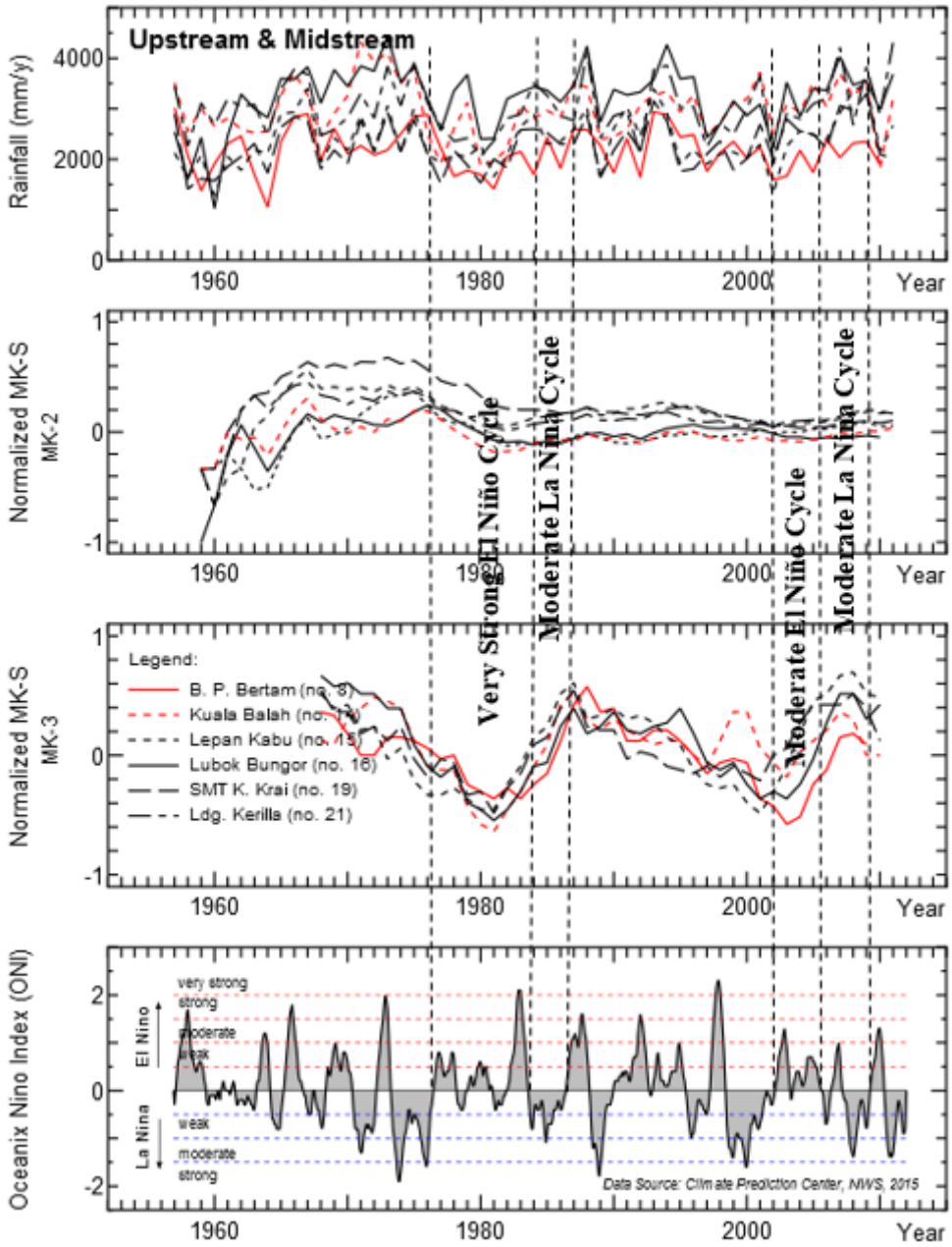

Figure 3.8. Upstream and midstream trends of Kelantan watershed (Ref. of ENSO: National Weather Service, 2015).

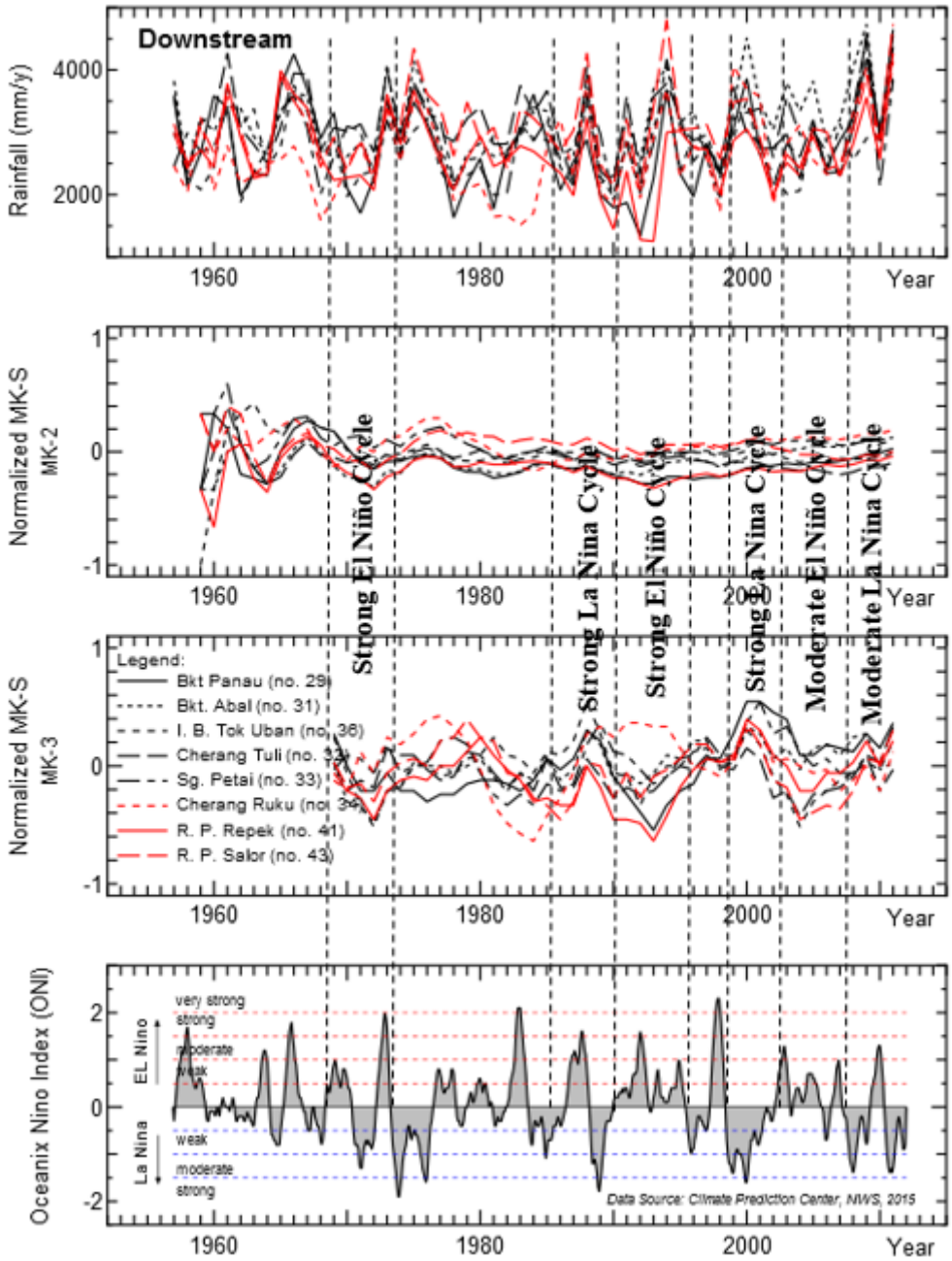

Figure 3.9. Downstream trends of Kelantan watershed (Ref. of ENSO: National Weather Service, 2015).

Table 3.5. El Niño and La Niña events from 1950 to 2012[a]

Event	Year
El Niño	1951–52 (weak)
	1957–58 (strong)
	1963–64 (strong)
	1965–66 (moderate)
	1968-70 (weak)
	1972–73 (strong)
	1982–1983 (very strong)
	1987–88 (strong)
	1997–98 (very strong)
	2002–03 (moderate)
	2009–10 (moderate)
La Niña	1950–51 (weak)
	1954–57 (weak)
	1964–65 (weak)
	1967–68 (weak)
	1970–72 (moderate)
	1973–76 (moderate)
	1984–85(weak)
	1988–89 (strong)
	1995–96(weak)
	1998–01(moderate)
	2007–08 (moderate)
	2010–11(moderate)

[a] Hsu et al., 2013; Climate Prediction Center, National Weather Service, 2015

3.5 *Conclusion*

The aim of this study was to check the reliability of time-series rainfall data by homogeneity tests, and investigate rainfall trends within the period of 1948 to 2011. Conclusion can be drawn as follows:

(1) Long historical data of 50 rainfall stations were tested to check the data reliability. As a result, 9 rainfall stations were found suspect or doubtful through absolute homogeneity tests. Comparing with the record of surrounding homogenous stations, 4 out of 9 stations were finally recognized as inhomogeneous.

(2) The Mann-Kendall test using the normalized MK-S value was applied to find out long-term and short-term characteristics of rainfall variability. The MK test of 30-years sampling period shows decreasing trend in 1957-1987 and increasing trend in 1981-2011.

(3) Using the MK-2 (sequential elongated sampling) and MK-3 (moving segmented sampling), the fluctuation trend which may exist behind the real rainfall variation was clearly found. In MK-3 with 10-years sampling, the turning points of the MK-3 values corresponded well to the cycle of El Nino and La Nina. The effect of them was different for upstream inland area and downstream area near coast of South China Sea.

Finally, extending the MK-3 plot, we might predict roughly that in Kelantan watershed high rainfall years after 2009 La Nina may slowly decrease up to around 2015 in inland area, remain high around 2015 in downstream area, then decrease and meet low rainfall years at next El Nino after around 2020. Therefore, from this analysis we are able to estimate the future trends of rainfall in this region and hence, understand its rainfall variability which corresponds to ENSO.

4 Observation-based Approach for Early Flood Prediction

4.1 *Introduction*

Flood forecasting system for warning and evacuation evolved slowly in the 1970s and 1980s in this watershed. However recent advance of technologies, such as development of data acquisition systems based on telemetry, radar/satellite observation and computer simulation, has enhanced significantly the potential for providing real-time flood warning. Currently, three approaches are available in flood forecasting, i.e., observation-based statistical models such as ARMA, conceptual models such as storage function, tank model, etc., and numerical simulation models called "physically-based, distributed parameter hydrologic model".

In this chapter, observation-based modelling is treated and a new model is developed for quick prediction of change of water level at observation points by using the statistical relationship without explicitly considering the physical processes.

4.2 *Review of Observation-based Models*

There are many traditional linear stochastic models both stationary and non-stationary, ARMA and ARIMA (Abrahart and See, 2000; Brath et. al., 2002; Galavi et al., 2013) and soft-computing, non-linear, linguistic variable data-driven approach such as Fuzzy Logic (See and Openshaw, 1999; See and Openshaw, 2000; Chang et al., 2005) and Artificial Neural Networks (ANNs) (Dawson et. al, 2002; Pan et. al, 2013).

4.2.1 *ARMA/ARIMA*

Mathematically based forecasting model can be either deterministic, attempting to reproduce actual observed or stochastic, reproducing a set of values having the same statistical properties as historical observed records. A stochastically-based model can predict the most likely future water level conditioned on the current data. The ARMA model, a representative stochastic model, utilizes its own past data to predict future value. ARMA model consists of two parts where the autoregressive (AR) part is composed of its past observed time-series values, and the moving average (MA) part uses the value of a random variable at time t are modelled not only affected by the shock at time t, but also the shocks that have taken place before time t.

Autoregressive Models (AR)

Autoregressive time series models make use of linear combination of past values of the process to be modelled, as a means of predicting future values. Following Box and Jenkins (1970) treatment, let z_{t-i} for $0 \leq i \leq n$ be the sampled values of an assumed stationary Gaussian process at equally spaced temporal intervals. Further let y_{t-i} be the deviations of the process from its mean. The process may then be modelled as an autoregressive process of order p, with the following form

$$\hat{y}_t = \phi_1 y_{t-1} + \phi_2 y_{t-2} \dots + \phi_p y_{t-p} + \varepsilon_t \tag{4.1}$$

where the ϕ_j's are the autoregressive weights and ε_t is a random shock term. The shock term is drawn from normal distribution assumed to have zero mean and a variance which must be estimated from past observations of the process to be modelled. The introduction of the backward shift operator B, for which $By_t = y_{t-1}$ and $B^i y_t = y_{t-1}$, allows the AR model to be written in a more condensed form as

$$\phi(B) y_t = \varepsilon_t \tag{4.2}$$

where the AR operator is

$$\phi(B) = 1 - \phi_1 B - \phi_2 B^2 - \cdots - \phi_p B^p \tag{4.3}$$

Moving Average Models (MA)

A moving average model defines the current value of a process as a linear combination of white noise shocks ε_t. Thus a moving average model of order q is

$$\hat{y}_t = a_t - \theta_1 \varepsilon_{t-1} - \theta_2 \varepsilon_{t-2} - \cdots - \theta_q \varepsilon_{t-q} \tag{4.4}$$

where the moving average weights θ_1 are not constrained to positive nor sum to unity. As was the case for the autoregressive model. As the same with autoregressive model, we can define a moving average operator

$$\theta(B) = 1 - \theta_1 B - \theta_2 B^2 - \cdots - \theta_q B^q \tag{4.5}$$

Or can be written as

$$\hat{y}_t = \theta(B)\varepsilon_t \tag{4.6}$$

<u>Autoregressive-Moving Average (ARMA)</u>

The general equation of ARMA(p, q) model can be written as

$$\hat{y}_t = -\phi_1 y_{t-1} + \phi_2 y_{t-2} \dots + \phi_p y_{t-p} + \varepsilon_t - -\theta_1 \varepsilon_{t-1} - \theta_2 \varepsilon_{t-2} - \cdots - \theta_q \varepsilon_{t-q} \tag{4.7}$$

Or can be written as

$$\phi(B)\hat{y}_t = \theta(B)\varepsilon_t \tag{4.8}$$

ARIMA model is extended of ARMA model as it includes the extra part of differencing by taking each data point and calculates the change from the previous data point.

4.2.2 *Artificial Neural Network (ANNs) & Fuzzy Logic*

ANNs is based on behaviour of the brain and nervous systems in a simplified computational form. They are constituted by highly interconnected simple elements, called artificial neurons which receive information, elaborate them through mathematical functions and pass them to other artificial neurons. The artificial neurons are organized in layers: an input layer, hidden layer and output layer as shown in Figure 4.1.

Fuzzy logic (Zadeh, 1973) is a logical mathematical procedure based on an “IF-THEN” rule system that allows for reproduction of the human way of thinking in a computational form. Fuzzy logic has the same structure as ANNs three layer network.

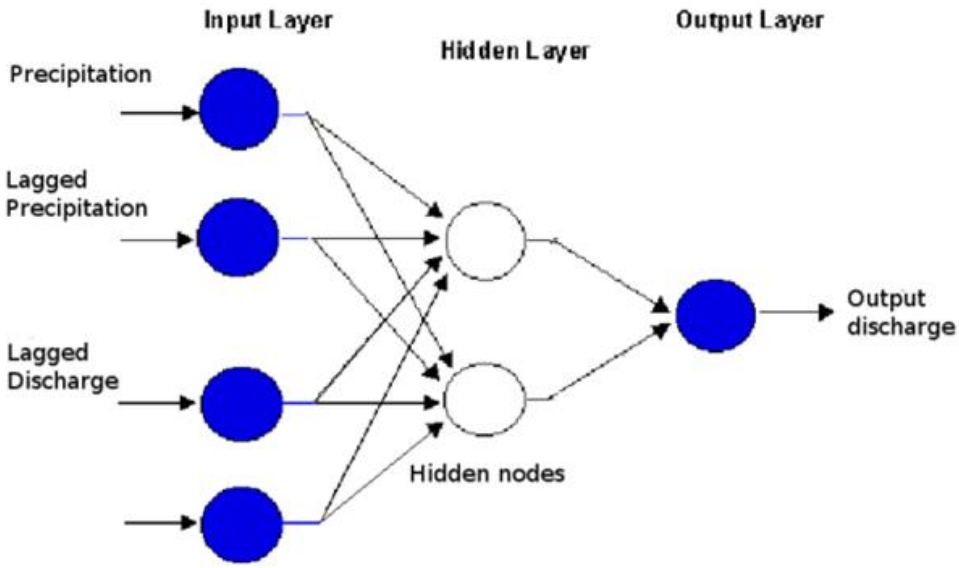

Figure 4.1. Schematic diagram of ANNs (Abrahart and See, 2000)

The two main disadvantages of this soft computing method are the computational time and the danger of over fitting (Kumari et. al., 2013). Unlike regression analysis where the coefficients can be efficiently calculated by matrix algebra regardless of the number of data points or variables, both ANNs and fuzzy logic require somewhat trial and error approach. Unlike hard computing schemes which strive for exactness and full truth, soft computing techniques exploit the given tolerance of imprecision, partial truth, and uncertainty for a particular problem (Malik, 2015).

4.3 *Development of an Upstream-Observation-based Model.*

4.3.1 *Objective*

The target of this chapter is to develop a new concept of observation-based model for early flood prediction at two forecasting points in Kelantan watershed; Guillemard Bridge and Kuala Krai. Guillemard Bridge station is located about 60 km from the river mouth, just before reaching the capital city of Kelantan state, Kota Bharu, and Kuala Krai station is located 33 km away upstream of Guillemard Bridge station as shown in Figure 4.2. The model is based on linear combination of the upstream information that flows in the river network and reaching to the forecasting point. This study aims to provide flood prediction as early as possible, therefore this model will only use upstream information without using its own past information like ARMA.

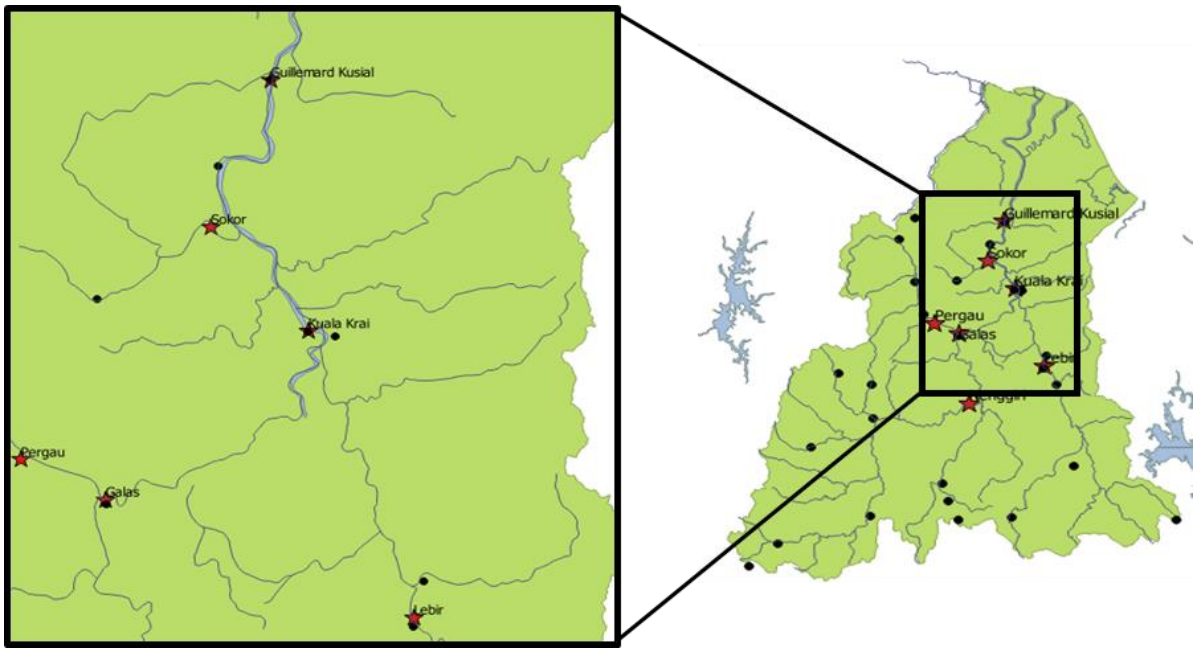

Figure 4.2. Location of water level and rainfall stations used in observation based approach

4.3.2 *Basic Assumptions*

Following assumptions are made in developing the model.

1) Upstream telemetry water level observation records are used for predicting water level at the downstream prediction point.
2) Observation records at the forecasting point are not used in this model as used in ARMA model, because such information runs away from the prediction point and becomes no relation with the future water level. The future water level at prediction point depends upon the upstream past records which are flowing on the way to forecasting point.
3) Upstream area experiences heavy rainfall earlier than downstream area, because in reversed case, normal relationship between upstream and downstream becomes ineffective. Such case is discussed in the later section.
4) Combination of multiple upstream observation records are used for predicting water level at a downstream prediction point.
5) The prediction model is described as linear combination of upstream past data, considering different delay times for respective combinations of upstream and prediction points.
6) Average delay time from upstream to prediction point is statistically calculated by using historical observation data.

The procedures in this new observation-based model consist of

- finding the average delay time, $\bar{\tau}$ and suitable lag range by using graphical and cross-correlation analysis
- finding coefficients of the linear model with least square method
- and making early prediction for several hours at the selected downstream points.

4.3.3 *The Mathematical Model*

A linear time series model based on least square method is developed for early flood prediction for Kelantan watershed by utilizing the information that flows in the river before reaching the forecasting point. This model consists of various upstream telemetry observation of Kelantan watershed in hourly scale. Figure 4.3 illustrates the schematic diagram of Kelantan river network where the information which passes at A and B at (t-j) is flowing towards station D. This represents the information sequence will reach D sometime in the future. Unlike ARMA method where the future value lies within the past self-value, in this method, the value at D is formed by the past time sequence of A and B. Table 4.1 and Figure 4.4 illustrate the distance and information of water level station used in this study.

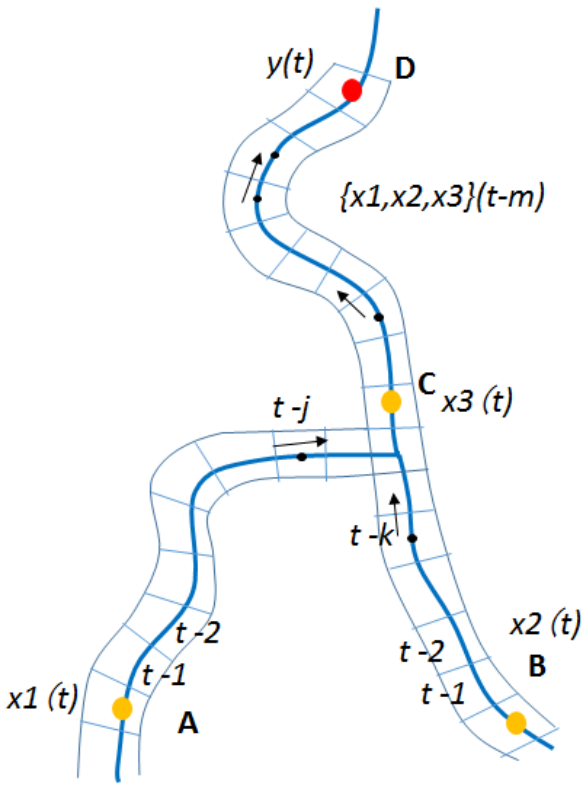

Figure 4.3. Schematic diagram of Kelantan River network in which the information passed at station A, B, C flows towards station D

The general term of the equation is

$$\hat{y}(t) = A_{1,0}x_1\left(t - \bar{\tau}_{1,0} - 0\right) + A_{1,1}x_1\left(t - \bar{\tau}_{1,0} - 1\right) + \cdots + A_{1,n}x_1\left(t - \bar{\tau}_{1,0} - n\right) + \cdots + A_{m,n}x_m\left(t - \bar{\tau}_{m,0} - n\right) \tag{4.9}$$

Or it can be written as

$$\hat{y}(t) = \sum_{i=1}^{m}\sum_{j=0}^{n} A_{i,j}x_i\,(t - \bar{\tau}_{i,0} - j) \tag{4.10}$$

where $\hat{y}$ is the predicted value at time *t*. $A_{i,j}$ is the coefficient and x_i is the upstream predictor variables that determines the downstream predicted values, $\bar{\tau}_{i,0}$ is the average delay time, m is the number of upstream stations used for prediction and n is the range delay.

The standard form of least square can be written as

$$J = \sum_{t=t0}^{tmax} [\hat{y}(t) - y(t)]^2 \tag{4.11}$$

Where at the minimum J, the following condition satisfied.

$$\frac{\partial J}{\partial A_{k,l}} = 2\sum_{t=t0}^{tmax}\left[\frac{\partial \hat{y}(t)}{\partial A_{k,l}}\right][\hat{y}(t) - y(t)] = 0 \tag{4.12}$$

$$\frac{\partial \hat{y}}{\partial A_{k,l}} = \left[x_k(t - \bar{\tau}_{k,0} - l)\right] \tag{4.13}$$

Equation 4.5 can be rearranged in the form of matrix of $C.A = D$ where

$$C = \begin{bmatrix} C_{11,11} & C_{11,12} & \cdots & C_{11,1n} & C_{11,21} & \cdots & C_{11,mn} \\ C_{12,11} & C_{12,12} & \cdots & C_{12,1n} & C_{12,21} & \cdots & C_{12,mn} \\ \vdots & \vdots & \vdots & \vdots & \vdots & \vdots & \vdots \\ C_{1n,11} & C_{1n,12} & \cdots & C_{1n,1n} & C_{1n,21} & \cdots & C_{1n,mn} \\ C_{21,11} & C_{21,12} & \cdots & C_{21,1n} & C_{21,21} & \cdots & C_{21,mn} \\ \vdots & \vdots & \vdots & \vdots & \vdots & \vdots & \vdots \\ C_{mn,11} & C_{mn,12} & \cdots & C_{mn,1n} & C_{mn,21} & \cdots & C_{mn,mn} \end{bmatrix}, A = \begin{bmatrix} A_{1,1} \\ A_{1,2} \\ \vdots \\ A_{1,n} \\ A_{2,1} \\ \vdots \\ A_{m,n} \end{bmatrix}, D = \begin{bmatrix} D_{1,1} \\ D_{1,2} \\ \vdots \\ D_{1,n} \\ D_{2,1} \\ \vdots \\ D_{m,n} \end{bmatrix}$$

where the value of C and D can be calculated from

$$C_{kl,ij} = \sum_{t=t0}^{tmax} x_k\left(t - \bar{\tau}_{k,0} - l\right) * x_i(t - \bar{\tau}_{i,0} - j) \tag{4.14}$$

$$D_{kl} = \sum_{t=t0}^{tmax} x_k(t - \bar{\tau}_{k,0} - l) * y(t) \tag{4.15}$$

By using the Gauss Elimination method, the values of A can be found.

Table 4.1. Distance between each water level station used.

Station	A: Galas	B: Lebir	C: Kuala Krai	D: Guillemard
A: Galas	-	-	38.4 km	71.4 km
B: Lebir	-	-	37.8 km	70.8 km
C: Kuala Krai	38.4 km	37.8 km	-	33.0 km
D: Guillemard	71.4 km	70.8 km	33.0 km	-

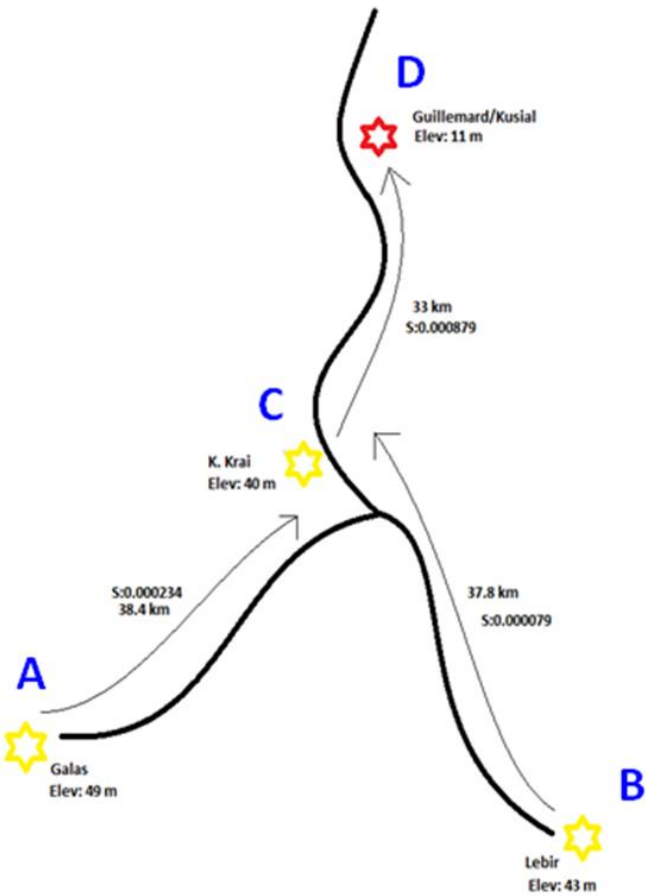

Figure 4.4. Schematic diagram of water level stations used in this method.

4.4 *Analysis of Average Delay Time*

4.4.1 *Conventional Graphical Approach*

Hourly data of water level were selected from 1st November to 31st January every year from 2004 to 2013 which was regular monsoon flood season in Kelantan**.** To find the delay time between two points, graphical based method was conducted by comparing the starting time of the rising limb and peak time of water level hydrograph. Table 4.2 summarized the result of graphical analysis. From the result, the delay time for each year varied. Even there were some events that gave negative values. Hence, no clear delay time could be identified.

Table 4.2. Delay time, τ by comparing peak and starting time of the hydrograph

Year	Event	A-C		A-D		B-C		B-D		C-D	
		Start	Peak	Start	Peak	Start	Peak	Start	Peak	Start	Peak
2004	1	6 hrs	7hrs	9 hrs	11 hrs	2 hrs	9 hrs	5 hrs	13 hrs	3 hrs	4 hrs
2005	1	1 hrs	1 hrs	9 hrs	6 hrs	13 hrs	4 hrs	21 hrs	9 hrs	8 hrs	5 hrs
	2	3 hrs	0 hrs	6 hrs	-4 hrs	64 hrs	1 hrs	70 hrs	- 3hrs	3 hrs	-4 hrs
	3	4 hrs	4 hrs	1 hrs	10 hrs	- 4hrs	- 3 days	- 31 hrs	- 3 days	- 3 hrs	6 hrs
2006	1	0 hrs	3 hrs	15 hrs	2 hrs	6 hrs	4 hrs	21 hrs	27 hrs	21 hrs	23 hrs
	2	-2 hrs	-7 hrs	17 hrs	12 hrs	1 hrs	11 hrs	20 hrs	31 hrs	19 hrs	20 hrs
2007	1	-	-	-	-	-8 hrs	6 hrs	-6 hrs	17 hrs	26 hrs	11 hrs
2008	1	5 hrs	-5hrs	22 hrs	12 hrs	4 hrs	7 hrs	21 hrs	26 hrs	17 hrs	20 hrs
	2	-7 hrs	3 hrs	- 8 hrs	17 hrs	19 hrs	8 hrs	20 hrs	24 hrs	25 hrs	16 hrs
	3	2 hrs	5 hrs	19 hrs	23 hrs	- 16 hrs	0 hrs	1 hrs	- 17 hrs	17 hrs	17 hrs
2009	1	5 hrs	-1hrs	26 hrs	17 hrs	-	-	-	-	21 hrs	18 hrs
	2	-48 hrs	-9 hrs	-29 hrs	9 hrs	-	-	-	-	31 hrs	17 hrs
	3	2 hrs	12 hrs	7 hrs	32 hrs	-	-	-	-	5 hrs	20 hrs
2010	1	2 hrs	16 hrs	4 hrs	17 hrs	4 hrs	0 hrs	6 hrs	1 hrs	2 hrs	1 hrs
	2	2 hrs	2 hrs	3 hrs	2 hrs	- 2 hrs	1 hrs	- 1 hrs	2 hrs	1 hrs	1 hrs
2011	1	-2 hrs	0 hrs	- 1 hrs	17 hrs	3 hrs	0 hrs	4 hrs	17 hrs	1 hrs	17 hrs
	2	-3 hrs	5 hrs	-3 hrs	9 hrs	3 hrs	13 hrs	3 hrs	15 hrs	0 hrs	5 hrs
	3	3 hrs	6 hrs	3 hrs	17 hrs	20 hrs	4 hrs	20 hrs	15 hrs	0 hrs	12 hrs
2012	1	-	-	-	-	2 hrs	0 hrs	4 hrs	0 hrs	0 hrs	0 hrs
	2	-	-	-	-	1 hrs	21 hrs	1 hrs	21 hrs	0 hrs	0 hrs
2013	1	20 hrs	23 hrs	33 hrs	24 hrs	20 hrs	-1 hrs	33 hrs	0 hrs	13 hrs	1 hrs
	2	2 hrs	0 hrs	0 hrs	2 hrs	0 hrs	0 hrs	- 2hrs	2 hrs	- 2hrs	2 hrs
	3	20 hrs	5 hrs	21 hrs	10 hrs	0 hrs	7 hrs	1 hrs	12 hrs	1 hrs	5 hrs

Via graphical analysis, it was difficult to find the proper delay time between the stations since there were influence of tributaries joining the mainstream in between and this tributaries maybe influenced by heavy rainfall. As shown in Figure 4.2, Kelantan has many additional tributaries before reaching to Guillemard Bridge station.

4.4.2 *Cross-correlation by mean value*

Cross-correlation analysis is a standard method of estimating the degree to which two series are correlated. Three cross correlation analyses were carried out to predict the delay time and delay range. The first cross correlation formula can be written as:

$$\gamma_1(\tau) = \frac{\sum(W_x(t) - mW_x) \times (W_y(t+\tau) - mW_y)}{\sqrt{\sum(W_x(t) - mW_x)^2} \times \sqrt{\sum(W_y(t+\tau) - mW_y)^2}} \tag{4.16}$$

where W_x and W_y are the water level at upstream and downstream, mW_x and mW_y are the mean of corresponding time series. The highest value γ_1 nearest to 1 indicates the strongest correlation at delay time τ.

4.4.3 *Cross-correlation by derivative*

The second cross correlation formula is a product of water level difference at station *x* at time *t* and station *y* at time $t + \tau$ and can be written as:

$$\gamma_2(\tau) = \frac{1}{n}\sum_{t=1}^{n}[dW_x(t) \times dW_y(t+\tau)] \tag{4.17}$$

where *n* is the number of sampling data and the difference of water level at station *x* and *y* are expressed as:

$$dW_x(t) = W_x(t+1) - W_x(t) \tag{4.18}$$

$$dW_y(t+\tau) = W_y(t+\tau+1) - W_y(t+\tau) \tag{4.19}$$

For the second cross-correlation formula, the highest value of γ_2 indicates the strongest correlation at delay time τ.

4.4.4 *Cross-correlation by double derivative*

The third cross correlation formula is the product of difference of the difference between each station *x* and *y* at time *t* and $t+\tau$ and can be written as:

$$\gamma_3(\tau) = \frac{1}{n}\sum_{t=1}^{n}[[dW_x(t) - dW_x(t+\tau)] \times [dW_y(t) - dW_y(t+\tau)]] \tag{4.20}$$

where $dW_x(t)$ and $dW_y(t)$ were calculated using Equations 4.10 and 4.11, respectively. The lowest value of γ_3 indicates the strongest correlation between the two water level stations at delay time τ. In this analysis, hourly data from 1st November to 31st January of year 2008, 2011 and 2013 were selected based on data availability at all stations i.e., Galas (A), Lebir (B), Kuala Krai (C) and Guillemard Bridge (D). Figures 4.5 to 4.7 show the observed water level at station A, B, C and D during monsoon season (1st November to 31st January) for year 2008, 2011 and 2013. It shows that all water level stations experienced the same major rainfall events. Cross-correlation between station A to C, station B to C, station A to D, station B to D and station C to D were determined using three cross correlation methods. Figures 4.8 to 4.12 show the results of the three cross correlation methods and Table 4.3 summarizes the delay time based on the three cross-correlation formula.

4.4.5 *Delay analysis from Galas (A) and Lebir (B) to Kuala Krai (C)*

The distance between station A to C and station B to C are almost the same as shown in Table 4.1. For year 2008 and 2011, the delay time is between 4 to 5 hours based on γ_1 and 4 hours calculated using γ_2 and γ_3 as illustrated in Figures 4.8 and 4.9. However in 2013, the result varied differently for γ_1 where the delay time from station A to C was 7 hours and station B to C was 4 hours, and for γ_2 and γ_3, 2 hours for both station A to C and station B to C. These results rely on the data and natural phenomenon of Kelantan watershed where in 2008 and 2011, station C has the same timing of the hydrograph rising limb with station A and B as shown in Figure 4.13 or sometime, much earlier. This situation might have happened when downstream area experienced the monsoon rainfall first before the north east winds brought the heavy rainfall to the upstream area, then resulted in longer delay time. Figure 4.14 illustrates this phenomenon, showing the movement of Kelantan watershed rainfall distribution from 22nd to 25th December 2011. Figure 4.15 shows estimated rainfall distribution derived from Inverse Distance Method discussed in Chapter 5, from 30th November to 3rd December 2013. It explains how the upstream of the watershed experienced the monsoon rainfall before downstream area.

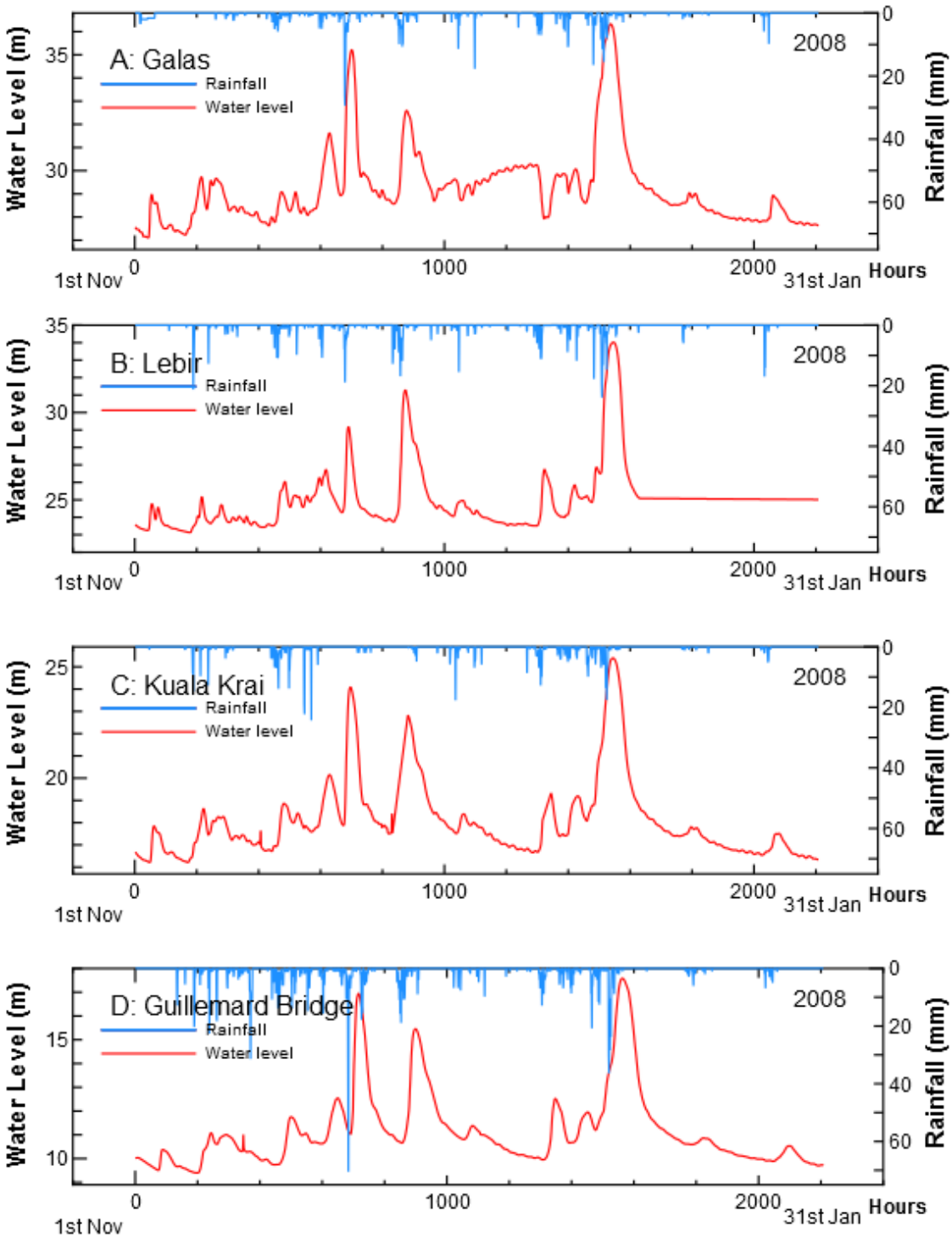

Figure 4.5. Observed water level and rainfall for station A, B C and D during the north east monsoon season in 2008.

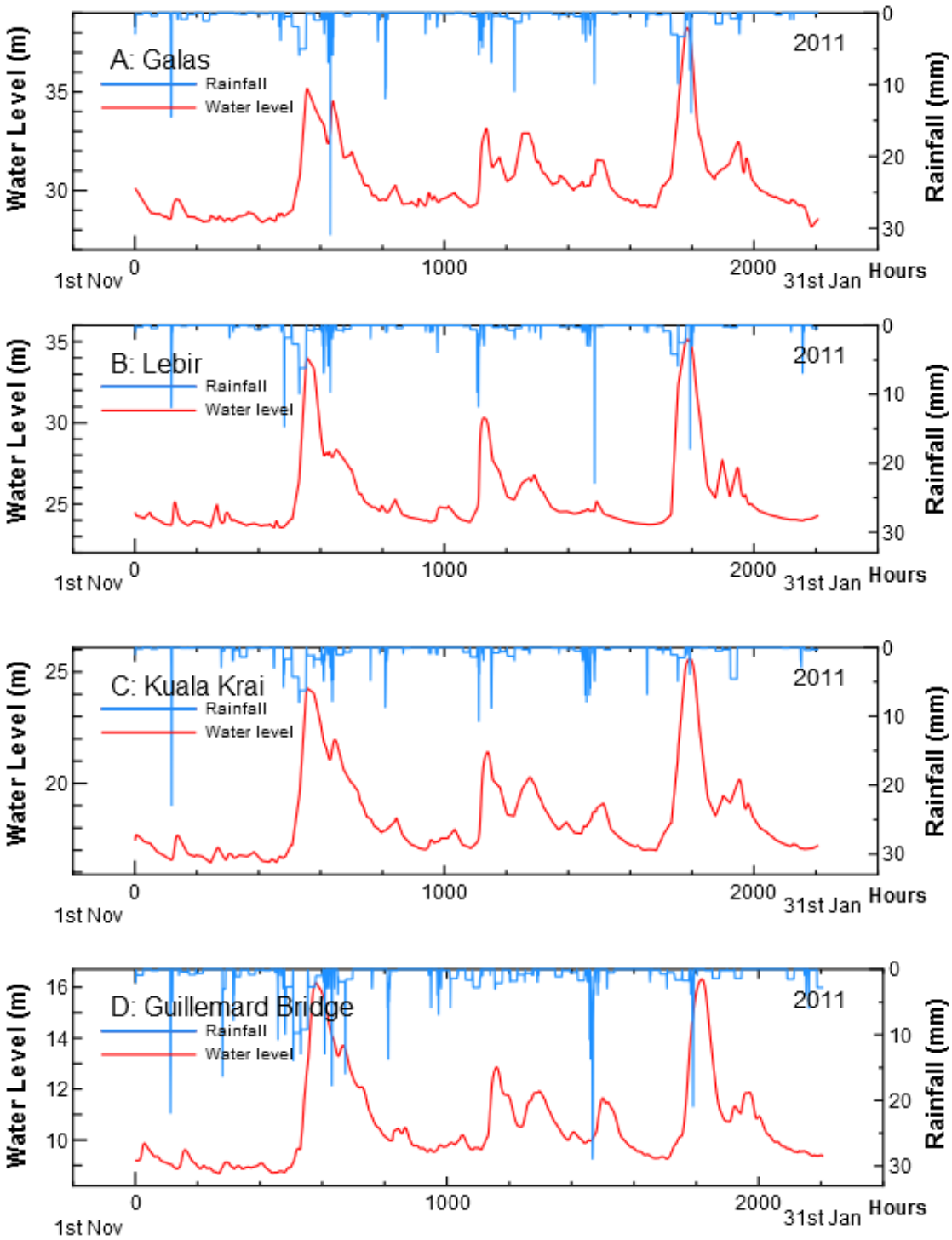

Figure 4.6. Observed water level and rainfall for station A, B, C and D during the north east monsoon season in 2011.

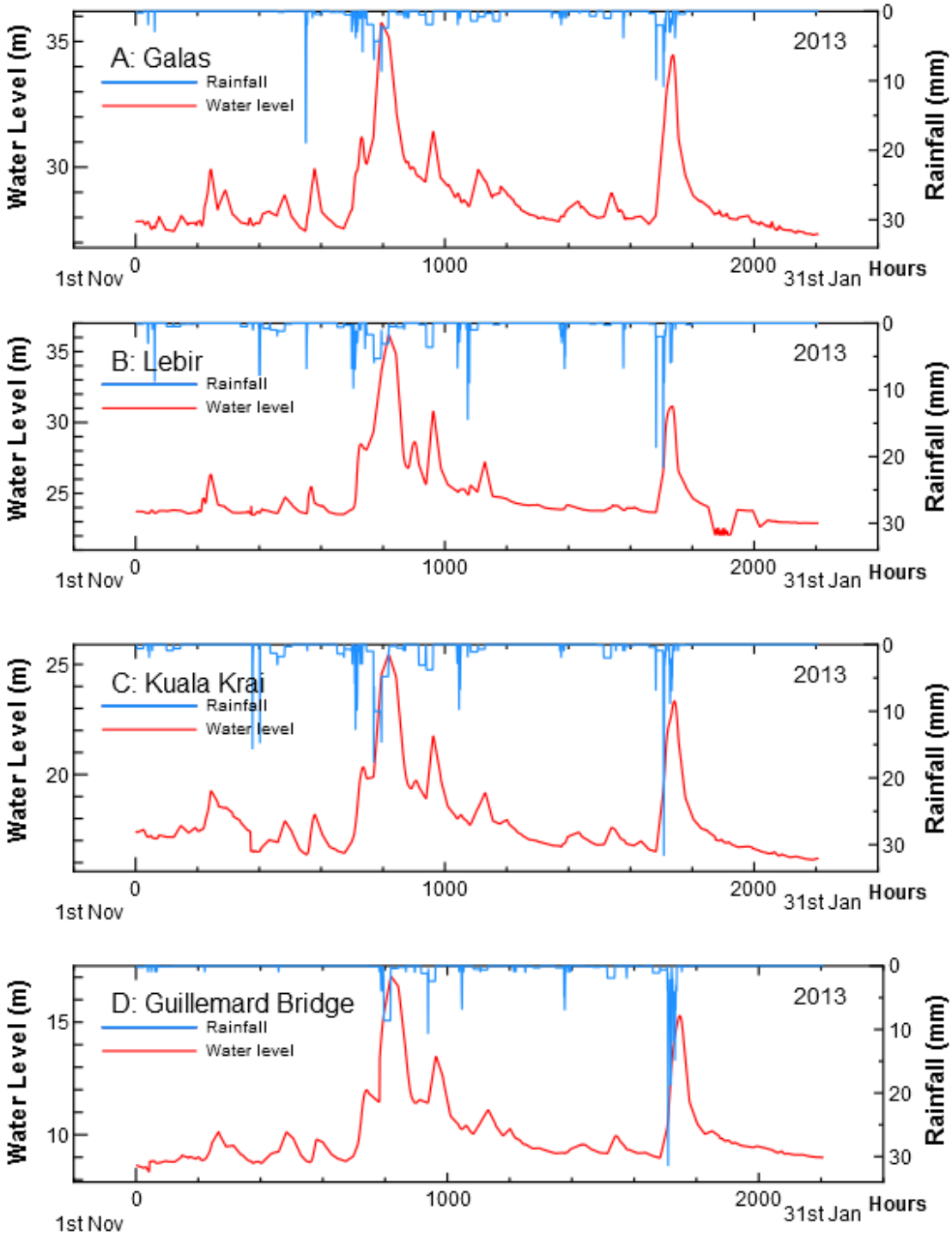

Figure 4.7. Observed water level and rainfall for station A, B and C during the north east monsoon season in 2013.

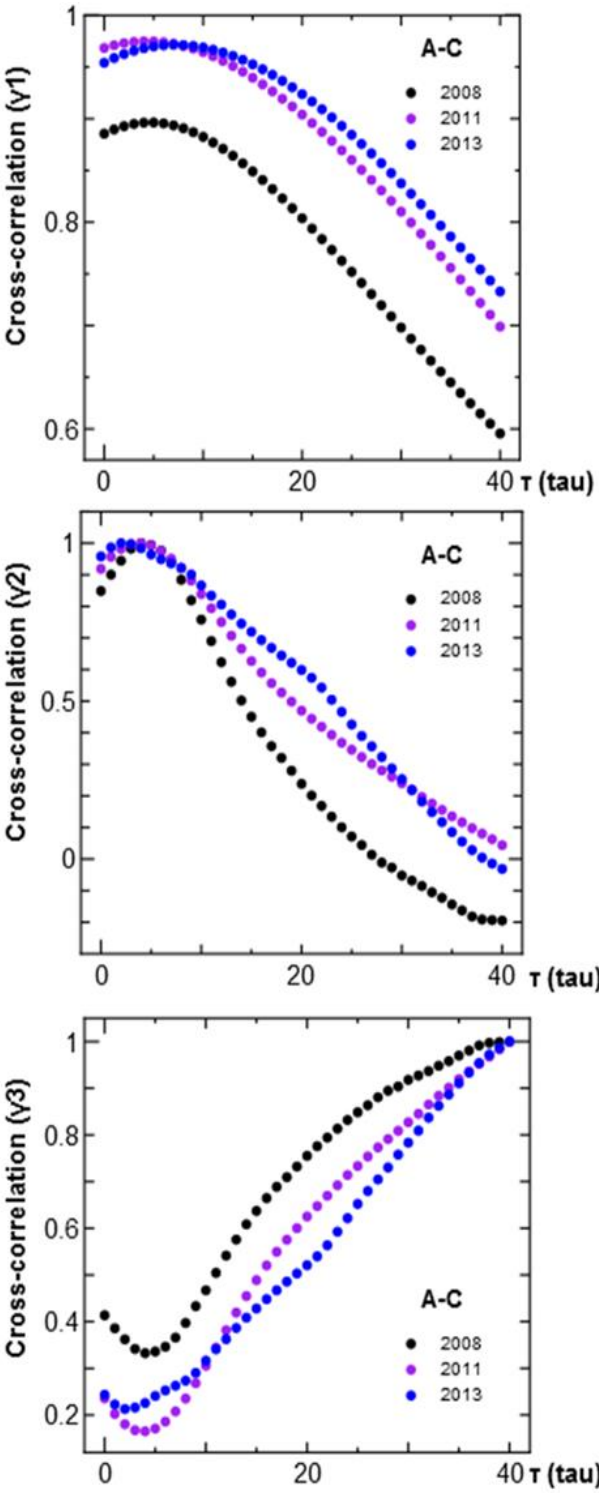

Figure 4.8. Cross correlation of three methods between A and C.

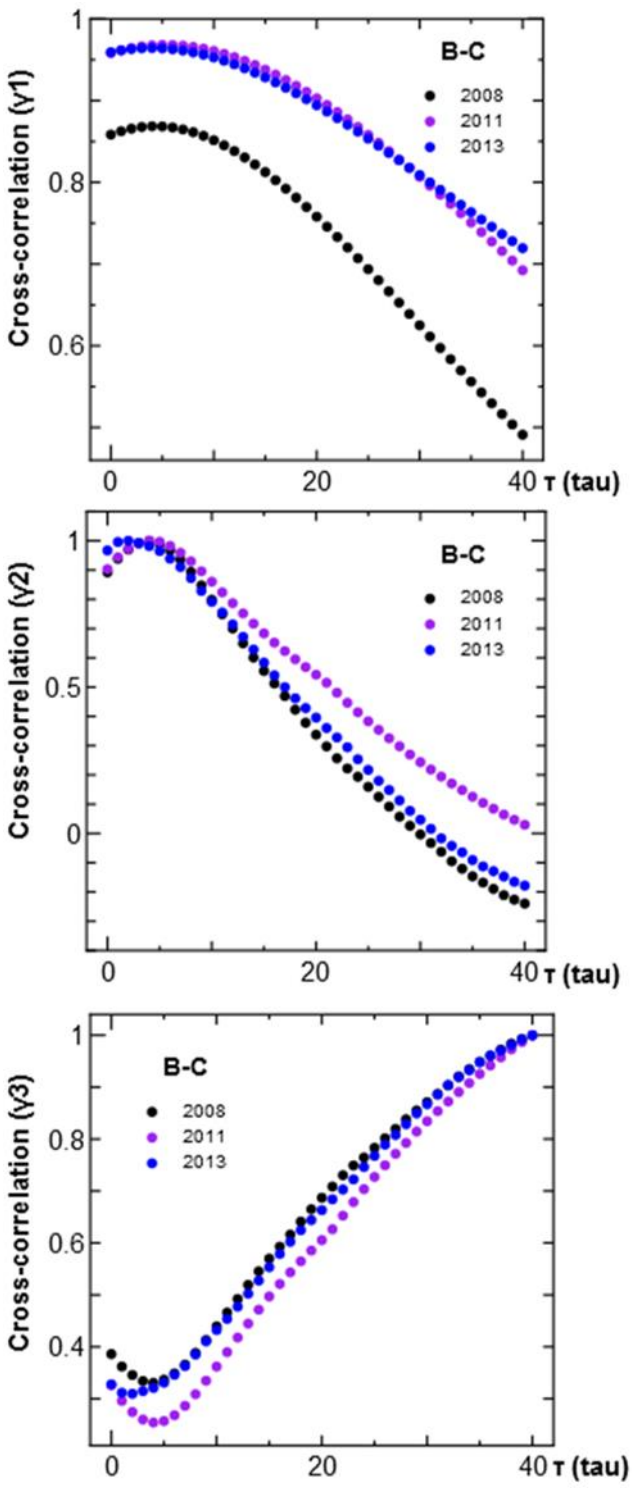

Figure 4.9. Cross correlation of three methods between B and C

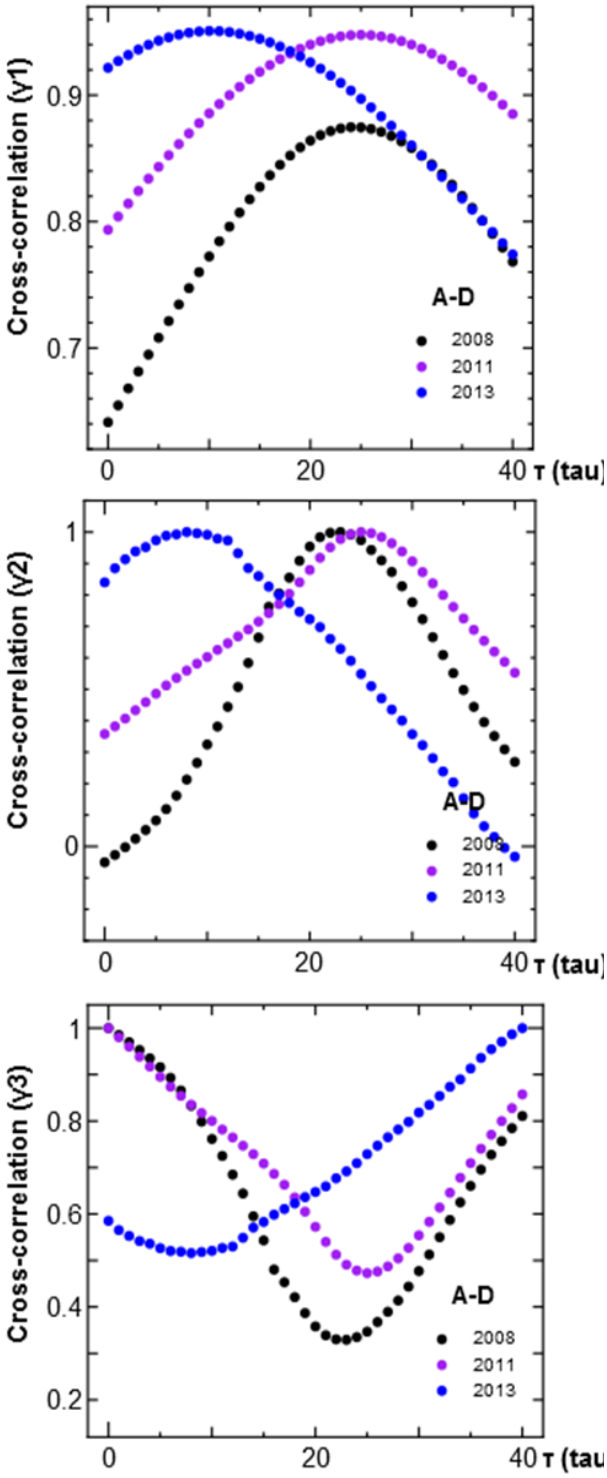

Figure 4.10. Cross correlation of three methods between A and D.

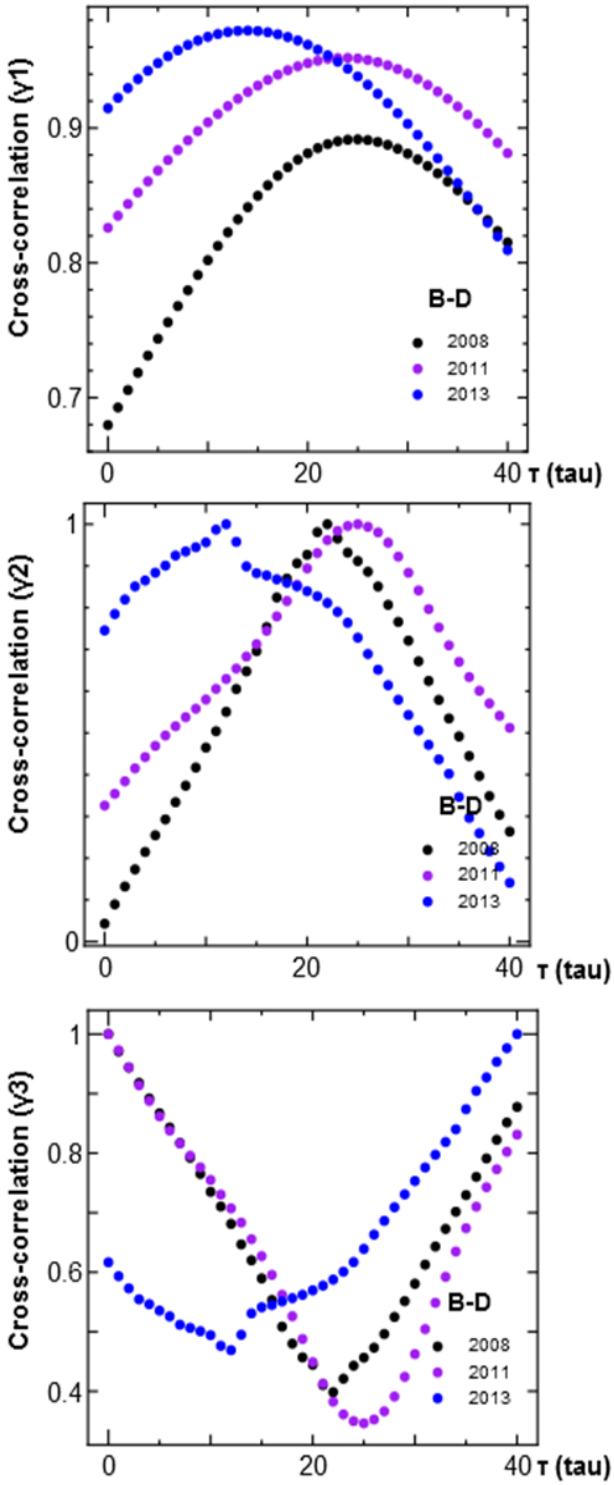

Figure 4.11. Cross correlation of three methods between B and D.

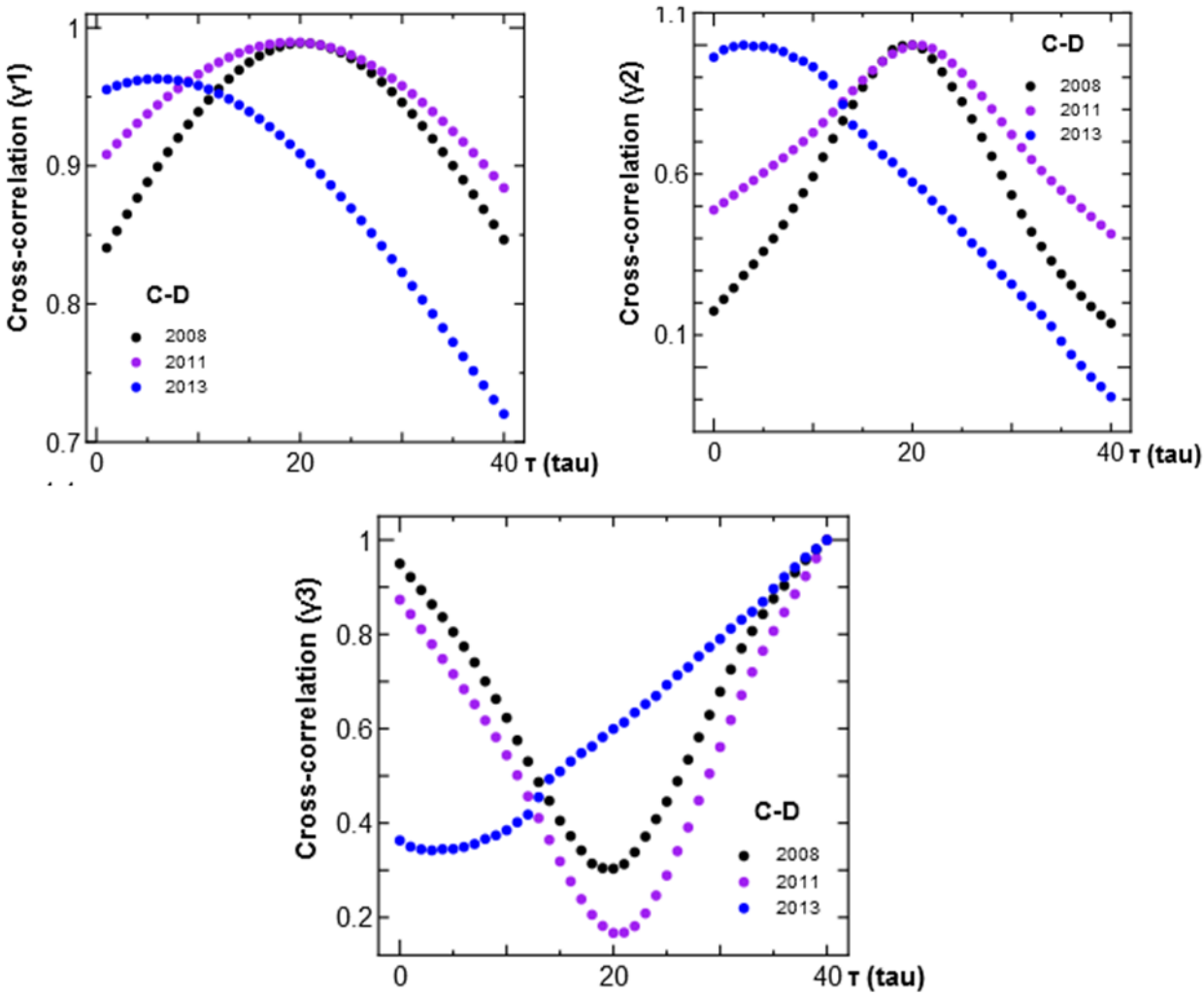

Figure 4.12. Cross correlation of three methods between C and D

Table 4.3. Delay time using three cross-correlation method

Year	Station Pair (Upstream – Downstream)														
	A-C			B-C			A-D			B-D			C-D		
	Delay time (τ) in hours														
	γ_1	γ_2	γ_3	γ_1	γ_2	γ_3	γ_1	γ_2	γ_3	γ_1	γ_2	γ_3	γ_1	γ_2	γ_3
2008	5	4	4	4	4	4	25	23	23	24	22	22	20	20	20
2011	4	4	4	5	4	4	24	25	25	25	25	25	19	20	20
2013	7	2	2	4	2	2	14	12	12	10	8	8	6	3	3

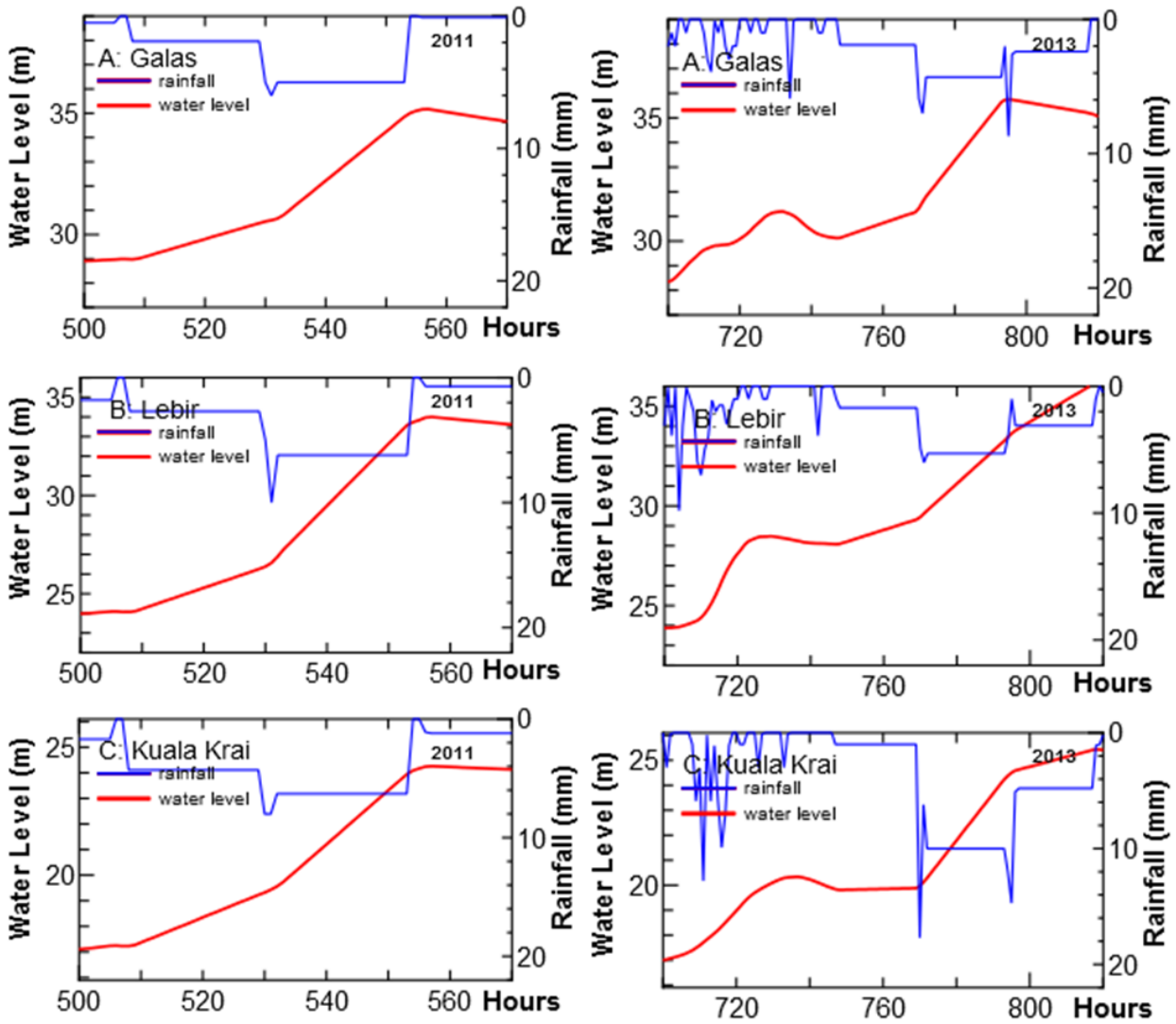

Figure 4.13. Starting time of hydrograph rising limb for station A, B and C in 2011 and 2013.

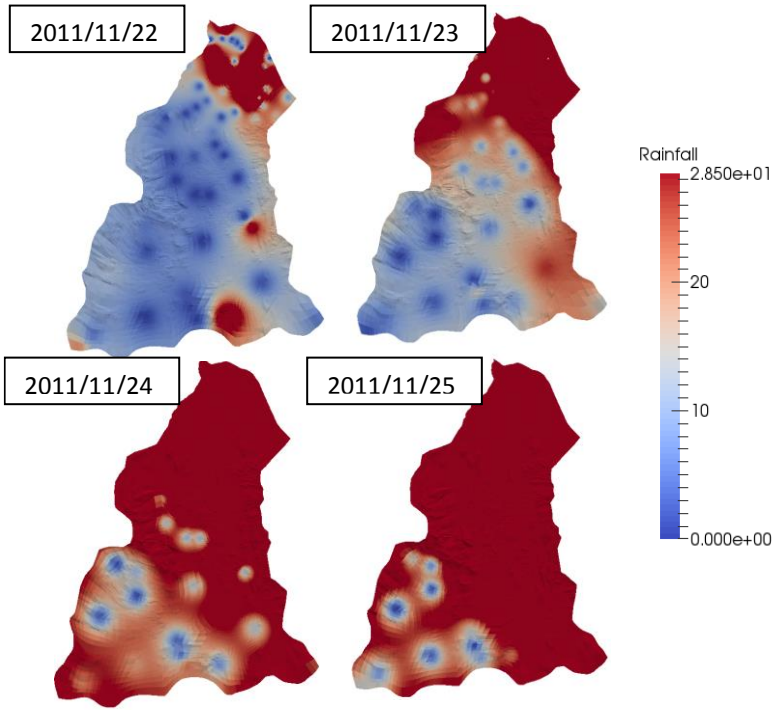

Figure 4.14. Kelantan watershed rainfall distribution in daily scale for year 2011.

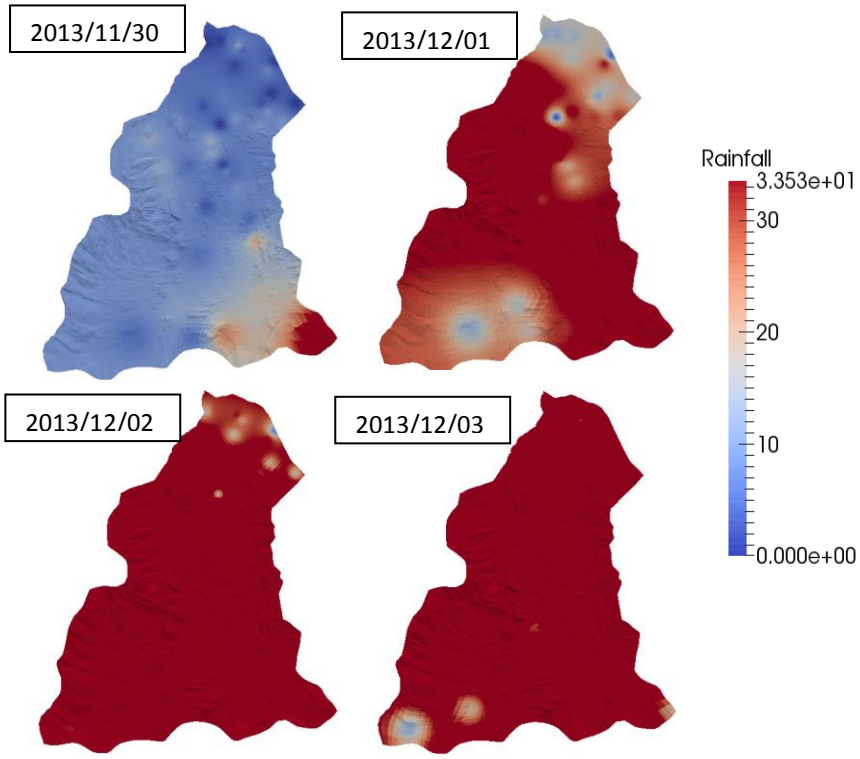

Figure 4.15. Kelantan watershed rainfall distribution in daily scale for year 2013.

4.4.6 *Delay analysis from Galas(A), Lebir (B) and Kuala Krai (C) to Guillemard Bridge (D)*

Cross-correlation between station A, B and C to D show longer delay time approximately around 20 hours in year 2008 and 2011 compared with 2013 as shown in Table 4.3. The reason behind this is the same as previous result of station A and B to C. Moreover, even though the distance between C to D is only 33 km away, the slope of the river is less steep making the travelling time slightly longer for the downstream area. By referring to Figure 4.2, there are a few tributaries that join into the Kelantan main stream after station C, which is also one of the factors that contributes to longer delay time from upstream station to station D.

4.5 *Sensitivity analysis of lag range*

Based on previous cross-correlation analysis, the size of lag range of 3 and 5 were found suitable for Kelantan watershed. Figure 4.17 shows the schematic diagram of how the model works for early flood prediction. For example, if the lag range 5 is selected, the lag for this model will start from 12 to 16 hours for Station A that has an average delay time of 14 hours to Station D.

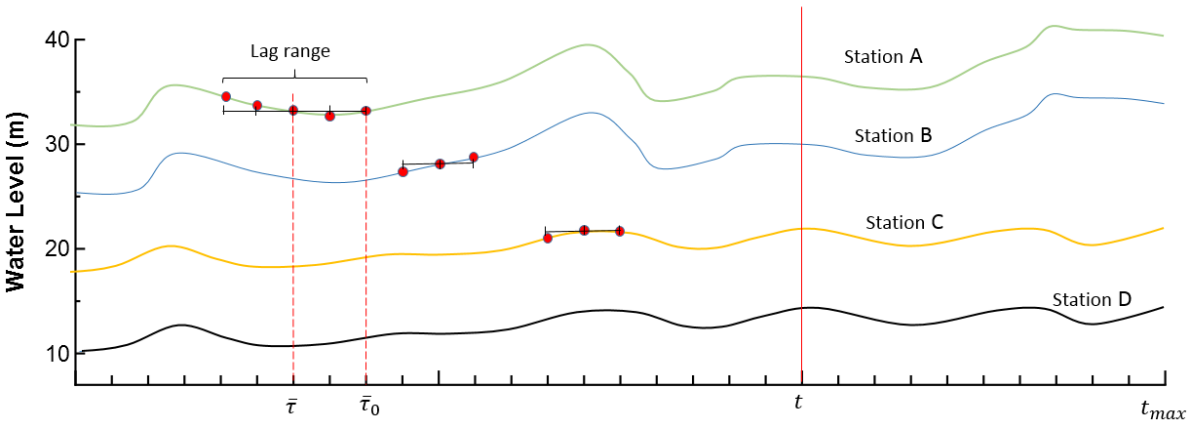

Figure 4.16. Schematic diagram of how the average delay time

To analyze the sensitivity of the lag range, early flood prediction for the first two events in 2011 at station C and D were used as shown in Figures 4.17 and 4.18. The selected lag range values were 3, 5 and 7 hours. From the results, it was found that the differences among them were very small. Since this method uses average delay time, lesser lag range can produce earlier flood prediction. Thus in this study, lag range of 3 was selected for early prediction at station C and D.

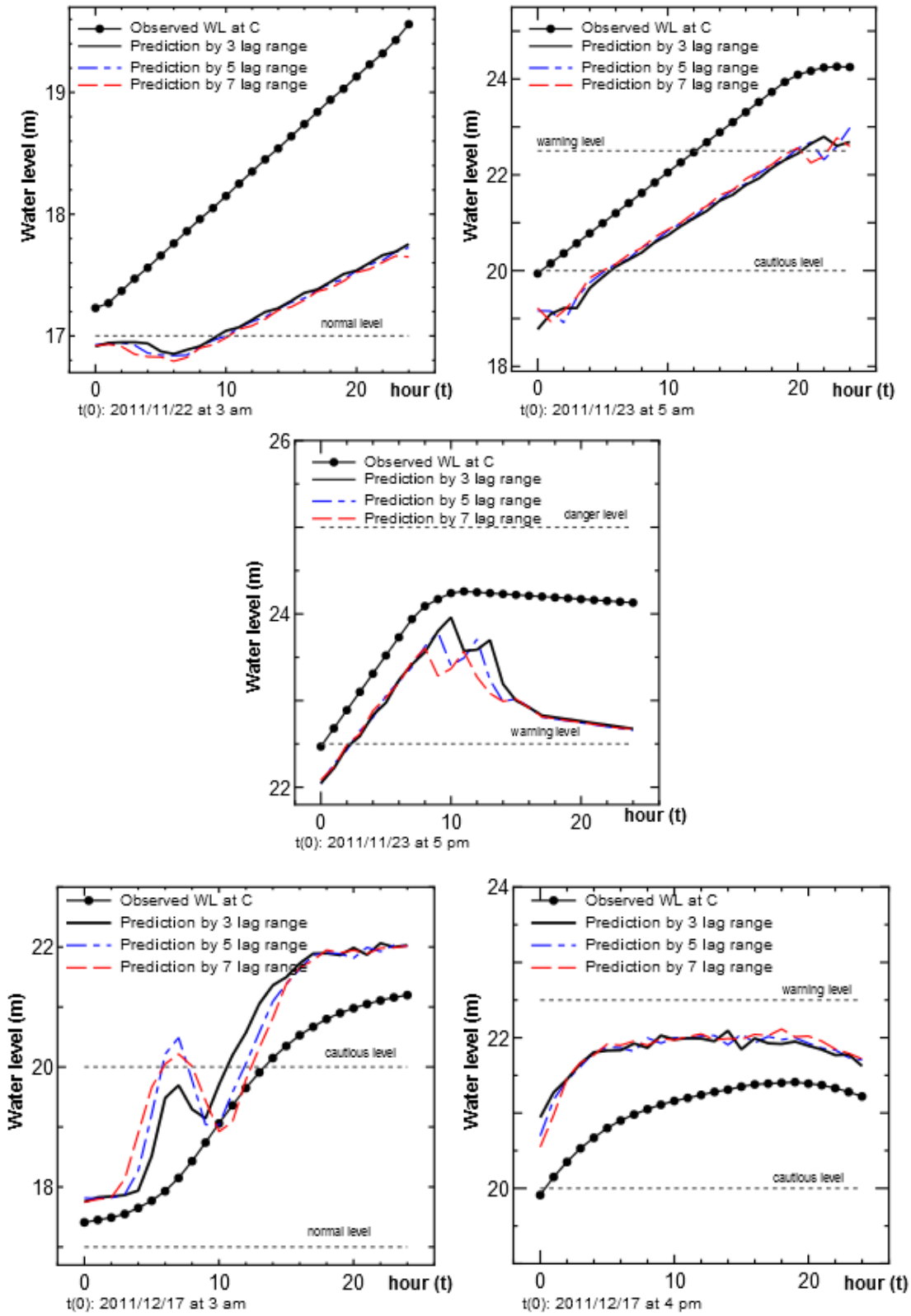

Figure 4.17. Sensitivity analysis of lag range at station C

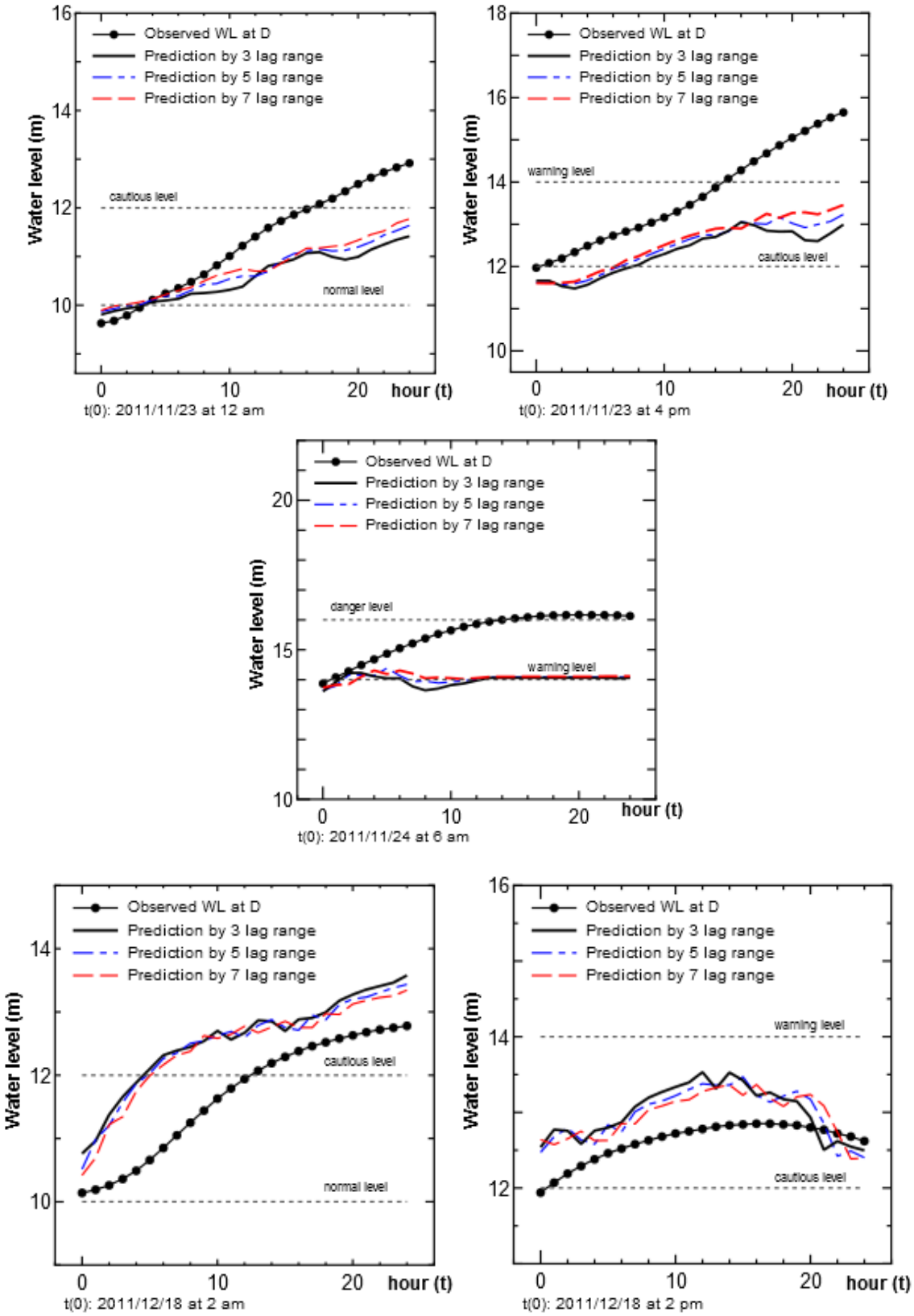

Figure 4.18. Sensitivity analysis of lag range at station D

4.6 *Early Flood Prediction*

For early flood prediction at C and D, three types of prediction were employed. Firstly, by using constant A coefficient determined at t, secondly, by updating the A coefficient at selected flood level at t=0, and thirdly, recalculation of A coefficients when the data were fed to the database system hourly. Root mean square error (RMSE) and Mean Absolute Error (MAE) were adopted to evaluate the performance of water level prediction

$$RMSE = \frac{1}{N}\sum_{i=1}^{N}(e_i^2)^{1/2} \tag{4.21}$$

$$MAE = \frac{1}{N}\sum_{i=1}^{N}|e_i| \tag{4.22}$$

where the difference between observed and predicted water level calculated as (e_i, i = 1, 2, …N).

4.6.1 *Early Flood Prediction at Kuala Krai (C)*

4.6.1.1. *Prediction at C by constant A coefficients*

For early flood prediction at station C for year 2011 and 2013 based on least square method, three types of predictions were made

- from A to C,
- from B to C, and
- from A and B to C,

as shown in Figure 4.19. A delay time of 5 hours had been chosen for A to C, and 4 hours from B to C based on cross-correlation analysis. From the results, early prediction using B was good enough for most high peak at C as illustrated in Figure 4.20 where RMSE and MAE value was the lowest for year 2011 and 2013. These results however were obtained using the same A coefficients determined with the sampling from 1st November to t = 0. By updating the A coefficients, good predictions were provided for early warning at station C, however it depends on certain situation and scenario as discussed in section 4.4.5.

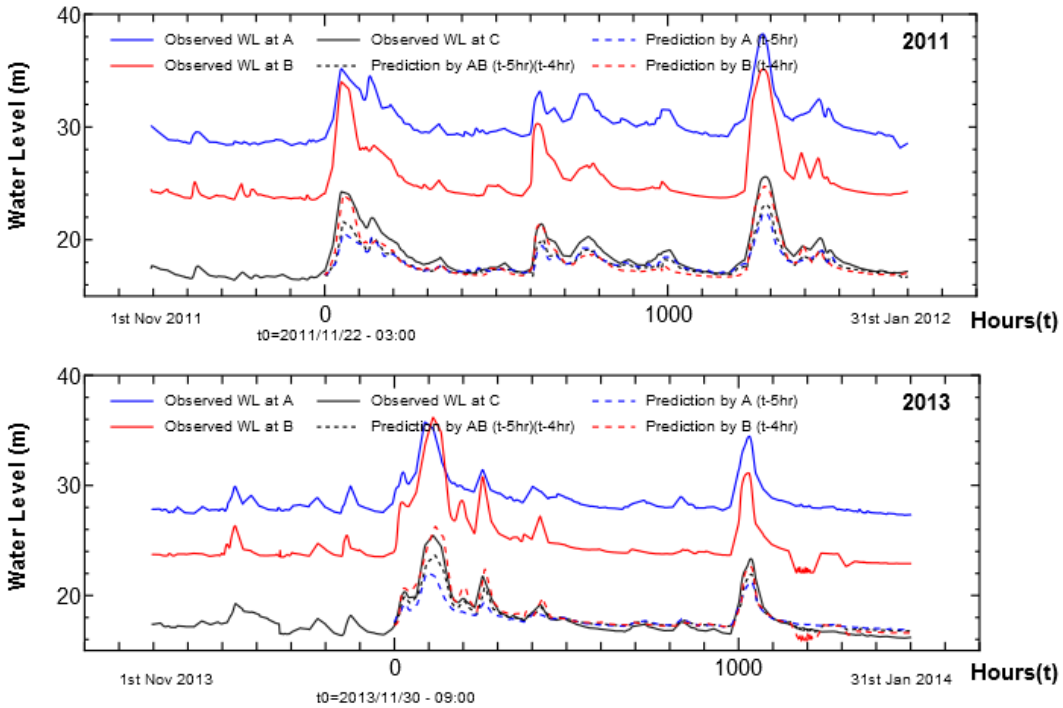

Figure 4.19. Observed water level at A, B and C and flood prediction at C by constant A coefficients for year 2011 and 2013

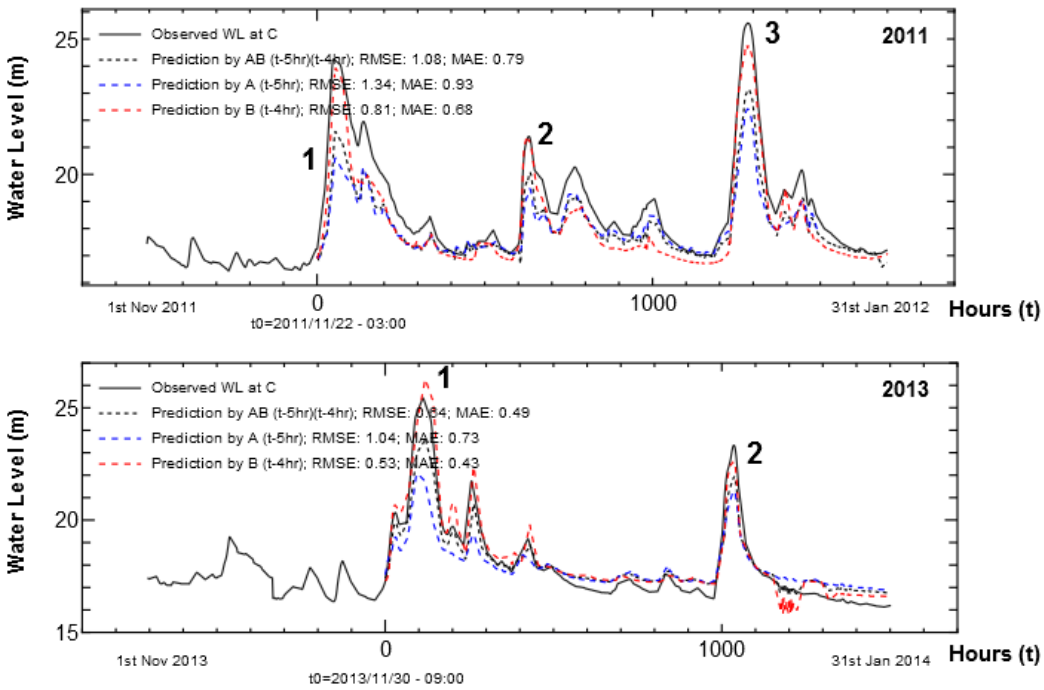

Figure 4.20. Flood prediction at C by constant A coefficients for year 2011 and 2013.

4.6.1.2. *Prediction at C by updated A coefficient at selected flood level*

Figures 4.21 to 4.25 show an example water level prediction at certain flood level indicator for peaks in 2011 and 2013 as marked in Figure 4.20. It is apparent from the results that by combination of A and B to predict C was superior than using either only A or B as shown in Figures 4.23 and 4.24, even though sometimes, B gave reliable results too as shown in Figures 4.21 and 4.22. This is because sub-watershed on the east side (Lebir) experienced intense heavy rainfall compared with the west side of Kelantan in the event, resulting higher water level at B as presented in Figure 4.19. Figure 4.21 shows prediction for peak 1, 2011. The prediction was very poor especially in Figure 4.21 (left and middle) since the downstream area experienced the monsoon rainfall first before the upstream area as discussed previously in Chapter 4.4.5. Poor prediction also can be seen in Figure 4.25 (right) where the prediction deteriorated earlier due to the effect of rainfall movement (from upstream to downstream). Overall, for most of the cases, the model predicted within 1 m from the starting time of prediction up to several hours.

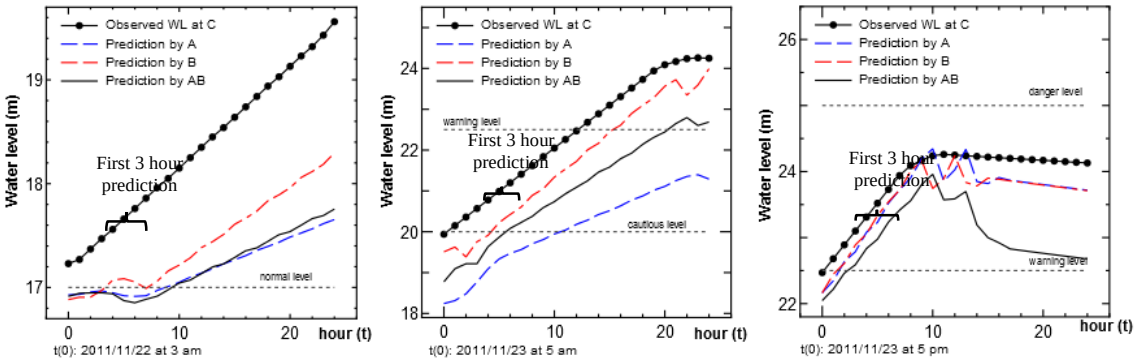

Figure 4.21. Flood prediction at C by updated A coefficients at certain flood level, peak 1 2011

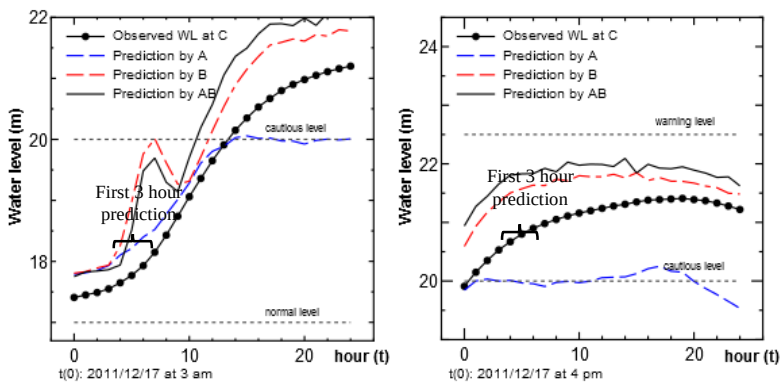

Figure 4.22. Flood prediction at C by updated A coefficients at certain flood level, peak 2 2011

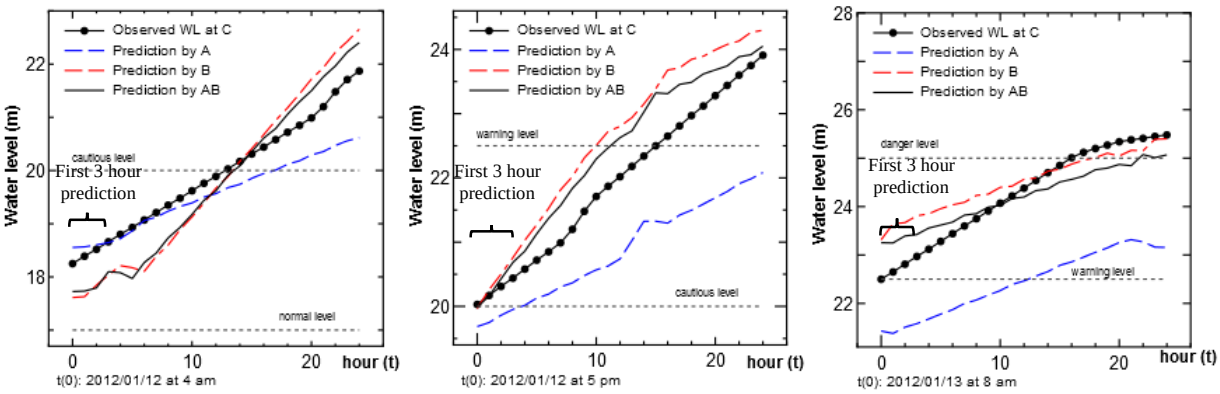

Figure 4.23. Flood prediction at C by updated A coefficients at certain flood level, peak 3 2011

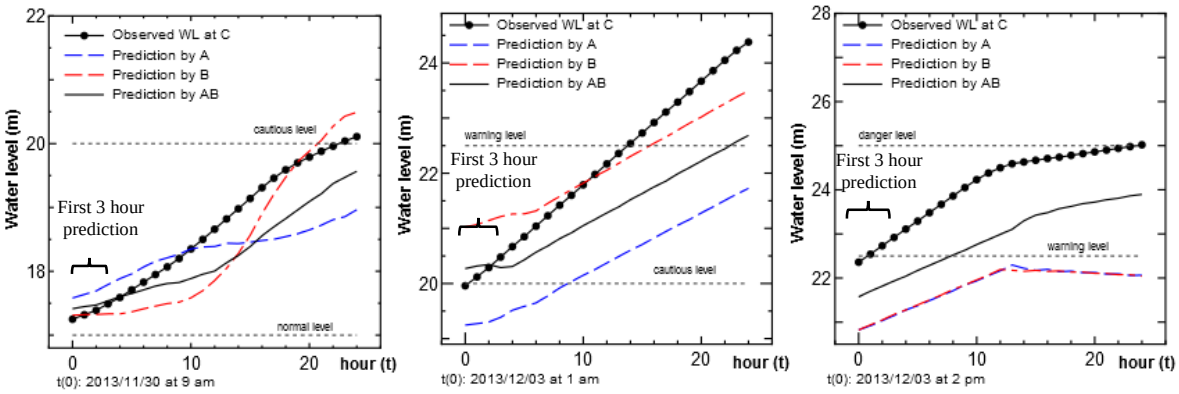

Figure 4.24. Flood prediction at C by updated A coefficients at certain flood level, peak 1 2013

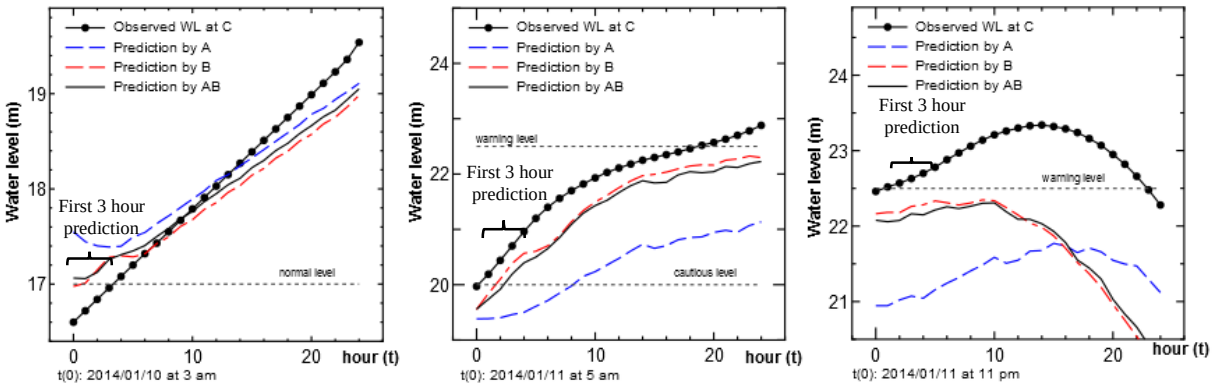

Figure 4.25. Flood prediction at C by updated A coefficients at certain flood level, peak 2 2013.

4.6.1.3. *Prediction at C by updated A coefficient - hourly*

Figures 4.26 and 4.27 show the results of flood prediction of hourly updated A coefficients up to 3 hours in 2011 and 2013 using combination of A and B for flood prediction at C. The prediction was very poor in the beginning especially in peak 1 2011 since the downstream area

experienced the monsoon rainfall first before the upstream area as discussed previously in Chapter 4.4.5. Toward the peak of the flood event in 2013, the prediction started to deteriorate due to the effect of rainfall movement (from upstream to downstream). Overall, the model produced MAE less than 1 m up to the highest peak of each flood event.

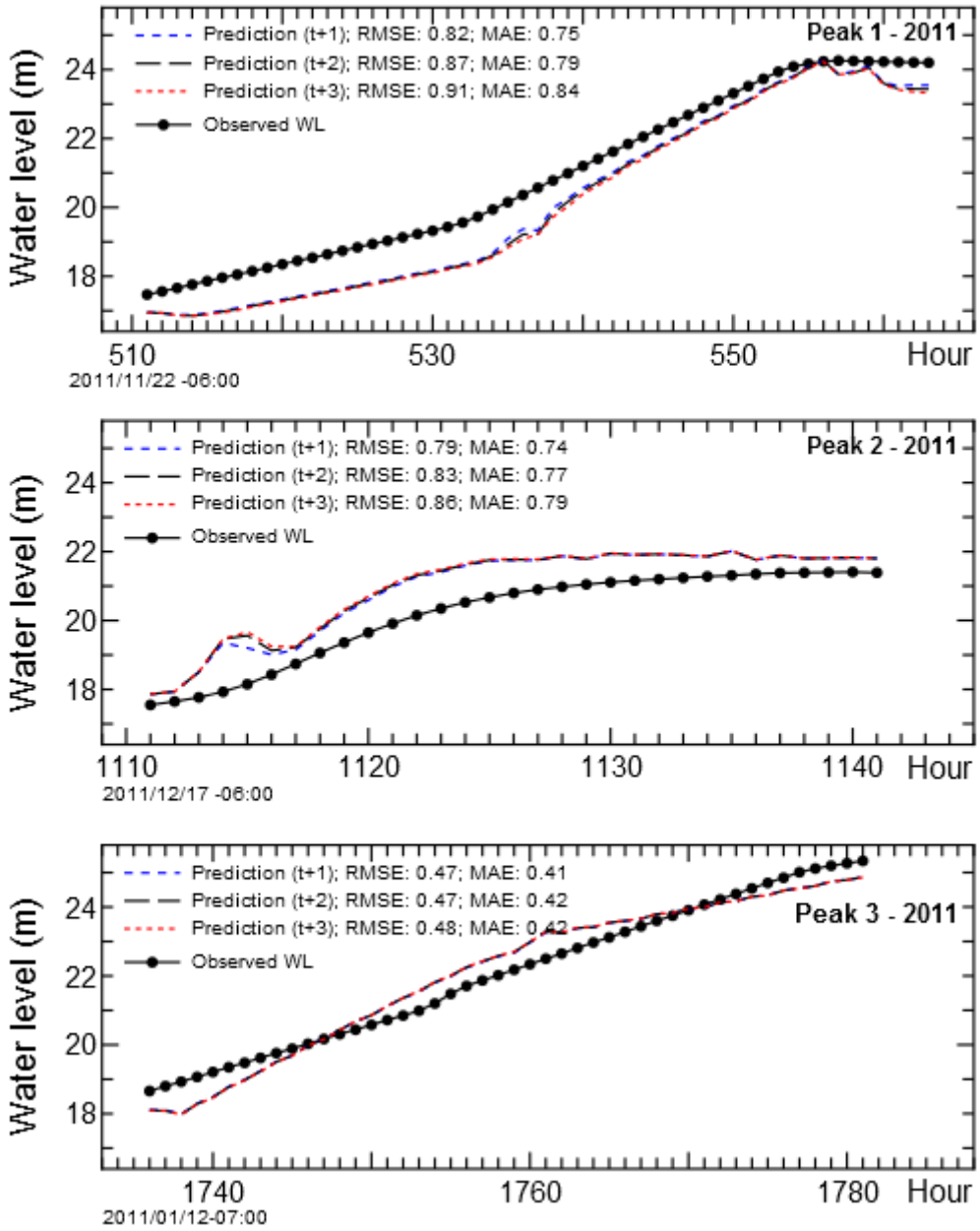

Figure 4.26. Flood prediction at C by updated A coefficients - hourly, 2011

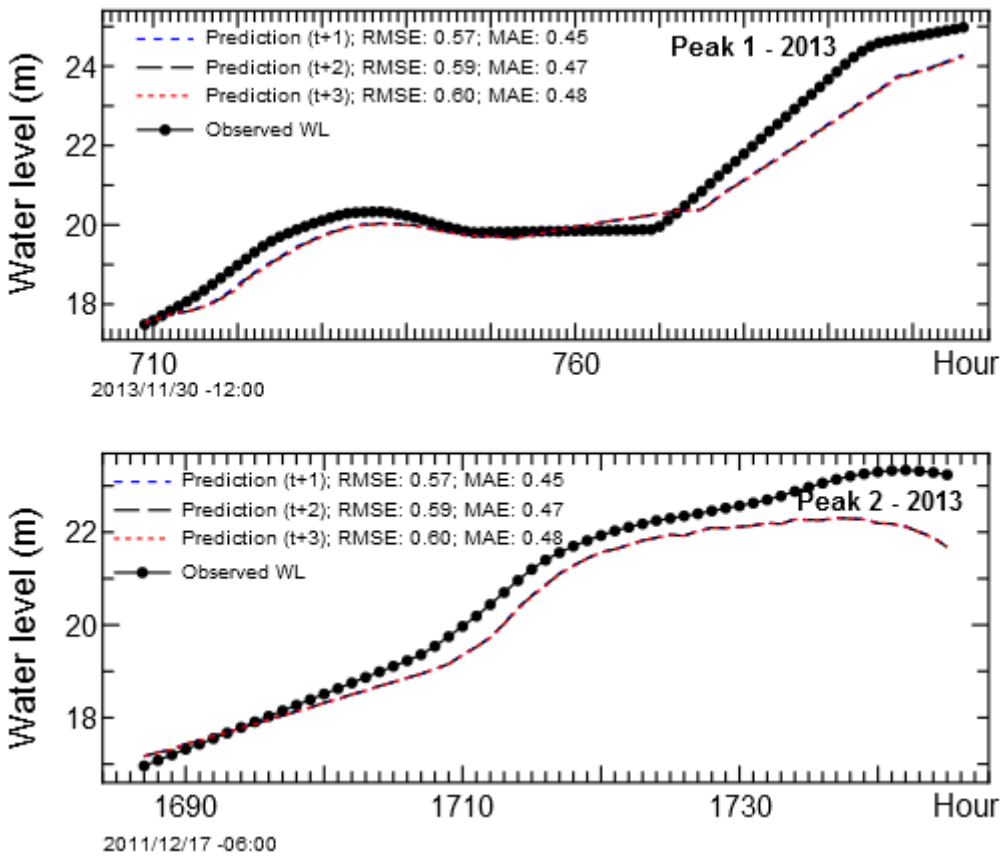

Figure 4.27. Flood prediction at C by updated A coefficients - hourly, 2013

4.6.2 *Early Flood Prediction at Guillemard Bridge (D)*

4.6.2.1. *Prediction at D by constant A coefficients*

Early flood prediction at station D for year 2011 and 2013 are shown in Figure 4.28. Five types of predictions were made:

- from A to D,
- from B to D,
- from C to D,
- from A and B to D, and
- from A, B and C to D.

Delay times were chosen as 14 hours for A, 10 hours for B and 6 hours for C, based on cross-correlation analysis. Early prediction was made using constant A coefficients, determined from early monsoon season data until the end of January as illustrated in Figure 4.28. However, the effect of joining tributaries located between C and D was clearly shown, especially during high peak as illustrated in Figure 4.29. By updating the A coefficients hourly will provide fairly

good predictions for early warning at station D depending on certain situation and scenario as discussed in section 4.4.5.

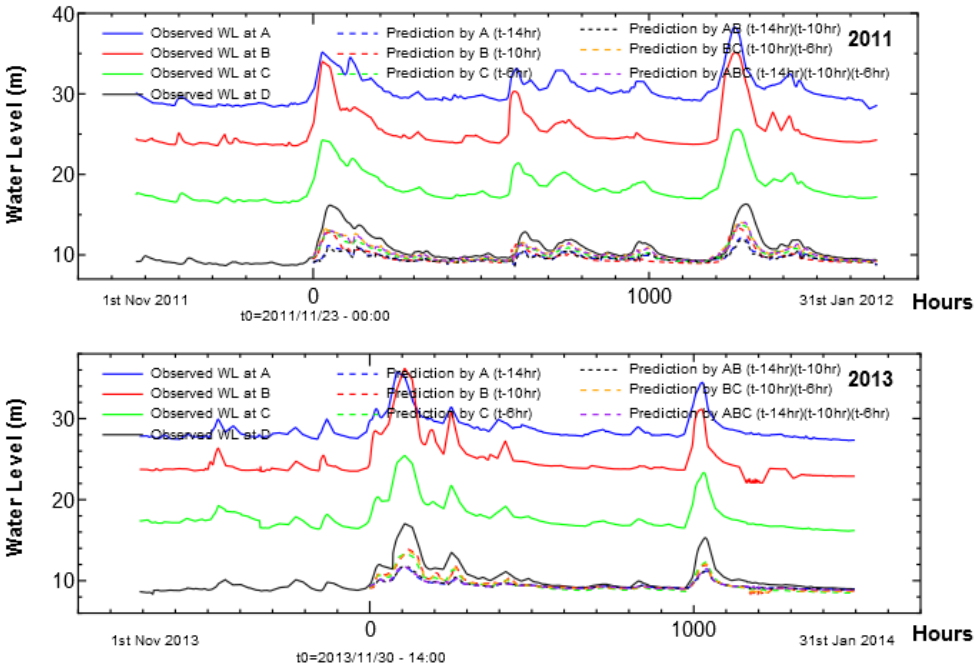

Figure 4.28. Observed water level at A, B, C and D and flood prediction at D by constant A coefficients for year 2011 and 2013

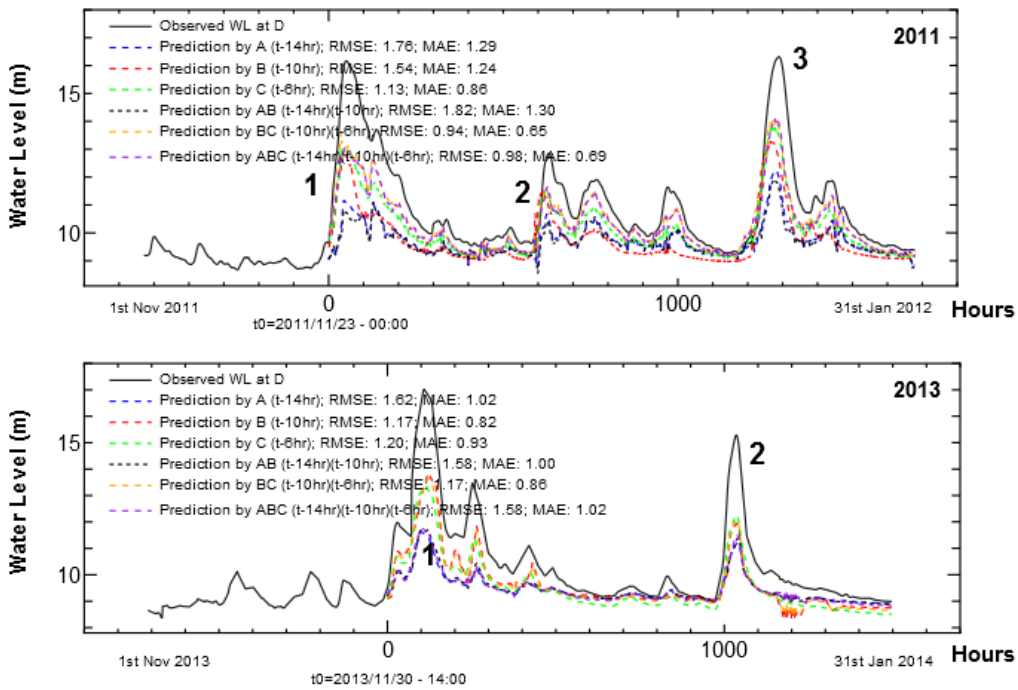

Figure 4.29. Flood prediction at D for year 2011 and 2013 by constant A coefficients for year 2011 and 2013

4.6.2.2. *Prediction at D by updated A coefficients at selected flood level*

Figures 4.30 to 4.34 show example forecasts at certain flood level indicator for peaks in 2011 and 2013 as marked in Figure 4.29. It appears that combination of all station A, B and C provides higher accuracy compared with single station or combination of A and B which can be seen in all figures. However, Figure 4.33 shows a very poor prediction, especially in the middle due to sudden shift in observation data at D.

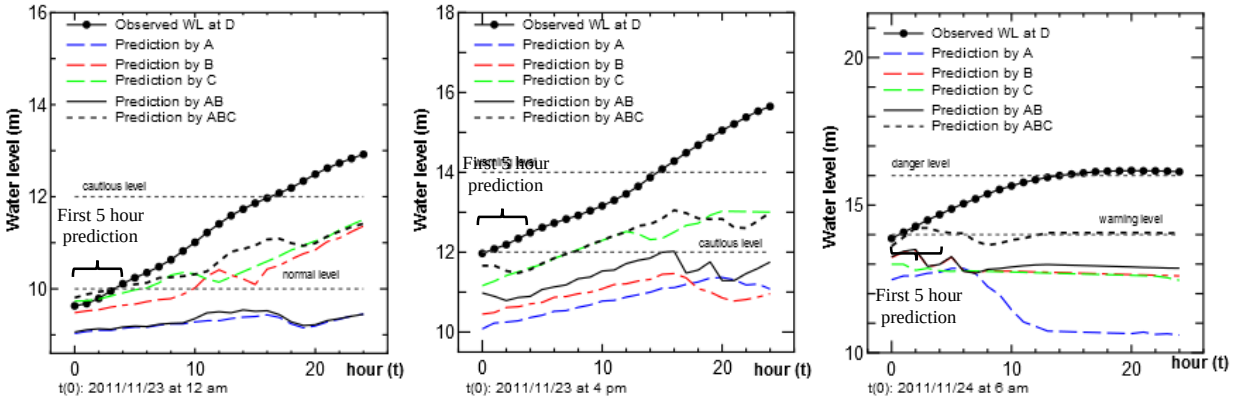

Figure 4.30. Flood prediction at D by updated A coefficients at certain flood level, peak 1 2011

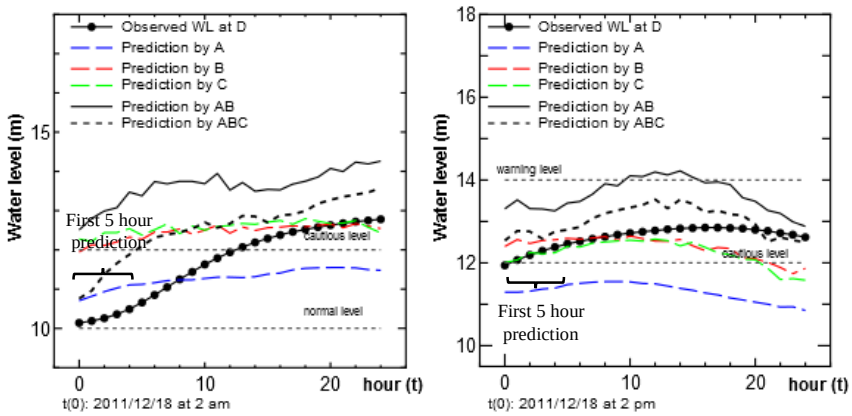

Figure 4.31. Flood prediction at D by updated A coefficients at certain flood level, peak 2 2011

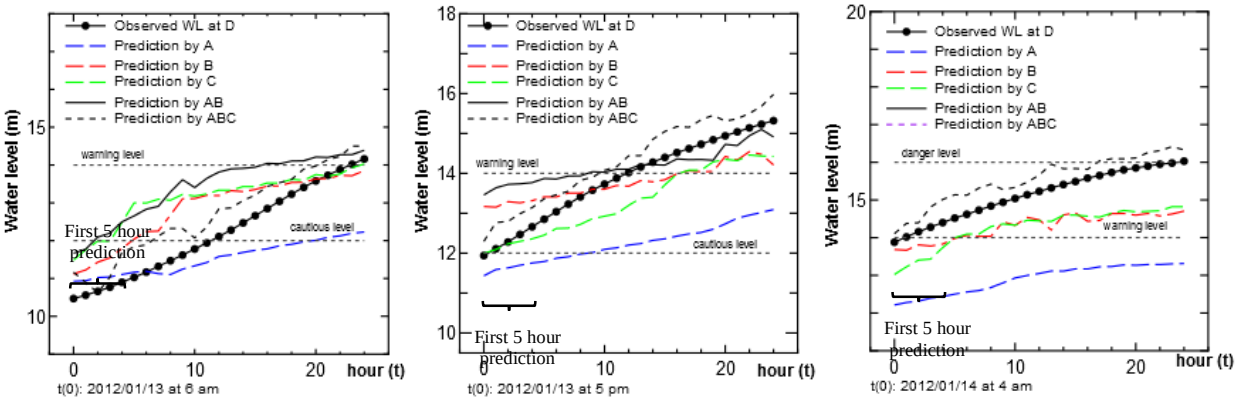

Figure 4.32. Flood prediction at D by updated A coefficients at certain flood level, peak 3 2011

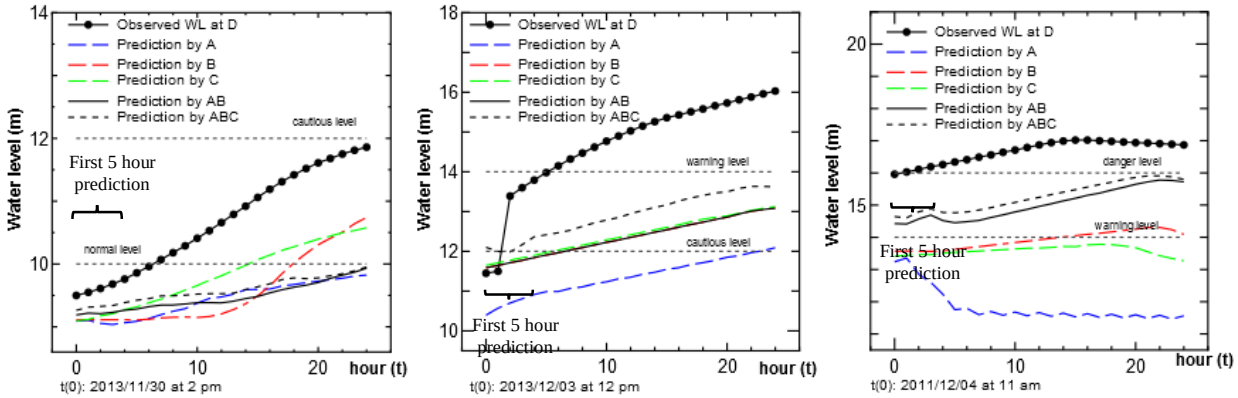

Figure 4.33. Flood prediction at D by updated A coefficients at certain flood level, peak 1 2013

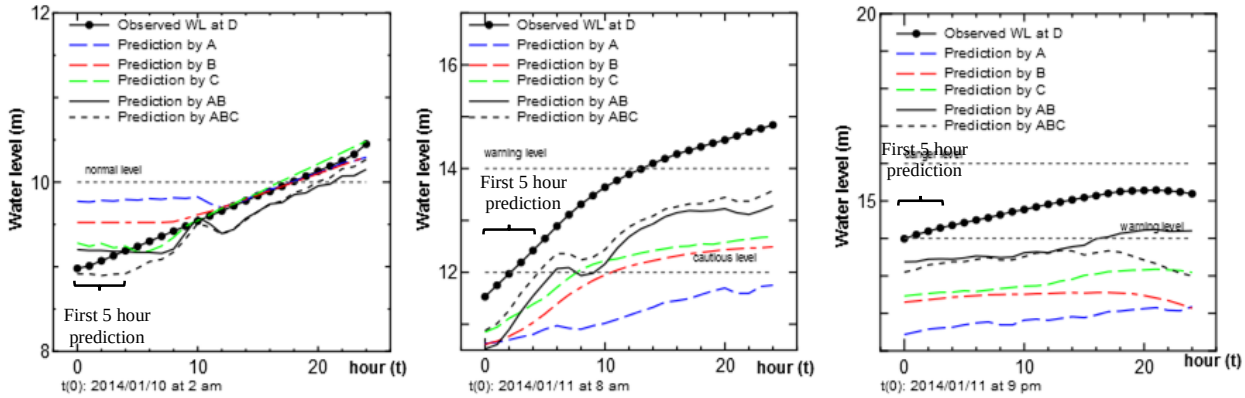

Figure 4.34. Flood prediction at D by updated A coefficients at certain flood level, peak 2 2013.

4.6.2.3. *Prediction at D by updated A coefficient – hourly*

Figures 4.35 and 4.36 show the results of flood prediction of updated hourly A coefficients, up to 5 hours in 2011 and 2013 using combination of A, B and C for flood prediction at D. Towards the peak of the flood event in 2013, the predictions started to deteriorate. This is due to the effect of rainfall movement (from upstream to downstream) as discussed in previous section. Overall, the model gave MAE less than 1 m up to the highest peak of each flood event, except for peak 1 in 2013 in Figure 4.35 where the flood prediction became worse due to the sudden shift in the observed data. This kind of serious prediction error seemed to occur when the downstream area experienced heavier rainfall (local effect), in addition to the effect of joining tributaries located in between C and D (ungauged tributaries).

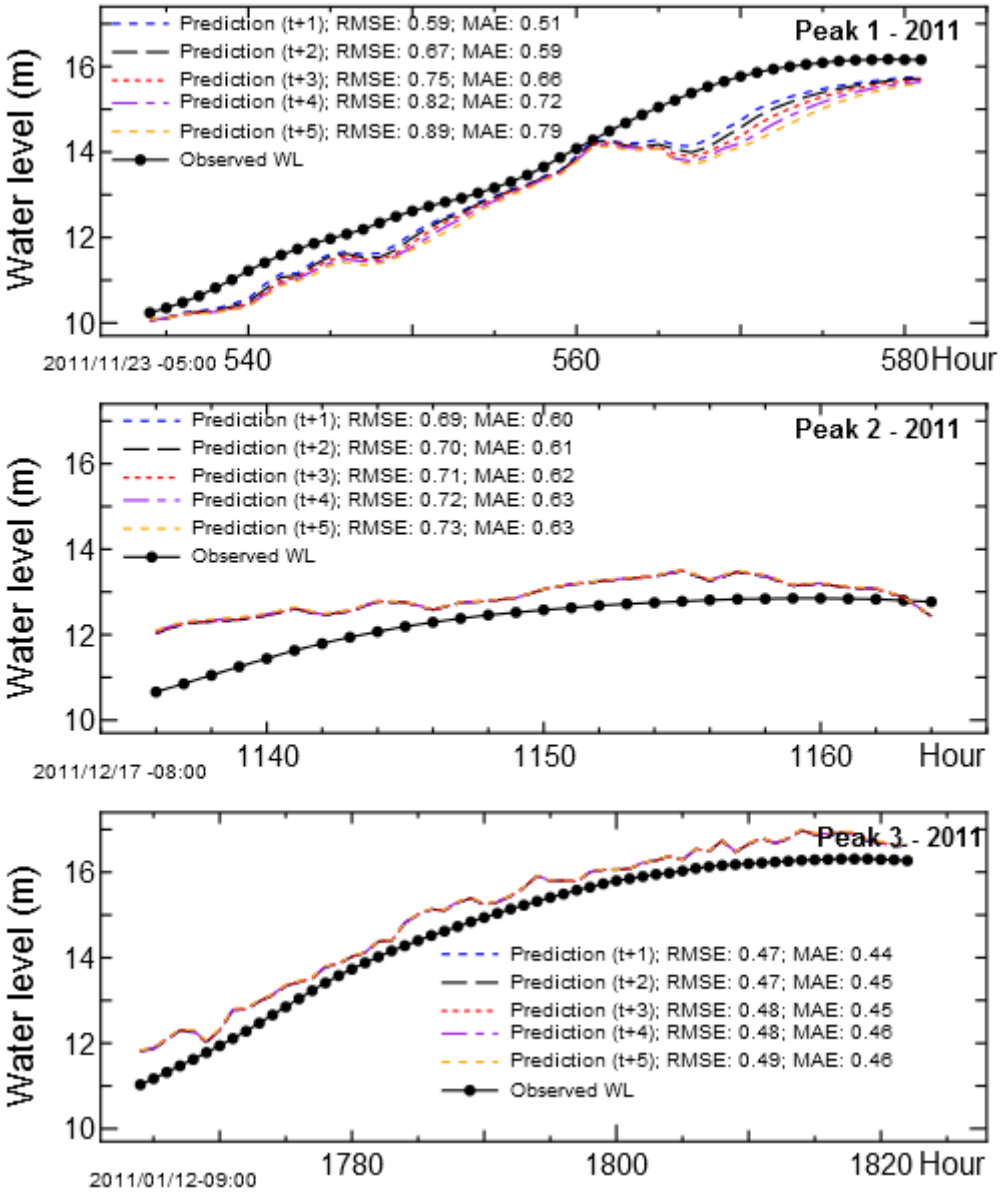

Figure 4.35. Flood prediction at D by updated A coefficients - hourly, 2011

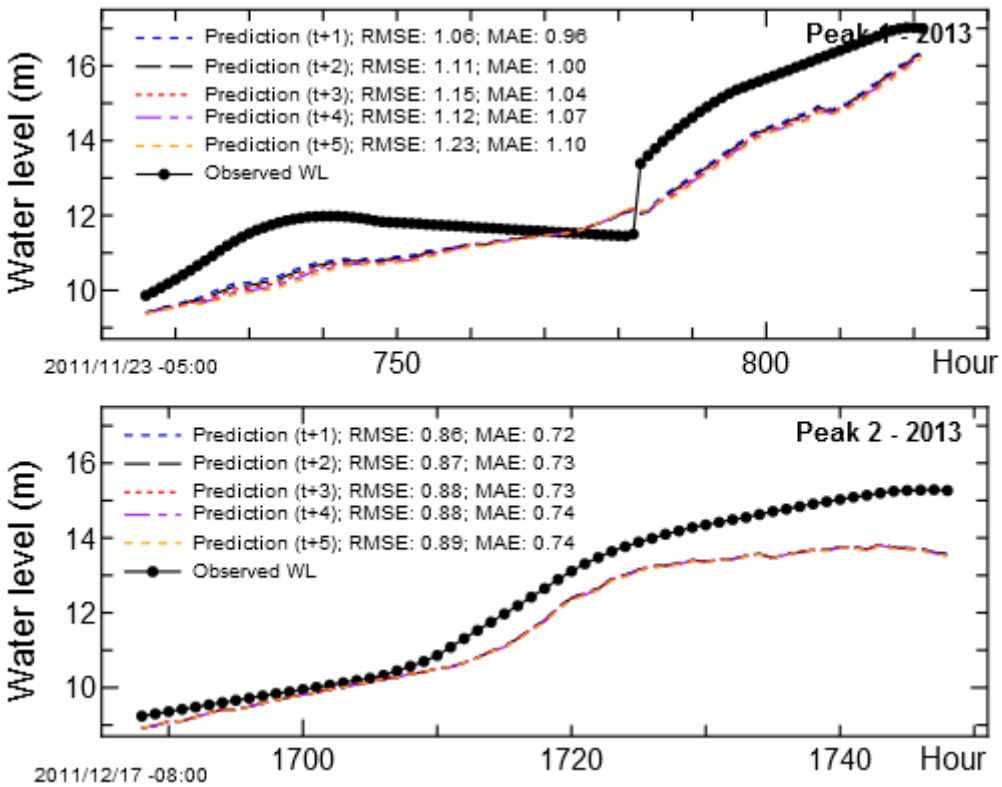

Figure 4.36. Flood prediction at D by updated A coefficients - hourly, 2013

4.7 *Improved Linear Observation-based Model.*

As stated in the previous section, future flood information is mostly contained in the flow from upstream, so that effect of the data at forecasting point itself was neglected. But taking into consideration the most recent observed data at forecasting point may work to improve the accuracy of the prediction. The ordinary ARMA models use a time series of forecasting station's observed data, but in this section, a semi-ARMA model which uses only most recent observation data at prediction point is developed.

4.7.1 *Auto-correlation of Kuala Krai (C) and Guillemard Bridge (D)*

In order to check statistical correlation of the time-series data at C and D, auto-correlation and variogram of C and D were calculated using the following equations.

<u>Auto-correlation:</u>

$$r_1 = \frac{1}{N}\sum_{j=1}^{\tau}[W_x(t-j) \times W_x(t)]^2 \tag{4.23}$$

Variogram:

$$r_2 = \frac{1}{N}\sum_{j=1}^{\tau}[W_x(t-j) - W_x(t)]^2 \tag{4.24}$$

where N is the number of samples and W_x is water level at respective stations. From the results as shown in Figure 4.37, station C gave good correlation up to 8 hours, while for station D up to 5-7 hours by auto-correlation. Variograms also indicated that strong correlations existed up to around 10 hours for both C and D. Therefore, including some of the past data of the forecasting stations seemed to improve the accuracy of prediction at C and D, especially at the beginning of the flood event.

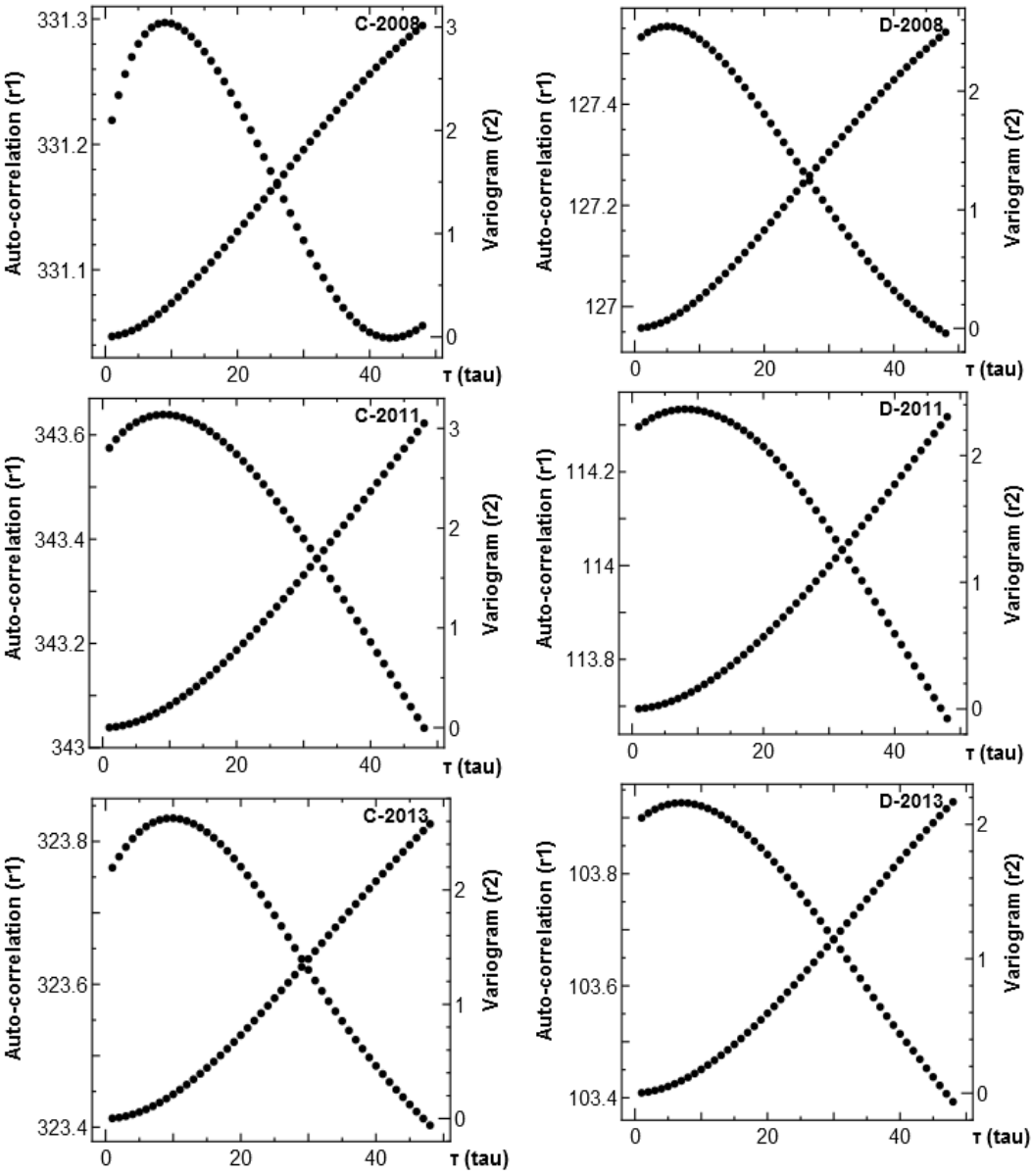

Figure 4.37. Auto-correlation and variogram of C and D for year 2008, 2011 and 2013.

4.7.2 *The Mathematical Model using forecasting point data*

In this section, the previous model is improved by adding most recent data of forecasting point. Most of the framework is the same as the previous model, but the new model includes past information of the forecasting point (past 1 hour). Unlike ARMA method where the future value lies within the past self-value, in this method, the value at D is formed by the past time sequence of A, B, C, and the most recent observation at D.

The general term of the equation is

$$\hat{y}(t) = A_0 y(t-1) + A_{1,0} x_1\left(t - \bar{\tau}_{1,0} - 0\right) + A_{1,1} x_1\left(t - \bar{\tau}_{1,0} - 1\right) + \cdots + A_{1,n} x_1\left(t - \bar{\tau}_{1,0} - n\right) + \cdots + A_{m,n} x_m\left(t - \bar{\tau}_{m,0} - n\right) \tag{4.25}$$

Or it can be written as

$$\hat{y}(t) = A_0 y(t-1) + \sum_{i=1}^{m} \sum_{j=0}^{n} A_{i,j} x_i \left(t - \bar{\tau}_{i,0} - j\right) \tag{4.26}$$

where $\hat{y}$ is the predicted value at time *t*, A_0 is the coefficient of *y*, $A_{i,j}$ is the coefficient for x_i (upstream predictor variables), $\bar{\tau}_{i,0}$ is the average delay time, m is the number of upstream stations used for prediction and n is the range of delay. The process of finding A_0 and $A_{i,j}$ coefficients is the same as shown in equation 4.4 – 4.8, by assuming y having range of delay of 1 hour. Prediction processes can be described as follows.

<u>Step.1</u> Using linear model written in Equation 4.19,

$$\hat{y}(t) = A_0 y(t-1) + \sum_{i=1}^{m} \sum_{j=0}^{n} A_{i,j} x_i \left(\mathrm{t} - \bar{\tau}_{i,0} - j\right)$$

and find out $A_0, A_{i,j}$ by minimizing $J = \sum_{t=\mathrm{t_s}}^{t_0-1} \{\hat{y}(t) - y(t)\}^2$

<u>Step 2.</u> Calculate $\hat{y}(t_0)$ and determine correction value

$$\hat{y}(t_0) = A_0 y(t_0 - 1) + \sum_{i=1}^{m} \sum_{j=0}^{n} A_{i,j} x_i \left(\mathrm{t}_0 - \bar{\tau}_{i,0} - j\right)$$

$$\varepsilon_0 = y(t_0) - \hat{y}(t_0) \tag{4.27}$$

Correction of predicted value:

$$\hat{y}(t_0) = \hat{y}(t_0) + \varepsilon_0 \tag{4.28}$$

<u>Step 3.</u> Predict water level at $\mathrm{t}_0 + k\ (k = 1,\ kmax)$ using the same equation above

$$\hat{y}(t) = A_0 y(t-1) + \sum_{i=1}^{m}\sum_{j=0}^{n} A_{i,j} x_i\,(\mathrm{t} - \bar{\tau}_{i,0} - j)$$

but if $\mathrm{t} > \mathrm{t}_0$, then $y(t-1)$ is replaced by $\hat{y}(t-1)$ which is already estimated.

After finding out $A_0, A_{i,j}$ by minimizing $J = \sum_{t=\mathrm{t_s}}^{t_0+k-1} \{\hat{y}(t) - y(t_0)\}^2$

$$\hat{y}(t_0 + k) = A_0 \hat{y}(t_0 + k - 1) + \sum_{i=1}^{m}\sum_{j=0}^{n} A_{i,j} x_i \left(\mathrm{t_0} + \mathrm{k} - \bar{\tau}_{i,0} - j\right) + \mathrm{cor_y} \tag{4.29}$$

where

$$\text{Correction 1} : Cor_y = \varepsilon_0 \text{ for } k = 1, \text{otherwise } 0$$

$$\text{Correction 2} : Cor_y = \varepsilon_0 \text{ for all } k$$

This model might be applicable to estimate the water level up to 3 hours at Kuala Krai, and 5 hours at Guillemard Bridge by using the predicted $\hat{y}(t)$value of previous hour. Figure 4.38 illustrates how the correction method 1 and 2 works in prediction.

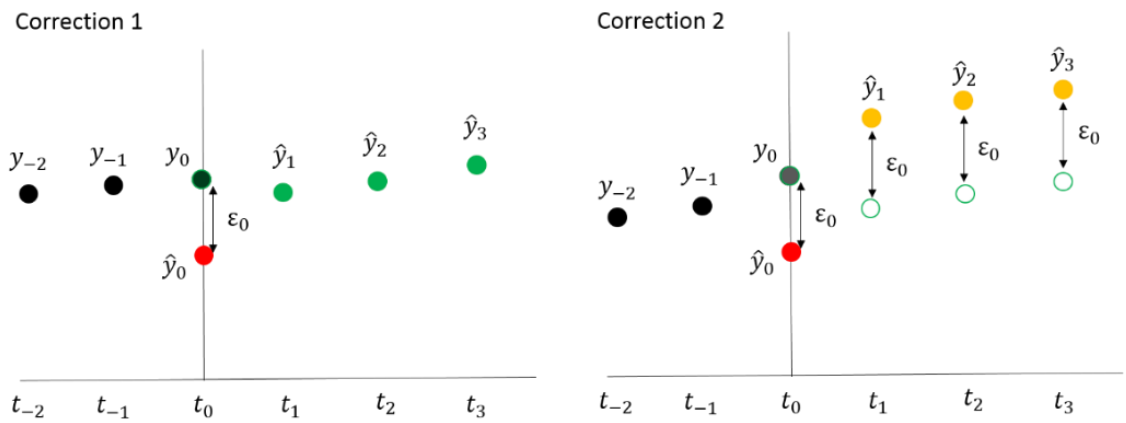

Figure 4.38. Illustration of correction 1 and 2 method.

4.7.3 *Improved Early Flood Prediction at Kuala Krai (C)*

In section 4.7.3.1, predictions were made by updating the A coefficient at selected flood level at t=0. Four prediction results are presented in each figure for comparison; first by utilizing only upstream information as shown in previous section 4.6, second by the improved model without correction, third and fourth by applying correction 1 and 2 of the improved model. Section 4.7.3.2 show the overall results when data were fed to the database system hourly. RMSE and MAE as shown in equations 4.14 and 4.15 were adopted to evaluate the performance of overall water level prediction for each event.

4.7.3.1. *Prediction at C at selected flood level*

Figures 4.39 to 4.41 illustrate water level prediction at C, up to 3 hours from different initial times for year 2011, while Figures 4.42 and 4.43 for 2013, and Figures 4.44 and 4.45 for 2014. Overall results show that by incorporating past forecasting station data of *t-1* improved the prediction regardless of any rainfall event, i.e., upstream-first rainfall, heavy local rainfall at the forecasting station, or downstream-first rainfall. By applying the correction method, the quality of prediction was much improved for most cases especially when the water level was in rising state. However the difference of correction method 1 and 2 (green and orange line) with non-correction (red) was very minimal, less than 50 cm as shown in Figure 4.39, bottom left.

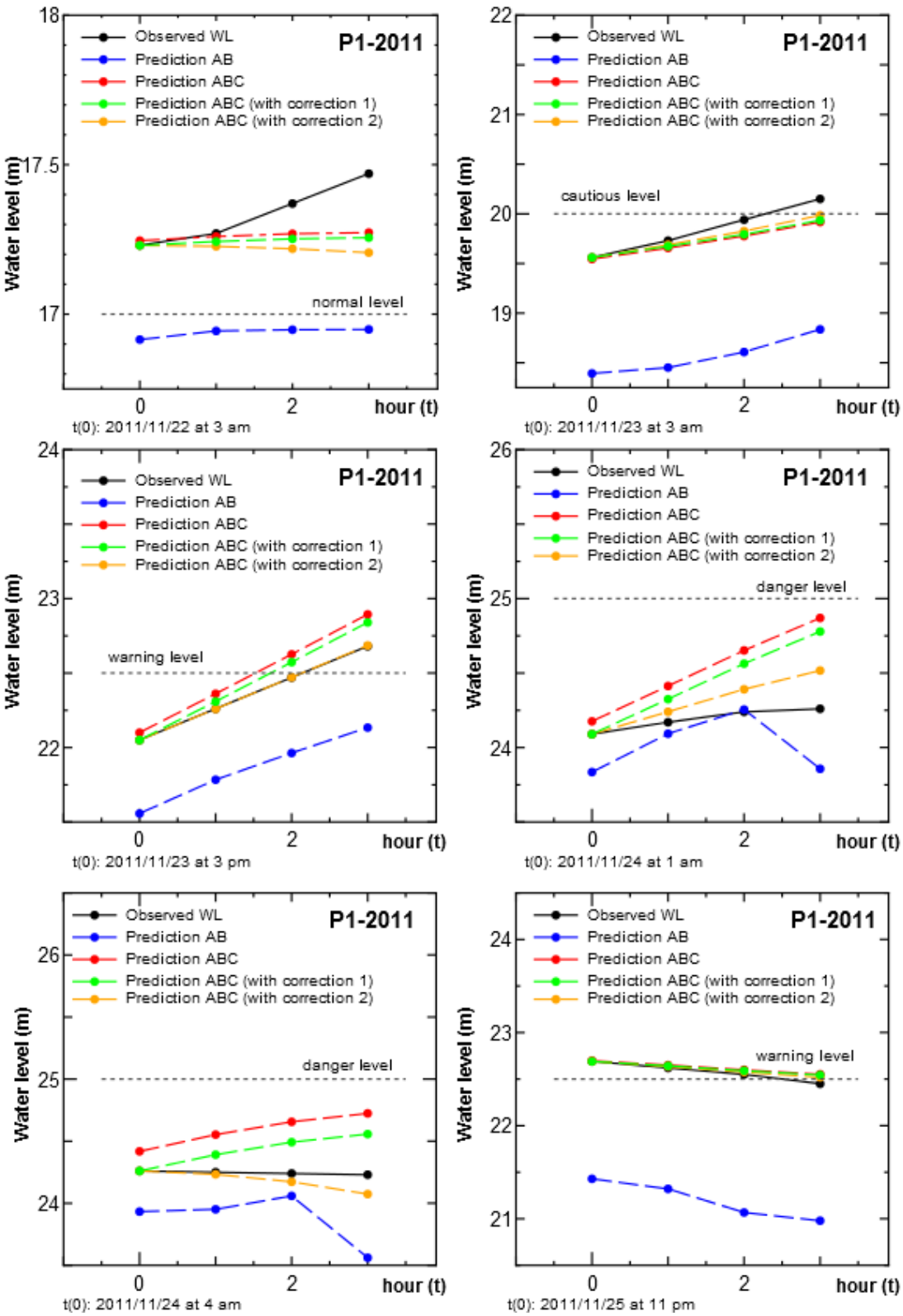

Figure 4.39. Improved flood prediction at C at certain flood level, peak 1 2011.

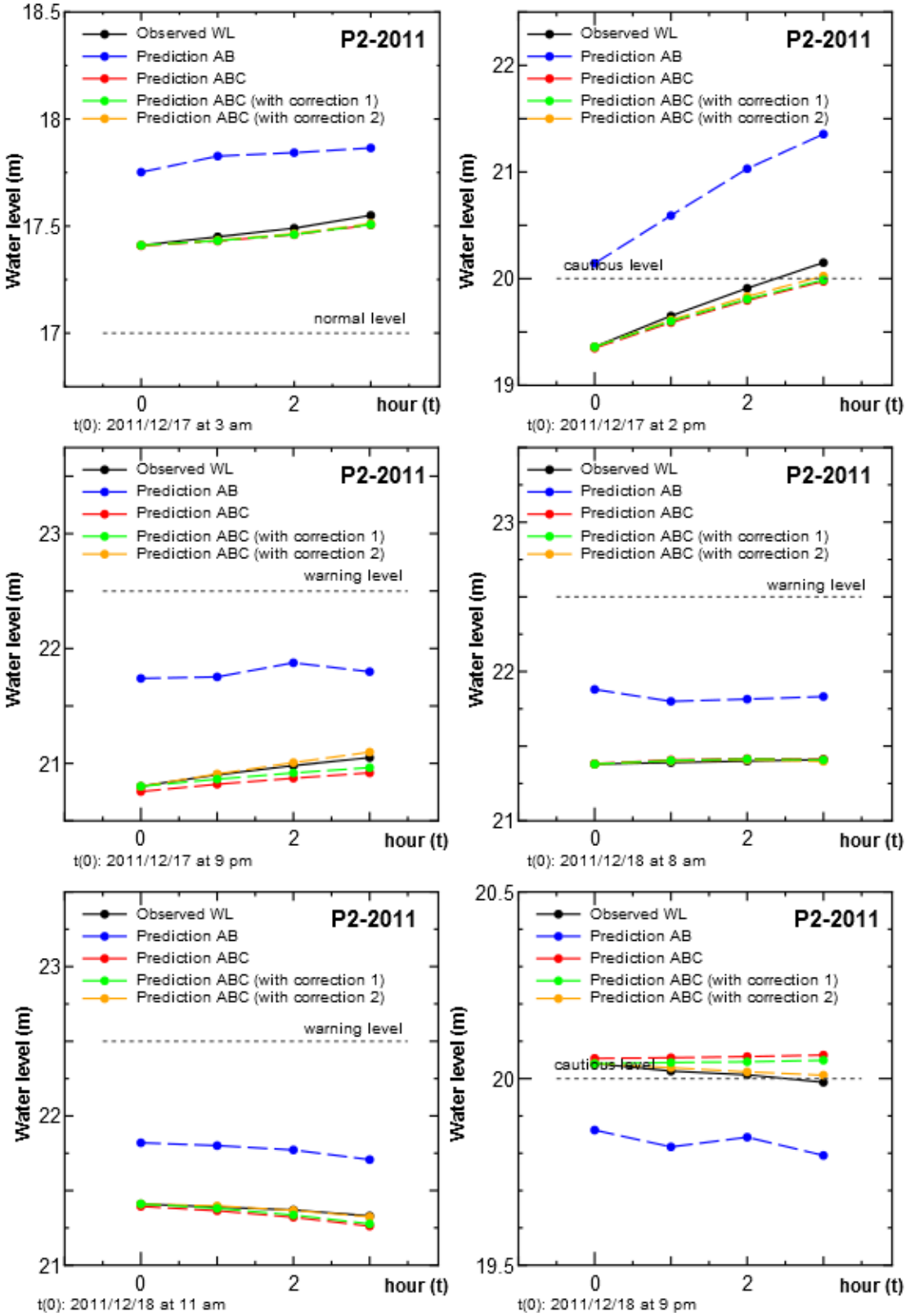

Figure 4.40. Improved flood prediction at C at certain flood level, peak 2 2011.

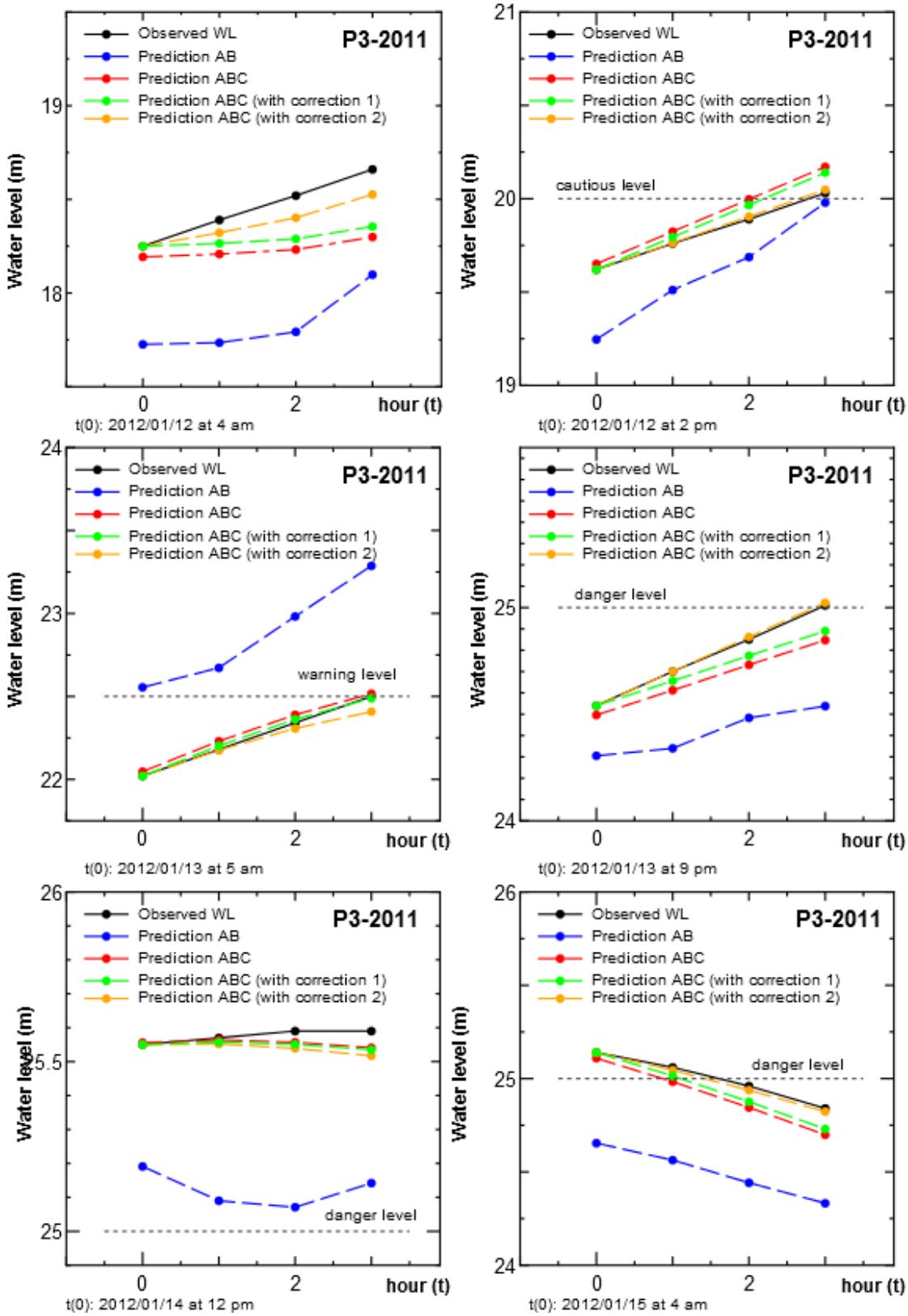

Figure 4.41. Improved flood prediction at C at certain flood level, peak 3 2011.

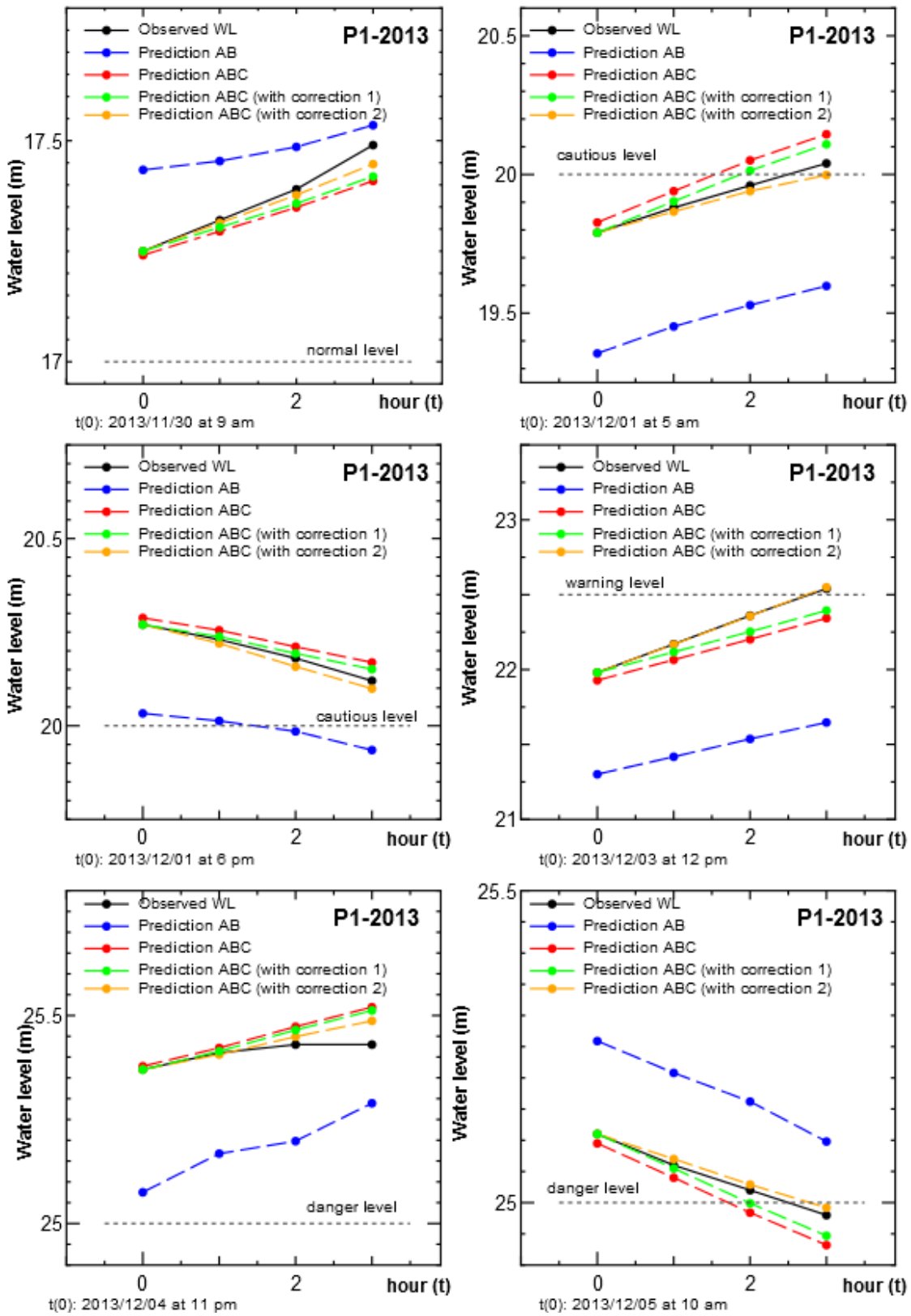

Figure 4.42. Improved flood prediction at C at certain flood level, peak 1 2013.

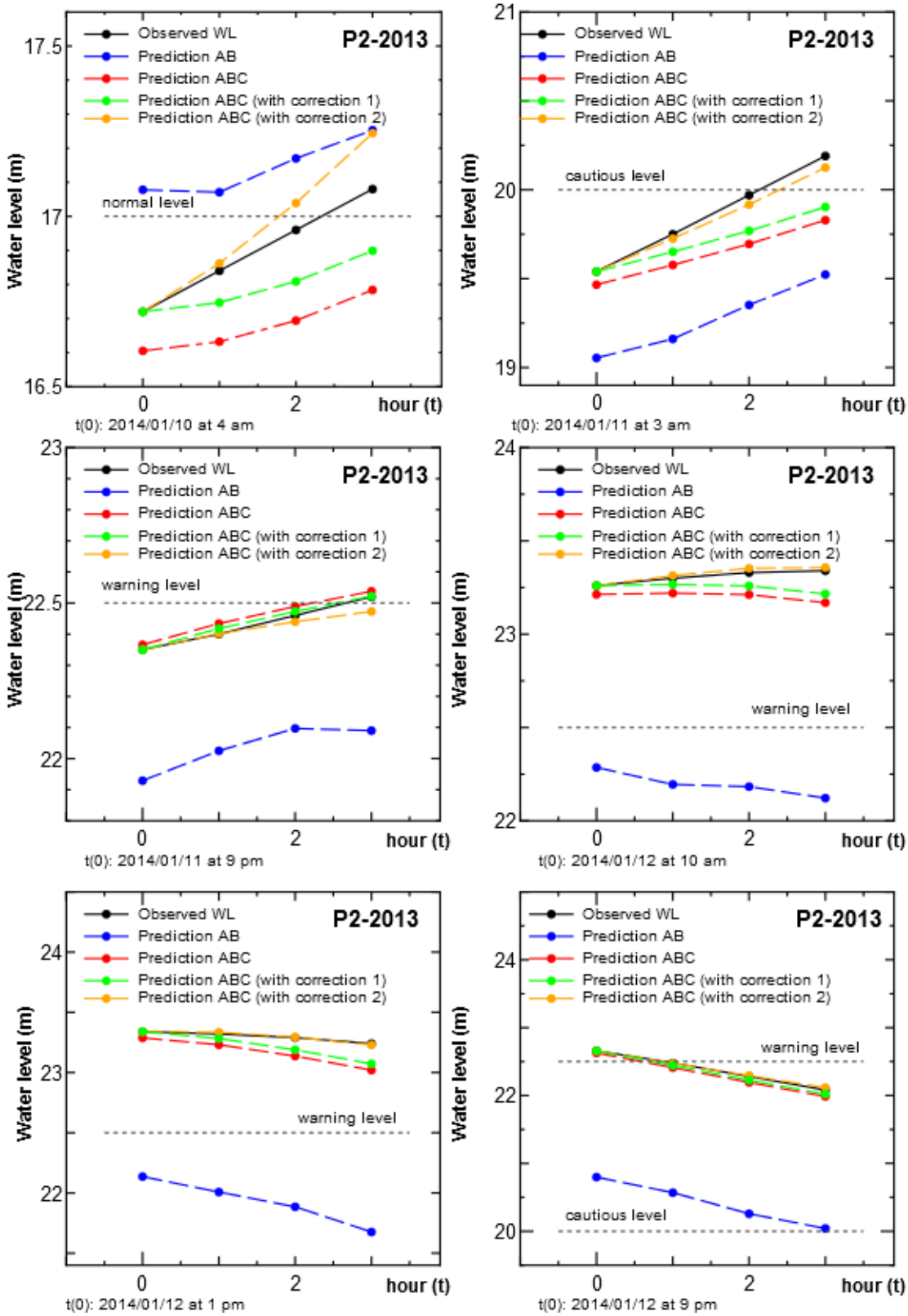

Figure 4.43. Improved flood prediction at C at certain flood level, peak 2 2013.

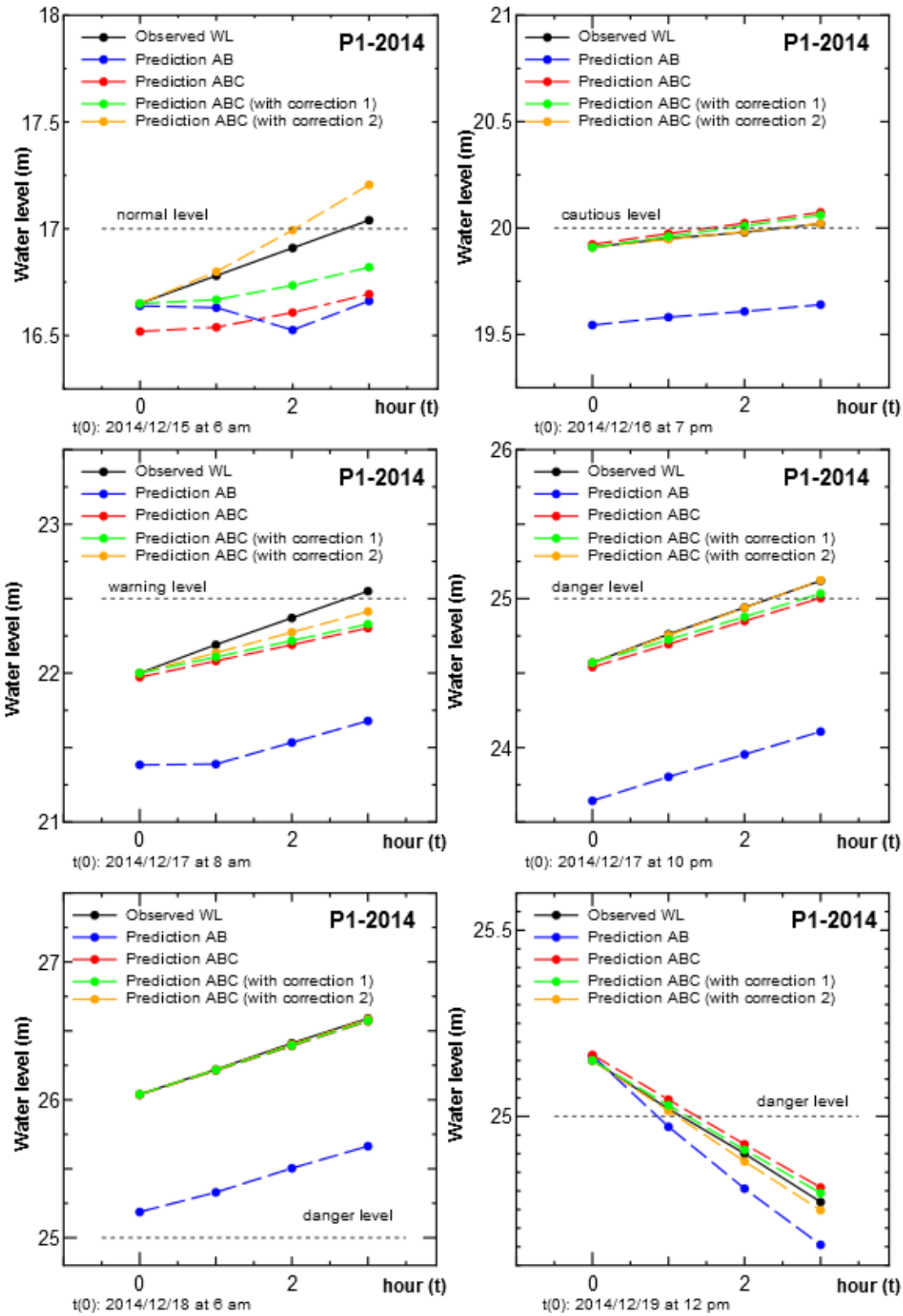

Figure 4.44. Improved flood prediction at C at certain flood level, peak 1 2014.

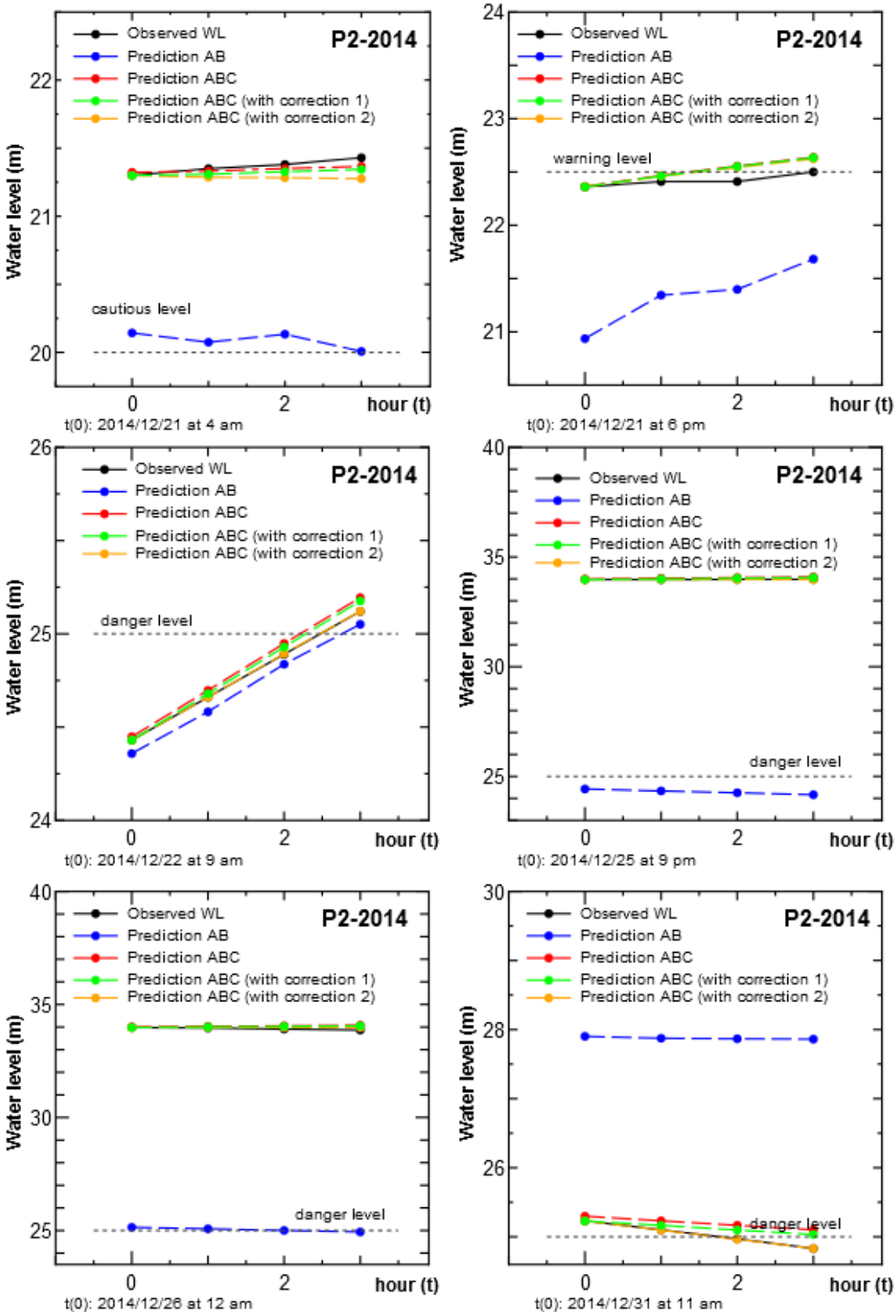

Figure 4.45. Improved flood prediction at C at certain flood level, peak 2 2014.

4.7.3.2. *Prediction at C by updated A coefficient hourly*

Figures 4.46 to 4.52 show the results of flood prediction of hourly updated A coefficient up to 3 hours in 2011, 2013 and 2014, from starting of the flood event, until the water level started to subside. The improved model managed to give good prediction for all cases as the RMSE and MAE improved very much compared with that utilizing upstream information only. The improved model also worked well if the upstream data deteriorated as shown in Figure 4.52 compared with the results of previous model. By applying the correction methods, quality of prediction has improved. The correction 2 method gave good prediction only if all past information was available (no missing or false data) or else, it provided somewhat deteriorated results (overestimate or underestimate) as the τ increases as shown in Figure 4.52.

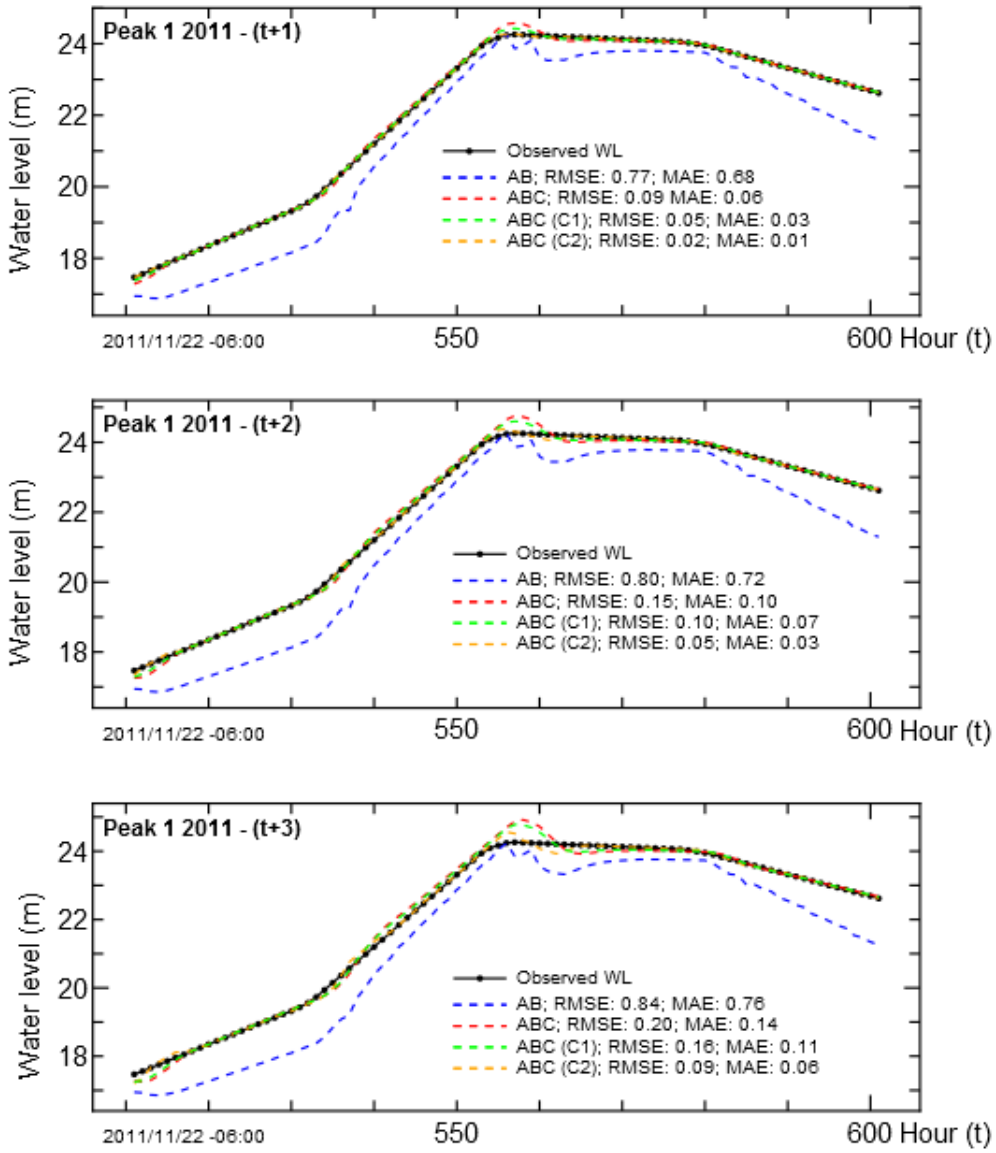

Figure 4.46. Improved flood prediction at C, peak 1 by updated A coefficients - hourly, 2011

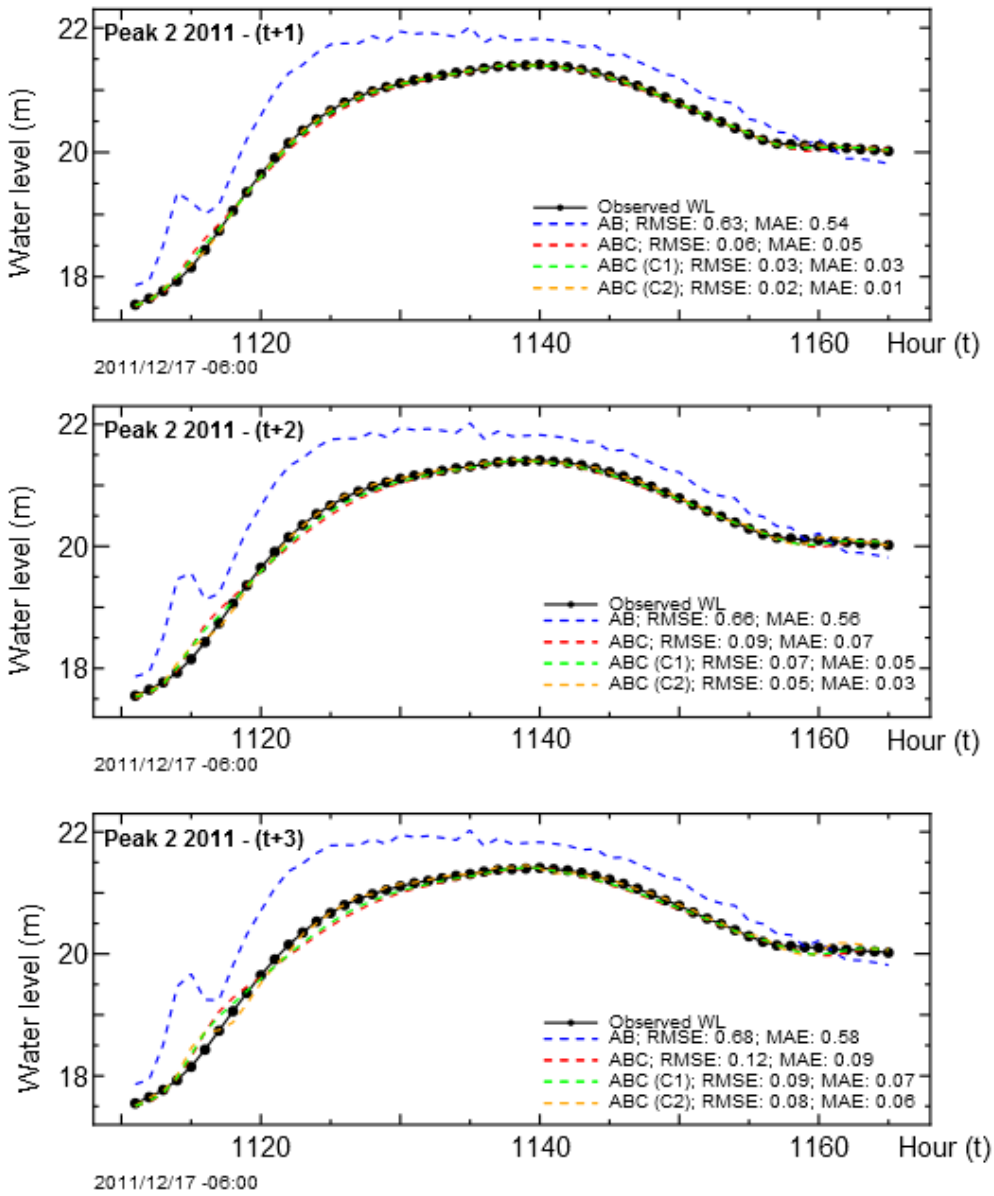

Figure 4.47. Improved flood prediction at C, peak 2 by updated A coefficients - hourly, 2011

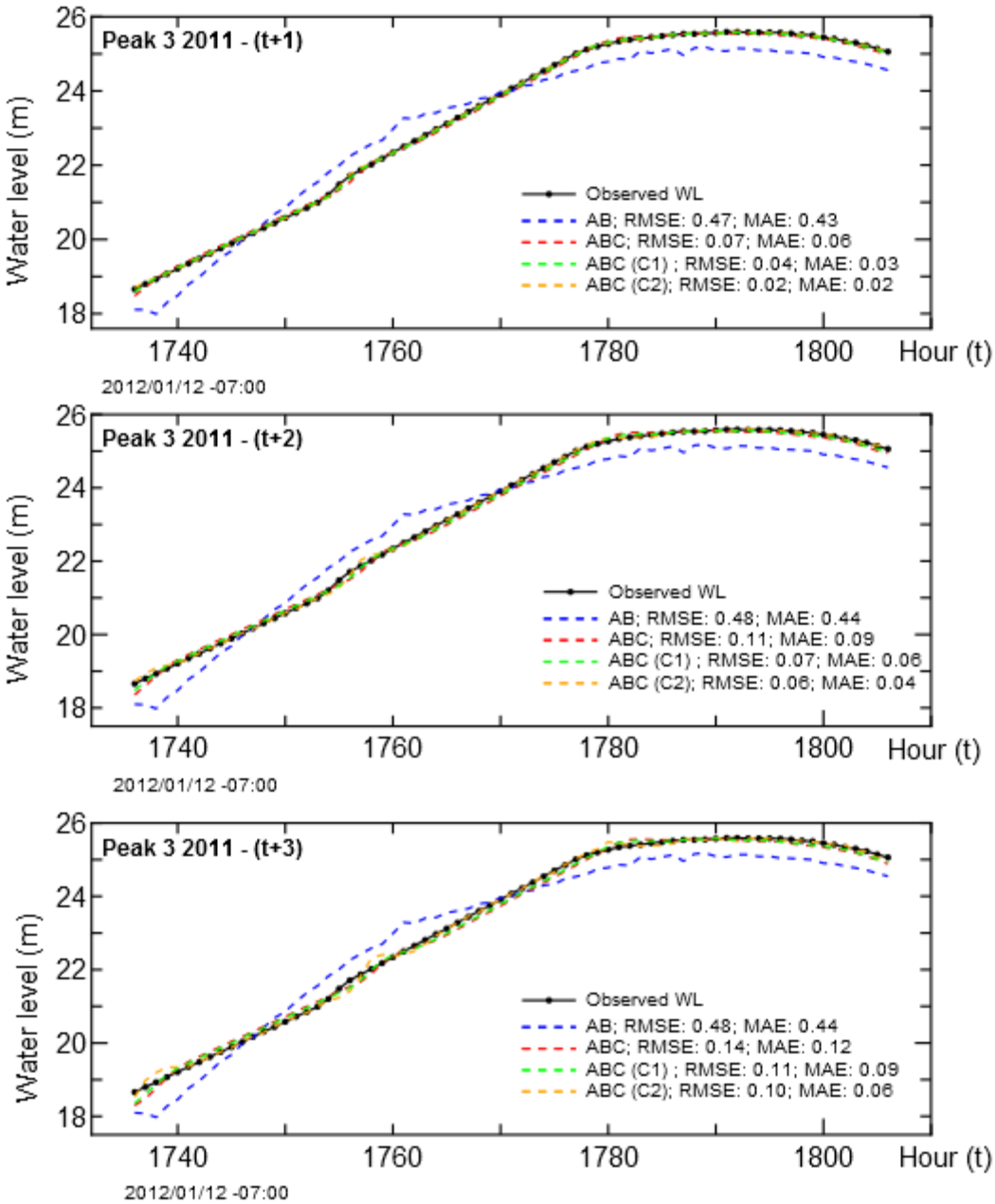

Figure 4.48. Improved flood prediction at C, peak 3 by updated A coefficients - hourly, 2011

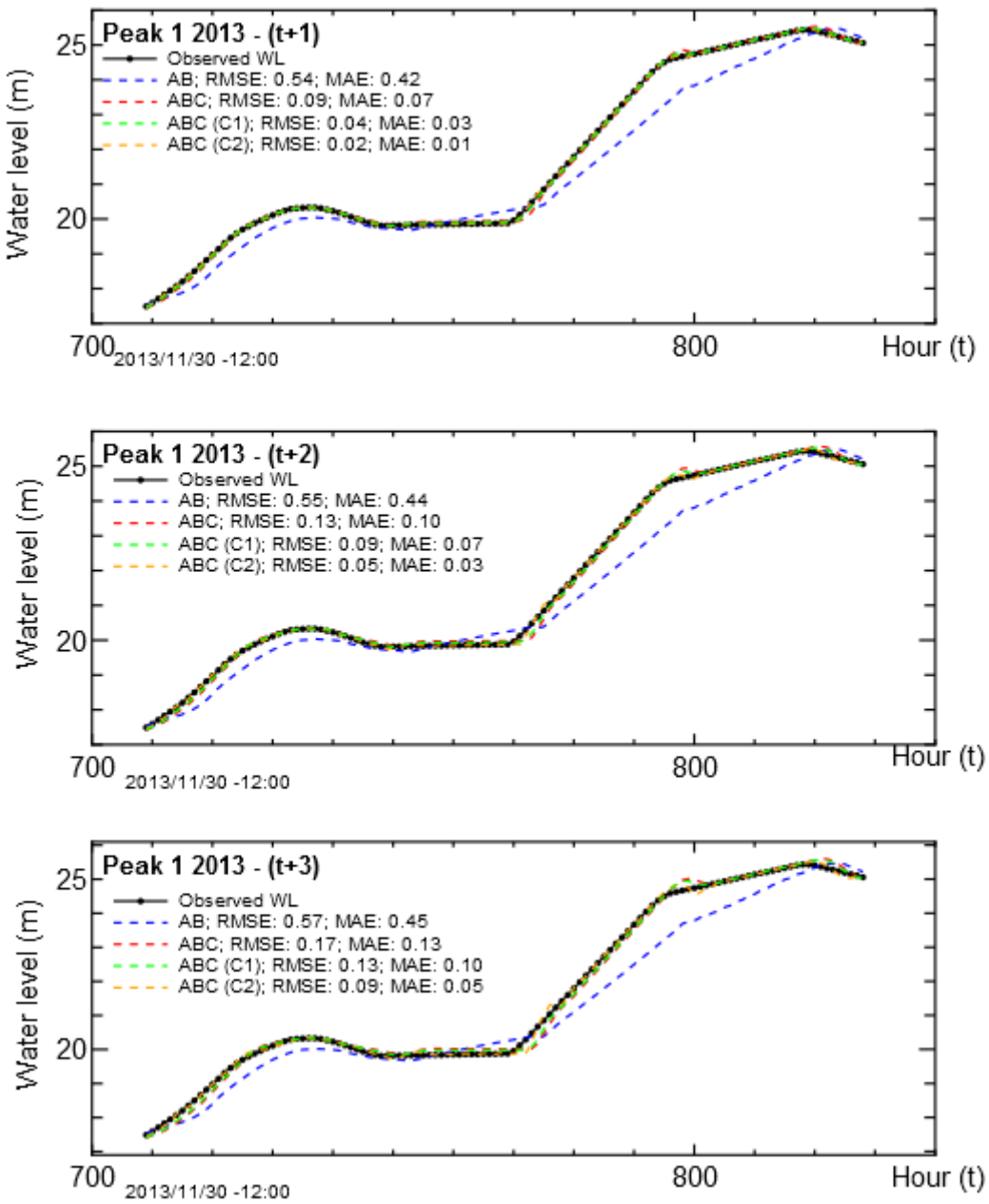

Figure 4.49. Improved flood prediction at C, peak 1 by updated A coefficients - hourly, 2013

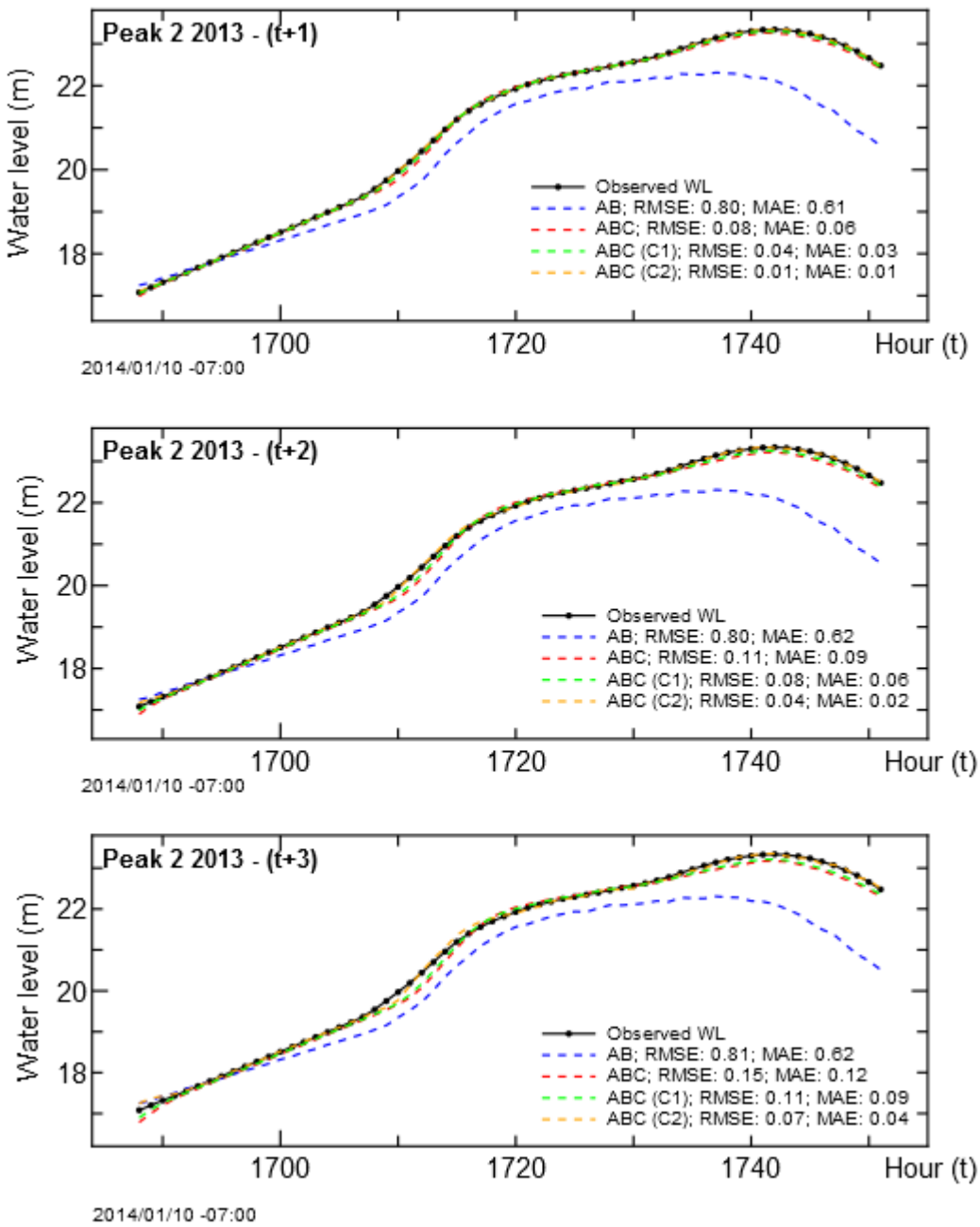

Figure 4.50. Improved flood prediction at C, peak 2 by updated A coefficients - hourly, 2013

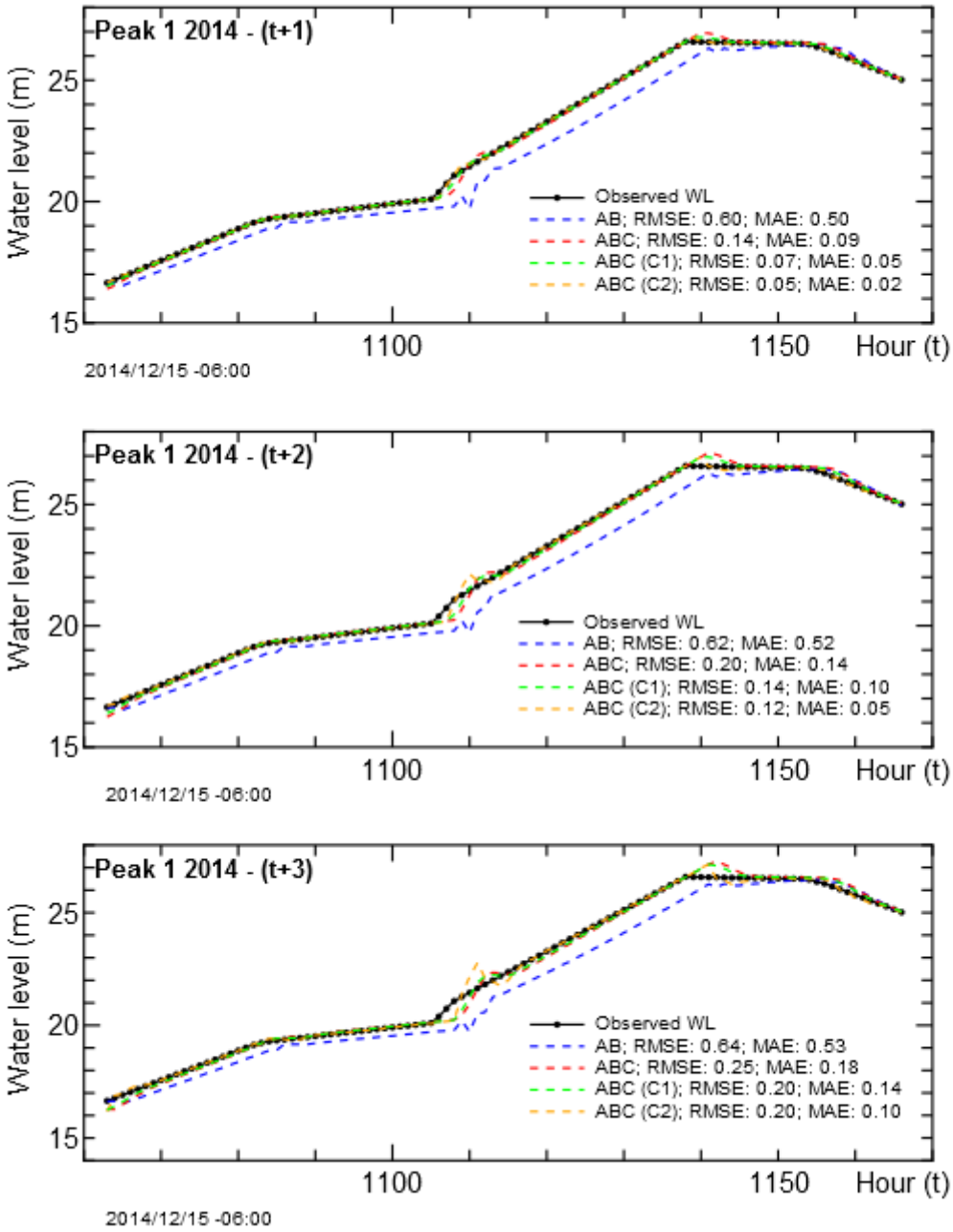

Figure 4.51. Improved flood prediction at C, peak 1 by updated A coefficients - hourly, 2014

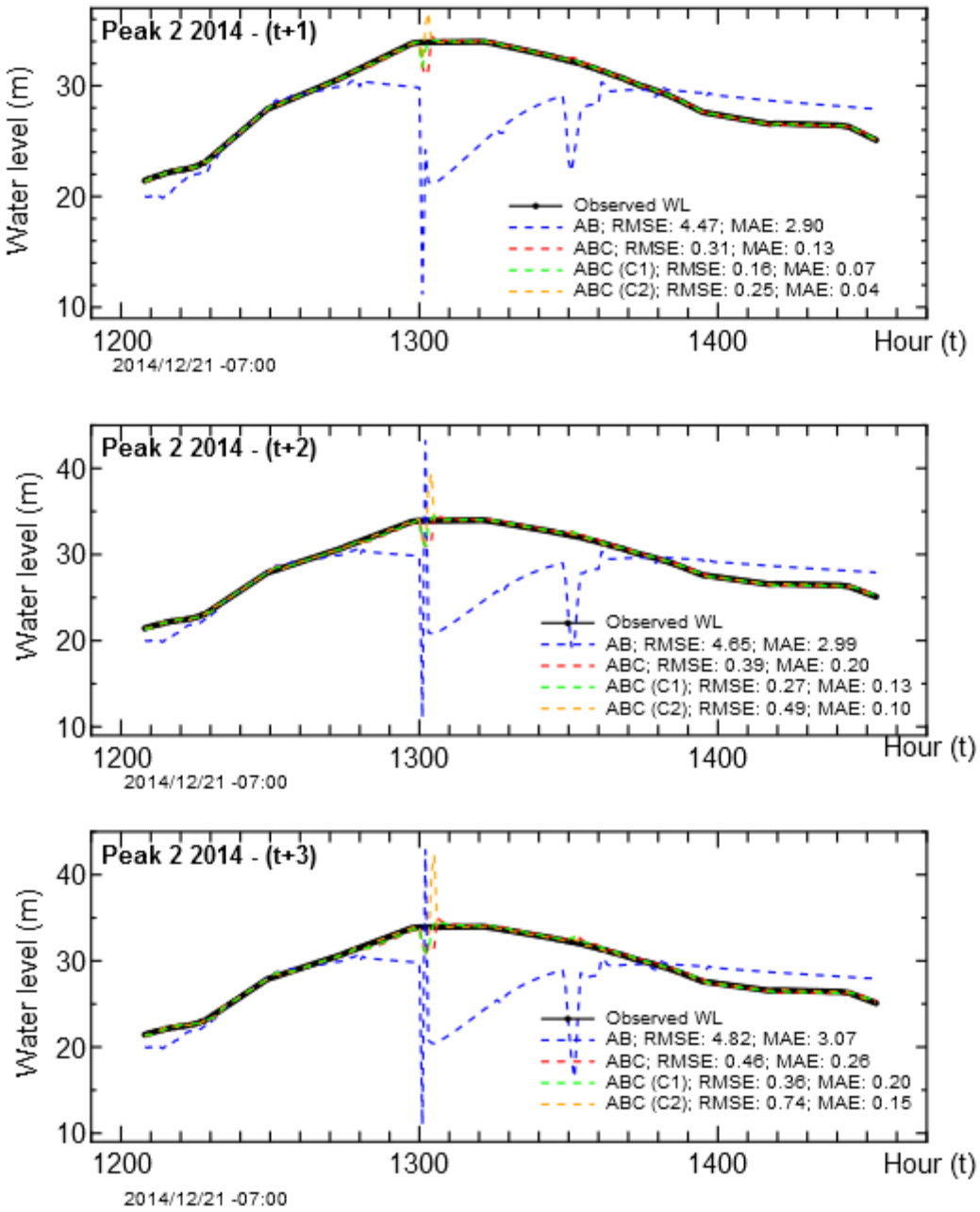

Figure 4.52. Improved flood prediction at C, peak 1 by updated A coefficients - hourly, 2014

4.7.4 *Improved Early Flood Prediction at Guillemard Bridge (D)*

4.7.4.1. *Prediction at D at selected flood level*

Figures 4.53 to 4.55 illustrate water level prediction at D up to 5 hours in advance for year 2011, while Figures 4.56 and 4.57 for 2013 and Figures 4.58 and 4.59 for 2014. Overall results show that by incorporating past forecasting station data of *t-1* improved the prediction regardless of any rainfall event, i.e., upstream-first rainfall, heavy local rainfall at the forecasting station and downstream-first rainfall. By applying the correction method, the quality of prediction was improved for most cases, especially when the water level was in rising state and decreasing state. However, the difference of correction method 1 and 2 (green and orange line) with non-correction (red) was very minimal, less than 50 cm as shown in Figure 4.53, upper right.

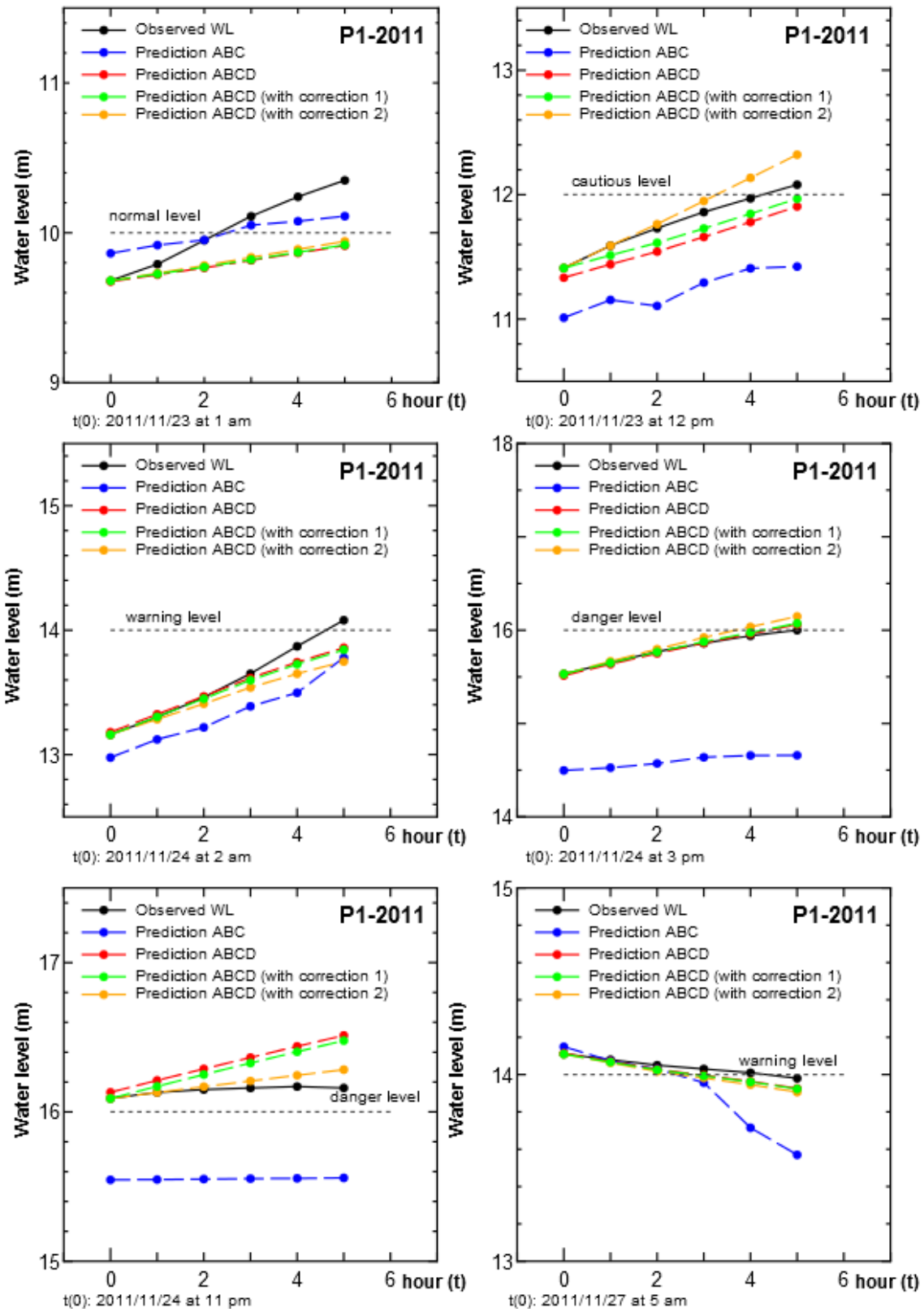

Figure 4.53. Improved flood prediction at D at certain flood level, peak 1 2011.

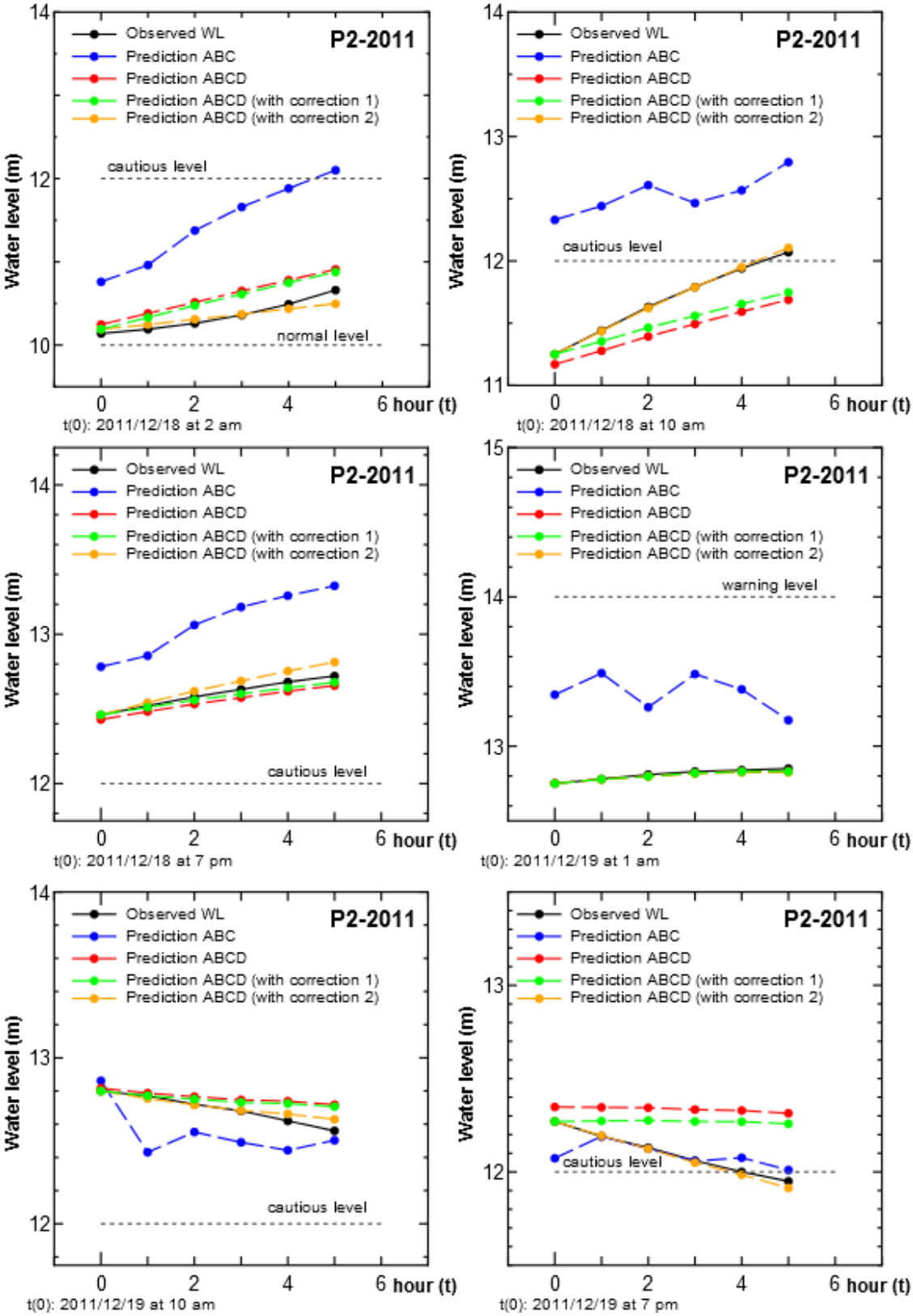

Figure 4.54. Improved flood prediction at D at certain flood level, peak 2 2011.

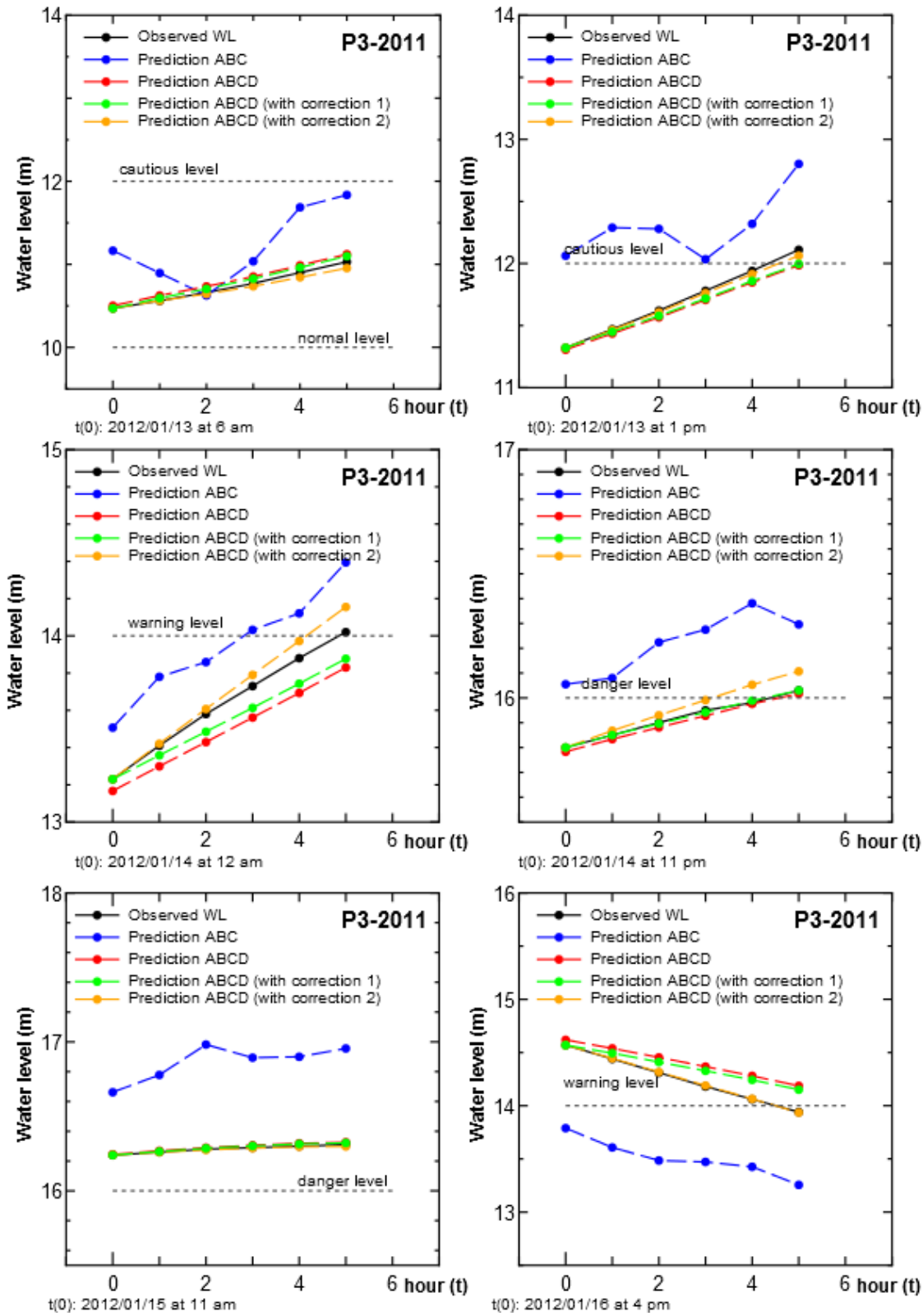

Figure 4.55. Improved flood prediction at D at certain flood level, peak 3 2011.

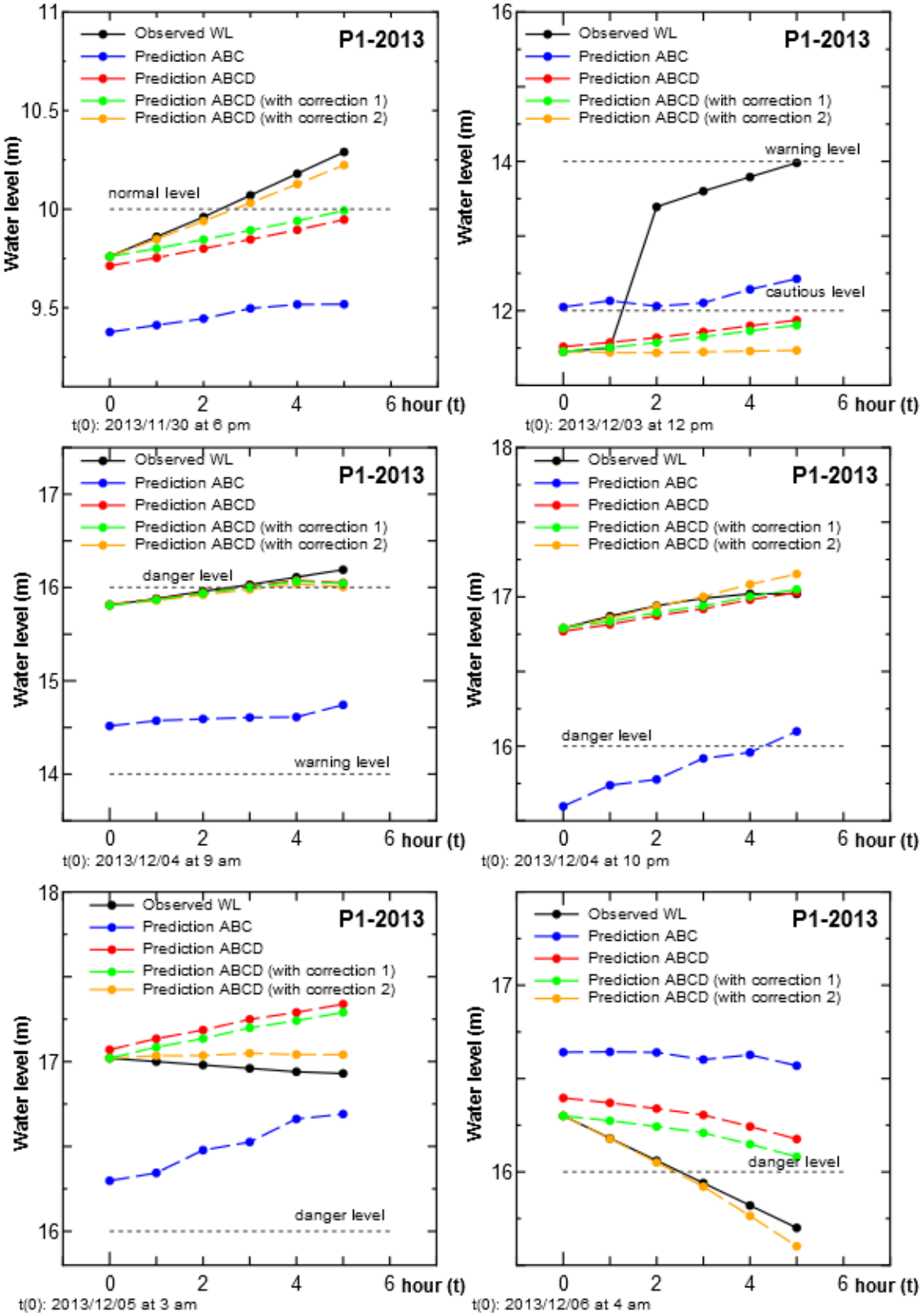

Figure 4.56. Improved flood prediction at D at certain flood level, peak 1 2013.

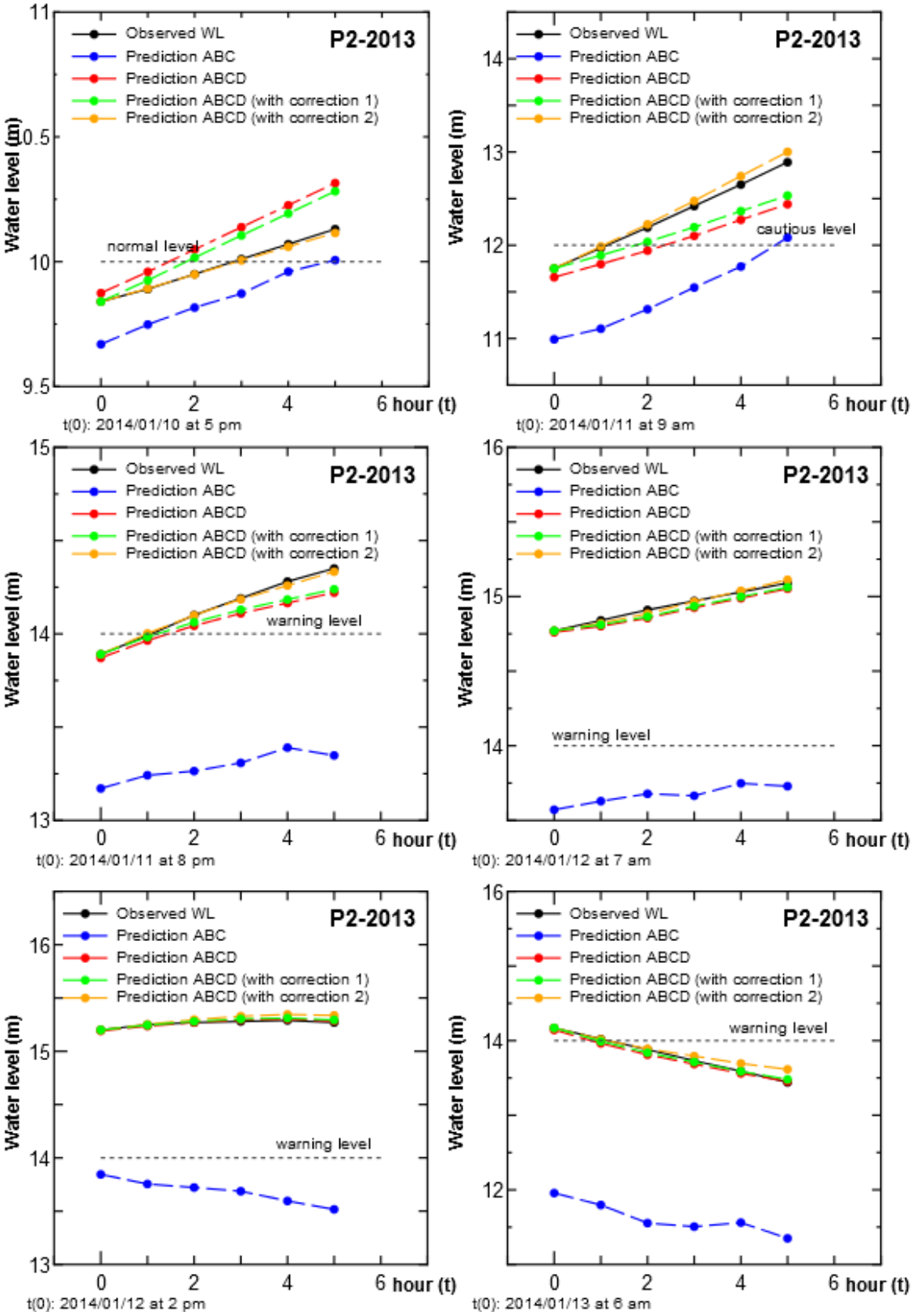

Figure 4.57. Improved flood prediction at D at certain flood level, peak 2 2013.

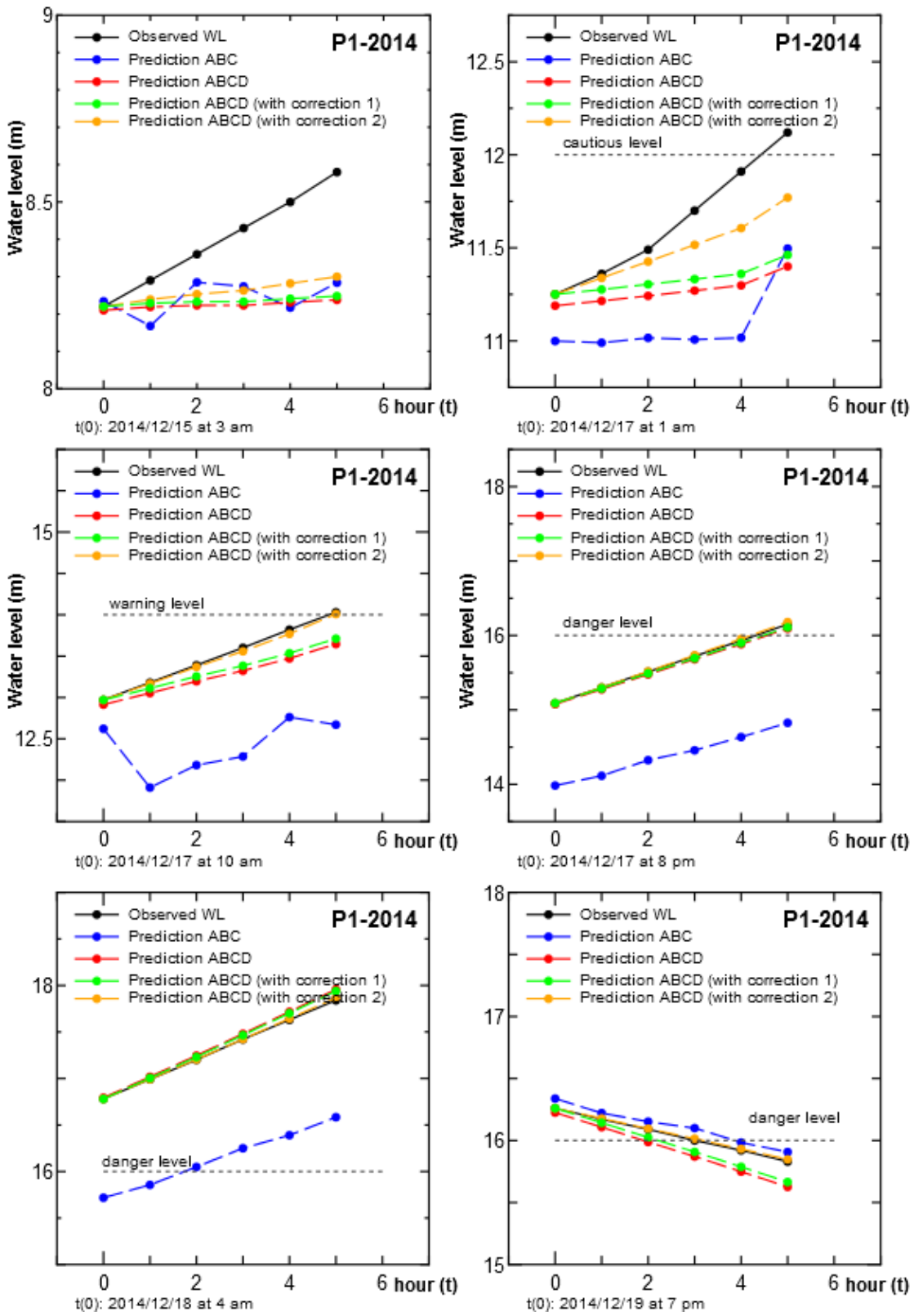

Figure 4.58. Improved flood prediction at D at certain flood level, peak 1 2014.

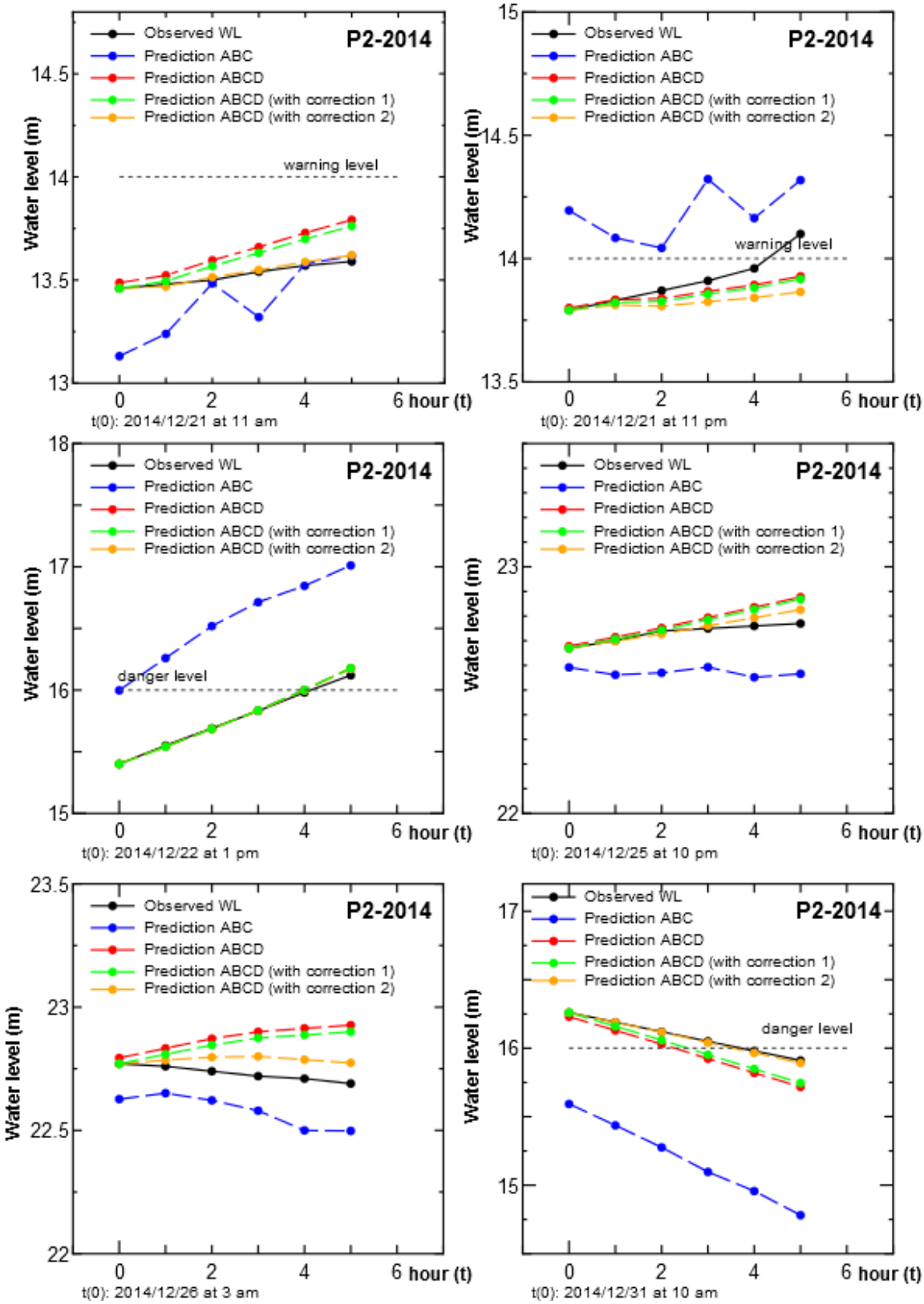

Figure 4.59. Improved flood prediction at D at certain flood level, peak 2 2014.

4.7.4.2. *Prediction at D by updated A coefficient hourly*

Figures 4.60 to 4.66 show the results of flood prediction of hourly updated A coefficient up to 5 hours in 2011, 2013 and 2014, from starting of the flood event, until the water level started to recede. The improved model showed good quality of prediction for all cases as the RMSE and MAE had improved very much compared with those utilizing upstream information only. By applying the correction methods, quality of prediction was also improved. However, the correction 2 method gave good prediction only if all past information was available (no missing or false data) similar to those as shown in the Kuala Krai (C) events. The reason of sudden jump seen in the observation data in Figure 4.63 in 2013 may be related to some mechanical trouble but not clear, and at that point, correction method 2 could not trace and showed somewhat increased overestimate or underestimate as the prediction time length increased.

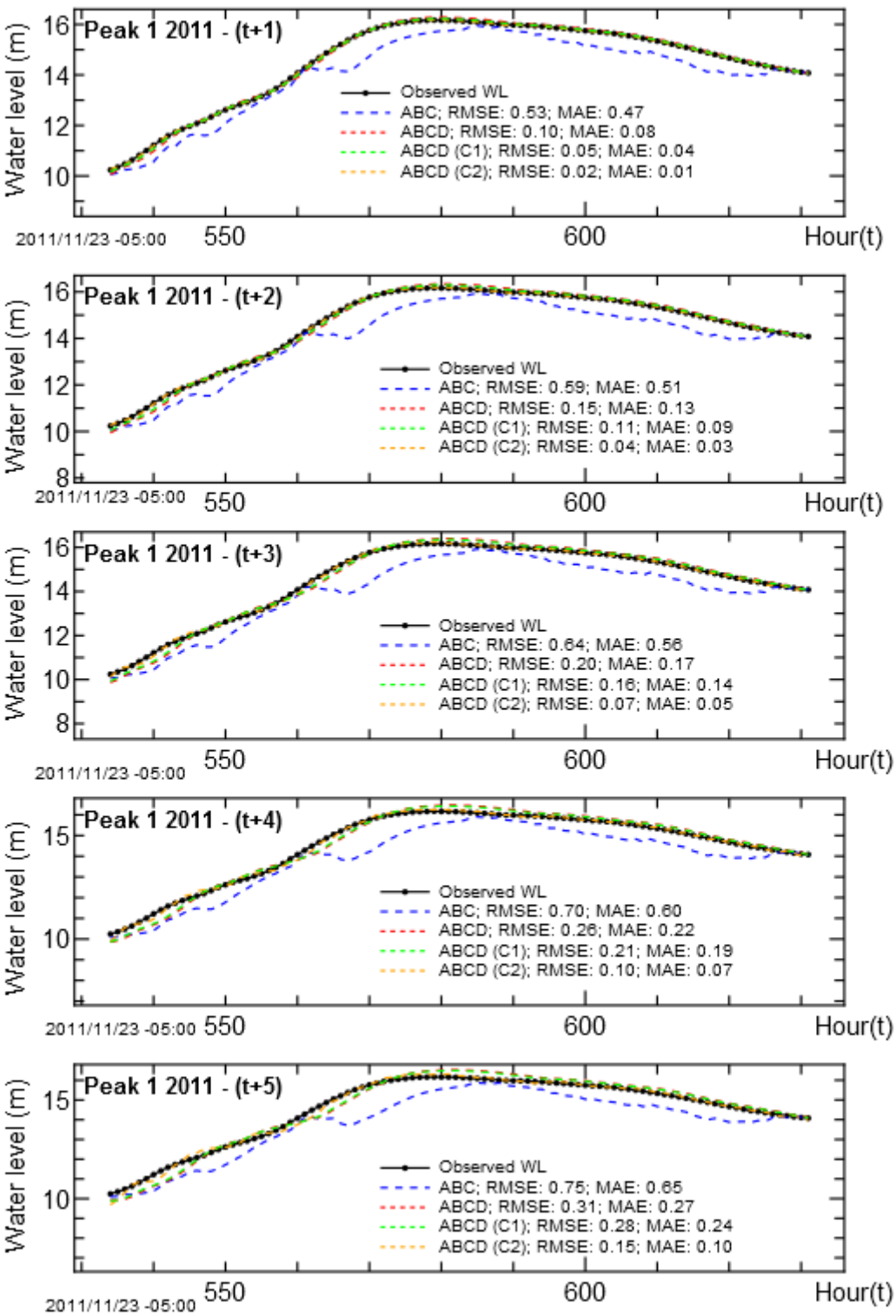

Figure 4.60. Improved flood prediction at D, peak 1 by updated A coefficients - hourly, 2011

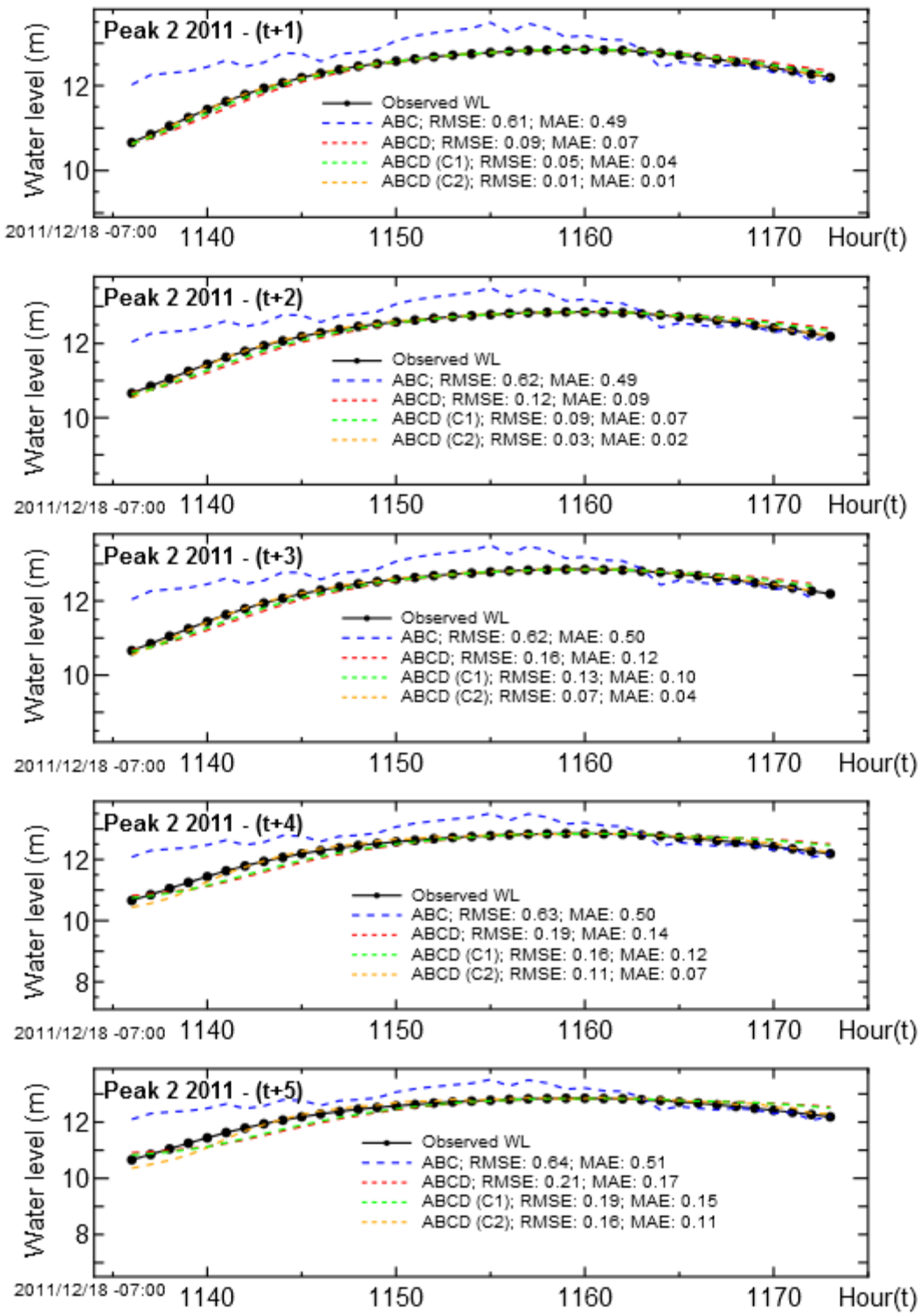

Figure 4.61. Improved flood prediction at D, peak 2 by updated A coefficients - hourly, 2011

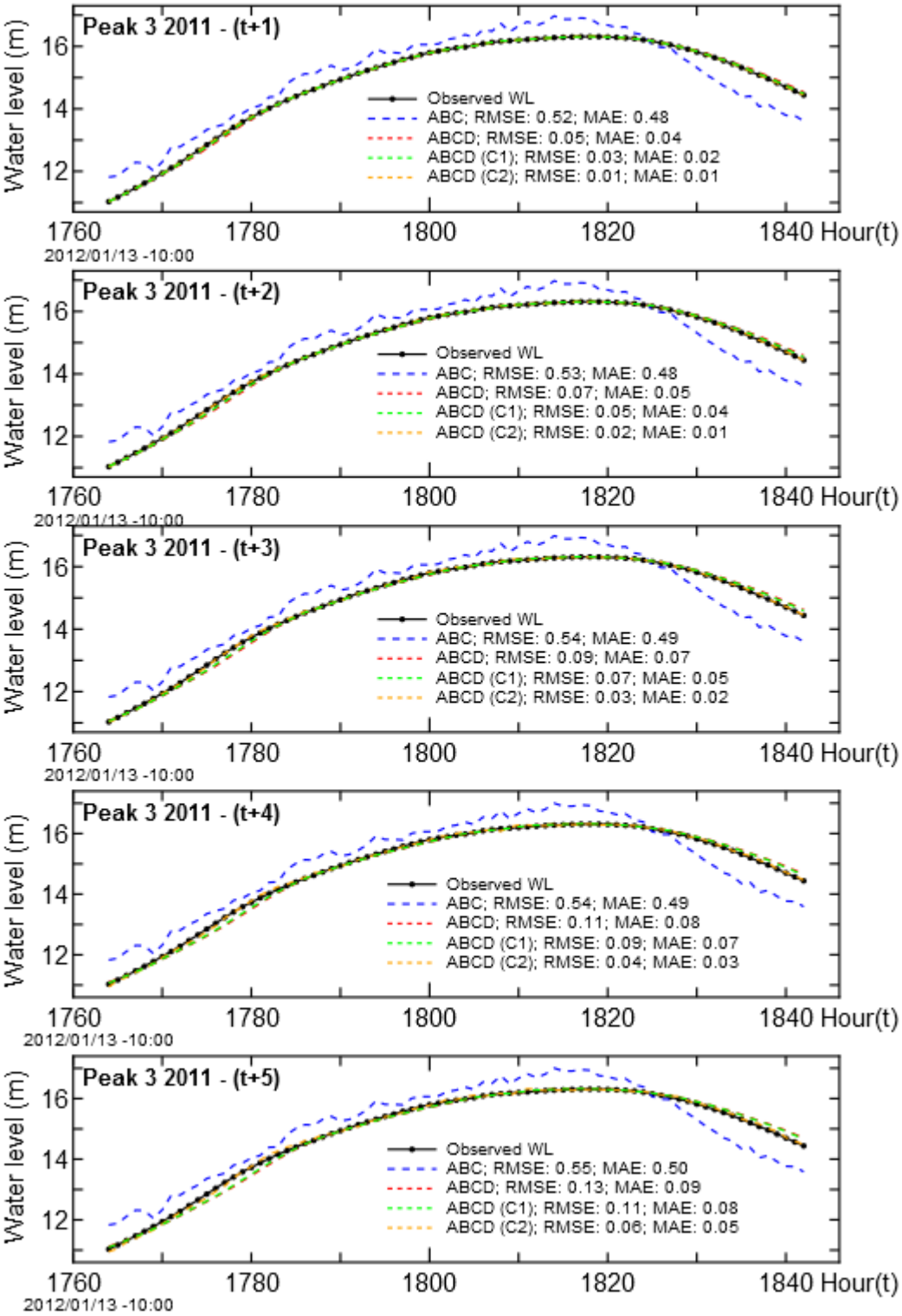

Figure 4.62. Improved flood prediction at D, peak 3 by updated A coefficients - hourly, 2011

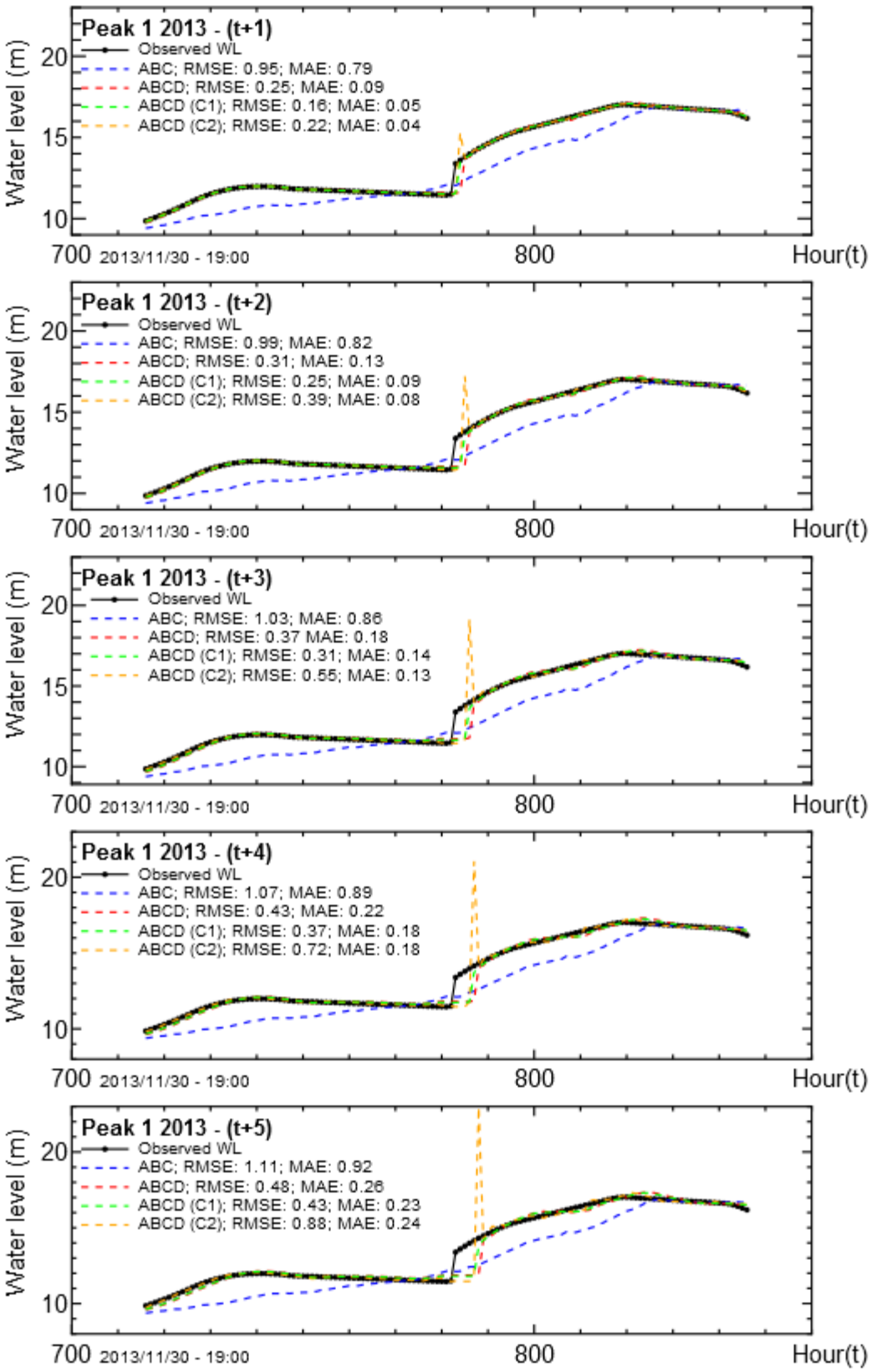

Figure 4.63. Improved flood prediction at D, peak 1 by updated A coefficients - hourly, 2013

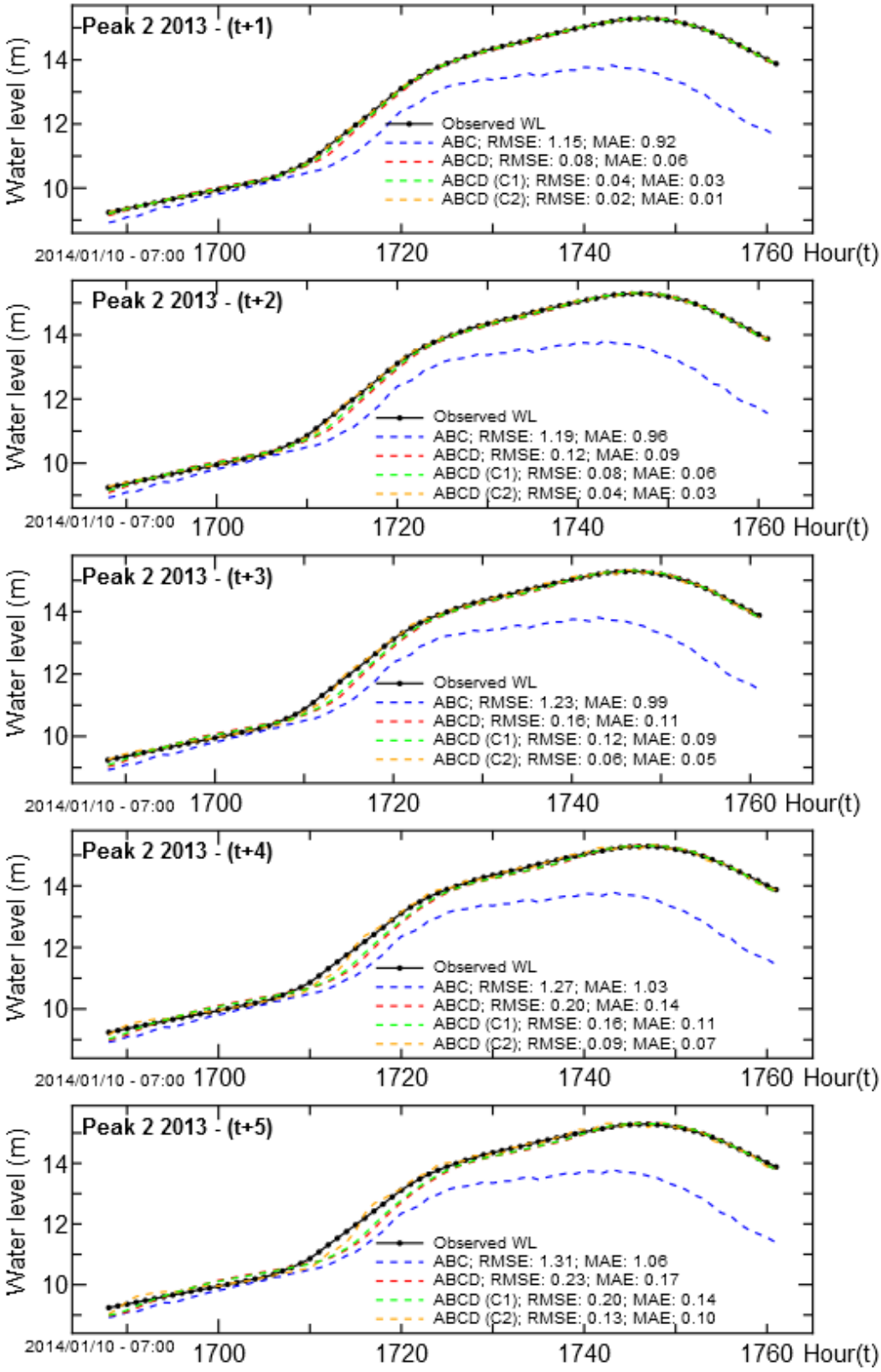

Figure 4.64. Improved flood prediction at D, peak 2 by updated A coefficients - hourly, 2013

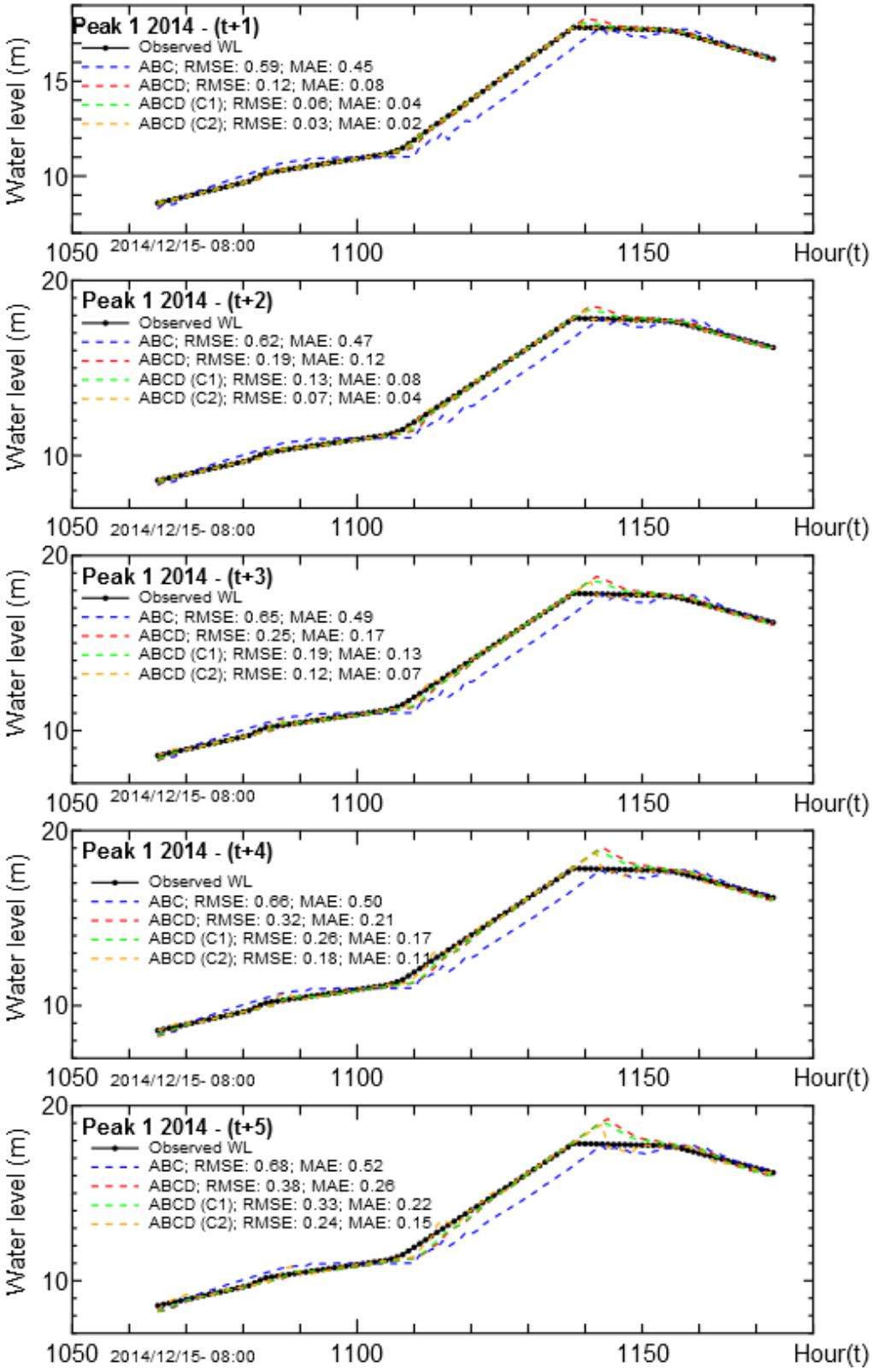

Figure 4.65. Improved flood prediction at D, peak 1 by updated A coefficients - hourly, 2014

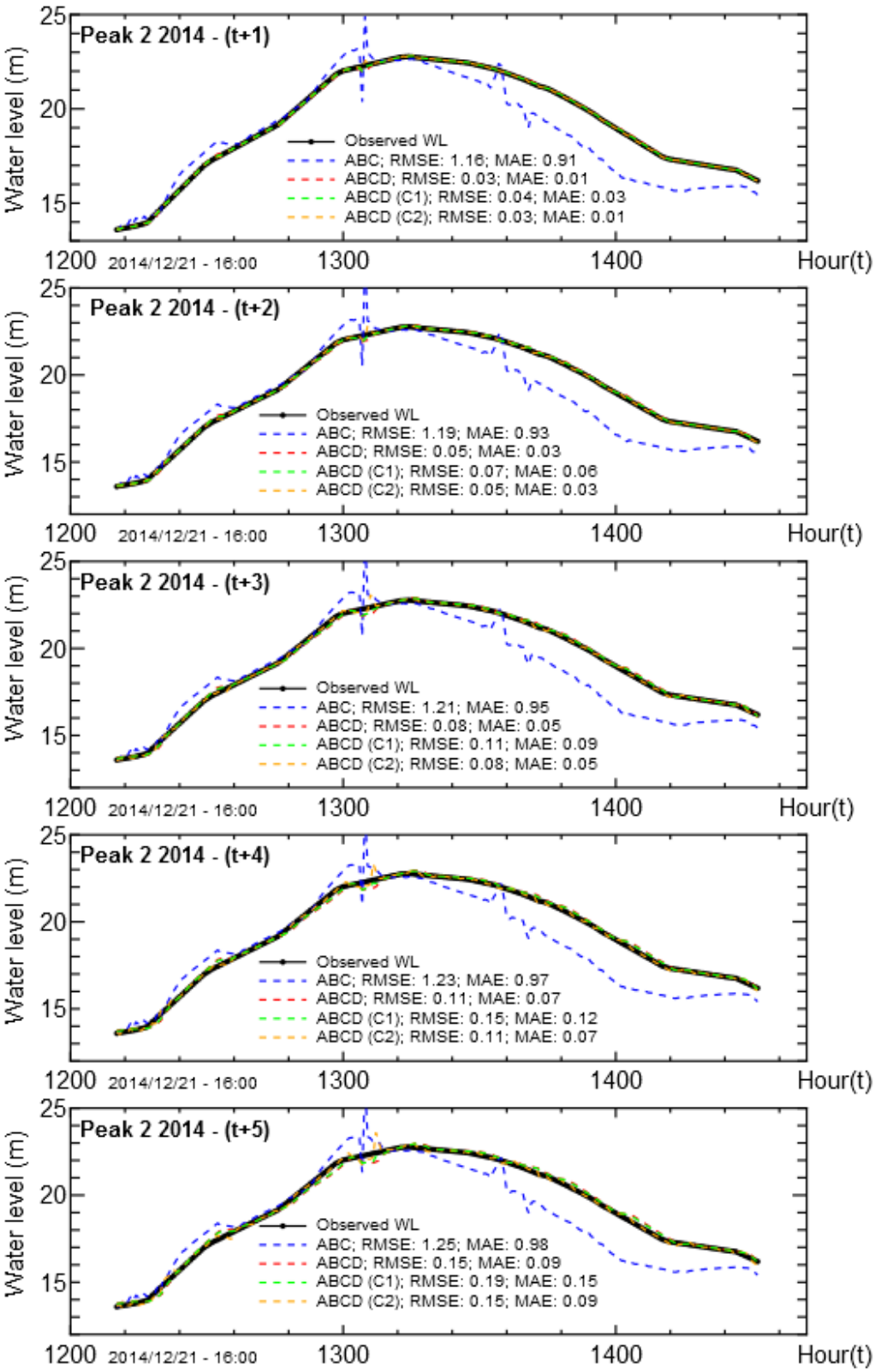

Figure 4.66. Improved flood prediction at D, peak 2 by updated A coefficients - hourly, 2014

4.7.5 *Performance of A Coefficients for Different Flood Event*

Basically there are roughly two types of monsoon scenario in Kelantan watershed as discussed in section 4.4.5: one, the heavy rainfall starts from upstream, then move to downstream, and another, from downstream moving to upstream. To investigate the performances of the observation-based model both original and improved models, A coefficients versus the variables used in calculating the coefficients for both scenarios were plotted as shown in Figures 4.67 and 4.68. The variables were arranged as shown in Table 4.4 for Kuala Krai and Table 4.5 for Guillemard Bridge.

Table 4.4: Kuala Krai Variables

Variables (X)	**Source**
1	Galas (t-4)
2	Galas (t-5)
3	Galas (t-6)
4	Lebir (t-3)
5	Lebir (t-4)
6	Lebir (t-5)
7	Kuala Krai (t-1)

Table 4.5: Guillemard Bridge Variables

Variables (X)	**Source**
1	Galas (t-13)
2	Galas (t-14)
3	Galas (t-15)
4	Lebir (t-9)
5	Lebir (t-10)
6	Lebir (t-11)
7	Kuala Krai (t-5)
8	Kuala Krai (t-6)
9	Kuala Krai (t-7)
10	Guillemard Bridge (t-1)

Figure 4.67 illustrates the value of A coefficients at selected flood level at D in 2011, where the downstream area experienced the first heavy rainfall. Blue line shows the value of A coefficients by original model and the red line is for the improved model. Both models show that the nearest station to the forecasting station gave highest coefficient value as shown in original model, variables no. 8 and 9 (Kuala Krai) and in improved model, variables no. 8, 9 and the forecasting station data itself, no 10.

Figure 4.68 shows the values of A coefficients at selected level at D in 2013 where the source of flood started from upstream. Upstream variables no. 1, 2 and 3 gave higher coefficient values compared with the nearest variables to the downstream forecasting station, except the past forecasting data itself as this value was superior and near to the observed forecasting data when calculating the A coefficients. By improved model, good prediction can be made regardless of any scenarios since via this method, incorporating the past forecasting station will improve the prediction since the variable provides higher coefficients values regardless of any rainfall scenarios.

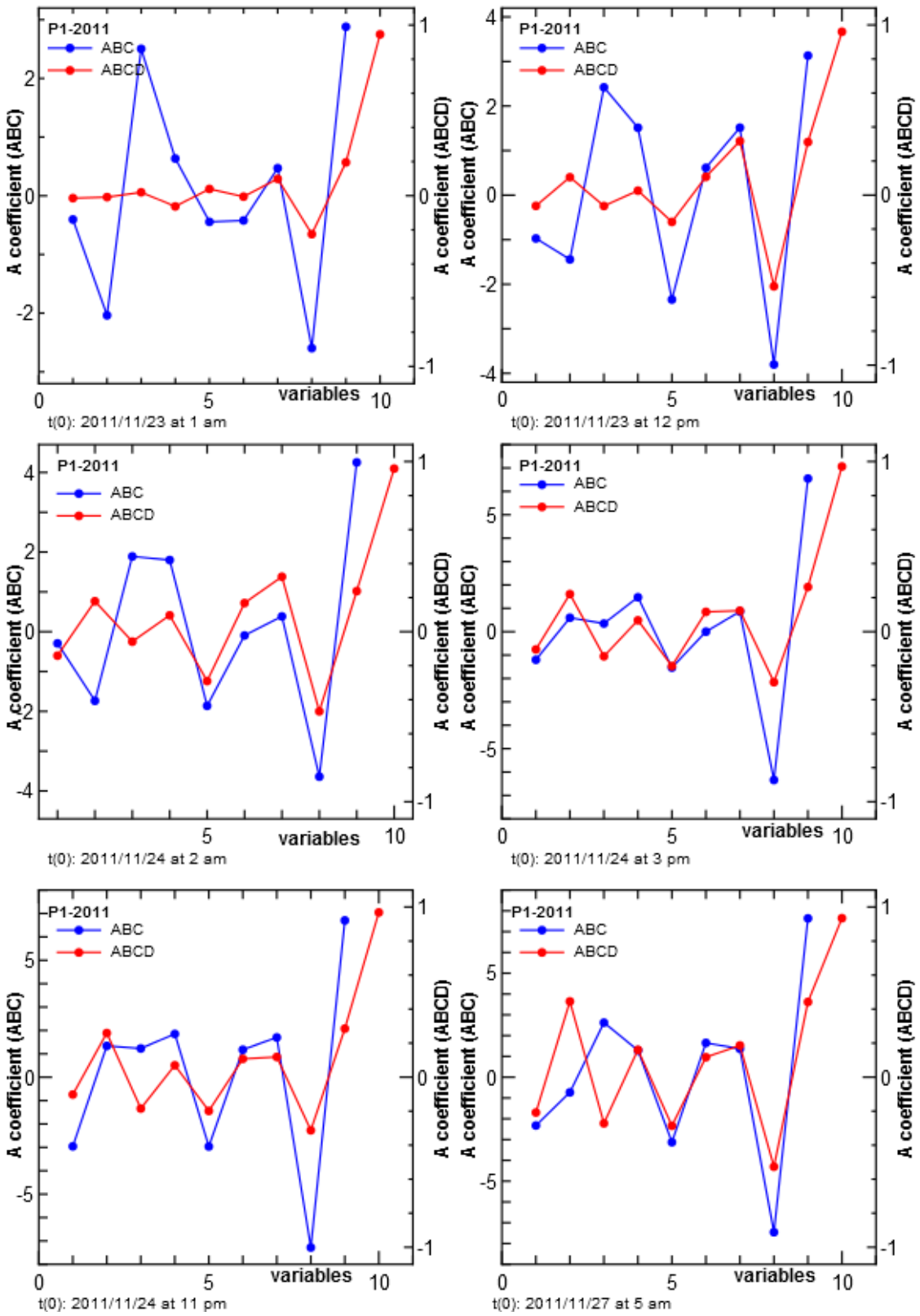

Figure 4.67. Comparison of A coefficients value for peak 1, 2011

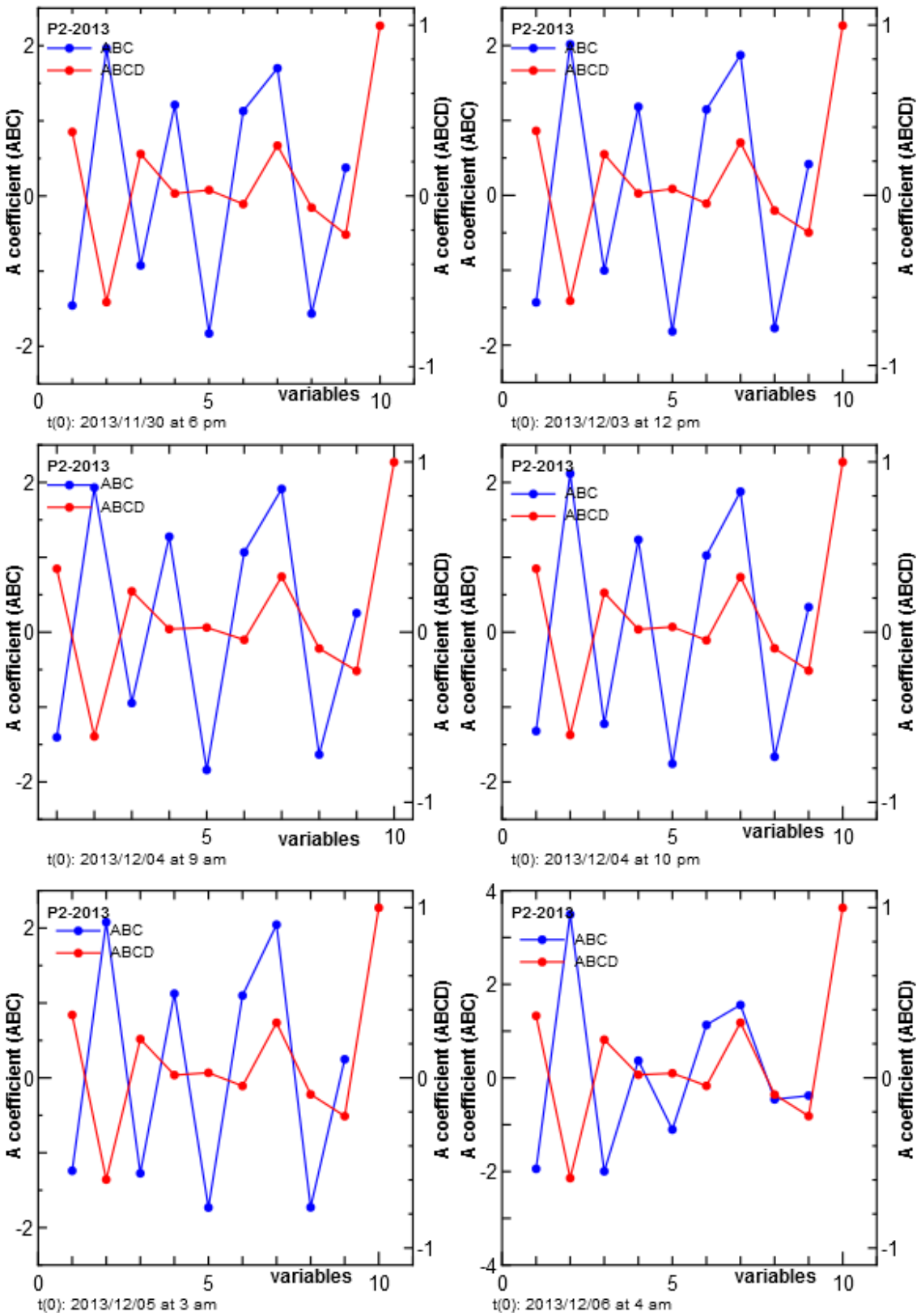

Figure 4.68. Comparison of A coefficients value for peak 2, 2013

4.8 *Discussion*

4.8.1 *Predictability of New Linear Observation-based Model*

Early prediction methods of water level at Kuala Krai (C) and Guillemard Bridge (D) has been discussed using the upstream observation-based approach. The method developed takes advantage of historical data obtained at upstream water level stations (telemetry stations) which reflect the future water level at downstream stations. A delay time of 5 hours is chosen from A to C and 4 hours from B to C. For station D, a delay time of 14 hours is chosen for A, 10 hours for B and 6 hours for C from cross-correlation analysis. Sensitivity of the lag range was conducted using lag range values of 3, 5 and 7 hours. From the results, the difference between lag range of 3, 5 and 7 is very small. Thus in this study, lag range of 3 is selected for early prediction at station C and D to produce earliest flood prediction. Three types of early flood prediction were made for year 2011 and 2013, constant coefficient, updated coefficient at certain flood level and updated hourly coefficients when new data were fed into the system. From the results using constant A for prediction at C, water level from B was good enough as it gave relatively good fit, especially during peak event. However for prediction at D, the effect of joining tributaries located in between C and D were clearly shown as all prediction using single stations and combinations failed to fit the hydrograph, especially during high peak event. By updating the A coefficient to predict flood at C, a combination of A with average delay time of 5 hours and B, 4 hours gave more reliable results compared with that by using single station. Similarly at D, the case by utilizing all upstream point A (14 hours), B (10 hours) and C (6 hours) provided higher predictability for most event in 2011 and 2013. Most of the cases, the model predicted within 1 m from the starting time of flood to several hours except peak 1 in 2013. However predictability at the beginning of flood is somewhat difficult if downstream rainfall comes earlier than in the upstream.

4.8.2 *Predictability of New Improved Linear Observation-based Model*

A new improved model was developed to enhance the accuracy of early prediction at C and D by incorporating past data of the forecasting station (t-1) together with upstream water level information. From the result, a good prediction can be made for both at C and D regardless of any rainfall and flood scenarios in Kelantan watershed. The new model produced MAE within 0.3 m (t+3) hours at C and (t+5) hours at D. By applying the correction method, it had improved the prediction for most cases especially when the water level was in rising state and decreasing

state, however the difference of correction method and non-correction was very minimal, less than 50 cm. The correction method 2 however will give reliable prediction if all information was sound and reliable.

4.8.3 *Highlights of Observation-based Modelling*

The new observation-based model (A) in this study utilized all information available in the upstream of forecasting station, where the time sequence of flood information that flowing into the river is used. Whereas ARMA model make uses of the past values of forecasting station to be modelled to predict future values. These values however run away from the prediction points hence becomes no relation with future water level as shown in Figure 4.69. To improve the flood prediction in Kelantan, a new improved model (B) incorporates the latest past information of forecasting point at $t-1$ hour and correction method to minimize the error.

As the delay time of Kelantan watershed varies each year based on graphical inspection, the model in this study introduced the average delay term, contrary to other models such as Multi-linear regression (MLR), and ANN that utilized only single average delay value. This model is suitable to be used regardless of any rainfall and flood scenarios occurred in this watershed.

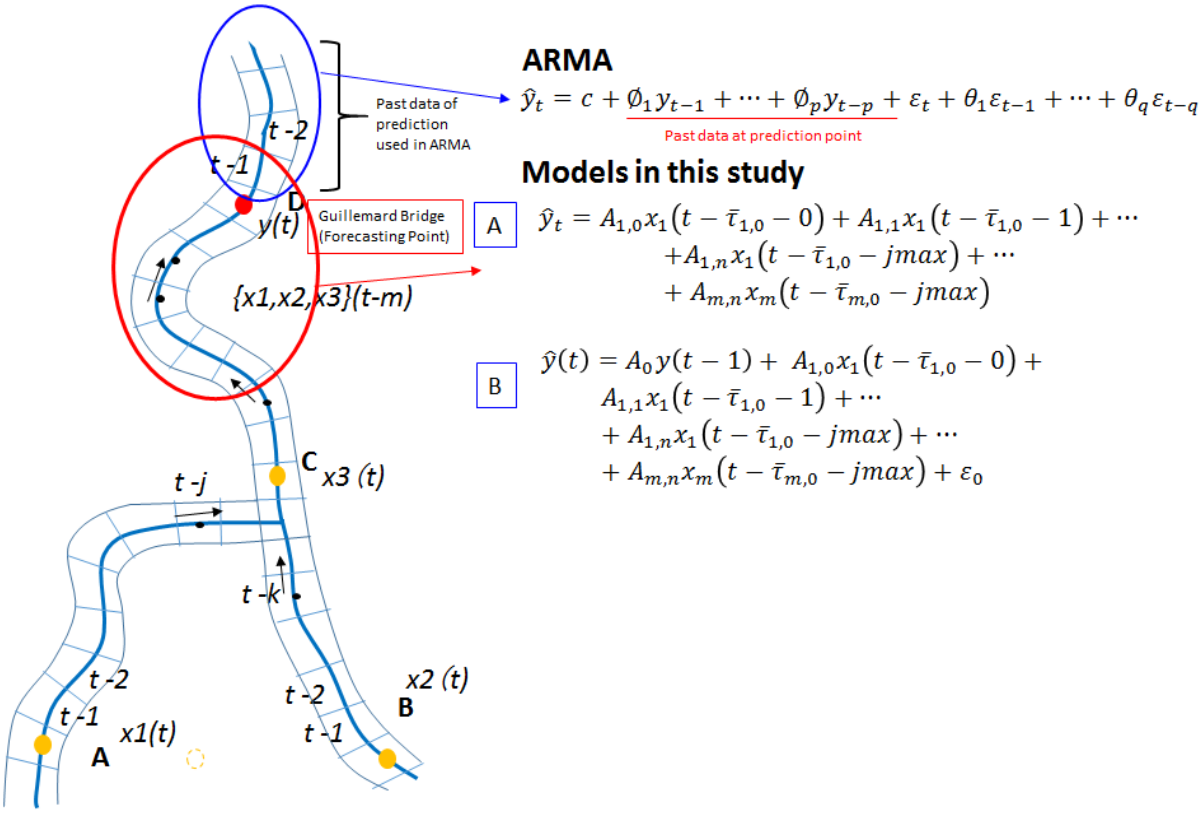

Figure 4.69. Comparison of ARMA and models in this study.

4.9 *Conclusion*

In this study, a new observation-based model for early flood prediction in Kelantan watershed was developed and presented.

1) Based on the idea that future water level at downstream point is formed by the information that is flowing in the river from upstream, not by the historical data of the prediction point itself, the developed model uses the linear combination of historical data at upstream water level stations (telemetry stations) to predict the water level at downstream point.
2) Conventional graphical method and cross-correlation analysis were conducted to find suitable parameters such as delay time and lag range. Using the former method, the delay time found for each year varies and some events give negative delay time. From cross-correlation analysis, a delay time of 4-5 hours are found from station Galas (A) and Lebir (B) to Kuala Krai (C) and 10-14 hours from A and B to Guillemard Bridge (D) , and 3-6 hours from C to D. From lag range sensitivity analysis, lag range of 3 hours was selected for early prediction at C and D.
3) Using linear combination of the upstream past data as the prediction equation, coefficients were regressed by the least square method through sampling over monsoon season from 2007 to 2013.
4) For early prediction at C, a combination of A with average delay time of 5 hours, and B with 4 hours gave more reliable results compared with that using single station. Similarly at D, the case by utilizing all upstream point A (delay time 14 hours), B (delay time 10 hours) and C (delay time 6 hours) provided higher predictability than using single upstream station for most events in 2011 and 2013. In most of the cases, the model predicted within 1 m from the starting time of flood to several hours.
5) For the case when downstream rainfall occurred earlier than in the upstream, it was found that predictability became somewhat deteriorated. To enhance predictability, a new improved model by incorporating the most recent data at forecasting station itself was developed.
6) The improved model successfully gave good prediction up to 3 hours for C and 5 hours for D with maximum Mean Average Error (MAE) of 0.3 meter for all events in years 2011, 2013 and 2014.

7) Correction method 1 and 2 were also introduced. However the difference of correction method and non-correction was very minimal, less than 50 cm. The correction method 2 gave reliable prediction if all information was sound and reliable.

This observation-based method can give reliable prediction of downstream point continuously by updating the A coefficients every 1 hour when new upstream telemetry data are added. For future work, the author plans to apply this model to the prediction at further downstream point in urban area located more downstream from Guillemard Bridge (D).

5 Numerical Approach for Early Flood Prediction

5.1 *Introduction*

Observation based approach may work for early prediction and give early flood warning for prediction point basis, however, it does not provide explicitly the knowledge of rainfall-runoff process taking place in the whole watershed. Since Kelantan watershed experience floods/inundations in many places almost every year during the north east monsoon season, it will be future requirement to understand the water flows in river and subsurface more dynamically than the observation-based prediction, and to use numerical prediction for early warning and for planning countermeasures to reduce damages by flood/inundations.

There are a number of numerical simulators, called as physically-based, distributed parameter hydrological model, such as TOPMODEL (Beven and Kirby, 1979; Beven et. al., 1984), TOPKAPI (Liu and Todini, 2002; Liu et al., 2005), MIKE-FLOOD (Danish Hydraulic Institute, 2007), IFAS (PWRI, 2009), GETFLOWS (Tosaka et. al, 2000) and so on. The results of such models can give far more concrete information than the statistical/conceptual models, at the expense of complicated preparation work and computer time (Singh, 1964; Pilgrim, 1976; Jakeman, 1993).

In this chapter, model construction processes of the Kelantan River watershed including gridding, parameter setting and initialization are described, then, as the main part of this chapter, the estimation methods of rainfall distribution, which is the most controlling input for the simulation, are discussed. Finally, reliability of the estimated distributions from all rainfall stations available and from only telemetry stations are compared and discussed using calibration runs for year 2007 to 2013.

5.2 *Summary of Numerical Simulator*

In this study, GETFLOWS (Tosaka, 2000) was used to develop numerical-based model for early flood prediction in Kelantan watershed. Figure 5.1 illustrates the schematic of terrestrial water flow within a watershed. The fluid dynamics in GETFLOWS is based on the generalized Darcy's law for multi-phase and multicomponent fluid flow system. In GETFLOWS, surface and subsurface coupled fluid-flows are realized as one of the main features including contaminant and heat transport. Various types of interactions between surface water and groundwater, water and air, freshwater and saltwater can be fully treated by this simulator.

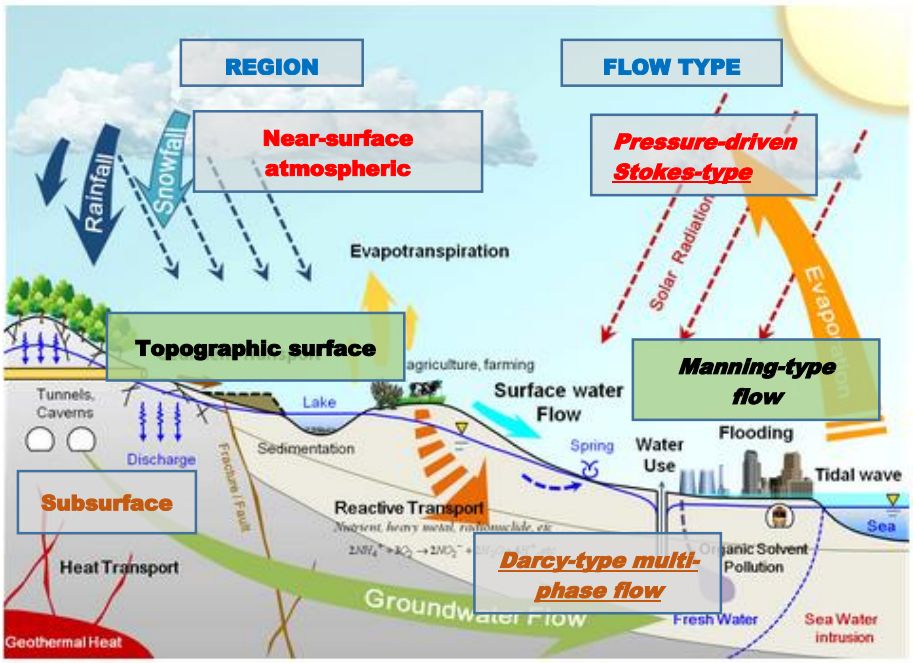

Figure 5.1. Schematic of terrestrial water flow (GETFLOWS's manual)

The mass balances equation in residual form can be written in gas composition (eq. 5.1) and water composition (eq. 5.2) as follows:

$$R_g = -\nabla.\left(\rho_g u_{g,x}\right) - \rho_g q_g - \frac{\partial(\rho_g \emptyset S_g)}{\partial t} = 0 \tag{5.1}$$

$$R_w = -\nabla.\left(\rho_w u_{w,x}\right) - \rho_w q_w + \rho_w \rho q_r - E - \frac{\partial(\rho_w \emptyset S_w)}{\partial t} = 0 \tag{5.2}$$

Here, R_g and R_w are residuals of gas and water component, respectively, and other subscripts g, w indicate gas and water phases, ρ is phase density, u is phase velocity, $\emptyset$ is rock porosity, S is phase saturation, q is source terms of water and gas components respectively, and E is the water mass lost by evapotranspiration effect.

The velocity laws of surface are based on diffusion wave approximation as shown in Eq. 5.3,

$$u_{w,x} = -\frac{R^{2/3}}{n}\frac{I}{|I|^{1/2}}, I = \left(\frac{\partial z}{\partial x} + \frac{\partial h}{\partial x}\right) \tag{5.3}$$

where, R is the hydraulic radius, n is Manning's roughness factor, I is the hydraulic gradient of channel flow with z:elevation of channel floor and h:water depth. For subsurface flow velocities, 2-phase Darcy's law is adopted as follows.

$$u_{w,x} = -\frac{Kk_{wg}}{\mu_w}\frac{\partial\psi_w}{\partial x} \tag{5.4}$$

$$u_{g,x} = -\frac{Kk_{rg}}{\mu_g}\frac{\partial\psi_g}{\partial x} \tag{5.5}$$

where, K is the permeability of porous media, μ_w, μ_g are phase viscosities, k_{rw}, k_{rg} are the relative permeability of water and gas phases, Ψ_w, Ψ_g are hydraulic potential of water and gas phases, respectively.

Table 5.1 shows functional comparison chart between GETFLOWS and other simulators that is currently available.

Table 5.1. Functional comparison of GETFLOWS and other simulators (www.getc.co.jp)

SIMULATOR	Dimension	Fluid Flow								Material Transport								Heat Transport						Sediment transport			Deformation			Discretization		Parallel Computing	Preprocessor	Manual		
		Surface Flow	Water	Air	Water Vapour	NAPL	Density Flow	Compressibility	Viscosity	Advection	Dispersion/Diffusi	Adsorption	Dissolution	Precipitation	Volatilization	Ion Exchange	Chemical Reaction	Decay	Advection	Conduction	Eradiation	Heat Exchange	Phase Transfer	Bed Load	Suspended Load	Landslide	Landform change	Elastic	Inelastic	Coupled Flow	Spatial	Temporal			Theoretical	Operating	V&V
GET FLOWS	3	X	X	X	X	X	X	X	X	X	X	X	X		X	X	X	X	X	X	X	X	X	X	X		X				IFDM	FI	X		X		
MIKE SHE	3	X	X							X	X	X						X						X	X		X				FDM			X	X	X	X
GFLOW	3	X	X																												FDM			X	X	X	
GS FLOW	3	X	X																												FDM				X	X	X
MT3DMS	3		X							X	X	X					X	X													FDM	FI			X	X	X
MOD FLOW-2000	3	X	X																									X	X	X	FDM	FI		X	X	X	
RT3D	3		X							X	X	X					X	X													FDM			X	X	X	X
FEHM	3		X	X	X			X	X	X	X	X	X				X	X	X	X		X	X								FEM	FI			X	X	X
TOUGH2	3		X	X	X	X	X	X	X	X	X	X	X		X			X	X	X			X								IFDM	FI	X		X		
DTRANSU	3		X				X			X	X	X																			FEM	FI		X	X	X	
CODE_BRIGHT	3		X	X	X			X	X	X	X		X						X	X			X					X	X	X	FEM	FI		X	X	X	X
Open GeoSys	3		X	X	X		X	X	X	X	X	X	X			X		X	X	X		X	X					X	X	X	FEM		X	X	X	X	X
TOUGH-FLAC	3		X	X	X	X	X	X	X	X	X	X	X	X					X	X			X					X	X	X	IFDM						
ROC MAS	3		X		X														X	X								X	X	X	FEM						
STOMP	3		X	X	X	X	X	X	X	X	X	X	X		X			X	X	X			X								IFDM	FI		X	X	X	X
HST3D	3		X					X	X	X	X	X						X	X	X											FDM			X	X	X	X
HYDROTHERM	3		X	X	X			X	X										X	X		X	X								FDM	FI		X	X	X	X

FDM: Finite Differential Method
IFDM: Integral Finite Differential Method
FEM: Finite Element Method
FI: Fully Implicit Method

5.3 *Basic Modelling Procedure*

5.3.1 *Grid Construction*

For constructing Kelantan watershed grid system, SRTM with 90 x 90m resolutions is used to generate over 393,185 meshes using the grid generator supplied by the simulation system. Data of digitized river networks were provided by DID in KML files.

Figure 5.2 (step 1) shows the river networks in the watershed, and the grid baselines are shown in Figure 5.2(step 2). Grid generator (Tosaka and Sasaki, 2014) was used to create grid system from the baseline as shown in step 3. And finally, a river-channel-fitted grid system was generated to give a detail representation of river channels especially along the river, confluence of Kelantan River as shown in the last of Figure 5.2. Figure 5.3 shows the final grid Kelantan watershed in three dimensional view.

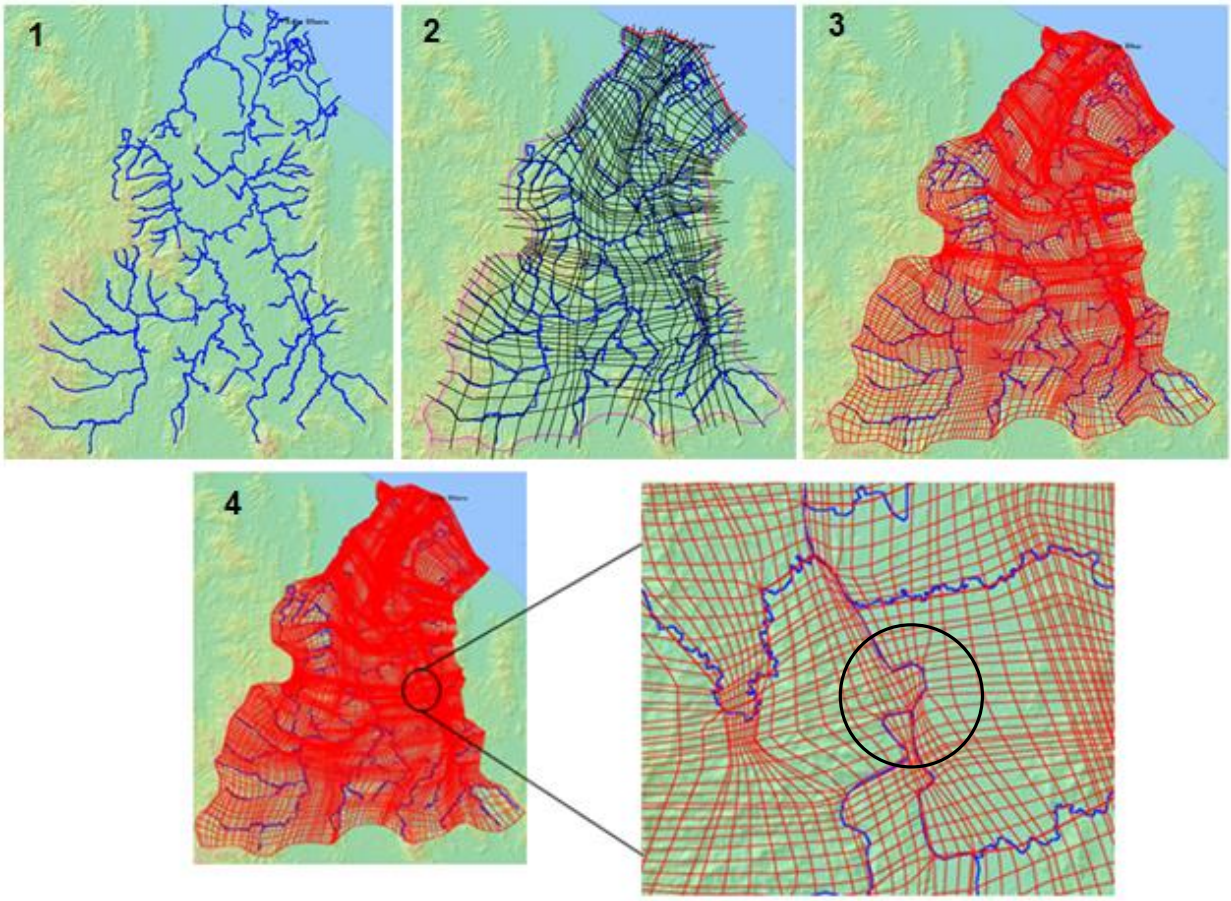

Figure 5.2. Steps of Kelantan watershed's grid constructions.

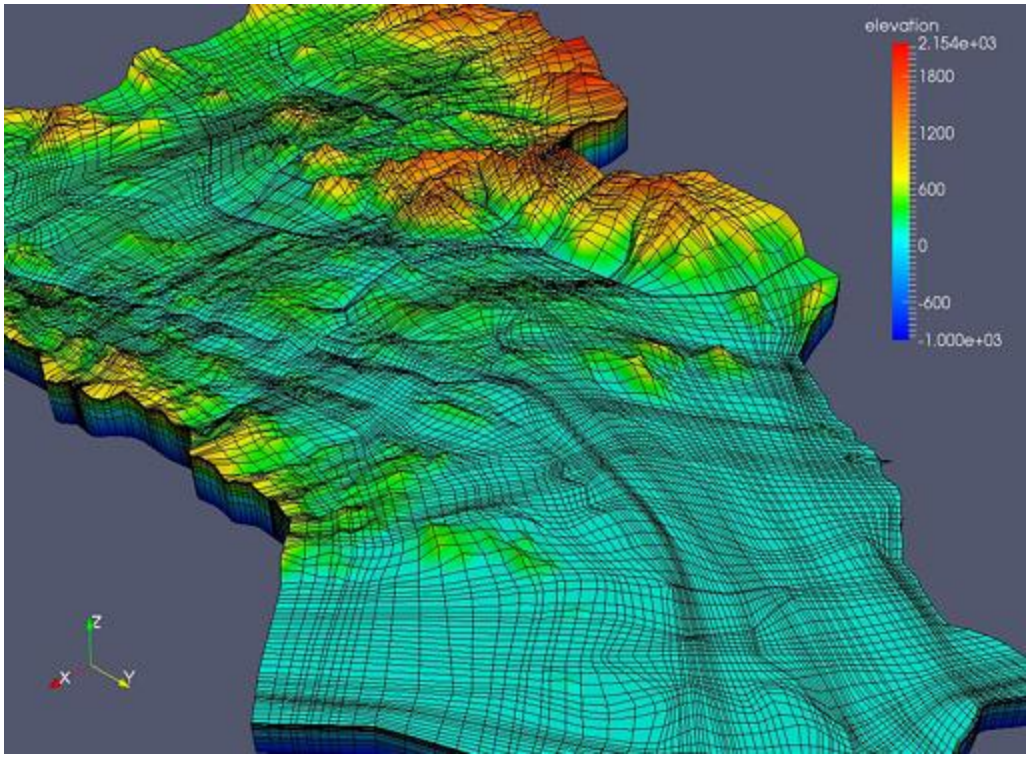

Figure 5.3. Three-dimensional view of Kelantan watershed, 115 x 263 x 13grids. (Elevation in meter)

5.3.2 *Model Initialization*

A two-stage initialization which consists of subsurface equilibration and surface-subsurface coupled equilibration were done by setting the necessary parameters such as permeability, porosity, surface manning's and evapotranspiration as shown in Table 5.2.

Table 5.2. Sensitive input parameters introduced to GETFLOWS simulator

Sensitive Parameters	**Approximate range**	**Remarks**
Manning's roughness (river channel)	0.01 to 0.02	Constant for all channel
Manning's roughness (other place)	0.05 to 10	Depend on land use
Top soil permeability	1E-11 to 3E-11 m^2	Depend on land use
Top soil porosity	0.5 to 0.8	Depend on land use
Evapotranspiration	5 to 10 mm/day	-

First stage is the subsurface equilibration where

- All water is cleared on the surface, and set the surface as infinite capacity layer
- Fully saturate subsurface layers with water under static pressure
- Give infiltration to the top soil layer of 2 mm/day at every time step

By this setting, when simulation start, the water in shallow subsurface layers springs up to the low land area of the surface and groundwater level decreases in high land. After several thousand days, the subsurface groundwater pressure and saturation distribution become stable. Such condition is used as the starting point of the next equilibration step. Figure 5.4 shows the saturation distribution of the top soil layer after 1st stage initialization.

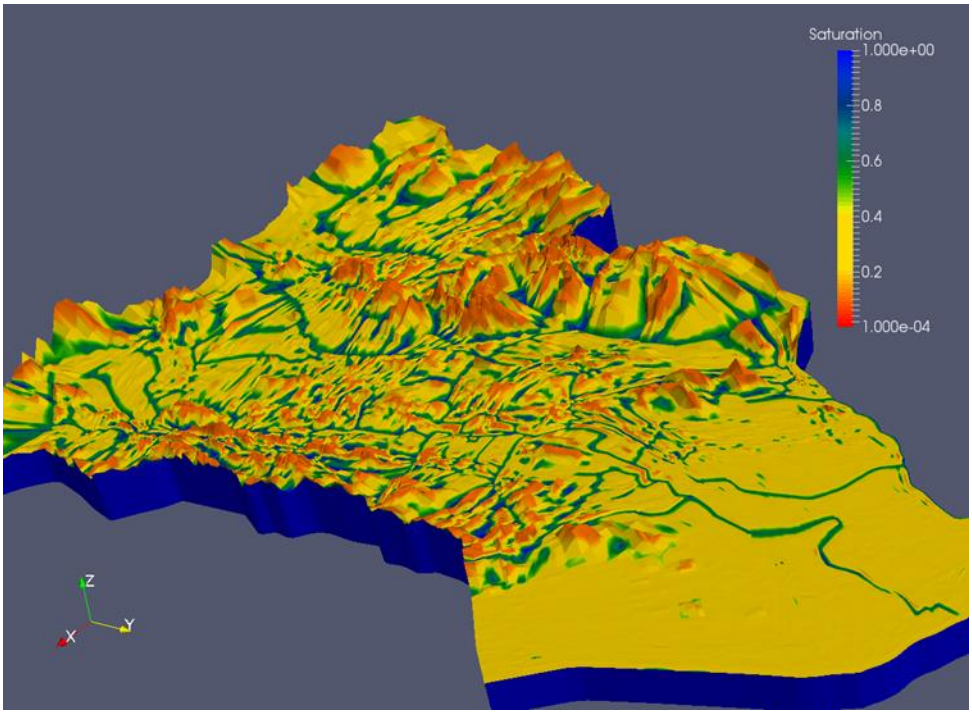

Figure 5.4: Saturation distribution of top soil after 1st stage initialization.
(Saturation fraction is from 0 to 1)

Second stage initialization of the surface-subsurface coupled equilibration consist of

- Set the porosity of the surface layer at 1.0
- Set the surface roughness distribution according to land use information
- Give average rainfall for dry season (2 mm/day for 183 days) and rainy season (7 mm/day for 182 days) to the surface layer (excluding evapotranspiration rate from the real rainfall)

Starting a simulation under this condition following the final results of the first stage initialization, river network will gradually formed on the surface under the balance of rain,

evapotranspiration, surface water and subsurface water. The final distribution of pressure and water saturation of this stage was used as the starting condition of the simulation for year 2007 up to 2013. Figure 5.5 shows the result of second stage initialization where river network of Kelantan appeared on the surface.

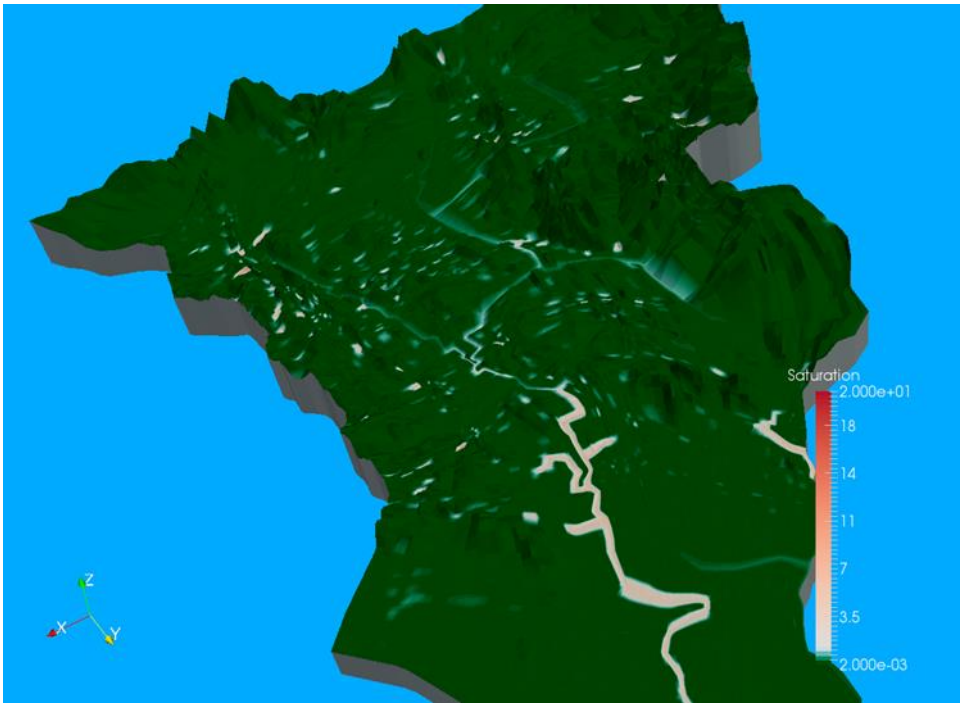

Figure 5.5. View of surface river networks appeared on the surface after the 2nd stage initialization. (Saturation fraction is from 0 to 1)

5.4 *Analysis of Rainfall Distribution*

5.4.1 *Review*

Assessing precipitation variability is the key element to develop any conceptual and predictive models in many fields such as water resource management and flood disaster prediction (Dawdy and Bergmann, 1969). Using rainfall gauge on its own as input carries great uncertainties regarding runoff estimation, especially when the area is large and the rainfall is measured and recorded at irregularly spaced gauging stations (Chaubey et al., 1999; Ly et. al., 2011; Wagner et. al., 2012). Hence spatial interpolation is the key to obtain continuous and orderly precipitation distribution at unknown points to be the input to the rainfall runoff processes via distributed and semi-distributed numerical modelling. The need to include rainfall spatial distribution becomes more significant if rainfall with a high degree of spatio-

temporal heterogeneity is the key driver of runoff (Wagner et. al, 2012; Tsai et. al., 2014). A few studies done by Arnaud et al. (2002), Schuurmans and Bierkens (2007) and Tramblay et. al (2011) indicated that using mean areal rainfall instead of spatially distributed rainfall inclines to undervalue the volumes and peak runoffs. However, the impact of spatial distribution of rainfall on runoff estimation is complex as it can be dependent on the rainfall's nature, catchment characteristics and the spatial scale used (Segond et al., 2007, Tao et al., 2009).

The estimation of rainfall distribution can be grouped into two; indirect and direct methods. Indirect rainfall estimation via satellite products, especially from radar remote sensing are increasingly used as covariates since they offer spatially detailed data information (Verworn and Haberlandt, 2011; Wagner et. al., 2012). Nordila et. al (2012) and He et al. (2011) conducted a study to compare spatial distribution of convective rainfall between meteorological radar data and ground-based data concluded that the distribution are poorly correlated. Therefore, the reliability of indirect methods have yet to be determined since it must be calibrated and validated using historical ground gauge stations by adjusting correction parameter (Lanza et. al., 2001; Ly et. al, 2011). However, by pairing the rainfall radar data with ground based data can improve the rainfall distribution and produce realistic runoff simulations especially when the rainfall measurements are scarce and the watershed contains coarse rain gauge networks as seen in a study conducted by Lange et. al (1999) and Tsai et. al (2014).

The direct ground-based method has a wide range of interpolation techniques ranging from simple to more complex calculations which can be divided into two main groups; deterministic and geostatistical. The mostly known deterministic approaches are Thiessen polygon (TH) introduced by Thiessen (1911) and inverse distance weighting (IDW) (Shepard, 1968) whereas the geostatistical methods constitute disciplines of mathematics and earth sciences, known as kriging method.

Mair and Fares (2011) compared TH, IDW, linear regression, ordinary kriging (OK) and simple kriging with varying local mean (SKlm) integrating distance and elevation in interpolating monthly, seasonally and yearly rainfall. 21 rain gauges were used across the mountainous leeward portion of the island of O'ahu (280km^2), Hawaii. They suggested the use of geostatistical interpolation over deterministic approach. TH produced the highest prediction error while OK produced the lowest error among all. Incorporation of elevation did not improve estimation accuracy for Sklm except the correlation between rainfall and elevation reached 0.82. Xu et. al (2014) used IDW, OK and ordinary co-kriging (OCK) to interpolate daily rainfall data in Sichuan province (487,000 km2) in China. The daily rainfalls of 43 meteorological stations from 2008 to 2013 were analyzed, and the result proved that OCK is

the best method as it can reduce system errors since environmental factors can be introduced as variables. In this study elevation, aspect and slope were incorporated in OCK.

Dirks et al (1998) compared areal mean methods, TH, IDW and kriging using 13 rain gauges in Norfolk Island (35 km2) in determination of hourly, daily, monthly and annually rainfall distribution. The paper concludes as to integrate watershed characteristics of spatially varying rainfall, IDW is the most advantageous method for interpolating an area with spatially dense networks. The same conclusion was achieved by Tao. et. al., (2009) on a small watershed in Lyon, France (15 km2) where superiority of geostatistical method was not obvious thus IDW result was preferred.

In another case study in China (Chen et al, 2010), the daily rainfall data from 753 rain gauges between 1951-2005 were analyzed using IDW, OK, radial basis function, local polynomials and nearest neighbour (NN) for the whole country. The IDW method was tried with four different powers ranging from 1 to 4. Among the eight used interpolation methods, OK and IDW with a power of 2 were ranked highest in terms of interpolation quality in the whole China. Ly et. al (2011), used different type of semivariogram models for kriging methods by using 30 year of daily rainfall data of 70 rain gauges in the hilly area of Ourthe and Ambleve watershed in Belgium (2,908km^2). Spatial interpolators used in this study were IDW, TH, OK, universal kriging (UNK) kriging with external drift (KED) and OCK, both incorporating elevation. 7 semivariograms model (logarithmic, power, exponential, Gaussian, rational quadratic, spherical and penta–spherical) were adopted to avoid negative interpolated rainfall in OK. The paper finds that Gaussian model for semivariogram was the most frequently best fitted however, spherical model provided a slightly better result for OK, UNK and KED. Using elevation as secondary variables did not improve the estimation accuracy for daily rainfall. This paper considered OK and IDW to be the best methods.

Verworn and Haberlandt (2011) incorporated additional information (radar and elevation) in producing hourly rainfall distribution by using multivariate geostatistical method in their studies. They suggest using radar as additional information as the effect of elevation in hourly temporal scale only plays a minor role. However, incorporating elevation in monthly and annually scale may improve the estimation (Goovaerts, 2000).

Haberlandt and Kite (1998) performed an alternative spatial interpolations methods by comparing various time-series of daily rainfall distribution using objective verification based on runoff simulation over Mackenzie River Basin in Canada. They used the NN, IDW, OK and KED. By performing cross-validation over the rainfall gauge, OK gave the lowest standard error followed by IDW and NN. The KED in this study was used to assimilate rainfall gauge

with atmospheric rainfall data. They found out that geostatistical method and the use of combined rainfall data managed to increase reliability of runoff simulation's results. In another study done by Ruelland et al (2008) found that IDW datasets shown to provide the most realistic results outperformed OK, TH and spline by applying to hydrological applications. Their study analysed the sensitivity of lumped and semi-distributed hydrological modelling to several interpolations method in West African watershed where the data was scarce.

Based from literature review above, researchers have contrasting views as each method has its advantage and disadvantages. This study aims to investigate the IDW method in estimating rainfall distribution of Kelantan watershed by considering the spatial effect (large vs small scale) and also by integrating elevation data into IDW, via IDEW method.

5.4.2 *Objective*

The objective of this study is to develop rainfall distribution over the large Kelantan watershed on daily basis to provide realistic simulation for year 2007 up to 2013. It is crucial to study and predict the behaviour of rainfall and river runoff to reduce flood damages of the affected area. Thus, a good knowledge on rainfall distribution is essential in early flood prediction studies. Up to 70 rainfall stations and their daily time-series were used to interpolate gridded rainfall surfaces using inverse distance weighting method (IDW) and inverse distance and elevation weighting method (IDEW). The IDW and IDEW were tried twice each by: a) applying to whole watershed and b) sub-watershed scale. So a total of 5 rainfall distributions for gridded surface were produced in one space-time rainfall series together with average rainfall distribution. Sensitivity analysis for distance and elevation parameters were conducted to see the variation produced. The accuracy of these interpolated datasets will be examined using two approaches: cross-validation assessment and validation by numerical simulations via GETFLOWS.

For the purpose of early flood prediction in Kelantan watershed, a quick telemetry-based rainfall distribution estimation was also being tested for years 2010 to 2013. The comparison of rainfall distribution between all rainfall stations and telemetry stations were investigated and discussed in terms of reliability and appropriateness to be used for early flood prediction.

5.4.3 *Estimation Methods*

5.4.3.1. *Average Areal Rainfall*

As the most basic case, the average rainfall over a watershed was computed from the rainfall data measured at a number of rainfall gauges. In areas where more than one rainfall gauge is located, the following methods are employed to compute the average rainfall:

- Arithmetic average method
- Thiessen polygon method
- Isohyetal method.

However in this study, only arithmetic average method was used to compute the average rainfall over the watershed and sub watershed. This method can be considered as the simplest method of computing the average rainfall. The result was obtained by the division of the sum of the rainfall recorded at different rain gauge stations of the watershed/sub-watershed by the number of available stations. If the rain gauges are uniformly distributed over the area and the rainfall varies in very regular manner, the results obtained by this method are quite satisfactory. This method can be used for storm rainfall, monthly and annual average computations.

In this study, the Kelantan watershed was delineated into eight sub-watersheds as shown in Figure 5.6. The delineation was based on the hydrological characteristics such as stream network and waterlines, and also the manner of rainfall based on reliable long term records.

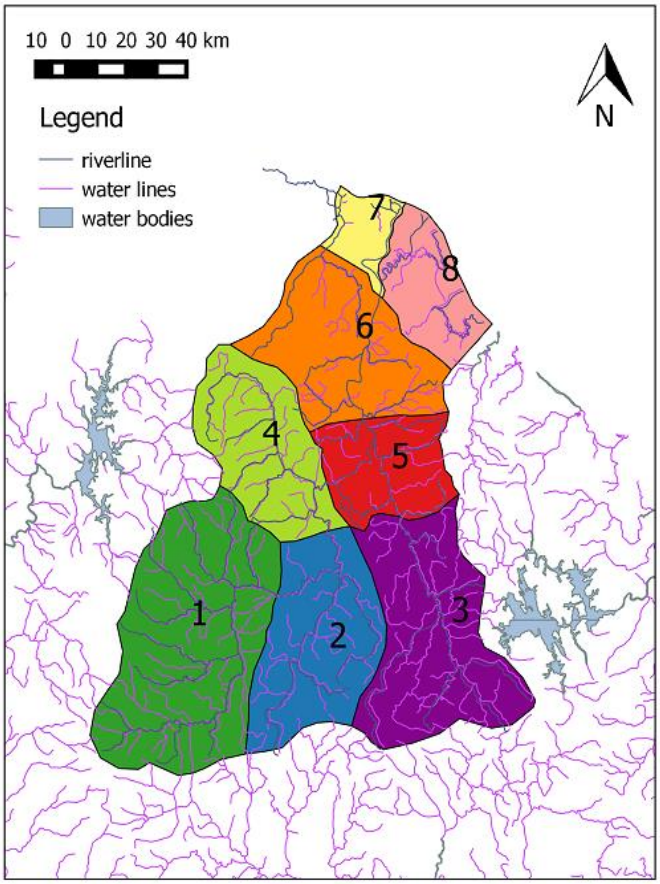

Figure 5.6. Kelantan watershed divided into 8 sub-watersheds.

5.4.3.2. *Inverse Distance Weighting Method (IDW)*

Inverse distance weighting method (IDW) is a famous conventional deterministic approach for spatial interpolation based on similarity or smoothness within a research area other than Thiessen method. The assigned values to unknown points are calculated as a weighted average of the values available at the known points (Franke, 1982). Weight increases as the distance decreases from the known points to unknown points (Ly et al., 2011 & Xu et. al., 2014). The mathematical form of the IDW is given below:

$$p_e = \sum_{i=0}^{N} \lambda_i p_i \tag{5.6}$$

where p_e is the interpolated rainfall for a grid cell; N is the number of gauges that are used in the interpolation for the current grid cell; λ_i is the corresponding weight of each known points where it reduces as the distance between known points and predicted points increases; p_i is the rainfall value in mm/day of the ith gauge station. The weighting factors is called Shepard method (Shepard, 1968) and determined by:

$$\lambda_i = \frac{d_{i0}^{-\alpha}}{\sum_{i=1}^{N} d_{i0}^{-\alpha}} \tag{5.7}$$

$$\sum_{i=1}^{N} \lambda_i = 1 \tag{5.8}$$

where the power of exponent α controls the influence of the distance among the sample points or gauge stations on the interpolations results. A low α leads to a greater weight towards a grid point value of rainfall from remote rain gauges. As the α decreases toward zero, the method approximates the Thiessen method (Ashraf et al., 1997; Dirks et al., 1998; Mair and Fares, 2011 & Ly et al.,2013). Dirks et. al., (1998) had concluded, to minimize the interpolation errors, α of 2 is used for daily and monthly steps, 3 for hourly and 1 for yearly. However most study (Goovaert, 2000; Llyod, 2005; Heistermann and Kneis, 2011; Ly et al., 2011 & Xu et. al., 2014) set α to 2 where inverse square distances were used in their estimation. During the process of prediction, the weights of gauge station are proportional and the sum of these weights is equal to 1.

5.4.3.3. *Inverse Distance and Elevation Weighting Method (IDEW)*

The IDW interpolation only incorporates a single influence factor which is horizontal distance. Therefore it is not suitable to be applied in an area with abrupt changes in elevation which could create uncertainty in estimating unknown information (Lloyd, 2005). Inverse distance and elevation weighting (IDEW) technique provides more suitable results for mountainous regions where topographic impacts on rainfall are important (Masih et al., 2011 & Ly et al., 2013). IDEW algorithm is part of hydrological data processing software called HyKit developed by UNESCO-IHE (Masih et. al., 2011). However in this study, C programming was used to do the interpolation by adopting the equations as shown below:

$$p_e = W_D \sum_{i=1}^{N} \frac{1}{D} w(d)_i p_i + W_Z \sum_{i=1}^{N} \frac{1}{Z} w(z)_i p_i \tag{5.9}$$

where W_D and W_Z are the importance factors for distances and elevations. Typical values for the importance factor is 0.8 for distance and 0.2 for elevation, respectively (Daly et. al., 2002). Similarly, $w(d)_i$ and $w(z)_i$ are the individual gauge weighting factors for distance and elevation respectively. Whereas D and Z are the normalization quantities given by the sum of individual weighting factors $w(d)$ and $w(z)$, respectively for all the gauges used in the grid interpolation. The weighting factors of $w(d)_i$ and $w(z)_i$ can be determined by:

$$w(d) = 1/d^{\alpha} \;\; for\; d > 0 \tag{5.10}$$

$$w(z) = \begin{cases} 1/z_{min}^{\beta} \;\; for\; z \leq z_{min} \\ 1/z^{\beta} \;\; for\; z_{min} < z < z_{max} \\ 0\; for\; z \geq z_{max} \end{cases} \tag{5.11}$$

where, d is the distance in kilometer between current grid and the gauge station used for interpolation, z is the absolute elevation difference in meter between the current grid ceall and the gauge station used for interpolation, α and β are exponent factors for distance and elevation weightings where the distance weighting exponent is 2 and 1, respectively (Daly et. al, 2002). z_{min} and z_{max} are the minimum and maximum limiting values of elevation differences for computing elevation weightings (Daly et. al., 2002 & Masih et. al., 2011). Limitations on z_{min}

and z_{max} help to avoid dominance of the stations having very small elevation difference and enables data point inclusion to be restricted to a local elevation range (Masih et. al., 2011). Typical values of z_{min} is 100 to 300 meter while z_{max} from 500 to 2,500 m depending on the study area (Masih. et. al., 2011).

5.4.4 *Cross-Validation Assessment*

The performance of the interpolation methods was assessed and compared by cross-validation procedure. The procedure consists of temporarily discarding one observation value at a time from the data sets and re-estimating the discarded value from the remaining sampled point using each interpolation method. Nash-Sutcliffe efficiency (NSE) (Nash and Sutcliffe, 1970) and root mean square error (RMSE) were adopted to evaluate the performance of interpolation methods:

$$NSE = \frac{1}{t}\sum_{j=1}^{t}[1 - (\sum_{i=1}^{N}(p_e - p_i)^2 / \sum_{i=1}^{N}(p_i - \bar{p}_i)^2)] \tag{5.12}$$

$$RMSE = \frac{1}{t}\sum_{j=1}^{t}\left\{\frac{1}{N}\sum_{i=1}^{N}[p_i - p_e]^2\right\}^{1/2} \tag{5.13}$$

where t is the number of days, N is the number of sampled gauges, and $\bar{p}_i$ is the average observed value over the period in days. NSE criterion is a form of normalized least squares where perfect agreement between the observed and estimated values yields an efficiency of 1, whereas a negative efficiency represents lack of agreement where the observed mean is a better predictor than the estimation value. RMSE indicates the deviation between estimated values and observed one hence, smaller RMSE contributes to better estimation capability.

The results of four interpolation methods were validated and ranked via RMSE and NSE as shown in Table 5.3. The RMSE validation indicates that each interpolation method has relatively similar deviations between estimated and observed values with a mean residual of 10.175 ± 0.233 It is also observed that the range of deviation values are significantly large for all interpolation methods, ranging from 0.05 to 78.5. This shows that despite similar deviation, the confidence level between estimation and observation value is not high as the external

factors need to be considered, such as the quality of the rainfall data. Hence, RMSE is not able to determine the best interpolation method in this case as illustrated in Figure 5.7.

Table 5.3. Cross-validation assessment performance and ranking of different interpolation methods based on root mean square error (RMSE) and Nash-Sutcliffe efficiency (NSE).

Interpolation Methods	Range RMSE	Mean RMSE	Rank of Mean RMSE	Range NSE	Mean NSE	Rank of Mean NSE
IDW	0.05-75.42	9.84	2	-0.87-0.76	0.09	4
IDEW	0.07-75.08	9.82	1	-0.28-0.99	0.93	2
AIDW	0.06-78.46	10.60	4	0.6-0.99	0.98	1
AIDEW	0.07-75.37	10.44	3	-0.97-0.99	0.92	3

On the other hand, the NSE validation shows that the IDW interpolation has the lowest mean value of NSE close to zero, while the rest of interpolation methods demonstrate a high mean value of NSE close to 1. Figure 5.8 illustrates the NSE cloud distributions for all interpolation methods and it can be clearly seen that the NSE value for IDW is much scattered within a wide range, both positive and negative efficiency, as compared with others. This shows that the quality of rainfall estimation in Kelantan can be improved by incorporating elevation and smaller sub-watershed in the interpolation. This is obvious since the geophysical and topography of Kelantan is mixed with mountainous terrain and valley.

It is also worth to note that integrating elevation in a smaller sub-watershed, i.e. AIDEW, did not significantly change the NSE value of AIDW. This could be due to the smaller elevation change that exists within the sub-watershed; hence elevation gives little impact in estimating the rainfall in smaller watershed. Overall, AIDW shows the best interpolation method to estimate the rainfall in entire Kelantan watershed according to NSE.

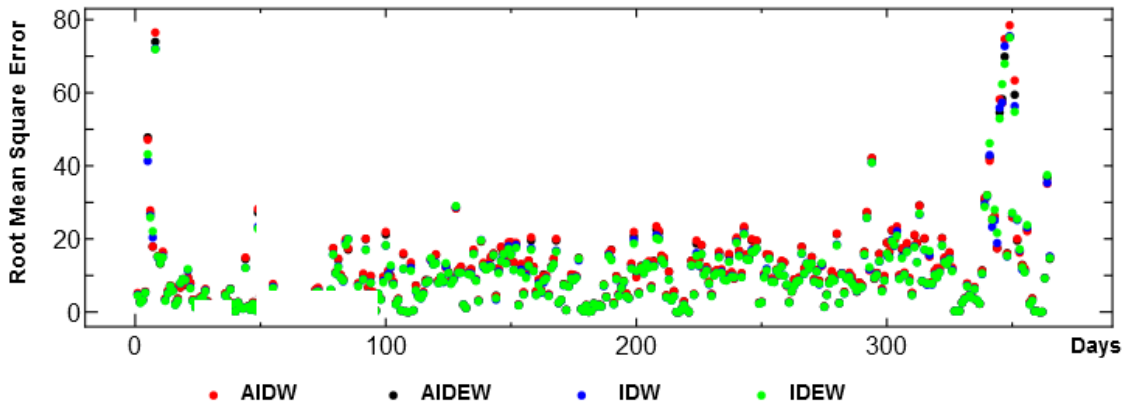

Figure 5.7. RMSE clouds from 1st January to 31st December 2007.

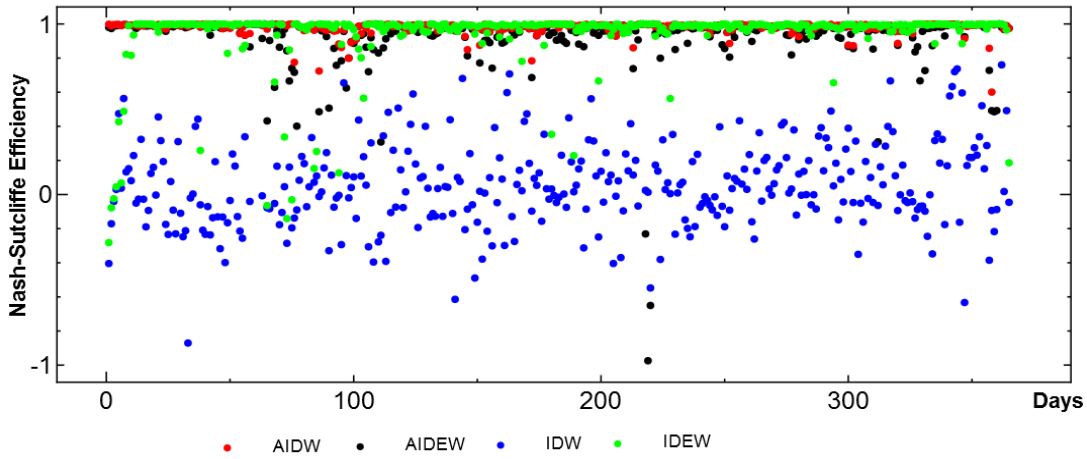

Figure 5.8. NSE clouds from 1st January to 31st December 2007.

5.4.5 *Sensitivity Analysis of Rainfall Distribution Parameter – All Stations.*

Sensitivity of rainfall distribution parameters was investigated to see variations in the pattern and amount of rainfalls produced by changing the α and z_{min} and z_{max}. Sensitivity analysis of α parameter as shown in Figure 5.9 shows that the greater of α will result in greater influence to area or grid that close to the interpolated points, whereas smaller α will result in interpolated values will be dominated by other points or rainfall gauges that are far away. This can be seen in day 341, year 2007 where when α equals to 1.5, weights of rainfall gauge that has high rainfall records in the east part was lesser compared with α equals 2 and 3. Same goes to day 346, year 2007 where when α equals to 3, both high rainfall and zero rainfall area gave greater influence to surrounding nearby grid compared with 2 and 1.5. Greater α value also results in greater amount of rainfall distributed over Kelantan watershed even though the number of rainfall gauges that have high rainfall value is small.

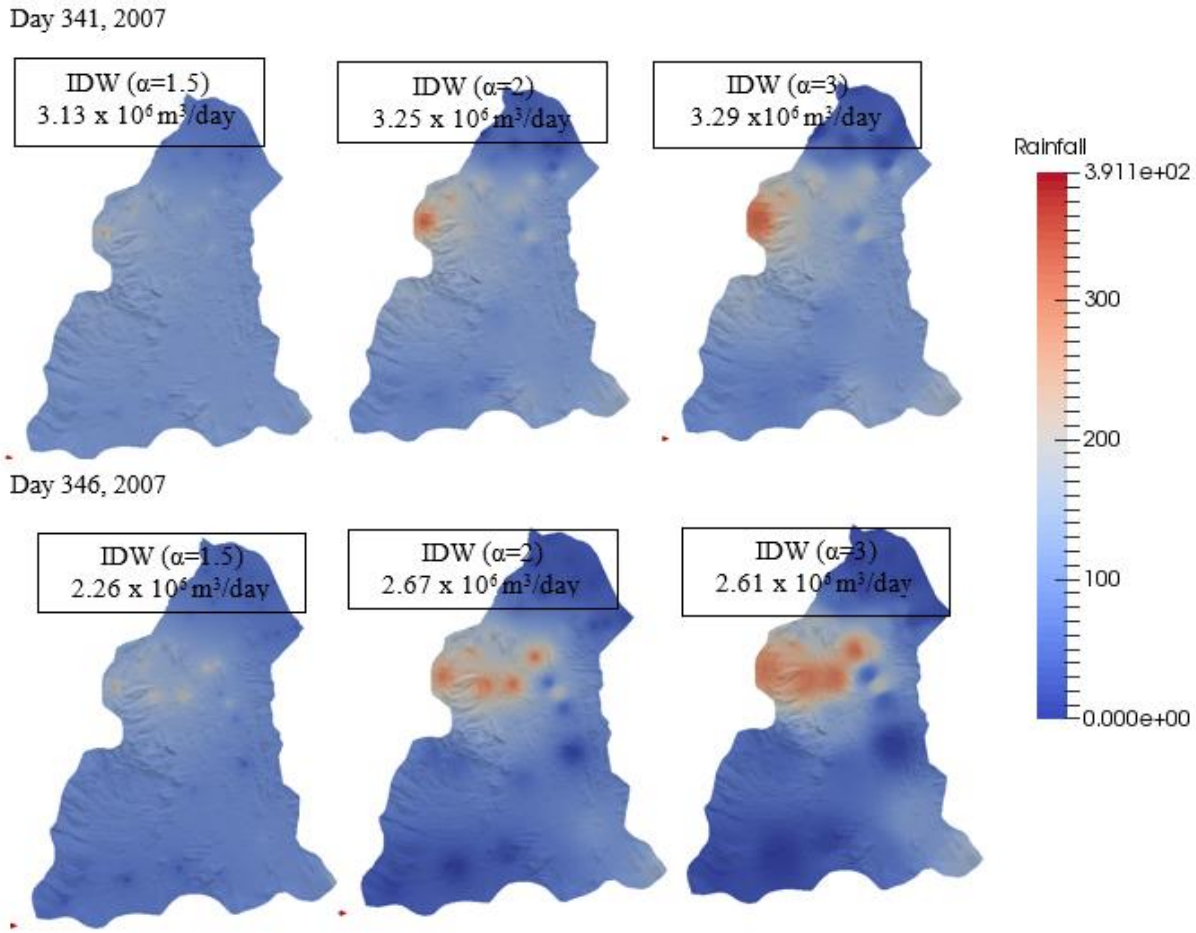

Figure 5.9. Sensitivity Analysis of IDW parameter α.

For IDEW elevation parameter, only z_{min} was adjusted since z_{max} for Kelantan watershed is known (around 1800m above sea level). Masih et al, suggested the range of z_{min} is around 100 to 300 m. Figure 5.10 illustrates the difference by applying z_{min} of 100 and 200 m. This shows that larger range of Δz leads to higher amount of rainfall across the watershed.

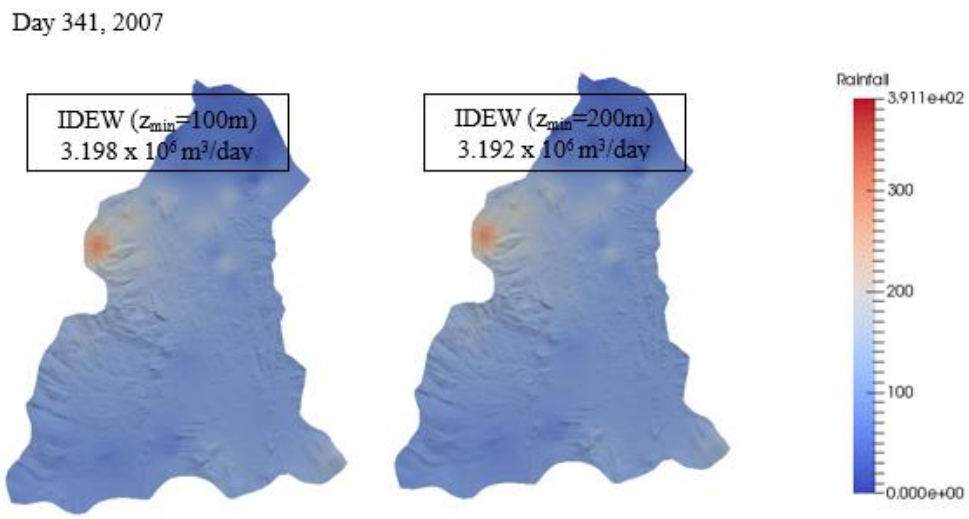

Figure 5.10. Sensitivity Analysis of IDEW parameter z_{min} (α = 2 and z_{max} = 1800m)

5.4.6 *Sensitivity Analysis of Rainfall Distribution Variation – All Stations*

Figure 5.11 shows the rainfall distribution of IDW, IDEW, Areal IDW (AIDW) and Areal) (IDEW for day 341, year 2007. AIDEW gave the most amount of rainfall followed by AIDW, IDW and IDEW. Dividing the watershed into sub-area in making rainfall distribution such as in AIDEW and IDEW controlled the amount of rainfall gauge used. This means to calculate the interpolation value, the rainfall gauges that falls within the area were used. To validate this result, Figure 5.12 was plotted by comparing the cumulative amount of rainfall generated across Kelantan watershed for year 2007. AIDEW produced the highest rainfall followed by AIDW, IDW and IDEW as shown in Figure 5.12. The accuracy of these interpolated rainfall were inspected by the GETFLOWS simulator by quantitative and qualitative comparison as shown in Figure 5.13.

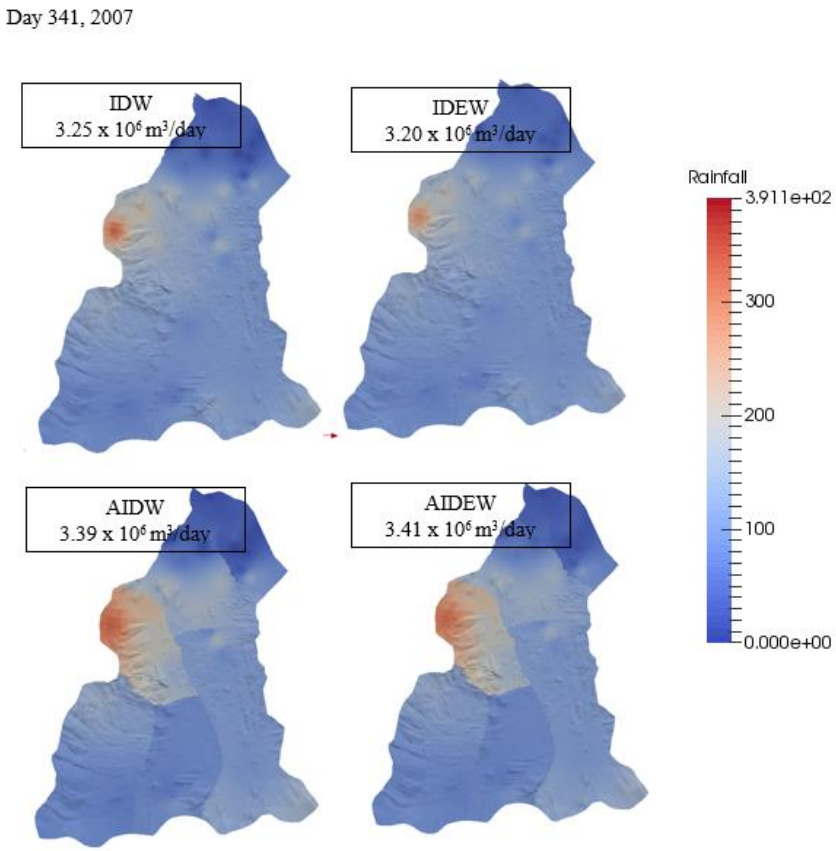

Figure 5.11. Sensitivity analysis of rainfall distribution types. (α = 2, z_{min} = 200 and z_{max} = 1800m)

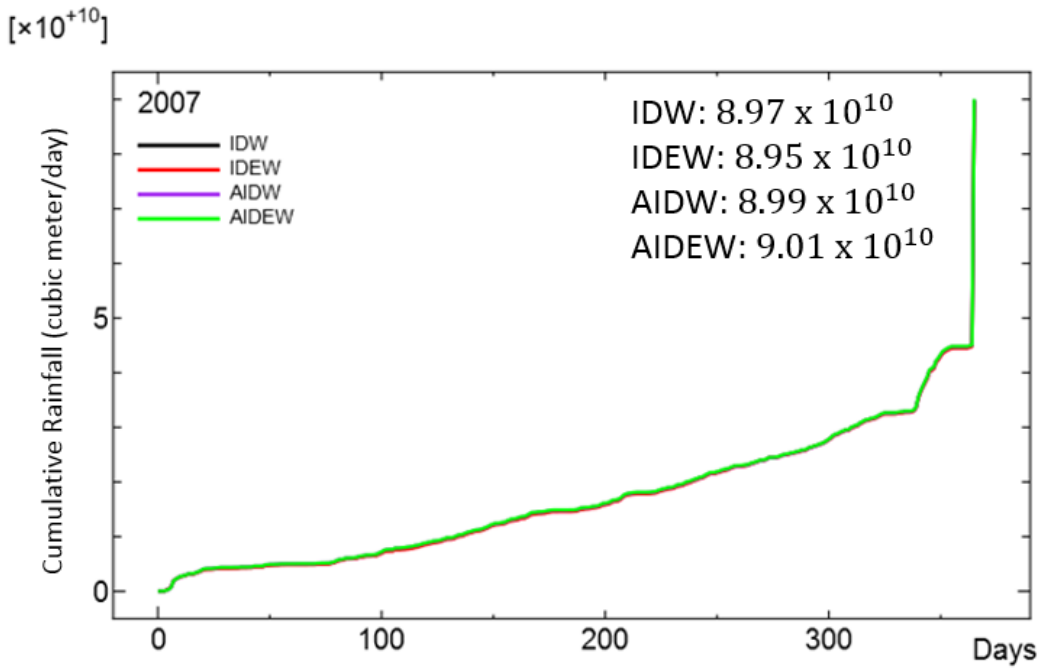

Figure 5.12. Cumulative rainfall by the four rainfall estimation methods

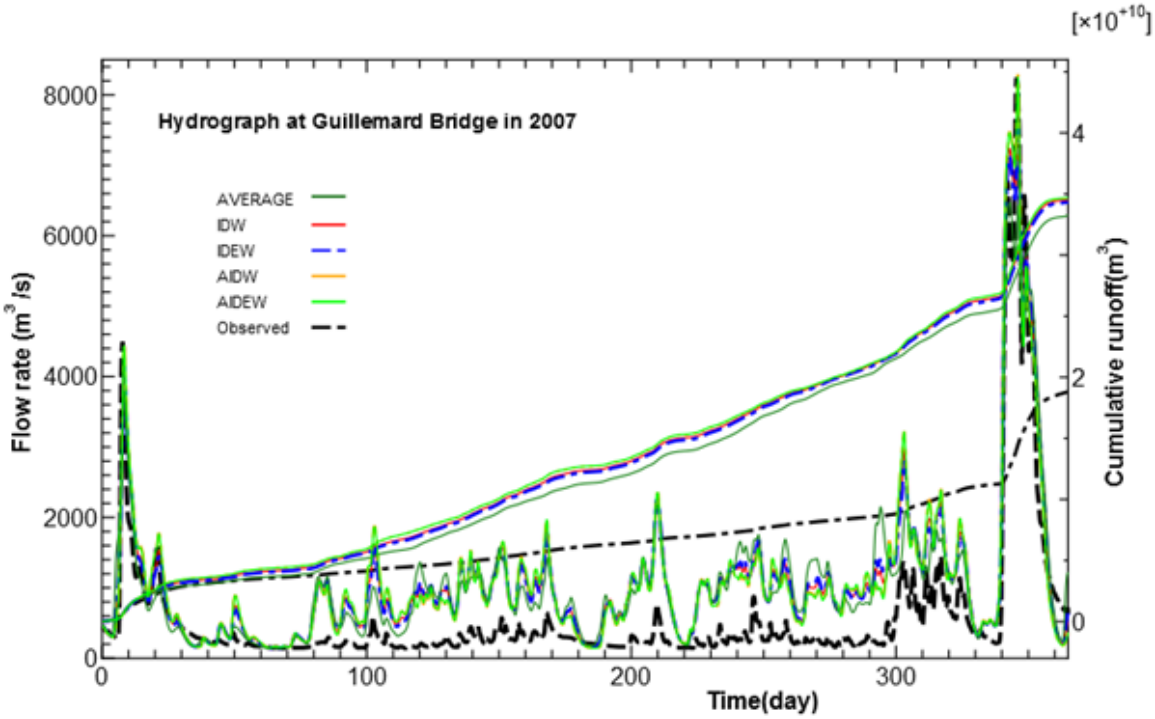

Figure 5.13. Hydrograph of Kelantan River at Guillemard Bridge in 2007.

The results for all rainfall distribution i.e IDW, IDEW, AIDW and AIDEW show very insignificant difference except average rainfall distribution. It is found that during low flood season, average rainfall tended to produce higher peaks whereas the volumes and peaks were undervalue during monsoon season as shown in Figures 5.15 and 5.16. From this analysis, the

simplest IDW method seems appropriate for Kelantan watershed hence, for early prediction, only IDW method will be used in this study.

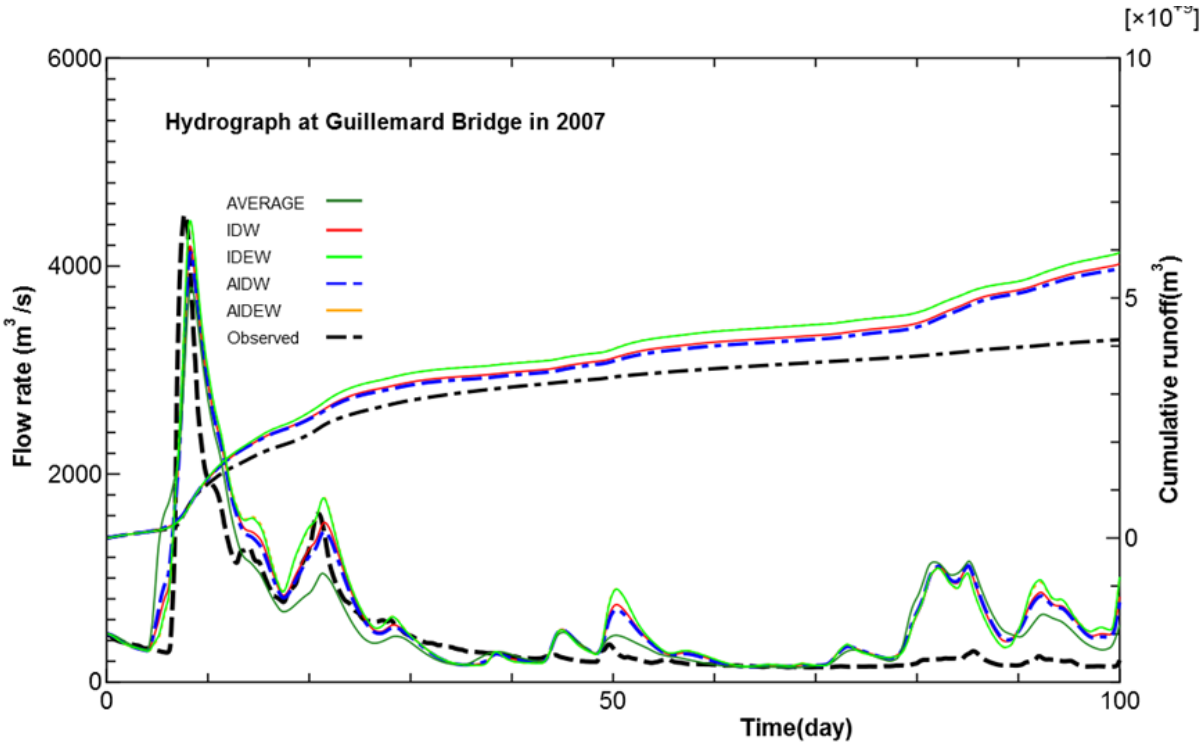

Figure 5.14. Hydrograph of Kelantan River at Guillemard Bridge for day 1-100 in 2007.

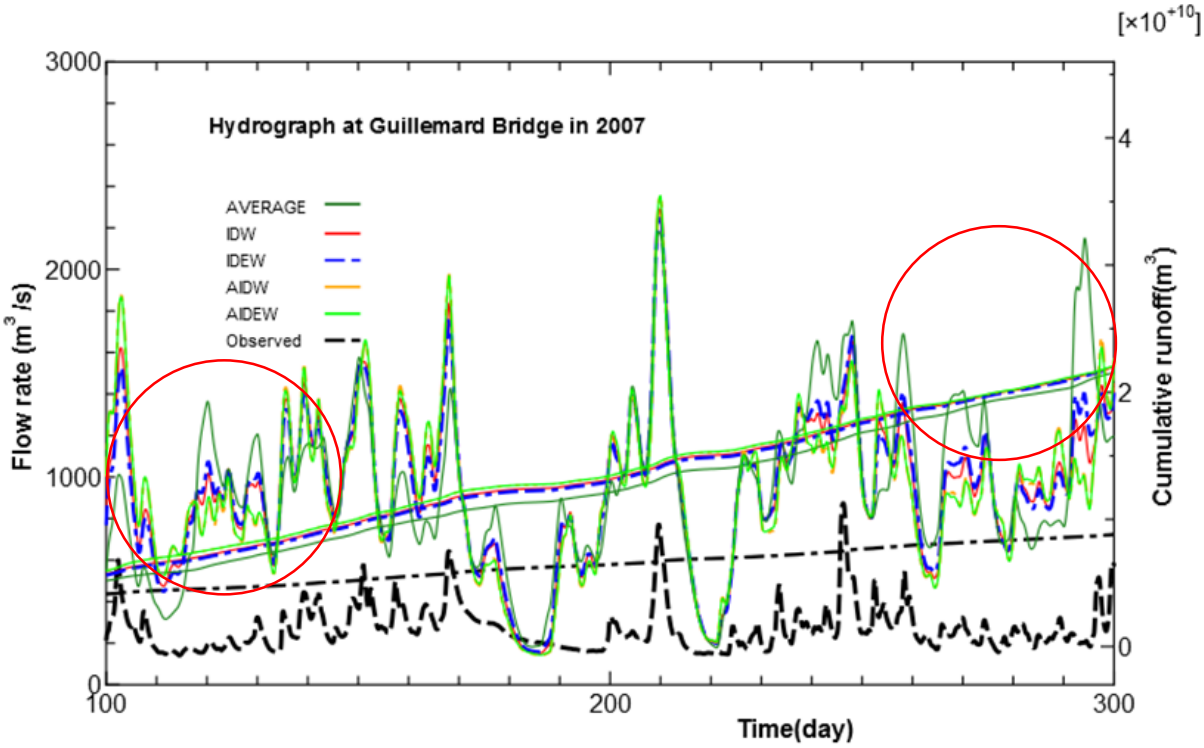

Figure 5.15. Hydrograph of Kelantan River at Guillemard Bridge for day 100-300 in 2007.

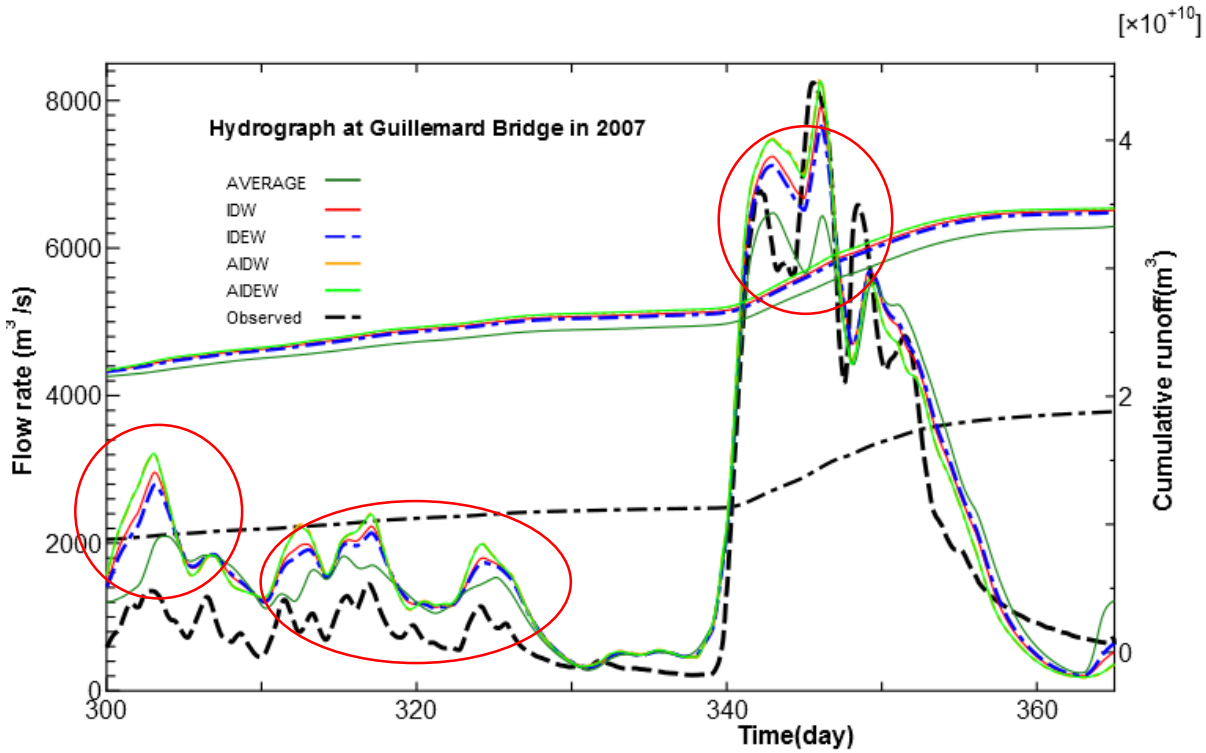

Figure 5.16. Hydrograph of Kelantan River at Guillemard Bridge for day 300-360 in 2007

5.4.7 *Sensitivity Analysis of Rainfall Distribution Parameter - Telemetry Stations*

Sensitivity analysis of α parameter for telemetry stations was conducted to evaluate the difference between rainfall distribution generated from telemetry stations (α = 0.5, 1, 2, 3) and all-stations (α =2). Figures 5.17 to 5.21 show the comparison of rainfall distribution during north east monsoon event in year 2011. It is found that by setting α value to 0.5, it will produce higher amount of rainfall closer to rainfall distribution generated using all stations. However, the distribution become non-distinguishable and is somewhat averaging the amount of rainfall across the Kelantan as shown in Figures 5.17 to 5.21 (α = 0.5). Figures 5.22 to 5.25 show the amount of cumulative rainfall generated from telemetry stations (α = 0.5, 1, 2, 3) and all-stations (α =2) for year 2010 ~ 2013. From the figures, α value of 0.5 gives higher amount of cumulative rainfall for each year and α value of 3 is the lowest. It is difficult to identify which α is suitable for early prediction using telemetry stations by comparing the amount of rainfall. But in terms of distribution, α of 2 is still applicable by comparing with distribution generated by all stations of the same α value.

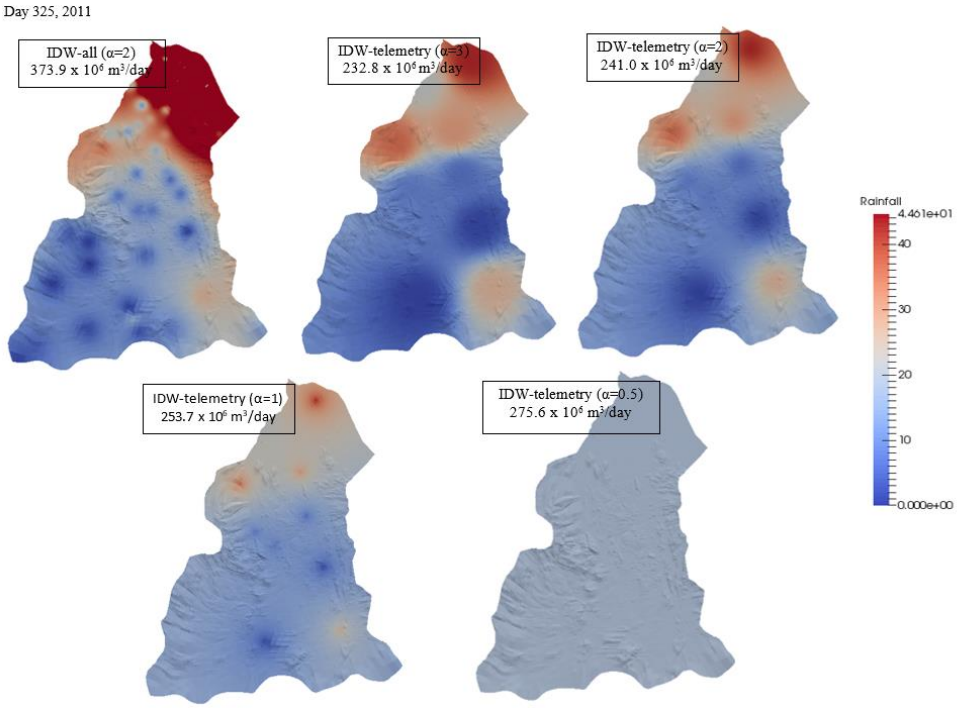

Figure 5.17. Comparison of rainfall distribution with various α, day 325 2011.

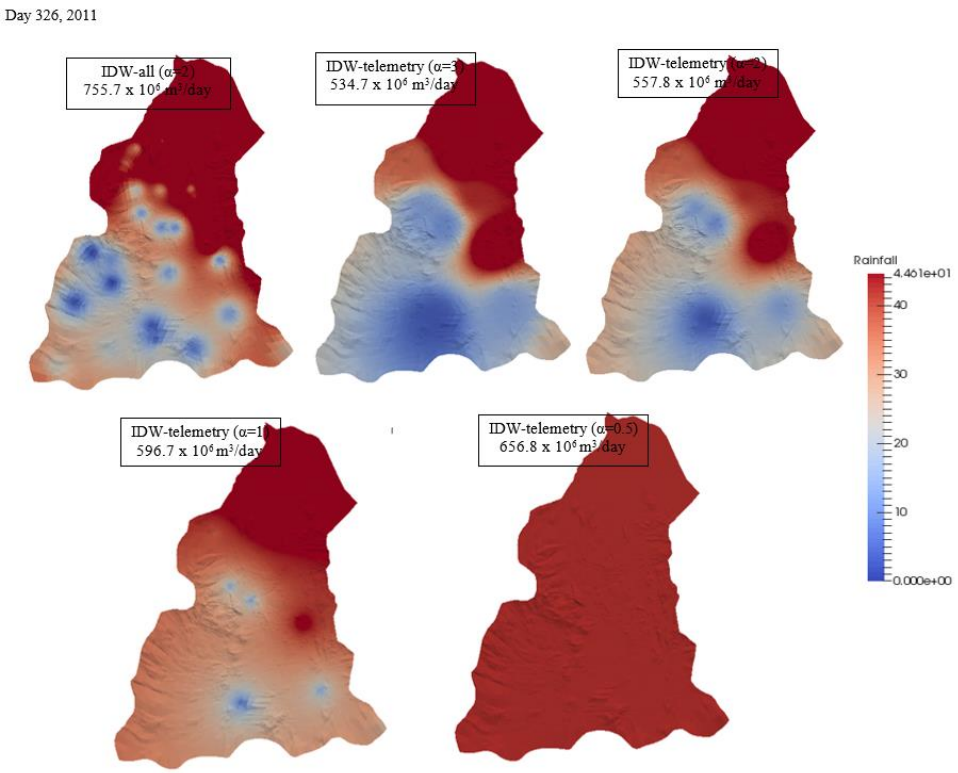

Figure 5.18. Comparison of rainfall distribution with various α, day 326 2011.

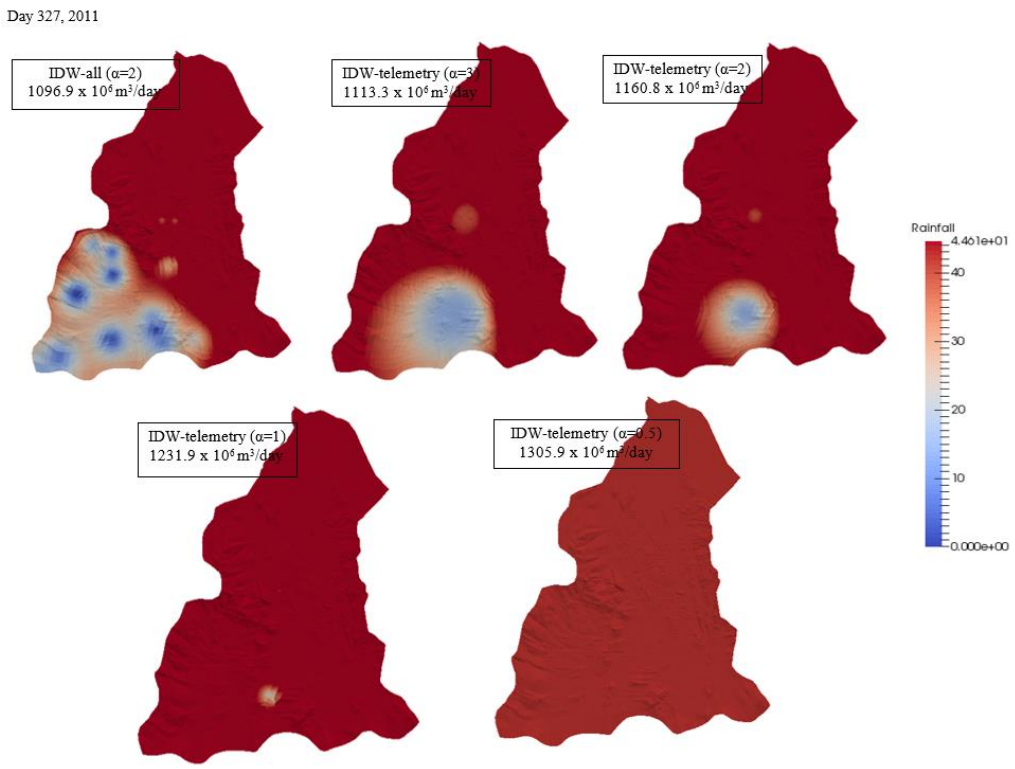

Figure 5.19. Comparison of rainfall distribution with various α, day 327 2011.

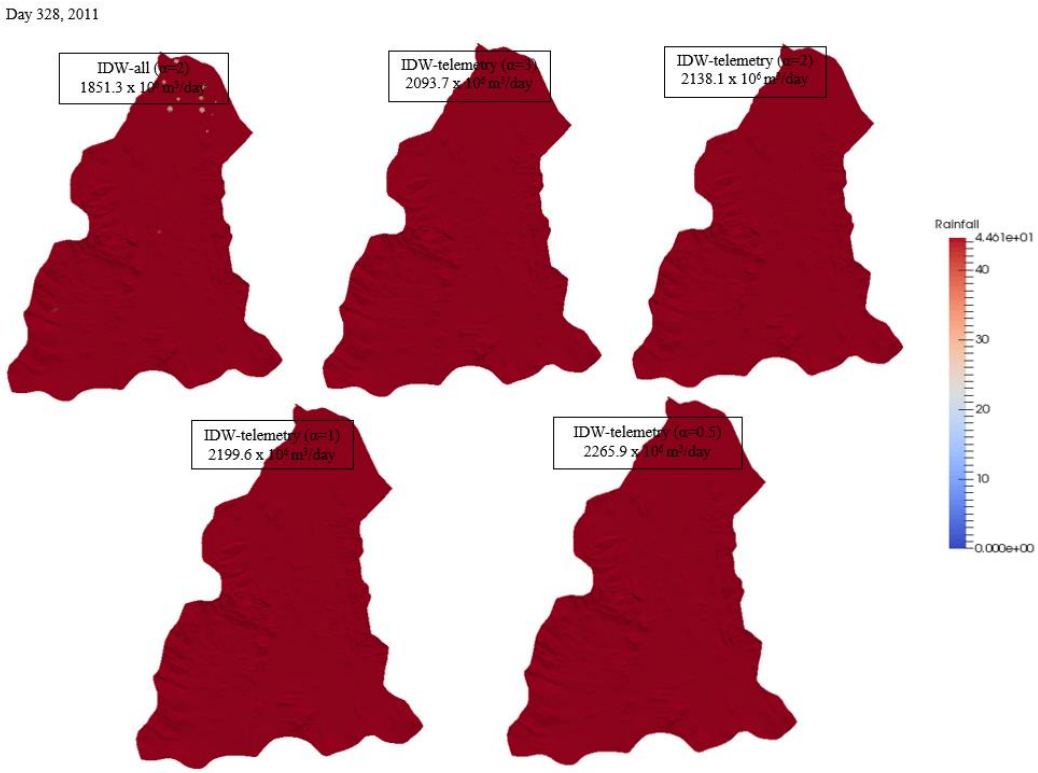

Figure 5.20. Comparison of rainfall distribution with various α, day 328 2011.

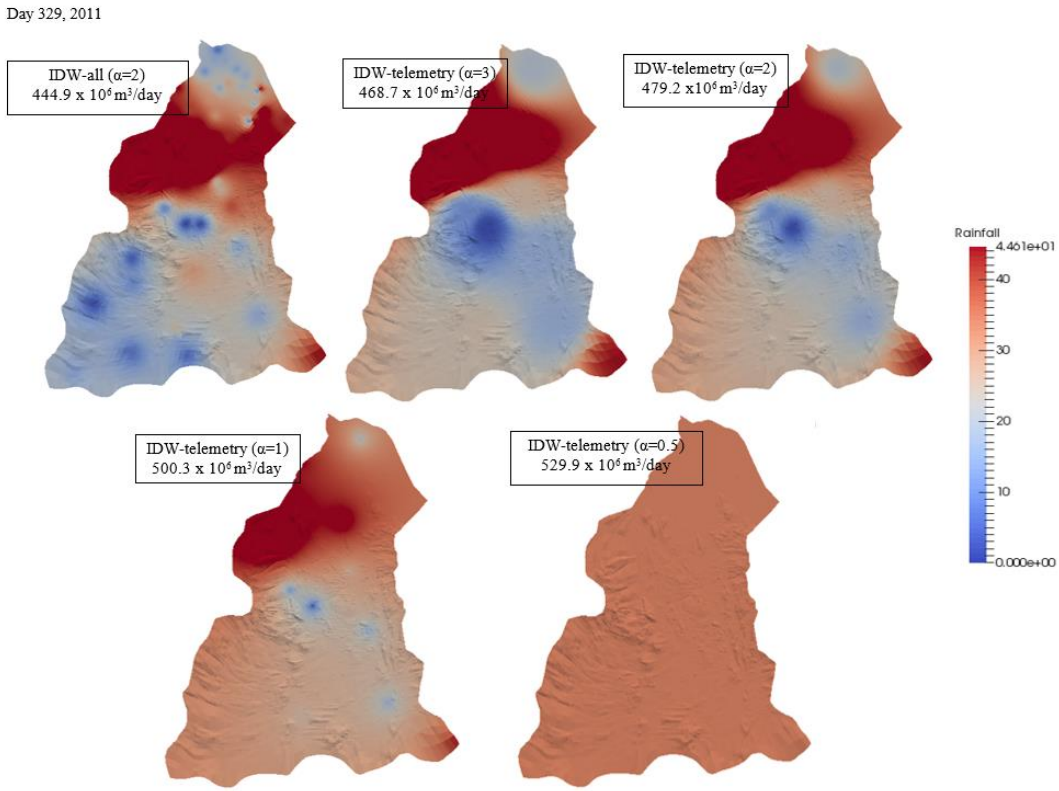

Figure 5.21. Comparison of rainfall distribution with various α, day 329 2011.

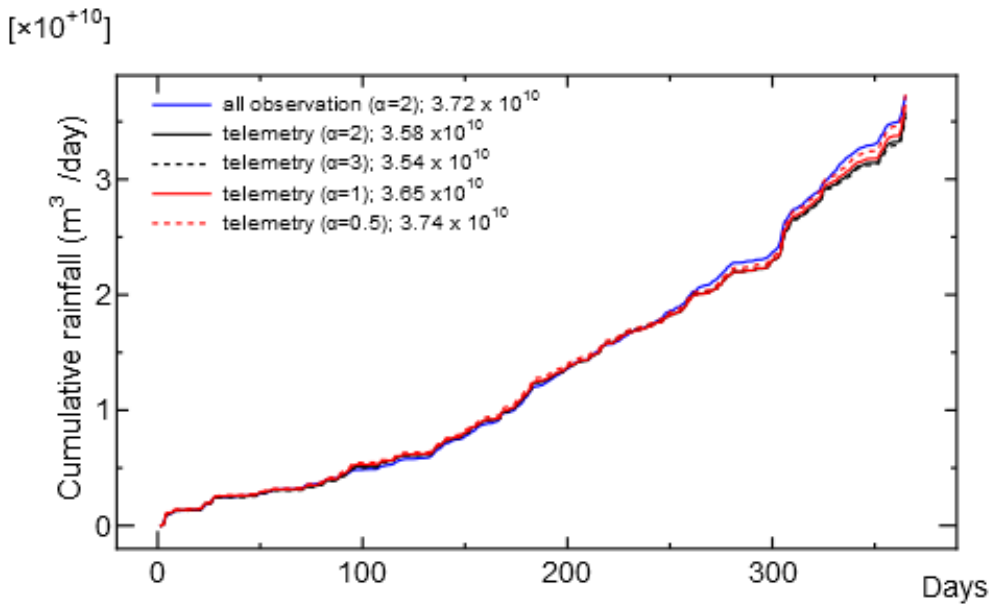

Figure 5.22. Cumulative rainfall by telemetry stations (α = 0.5, 1, 2, 3) and all-stations (α =2) for year 2011.

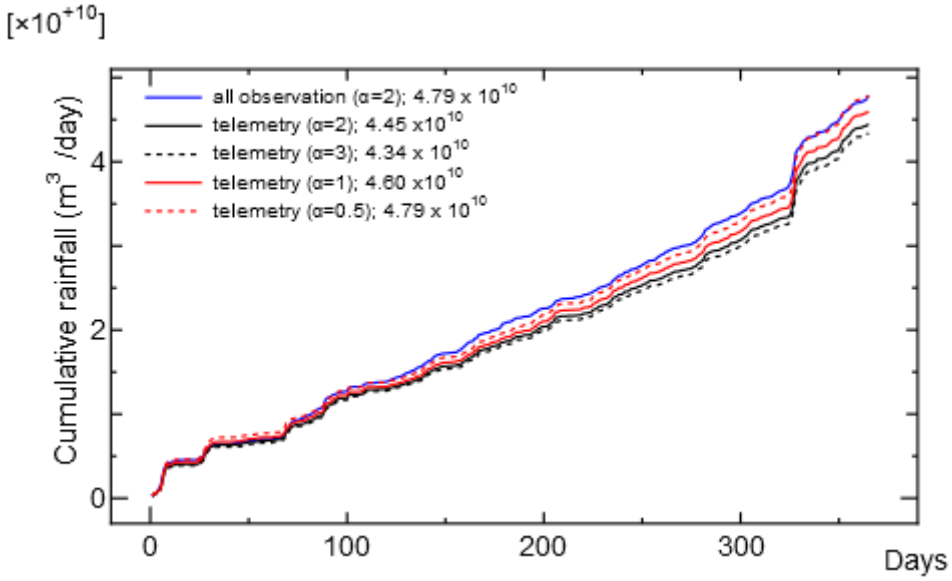

Figure 5.23. Cumulative rainfall by telemetry stations (α = 0.5, 1, 2, 3) and all-stations (α =2) for year 2011.

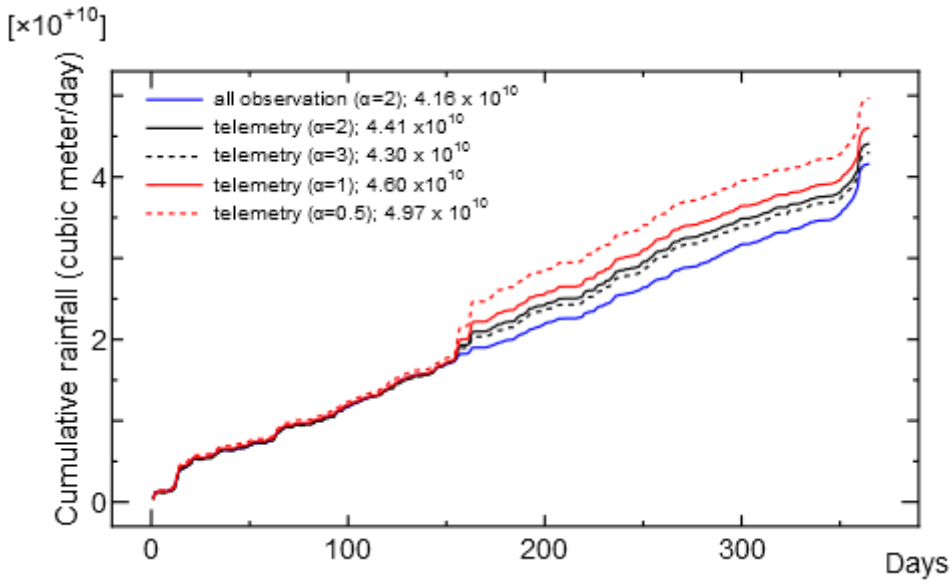

Figure 5.24. Cumulative rainfall by telemetry stations (α = 0.5, 1, 2, 3) and all-stations (α =2) for year 2012.

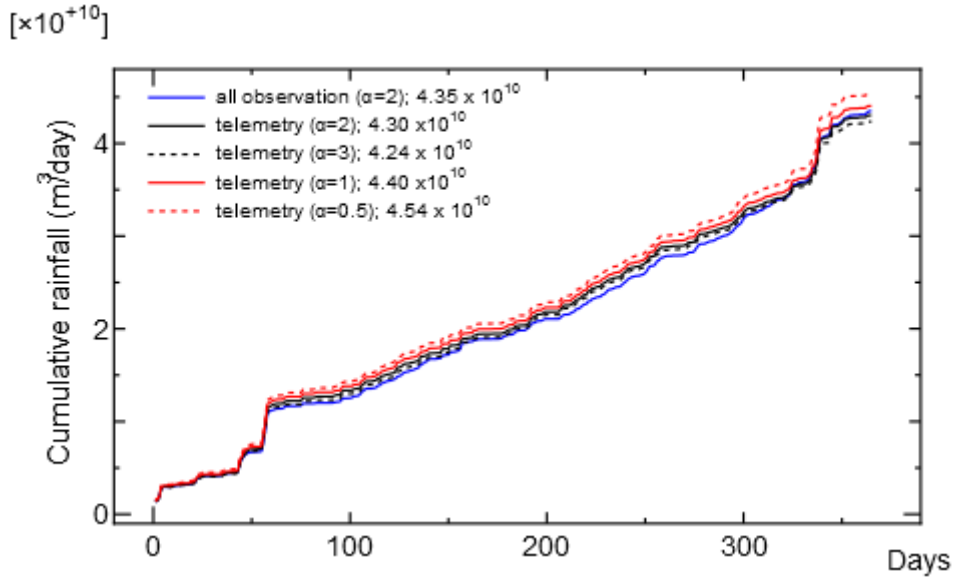

Figure 5.25. Cumulative rainfall by telemetry stations (α = 0.5, 1, 2, 3) and all-stations (α =2) for year 2013.

5.5 *Discussion on Rainfall Distribution by Numerical Simulation*

5.5.1 *Assumption of Simulation*

Rainfall distributions over the large Kelantan watershed were developed on daily basis to provide realistic simulation for year 2007 up to 2013. In this analysis, canopy interception and evapotranspiration effect were not considered. Up to 70 rainfall stations and their daily time-series were used to interpolate gridded rainfall surfaces using inverse distance weighting (IDW), inverse distance and elevation weighting (IDEW). The IDW and IDEW were tried twice each by: a) applying on whole watershed and b) sub-watershed scale. So a total of 5 rainfall distribution gridded surface was produced in one space-time rainfall series together with average rainfall distribution

5.5.2 *Comparison Among Rainfall Distribution Estimation Methods*

The sensitivity analysis of rainfall distribution parameters was done to see variations in rainfall pattern and amount of rainfall produced by changing the α and z_{min}. From the analysis, a low α leads to a greater weight towards a grid point value of rainfall from remote rain gauges. As the α decreases toward zero, the method approximates the Thiessen method, whereas larger range

of elevation leads to higher amount of rainfall produced across the watershed. For elevation parameter, larger range of Δz leads to higher amount of rainfall across the watershed.

The accuracy of all rainfall variability was inspected by GETFLOWS in quantitative and qualitative comparison. The results for all rainfall distribution i.e IDW, IDEW, AIDW and AIDEW show very insignificant difference. However, hydrographs generated using average rainfall tended to produce higher peaks during low-flood season whereas the volumes and peaks were undervalue during monsoon season. From this analysis, it is found that the simplest IDW method is appropriate for Kelantan watershed.

5.5.3 *Estimation by Telemetry Stations*

In Kelantan watershed, there are 11 telemetry rainfall stations located sparsely. For early flood prediction, quick rainfall distribution will be generated from this 11 telemetry stations.

Sensitivity analysis of α parameter for telemetry stations was conducted to evaluate the difference between rainfall distribution generated from telemetry stations (α = 0.5, 1, 2, 3) and all-stations (α =2). It was found that by setting α value to 0.5, it will produce higher amount of rainfall closer to rainfall distribution in years 2010 and 2011, generated using all stations. However, the distribution become non-distinguishable and was somewhat averaging the amount of rainfall across the Kelantan watershed.

Comparing quantitatively, α value of 0.5 gives higher amount of cumulative rainfall for each year and α value of 3 is the lowest. It is difficult to identify which α is suitable for early prediction using telemetry stations by comparing the amount of rainfall. But in terms of distribution, α of 2 is still applicable by comparing with distribution generated by all stations of the same α value.

5.6 ***Reproducibility of Guillemard Bridge Runoff Hydrograph***

5.6.1 *Proto-type Model Performance*

Figure 5.26 shows preliminary results of GETFLOWS using average areal rainfall as shown in Figure 5.6 for years 2007 to 2013. The results produced by GETFLOWS corresponded well with observation data. However, the amount of flows generated during high peak event is relatively low. This can be observed in each year during north east monsoon season (day 300 and above).

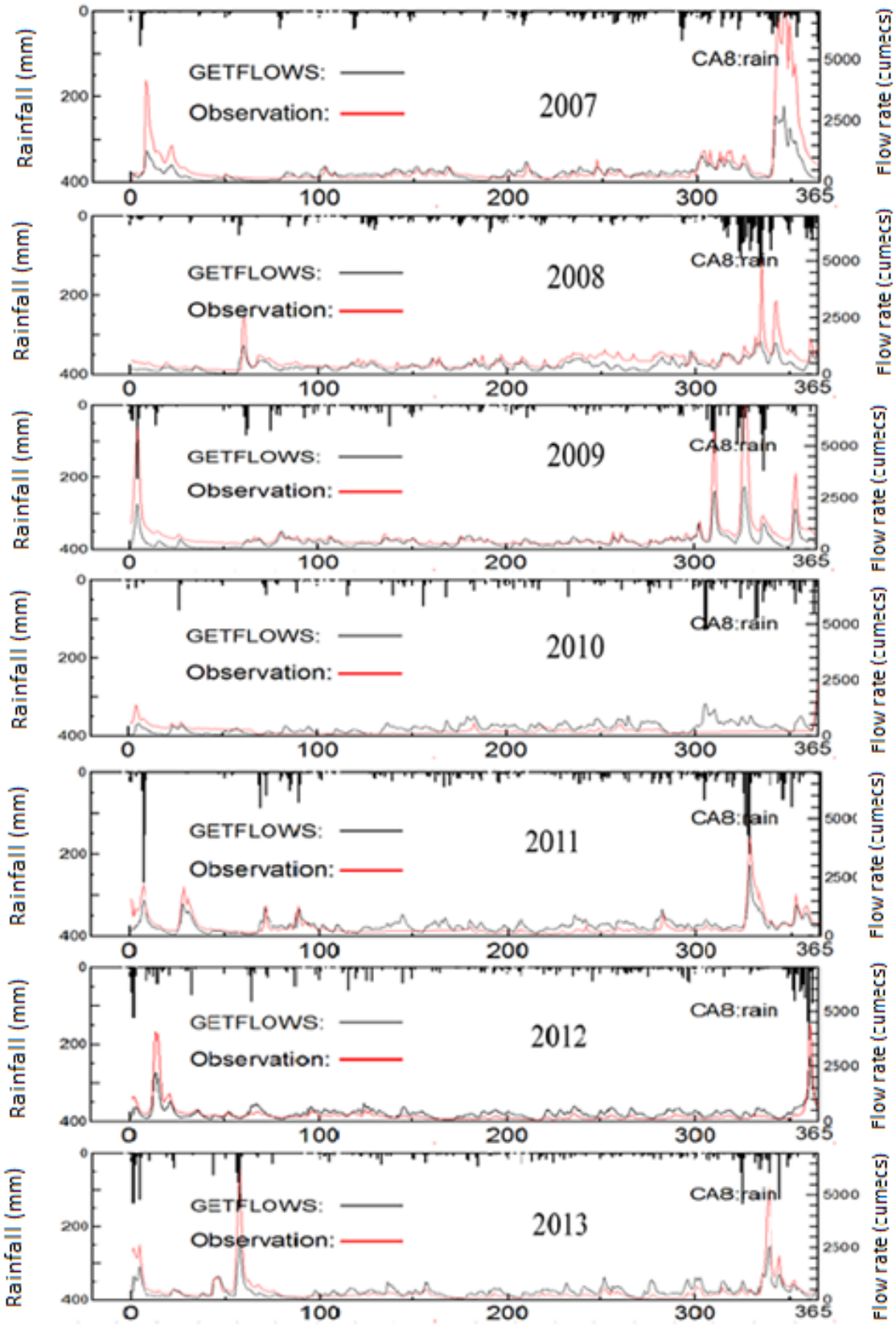

Figure 5.26. Hydrograph of Kelantan river at Guillemard Bridge by proto-type model for year 2007 to 2013.

5.6.2 *Improved Model Performance*

In this section, results from improved GETFLOWS model are presented. Based on sensitivity analysis, α value of 2 was chosen for both, all-stations and telemetry rainfall distribution. From the results in Figures 5.27 to 5.33, rainfall distribution using all-rainfall stations (red) gives relatively good fit during high-peak monsoon season but during low-flood season, the produced volume is higher than the observed flow.

Figures 5.30 to 5.33 show the results of telemetry stations (blue) starting 2010 to 2013. The results shows a very good match with all-stations (red) especially during the north east monsoon season. This proves that even though the amount of telemetry stations is small, using very rough rainfall distribution generated using telemetry stations is possible for early flood prediction for Kelantan watershed during the north east monsoon season. This is due to the low rainfall variability across the watershed during the north east monsoon season.

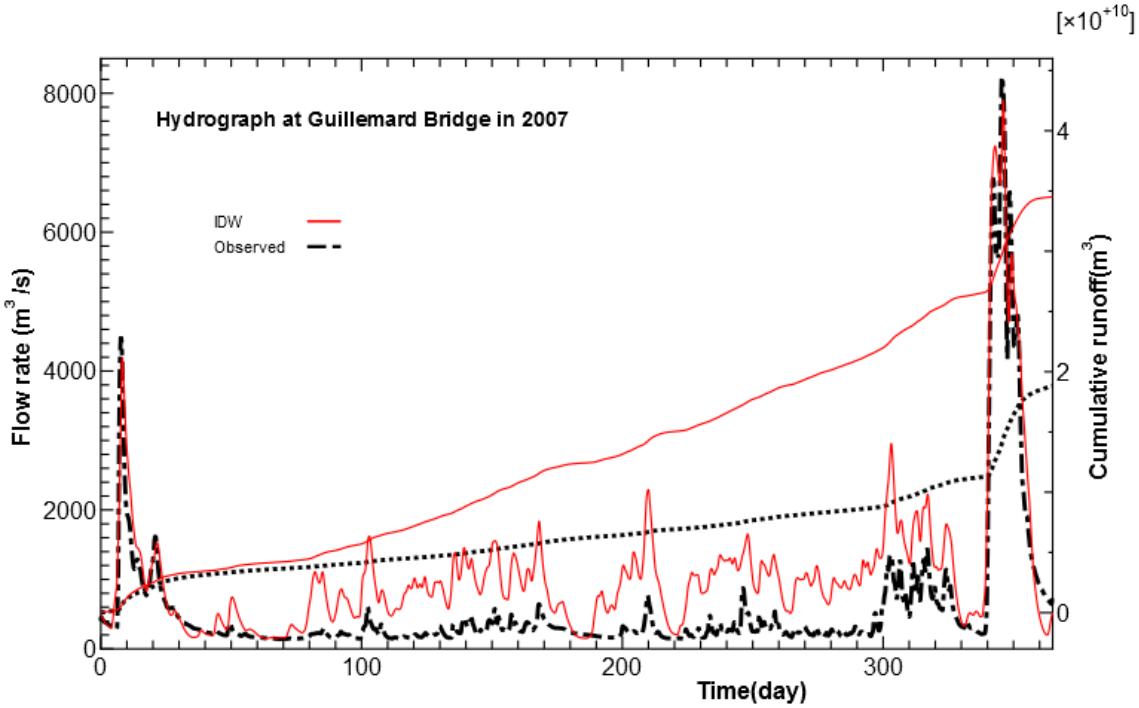

Figure 5.27. Hydrograph of Kelantan River at Guillemard Bridge in 2007 of improved model.

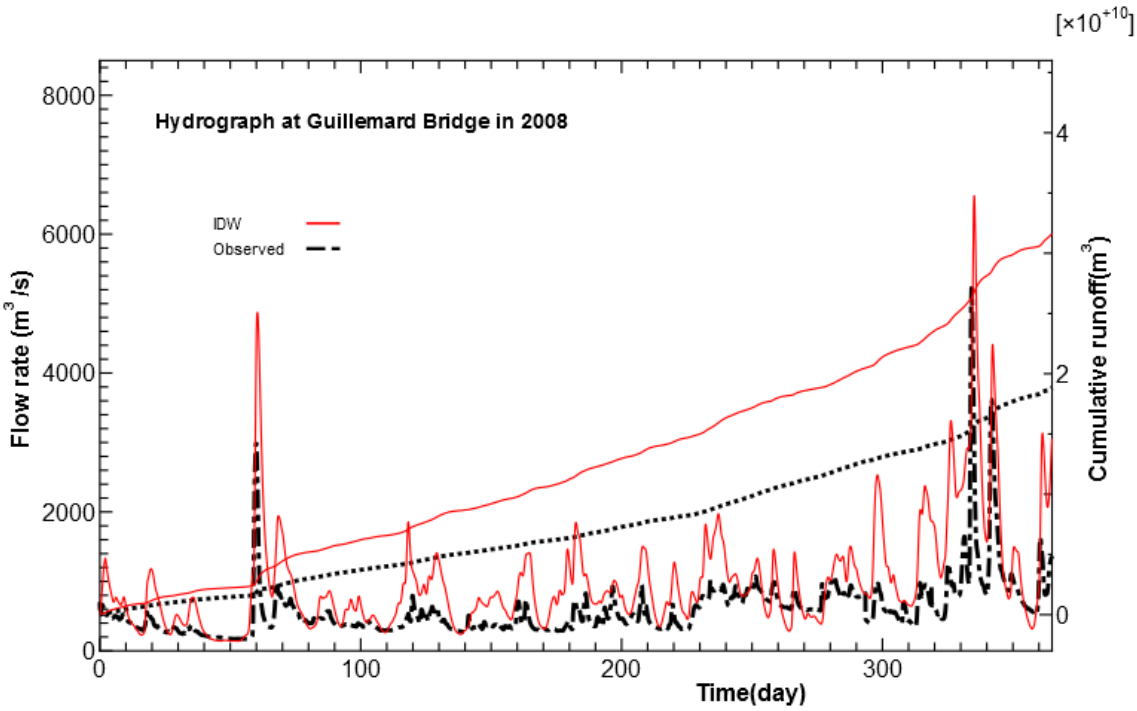

Figure 5.28. Hydrograph of Kelantan River at Guillemard Bridge in 2008 of improved model.

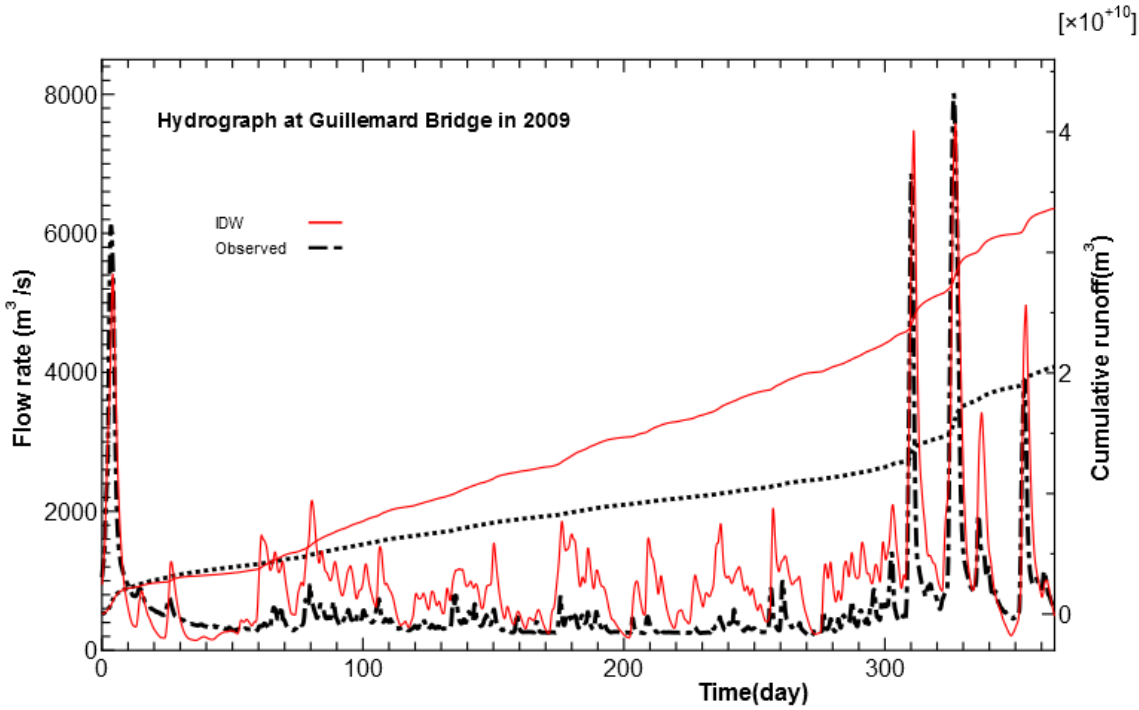

Figure 5.29. Hydrograph of Kelantan River at Guillemard Bridge in 2009 of improved model.

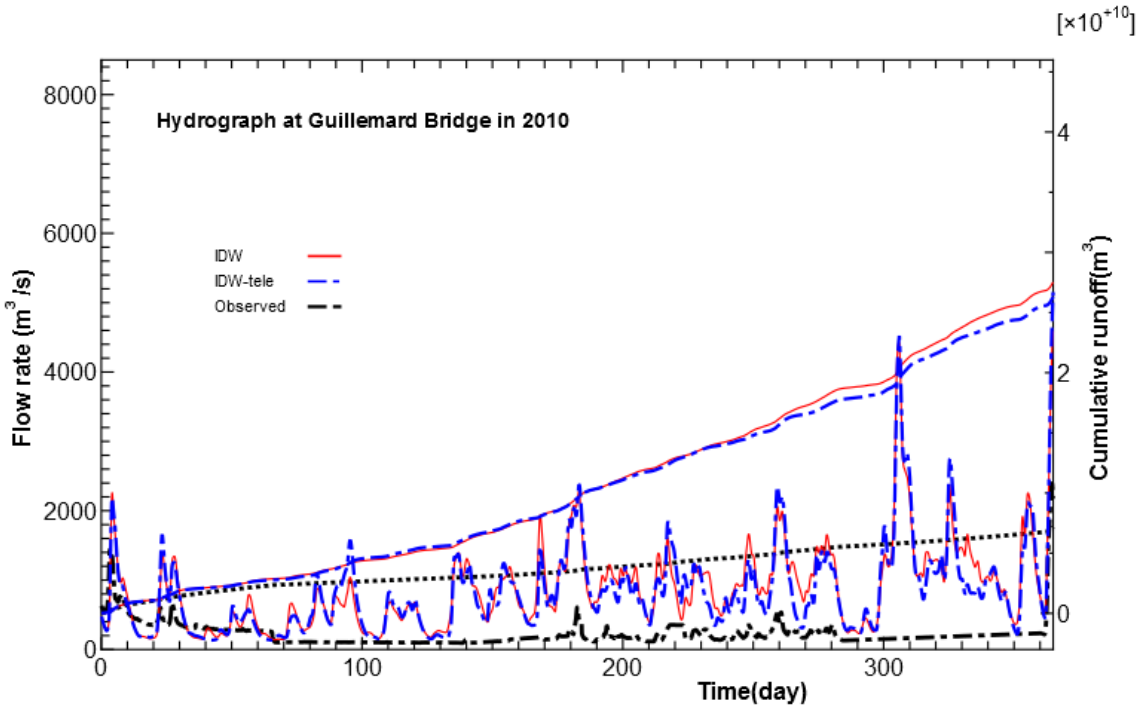

Figure 5.30. Hydrograph of Kelantan River at Guillemard Bridge in 2010 of improved model.

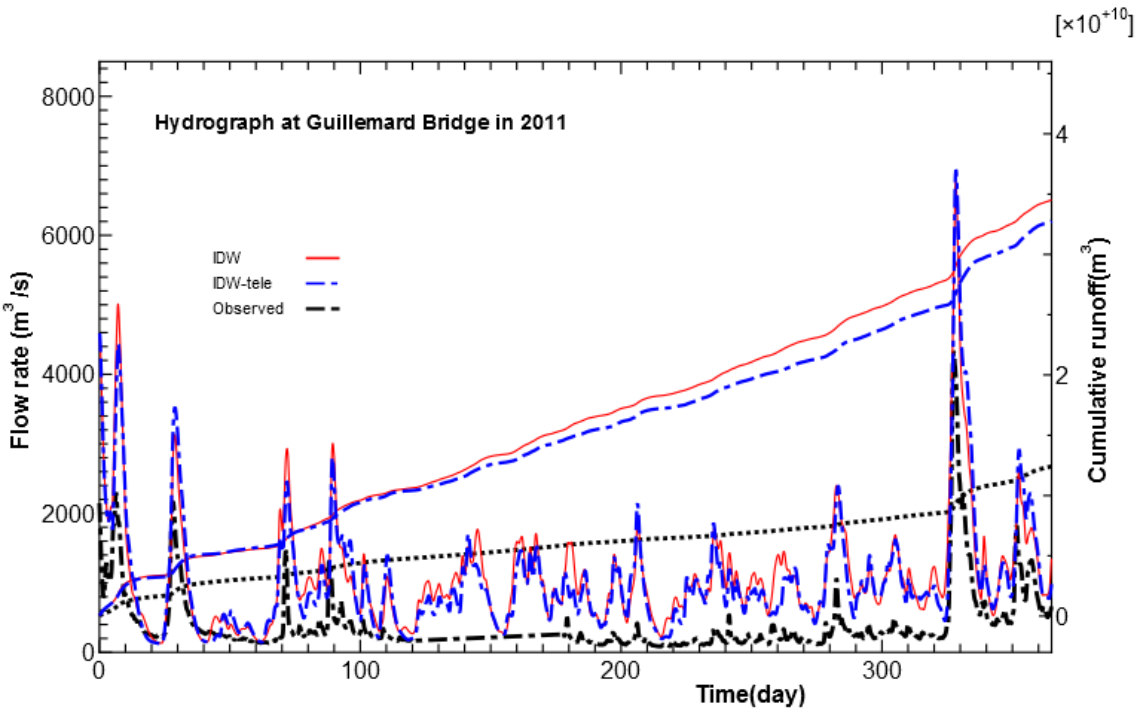

Figure 5.31. Hydrograph of Kelantan River at Guillemard Bridge in 2011 of improved model.

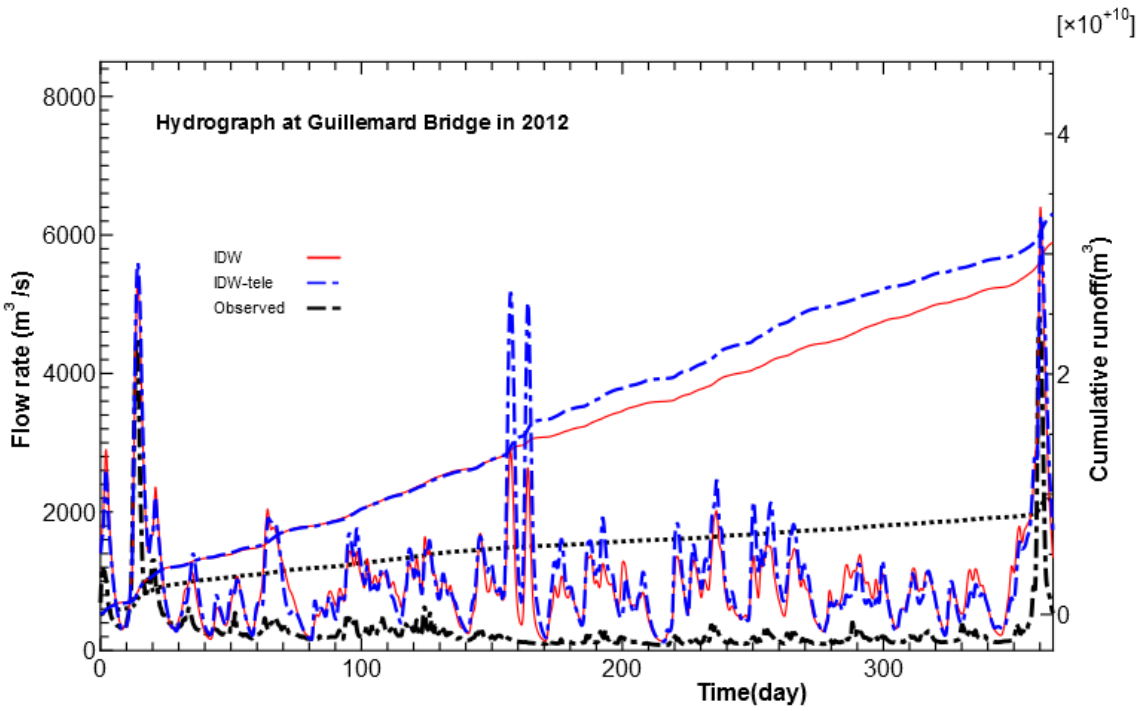

Figure 5.32. Hydrograph of Kelantan River at Guillemard Bridge in 2012 of improved model.

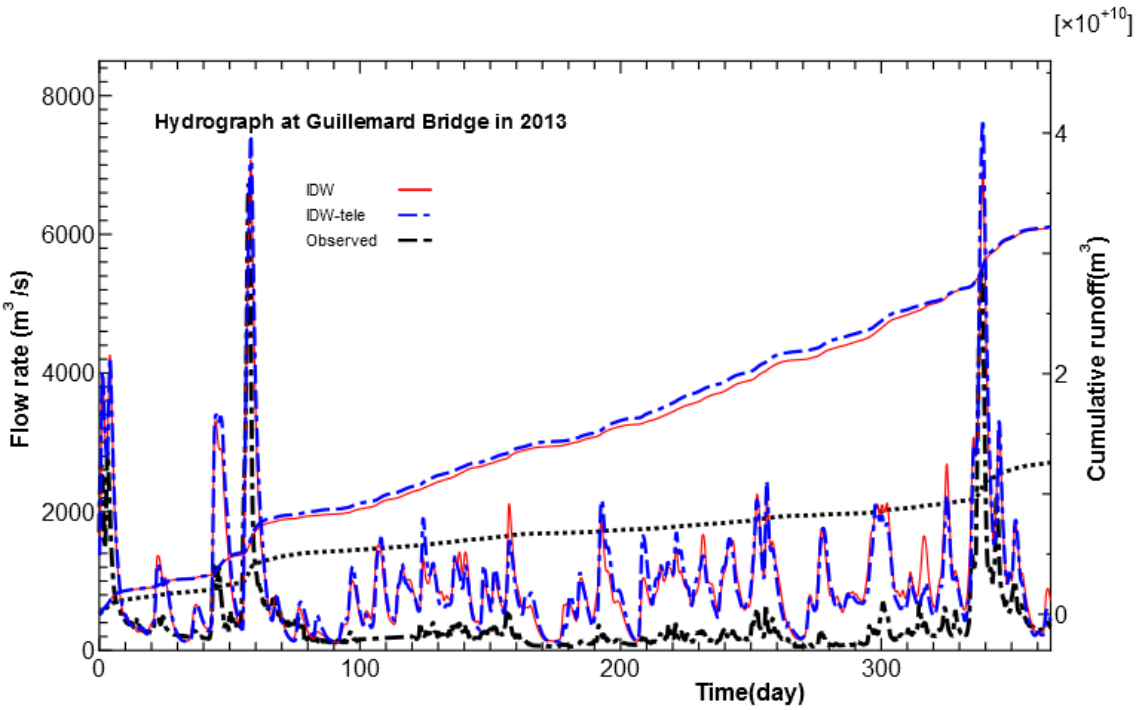

Figure 5.33. Hydrograph of Kelantan River at Guillemard Bridge in 2013 of improved model.

5.6.3 *Future Work to Improve Calibration*

Future work to improve flow estimation are

- Incorporating the effect of canopy interception and evapotranspiration to obtain full matching, especially during low flood season.
- To validate numerical model using the recent 2014 flood.
- To include all streamflow stations (telemetry) for optimum calibration result
- Visualization of streamflow in the river during flood event/inundation process.

5.7 *Conclusion*

For the purpose of realizing numerical prediction in the Kelantan watershed, basic numerical studies were conducted. Starting from the construction and initialization of the model by GETFLOWS, then, focusing on rainfall distribution which was the biggest governing factor of the watershed runoff behaviour, detail discussions were made in this study.

1) <u>Construction of basic numerical model</u>

   Topographic SRTM data with 90 x 90 m resolutions, river network and landuse information were used to construct basic Kelantan River watershed grid system. A two-stage initialization was done by setting the sensitive parameter such as permeability, porosity, surface manning's and evapotranspiration. Basic performance of the model was checked by comparing with observed flow rate at Guillemard Bridge.

2) <u>Estimation and comparison of rainfall distribution</u>

   A detail investigation on rainfall distribution variability is conducted by using the Inverse Distance Weight (IDW) family methods. The sensitivity analysis of rainfall distribution parameters was investigated to see variations in rainfall pattern and amount of rainfall produced by changing the α and z_{min}. From the analysis, a low α leads to a greater weight towards a grid point value of rainfall from remote rain gauges. As the α decreases toward zero, the method approximates the Thiessen method, whereas larger range of elevation leads to higher amount of rainfall produced across the watershed. The accuracy of all rainfall variability was inspected by GETFLOWS in quantitative and qualitative comparison.

3) Reliability of quick estimation by telemetry station

For early warning in the Kelantan River watershed, reliability of estimated distribution by using sparsely distributed stations has been discussed. It is found that α of 2 is still appropriate to be used for early flood prediction during the north east monsoons season since rainfall variability is very low during this season. The hydrographs from telemetry stations for year 2010 to 2013 give relatively good match with the simulated hydrographs by all stations.

4) Calibration of numerical model

The difference and adaptability of estimated rainfall distribution was checked and was found that the simplest IDW method may be appropriate for Kelantan watershed. The numerical model was calibrated with observed stream flow data for year 2007 and validated using 2008-2013 in daily scale. Simulation results show that calculated hydrographs were generally in good agreement with the observation flow rate during high peak monsoon. However, simulated hydrographs show significant differences from the observed hydrographs during low-flood season due to interception and evapotranspiration effect were not considered in these trials.

In this study, historical calibrations of the model to the observed flow rate were not the main target because some ambiguous factors regarding canopy interception and evapotranspiration could not be fully identified due to lack of historical meteorological data. Future plan in this will be to incorporate such effects to attain full historical matching, to validate the numerical model using recent 2014 flood, including all streamflow stations (telemetry) for optimum calibration result and visualization of streamflow in the river during flood event/inundation process.

6 Conclusion and Future Work

6.1 *Conclusion*

In Malaysia, flood is the most serious natural disaster in terms of frequency, areal extent and the number of population affected. In this study, targeting to develop practical methods for early flood prediction in the Kelantan River watershed, the author took three main steps; 1) historical data collection and consistency/trend check, 2) development of observation-based statistical models, 3) construction of physically based, distributed numerical model and estimation methods of rainfall distribution. Followings are the contents and major results covered in this thesis.

1) <u>Collection of historical observation data, consistency check and trend analysis</u>
   - The historical rainfall data at distributed gauge stations were collected from 1948 through 2013, and they were arranged and stored with continuous time stamp in the data base together with water level observations and other hydrologic data.
   - It was found that among fifty rainfall stations within the river basin, nine were flagged as doubtful or suspected in terms of consistency or homogeneity by the absolute homogeneity tests. Of these, four stations were identified as inhomogeneous and omitted from further analysis.
   - The Mann-Kendall tests (MK) with different sampling period were devised and applied to the trend analysis. The MK test of 30-year sampling period showed that weakly decreasing trend of rainfall persisted in 1957-1987 and some clear increasing trend in 1981-2011. The MK with 10-year sampling clearly gave the turning points and trend of rainfall which was not clearly seen in the observation data itself. The turning points found by this method corresponded well to the cycle of El Nino and La Nina. The effect of them was found different for upstream inland area and downstream area near coast of South China Sea.
   - Extending the above, it was predicted roughly that in Kelantan watershed high rainfall years after 2009 La Nina would slowly disappear up to around 2015 in inland area, remain high around 2015 in downstream area, then might decrease and meet low rainfall years at next El Nino after around 2020. Therefore, this analysis is expected to be effective for quantifying regional meteorological trends affected by ENSO.

2) Observation-based approach for early flood prediction

- To realize quick and reliable early flood prediction, two statistical models that estimate the water level at downstream forecasting point were developed based on the information of upstream gauge stations. Unlike ARMA or any other statistical linear runoff models that use time-series data of forecasting point itself, the first model developed here depends on mainly the information coming to the forecasting point from various upstream gauge stations in hourly scale, while in the second model, most recent observed data at forecasting point was considered to improve predictability.
- The basic form of model consists of a linear combination of the time-series data of multiple upstream stations considering the time lags and its ranges for respective stations. Cross-correlation analyses were conducted to find suitable time lags and lag ranges for respective pairs of gauge stations through monsoon season of the year. In determining coefficients of the linear system, the least square method was used for the summated data sampled over the period from the beginning of monsoon season in November to the end in next January.
- The first model was applied for the prediction of water level at Kuala Krai (C) using the observed data at two upstream stations, Galas (A) and Lebir (B), while for the prediction of water level at Guillemard Bridge (D), upstream data at A, B and C were used. It was found that a combination of station A with average delay time of 5 hours and station B of 4 hours gave more reliable results than using a single station. Similarly, at station D, the case by utilizing all upstream point A (14 hours), B (10 hours) and C (6 hours) provided higher predictability. In most of the cases, the water level predicted from the model has the Absolute Mean Error (MAE) within 1 m from the starting time of flood up to the peak of flood event. However, the predictability of the model deteriorates when the downstream area received rainfall earlier than the upstream area.
- To improve the predictability, the second model which included the most recent observation data at forecasting station successfully attained good prediction up to 3 hours and 5 hours for station C and D, respectively, with MAE of 0.3 meter for all events in year 2011, 2013 and 2014. This improved method could produce a continuous reliable prediction by updating the coefficients hourly assuming the upstream telemetry data is updated in monitoring system.

3) Numerical approach for early flood prediction

- To realize numerical prediction which can trace water flow over the watershed beyond point-wise prediction by the observation-based statistical model, a numerical model of the Kelantan watershed was constructed and used for the discussion of the estimation methods of rainfall distribution.
- A basic 3-D numerical model for the Kelantan watershed was constructed using topographic data (SRTM 90m resolution), river network and land-use information. Two-stage initialization was done to make initial distributions of pressure and surface/subsurface water saturation by setting the sensitive parameters such as permeability, porosity, surface manning's roughness factor, etc. Basic performance of the model was checked by comparing with observed flow rate at Guillemard Bridge.
- Detailed investigation on grid-wise rainfall distribution on daily basis was conducted by using the Inverse Distance Weight (IDW) family methods. It was found that the simplest IDW method was appropriate for the vast Kelantan watershed since the differences among the family methods were insignificant in terms of cumulative amounts and the performances of hydrographs obtained by the numerical simulator under the same simple condition neglecting unclear canopy interception and evapotranspiration effects.
- Considering the necessity of quick timely estimation of rainfall distribution for the numerical prediction, reliability of the estimated distribution by using only telemetry stations sparsely distributed in the watershed was discussed. It was found that the same IDW parameter used for the case of all available stations could be applied to telemetry-based estimation, and difference between two distributions was not significant in terms of cumulative amount over watershed. The simulated hydrographs using two distributions for year 2010 to 2013 gave relatively small difference and it was concluded that telemetry-based estimation might work for the early prediction purpose by the numerical model.
- The numerical simulations were run for checking data adaptability using basic parameters and estimated rainfall distributions for years 2007-2013 on daily scale. Simulation results showed that calculated hydrographs were generally in good agreement with the observed flow rate during high peak in monsoon, while

they showed significant difference from the observed during low-flood season. As the results of trial runs considering evapotranspiration effect made the difference much smaller in the low-flood period, it was suggested that in tuning model parameters to attain good matching, quantitative evaluation of canopy interception and evapotranspiration processes should be properly reflected.

The author expects the discussions and the developed models in this thesis could contribute to practical prediction of flooding in this watershed. The trend analysis might provide information about regional meteorological background to be considered in administrative policy. The proposed observation-based model might be introduced easily into practical use, and the numerical model, if satisfactory calibration is done, will provide us information what flow is occurring in the surface and subsurface of the whole watershed and help us planning countermeasures to minimize flood/inundation damages in this watershed.

6.2 *Limitations and Future Works*

Limitations and future works for both models are listed below:

1) A quick and reliable prediction of downstream water level can be done applying the developed observation-based method. Utilizing telemetry data of multiple upstream water level stations, continuous running of this model would predict the water level at downstream stations. However, if the downstream rainfall comes earlier than in the upstream, predictability might be deteriorated seriously. Even in such case, incorporating the newest data of the forecasting water level station may improve the predictability. Future work for observed-based model is to apply it at the water level observation point in urban area located more downstream from Guillemard Bridge (D) for early prediction.
2) The final target of the numerical simulation is to complete satisfactory matching between the observed and calculated, but it is left unrealized. To incorporate meteorological effects concerning canopy and evapotranspiration is the remaining work for the author, in order to know what is occurring in the whole watershed and to make countermeasure to minimize flood damage in this watershed.

References

Chapter 1 & 2

Abbott, M.B., Bathurst, J.C., Cunge, A.J., O'Connel, P.E. and Rasmussen, J., 1986. An introduction to the European Hydrological System – Système Hydrologique Européen, ''SHE'', 1. History and philosophy of a physically-based distributed modelling system. *J. Hydrol*, 87: 45–59.

Abbott, M.B., Bathurst, J.C., Cunge, J.A., O'Connell, P.E. and Rasmussen, J., 1986. An introduction to the European Hydrological System - Systeme Hydrologique Europeen, "SHE", 2: Structure of a physically-based, distributed modelling system *J. Hydrol*, 87(1-2): 61-77.

Awadalla, S, Noor IM., 1991. Induced climate change on surface runoff in Kelantan Malaysia. *International Journal of Water Resources Development*. 7: 53-59.

Beven, K.J., 1991. Spatially distributed modelling: conceptual approach to runoff prediction. In: D.S. Bowles and P.E. O'Connell (Editors), Recent Advances in the Modelling of Hydrologic Systems. Kluwer Academic, 373-387.

Chan N. W, 2002. Reducing flood hazards exposure and vulnerability in Peninsular Malaysia floods. Taylor & Francis Publisher: London.

Chan, N. W & Parker, D. J, 1996. Response to dynamic flood hazard factors in Peninsular Malaysia. *The Geographic Journal* 162: 313 -325.

DID, 2000.Drainage and Irrigation Department. Laporan Banjir Tahunan bagi Semenanjung Malaysia. Unpublished report. Kuala Lumpur.

DID, 2003. Drainage and Irrigation Department. Laporan banjir tahunan bagi Semenanjung Malaysia. Unpublished report. Kuala Lumpur.

DID, 2012. Drainage and Irrigation Department. Laporan banjir tahunan bagi Semenanjung Malaysia. Unpublished report. Kuala Lumpur.

DID, 2013. Drainage and Irrigation Department. Laporan banjir tahunan bagi Semenanjung Malaysia. Unpublished report. Kuala Lumpur.

Hoong, C. C., 2007. Development of flood forecasting model for Sungai Kelantan (Tank Model). *Undergraduate Thesis*. Universiti Teknologi Malaysia.

JICA, 1982. National water resources study in Malaysia. Sectoral Report, Vol. 5: River Conditions. Japan International Cooperation Agency.

Malaysia National Committee, 1976. Flood control in Malaysia. In Framji KK and Garg BC (Eds). Flood control in the world: A global review. International Commission on Irrigation and Drainage, New Delhi 2: 561-569.

Mohamed Desa, M. N, Mohd Sidek, L., Che Ros, F, Tabios III, G. Q., Pawitan, H.,Tuyen H. M. and Fukami K., 2010. State of the art report: Assessment of flood forecasting and warning system for tropical region. CSGM COE UNITEN-Technical Report No. 7.

MMD, 2007. Malaysian Meteorological Department (MMD). Report on heavy rainfall that caused floods in Kelantan & Terengganu. Unpublished Report. Kuala Lumpur.

Raj. J.K, 2009. Geomorphology. In: Hutchison, C.S and Tan, D.N.K., Eds., Geology of Peninsular Malaysia, Geological Society of Malaysia, Kuala Lumpur, 5-29.

Theresa, M.C & Konstantine, O.G., 2006. Intercomparison of lumped versus distributed hydrologic model ensemble simulations on operational forecast scales. *J. Hydrol.*, 329, 174 – 185.

Tosaka, H., Itoh, K. and Furuno, T., 2000. Fully coupled formulation of surface flow with 2-phase subsurface flow for hydrological simulation. *Hydrol. Process.* 14, 449-464.

World Bank, 2011. "The World Bank Supports Thailand's Post-Floods Recovery Effort". http://www.worldbank.org/en/news/feature/2011/12/13/world-bank-supports-thailands-post-floods-recovery-effort

Zakaria AS., 1975. The geomorphology of Kelantan delta (Malaysia). *CATENA* 2: 37-350.

Chapter 3.

Alexandersson, H., and Moberg, A., 1997. Homogenization of Swedish temperature data. Part 1: homogeneity test for linear trends, *Int. J. Climatol.*, 17, 25–34.

Bingham, C., and Nelson, L. S., 1981. An approximation for the distribution of the von Neumann ratio, *Technometrics*, 23(3), 285–288.

Birsan, M., Molnar P., Burlando, P., and Pfaundler, M., 2005. Streamflow trends in Switzerland, *J. Hydrol.*, 314(1–4), 312–329.

Buishand, T. A., 1982. Some methods for testing the homogeneity of rainfalls records, *J. Hydrol.*, 58, 11–27.

Cao, L.-J., and Yan, Z.-W., 2012. Progress in research on homogenization of climate data, *Adv. Clim. Change Res.*, 3(2), 59–67

Climate Prediction Center. 2015. *Changes to the Oceanic Niño Index (ONI)* [online]. NOAA, USA. Available from: http://www.cpc.noaa.gov/products/analysis_monitoring/ensostuff/ensoyears.shtml [Accessed 31st May 2015].

Costa, A. C., and Soares, A., 2009. Homogenization of climate data; review and new perspective using geostatistics, *Math Geosci.*, 41, 291–305.

Cubasch U., D. Wuebbles, D. Chen, M.C. Facchini, D. Frame, N. Mahowald, and J.-G.Winther(2013).Introduction. In: Climate Change 2013: Cambridge University Press, Cambridge, United Kingdom and New York, NY, USA.

Gilbert, R. O., 1987. *Statistical methods for environmental pollution monitoring*. New York: Van Nostrand Reinhold.

Hamed, K. H., 2008. Trend detection in hydrologic data: the Mann-Kendall trend test under the scaling hypothesis, *J. Hydrol.*, 349(3–4), 350–363.

Hartmann, D.L., A.M.G. Klein Tank, M. Rusticucci, L.V. Alexander, S. Brönnimann, Y. Charabi, F.J. Dentener, E.J. Dlugokencky, D.R. Easterling, A. Kaplan, B.J. Soden, P.W. Thorne, M. Wild and P.M. Zhai (2013). Observations: Atmosphere and Surface. In: Climate Change 2013: Cambridge University Press, Cambridge, United Kingdom and New York, NY, USA.

Hawkins, P. M., 1977. Testing a Sequence of observations for a shift in location, *J. Am. Stat. Assoc.*, 72, 180–196.

Heino, R., 1994. *Climate in Finland during the Period of Meteorological Observations*, Academic dissertation. Finnish Meteorological Institute.

Helsel, D. R., and Hirsch, R. M., 2002. *Statistical Method in Water Resources Techniques of Water Resources Investigations*, Book 4, Chapter A3, U.S Geological Survey. Available from: http://water.usgs.gov/pubs/twri/twri4a3. [Accessed 2nd June 2014].

Hsu P-C., Ho C-R., Liang S-J., and Kuo N-K., 2013. Impacts of two types of El Niño and La Niña events on typhoon activity. *Adv. Meteor*. 2013, 8.

IPCC. Climate Change 2001: Impacts, Adaptation, and Vulnerability. Contribution of Working Group II to the 3rd Assessment Report of the Intergovernmental Panel on Climate Change, Cambridge University Press, Cambridge, 2001.

Jarušková, D., 1996. Change-point detection in meteorological measurement, *Am. Meteor. Soc.*, 124, 1535–1543.

Kang, H. M., and Fadhilah, Y., 2012. Homogeneity tests on daily rainfall series in Peninsular Malaysia, *Int. J. Contemp. Math. Sciences*, 7(1), 9–22.

Kendall, M. G., 1975. *Rank Correlation Methods*. London: Griffin.

Kisi, O. and Ay, M., 2014. Comparison of Mann-Kendall and innovative trend method for water quality parameters of the Kizilirmak River, Turkey. , *J. Hydrol.*, 513(26), 362-375.

Klein Tank, A. M. G., 2007. *Algorithm theoretical basis document (ATBD)*, European Climate Assessment & Dataset (ECA&D) project document, KNM 38.

Mann, H. B., 1945. Nonparametric tests against trend, *Econometrica*, *13*, 245–259.

Mestre, O., Domonkos, P., Picard, F., Auer, I., Robin, S., Lebarbier, E., Böhm, R., Aguilar, E., Guijarro, J., Vertachnik, G., Klancar, M., Dubuisson, B., and Stepanek, P., 2013. HOMER: A homogenization software—methods and applications, *Quart. J. Hungarian Meteor. Serv.*, 117(1), 47–67.

Peterson, T. C., Easterling, D. R., Karl, T. R., Groisman, P., Nicholls, N., Plummer, N., Torok, S., Auer, I., Boehm, R., Gullett, D., Vincent, L., Heino, R., Tuomenvirta, H., Mestre, O., Szentimrey, T., Salinger, J., Førland, E. J., Hanssen-Bauer, I., Alexandersson, H., Jones, P., and Parker, D., 1998. Homogeneity adjustment of in situ atmospheric climate data: a review, *Int. J. Climatol*., 18(13), 1493–1517.

Pettitt, A. N., 1979. A non-parametric approach to the change-point problem, *Appl. Stat. J.*, 28, 126–135.

Philbert, M. L., Edmund, M., Hashim, K. N., 2014. Homogeneity of monthly mean air temperature of the United Republic of Tanzania with HOMER, *Atmos. Clim. Sci.*, 4, 70–77. doi.org/10.4236/acs.2014.41010

Roberts, G., 1998. The effects of possible future climate change on evaporation lossess from four contrasting UK water catchment areas. *Hydrological Processes*, 12(5): pp. 727-739.

Sahin, S. and Cigizoglu, H. K., 2010. Homogeneity analysis of Turkish meteorological data set, *Hydrol. Process*, 24(8), 981–992.

Suhaila, J., Sayang, M. D., and Jemain, A. A., 2008. Detecting inhomogeneity of rainfall series in Peninsular Malaysia, *Asia-Pac. J. Atmos. Sci.*, 44(4), 368–380.

Suhaila, J., Sayang, M. D., Wan Zawiah, W. Z., and Jemain, A. A., 2010. Trends in Peninsular Malaysia rainfall data during the southwest monsoon and northeast monsoon seasons: 1975–2004, *SainsMalaysiana.* 39(4), 533–542.

Tuomenvirta, T., 2002. Homogeneity testing and adjustment of climatic times-series in Finland, *Geophysica*, 38(1–2), 15–41.

Von Neumann, J., 1941. Distribution of the ratio of the mean square successive difference to the variance, *Annals of Math. Stat*., 12, 367-395.

Wijngaard, J. B., Klein Tank, A. M. G., and Können, G. P., 2003. Homogeneity of 20th Century European Daily Temperature and Precipitation Series, *Int. J. Climatol.*, 23, 679–692.

Yue, S., Pilon, P., and Cavadias, G., 2002. Power of the Mann-Kendall and Spearman's Rho tests for detecting monotonic trends in hydrological series, *J. Hydrol.*, 259(1–4), 254–271.

Abrahart, R. J. and See L., 2000. Comparing neural network and autoregressive moving average techniques for the provision of continuous river flow forecasts in two contrasting catchments. *Hydrol. Process.* 14, 2157-2172.

Box, G. E. P and Jenkins, G. M., 1970. Time series analysis forecasting and control, *Holden-Day*, San Francisco, California.

Brath, A., Montanari, A. and Toth, E., 2002. Neural networks and non-parametric methods for improving real-time flood forecasting through conceptual hydrological models. *Hydrol. Earth Syst. Sci.*, 6(4), 627-640.

Chang, L. C., Chang, F. J., and Tsai, Y. H, 2005. Fuzzy exemplar-based inference system for flood forecasting, *Water Resources Research* 41, W02005, doi: 10.1029/2004WR003037.

Dawson, C. W., Harpham, C., Wilby, R. L. and Chen, Y., 2002. Evaluation of artificial neural network technique in the River Yangtze, China. *Hydrol. Earth Syst. Sci.*, 6, 619-626.

Galavi, H., Mirzaei, M., Shui L. T and Valizadeh, N., 2013. Klang River-level forecasting using ARIMA and ANFIS models. *American Water Works Association*. 496-506.

Kumari, N., Sunita and Smita, 2013. Comparison of ANNs, Fuzzy Logic and Neuro-Fuzzy integrated approach for diagnosis of coronary heart disease: a survey. *Int. Journal of Computer Science and Mobile Computing*. 2, 216-224.

Malik, N., 2015. A comparative study on computational intelligence, granular computing and soft computing technique. *Int. Journal of Enhanced Researched in Management & Computer Applications*.6,1-6.

Pan, T., Yang, Y., Kuo, H., Tan, Y., Lai, J., Chang, T., Lee, C., and Hsu, K., 2013. Improvement of watershed flood forecasting by typhoon rainfall climate model with and ANN-based southwest monsoon rainfall enhancement. *J. Hydrol*., 506, 90-100.

See, L. and Openshaw, S., 1999. Applying soft computing approaches to river level forecasting. *Hydrol. Sci. J.*, 44(5) 763-778.

See, L. and Openshaw, S., 2000. A hybrid multi-model approach to river level forecasting. *Hydrol. Sci. J.*, 45(4) 523-536.

Zadeh, L. A., 1973. Outline of a new approach to the analysis of complex systems and decision processes. IEEE Transitions on Systems, Man, and Cybernetics, 3(1), 28-44.

Chapter 5.

Arnaud, P.,Bouvier, C., Cisner, L., and Dominguez, R., 2002. Influence of rainfall spatial variability on flood prediction, *J. Hydrol.*, 260, 216-230.

Ashraf, M., Loftis, L. C. & Hubbard, K. G., 1997. Application of geostatistics to evaluate partial weather stations network. *Agric. For Meteorol*., 84: 255-271.

Beven, K. J and Kirby, M. J., 1979. A physically based variable contributing area model of basin hydrology. *Hydrol. Sci. Bull*., 24, 1-3.

Beven, K. J., Kirby, M. J. Schofield, N., and Tagg, A. F., 1984. Testing a physically-based flood forecasting model (TOPMODEL) for three U. K. catchments, *J. Hydrol*., 69, 119-143.

Chaubey, I., Haan C. T., Grunwald, S. & Salisbury, J. M., 1999. Uncertainty in the model parameters due to spatial variability of rainfall. *J. Hydrol*. 220(1), 48-61.

Chen, D. Ou, T., Gong, L., Xu, C.-Y., Li, W., Ho, C.-H. & Qian, W., 2010. Spatial interpolation of daily precipitation in China: 1951-2005. *Advances in Atmospheric Sciences*. 27(6), 1221-1232.

Daly, C., Gibson, W. P., Taylor, G. H., Johnson, G. L. & Pasteris, P., 2002. A knowledge-based approach to the statistical mapping of climate. *Climate Research* 22. 99-113.

Dawdy, D. R. & Bergmann, J. M., 1969. Effect of rainfall variability on streamflow simulation, *Water Resources Research* 5, 958-966.

Dirks, K.N., Hay, J.E., Stow, C. D. & Harris, D., 1998. High-resolution studies of rainfall on Norfolk Island. Part II: Interpolation of rainfall data. *J. Hydrol.*, 208(3-4), 187-193.

Franke, R., 1982. Scattered data interpolation: Test of some methods. *Mathematics of Computations*, 33, 181-200.

Goovaerts, P., 2000. Geostatistical approaches for incorporating elevation into the spatial interpolation of rainfall. *J. Hydrol*. 228(1), 113-129.

Haberlandt, U., and Kite, G. W., 1998. Estimation of daily space-time precipitation series for macroscale hydrological modelling. *Hydrol. Process.* 12. 1419-1432.

Heistermann, M. & Kneis, D., 2011. Benchmarking quantitative precipitation estimation by conceptual rainfall-runoff modeling. *Water Resour. Res*. 47, W06514.

He, X., Refsgaard, J. C., Sonnenborg T. O., Vejen, F. & Jensen, K. H, 2011. Statistical analysis of the impact of radar rainfall uncertainties on water resources modeling. *Water Resour. Res*. 47, W09526.

Jakeman, A. J, 1993. How much complexity is warranted in a rainfall-runoff model?, *Water Resources Research* 29, 2637-2649.

Lanza, L. G., Ramirez, J. A. & Todini, E., 2001. Stochastic rainfall interpolation and downscaling,. *Hydrol. Earth Syst. Sci.*, 5, 139-143.

Lange, J., Leibundgut C., Greenbaum N., & Schick A. P., 1999. A noncalibrated rainfall-runoff model for large, arid catchments. *Water Resour. Res*. 35(7), 2161-2172.

Lloyd, C. D. 2005. Assessing the effect of integrating elevation data into the estimation of monthly precipitation in Great Britain. *J. Hydrol*., 308, 128-150.

Liu, Z. and Todini, E., 2002. Towards a comprehensive physically based rainfall-runoff model. *Hydrol. Earth Syst. Sci.*, 6, 859-881.

Liu, Z., Martina, M. L. V. and Todini, E., 2005. Flood forecasting using a fully distributed model: application of TOPKAPI model to the Upper Xixian Catchment. *Hydrol. Earth Syst. Sci.*, 9(4), 347-364.

Ly, S., Charles, C. & Degre, A., 2011. Geostatistical interpolation of daily rainfall at catchment scale: the use of several variogram models in the Ourthe and Ambleve catchments, Belgium.

Ly, S., Charles, C. & Degre, A., 2013. Different methods for spatial interpolation of rainfall data for operational hydrology and hydrological modeling at watershed scale. A review. *Biotechnol. Agron. Soc. Environ*. 17(2), 392-406.

Mair, A., & Fares, A., 2011. Comparison of rainfall interpolation methods in a mountainous region of a tropical island. *Journal of Hydrologic Engineering*. 16(4), 371-383.

Masih, I., Maskey, S., Uhlenbrook, S. & Smakhtin, V., 2011. Assessing the impact of areal precipitation input on streamflow simulations using the SWAT model. *J. Am. Water Resour. Assoc*., 47(1), 179-195.

MIKE-FLOOD User Manual, Danish Hydraulics Institute, 2007.

Nash, J. E. & Sutcliffe, J. V., 1970. River flow forecasting through conceptual models; Part 1- a discussion of principles. *J. Hydrol.*, 10, 282-290.

Nordila A., Jestin J. & Siti K. C. O., 2012. Analysis of convective structures using meteorological radar data and surface data. *International Journal of Engineering and Applied Sciences.* 1(2), 53-63.

Pilgrim, D. H., 1976. Travel times and non-linearity of flood runoff from tracer measurements on a small watershed, *Water Resources Research*, 12(3), 487-496.

PWRI Technical Note No. 4148 (2009), *ICHARM Publication No. 14*. IFAS Version 1.2, User's Manual.

Ruelland, D., Ardoin-Bardin, S., Billen, G., & Servat, E., 2008. Sensitivity of a lumped and semi-distributed hydrological model to several methods of rainfall interpolation on a large basin in West Africa. *J Hydrol.*, 361, 96-117.

Schuurmans, J. M. & Bierkens M. F. P., 2007. Effect of spatial distribution of daily rainfall on interior catchment response of a distributed hydrological model. *Hydrol. Earth Syst. Sci.*, 11.677-693.

Segond, M. L., Wheater, H. S., Onof, C., 2007. The significance of spatial rainfall representation for flood runoff estimation: A numerical evaluation based on the Lee catchment, UK. *J Hydrol.*, 347, 116-131.

Shepard, D., 1968. A two-dimensional interpolation function for irregularly-spaced data. *ACM Annual Conference/Annual Meeting*, 517-524.

Tao, T., Chocat, B., Liu, S. & Xin, K., 2009. Uncertainty analysis of interpolation methods in rainfall spatial distribution – a case of small catchment in Lyon. *Journal of Environmental Protection*, 1, 50-58.

Thiessen, A. H., 1911. Precipitation averages for large areas. *Mon. Weather Rev.* 39(7), 1082-1084.

Tosaka, H., Itoh, K. and Furuno, T., 2000. Fully coupled formulation of surface flow with 2-phase subsurface flow for hydrological simulation. *Hydrol. Process.* 14, 449-464.

Tramblay, Y., Bouvier C., Ayral. P. –A., & Marchandise A., 2011. Impact of rainfall spatial distribution on rainfall-runoff modelling efficiency and initial soil moisture conditions estimation. *Nat. Hazards Earth Syst. Sci.*, 11, 157-170.

Tsai, M.-J., Abrahart, R. J., Mount, N. J. & Chang, F.-J., 2014. Including spatial distribution in a data driven rainfall-runoff model to improve reservoir inflow forecasting in Taiwan. *Hydrol. Processes*. 28, 1055-1070.

Verworn, A. & Haberlandt, U., 2011.Spatial interpolation of hourly rainfall – effect of traditional information, variogram inference and storm properties. *Hydrol. Earth Syst. Sci.*, 15, 569-584.

Wagner, P.D., Fiener, P., Wilken, F., Kumar, S. & Schneider, K., 2012. Comparison and evaluation of spatial interpolation schemes for daily rainfall in data scarce regions. *J. Hydrol.*, 464, 388-400.

Xu W., Zou. Y., Zhang G. & Linderman M., 2014. A comparison among spatial interpolation techniques for daily rainfall data in Sichuan Province, China. *Int. J. Climatol.*

Appendix

This section contains figures that were generated from historical data for a purpose of comparison of selected data used in the analysis and to understand the phenomenon for each flood event that occurred during north east monsoon season. List of the appendices are:

1) A-1

   Hydrographs of various water level stations available in Kelantan watershed during north east monsoon season from 2004 to 2013.

2) A-2

   Hydrograph of Galas water level station together with available rainfall stations in Galas sub-watershed from 2007 to 2011

3) A-3

   Hydrograph of Lebir water level station together with available rainfall stations in Lebir sub-watershed from 2007 to 2011

4) A-4

   Hydrograph of Kuala Krai water level station together with available rainfall stations in Kuala Krai from 2007 to 2011

5) A-5

   Hydrograph of Guillemard Bridge water level station together with available rainfall stations in Guillemard Bridge from 2007 to 2011

6) A-6

   Comparison of rainfall distribution for selected days during north east monsoon season in 2007 calculated using IDW, IDEW, AIDW and AIDEW.

A-1) Water level in Kelantan watershed during NEM from year 2004 to 2013.

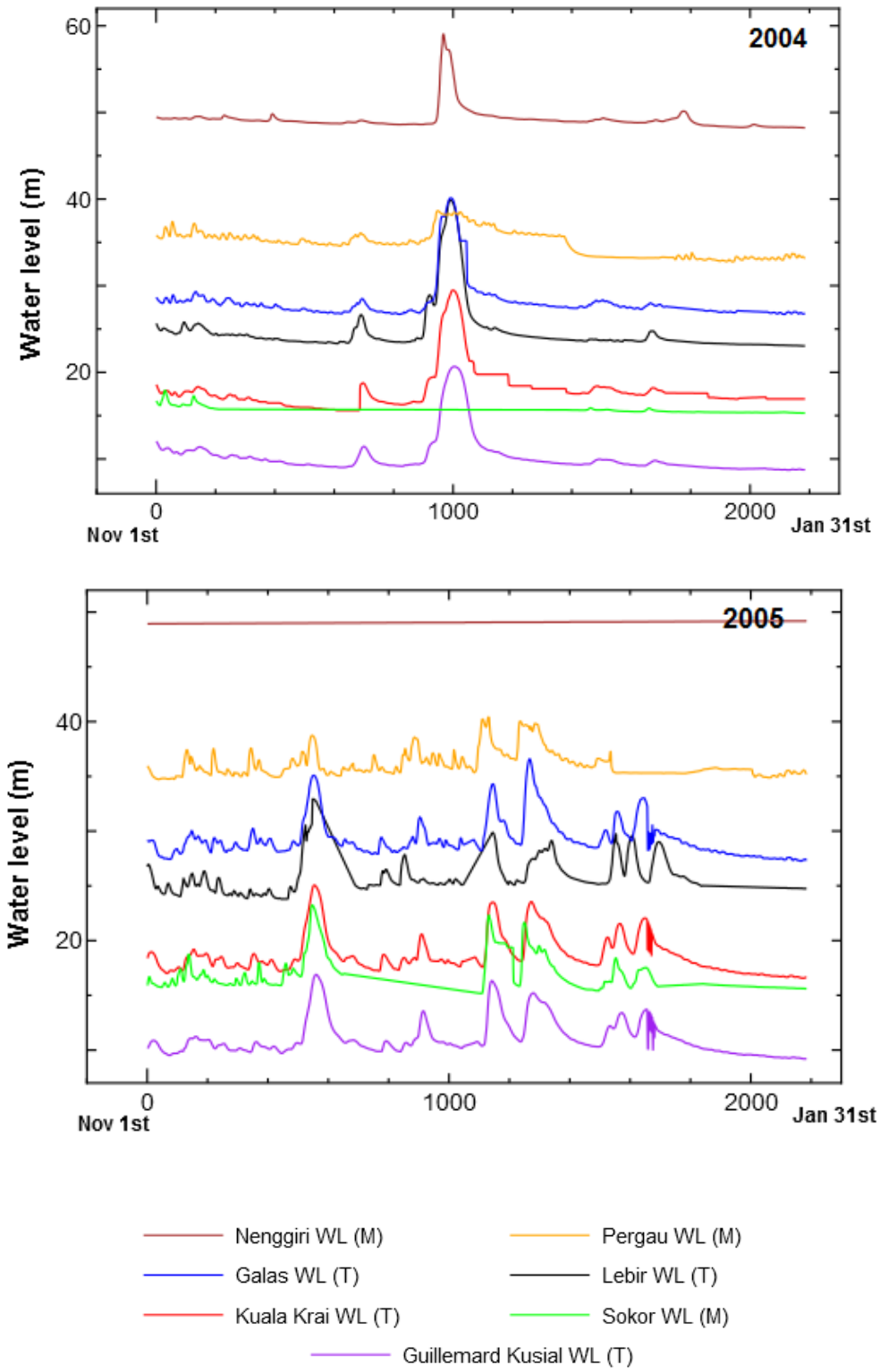

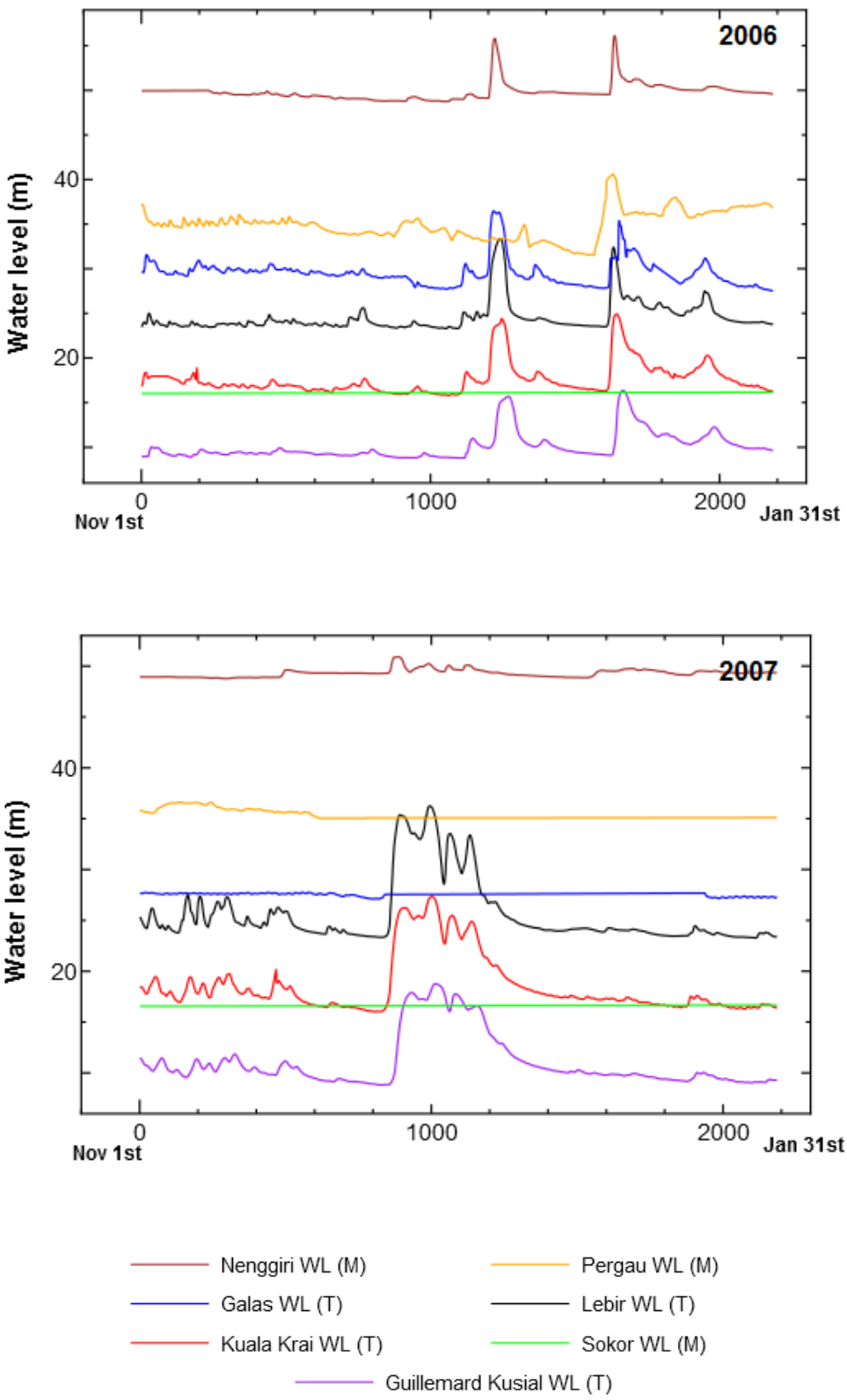
2006
Water level (m)
40
20
0
1000
2000
Nov 1st
Jan 31st
2007
Water level (m)
40
20
0
1000
2000
Nov 1st
Jan 31st
Nenggiri WL (M)
Pergau WL (M)
Galas WL (T)
Lebir WL (T)
Kuala Krai WL (T)
Sokor WL (M)
Guillemard Kusial WL (T)

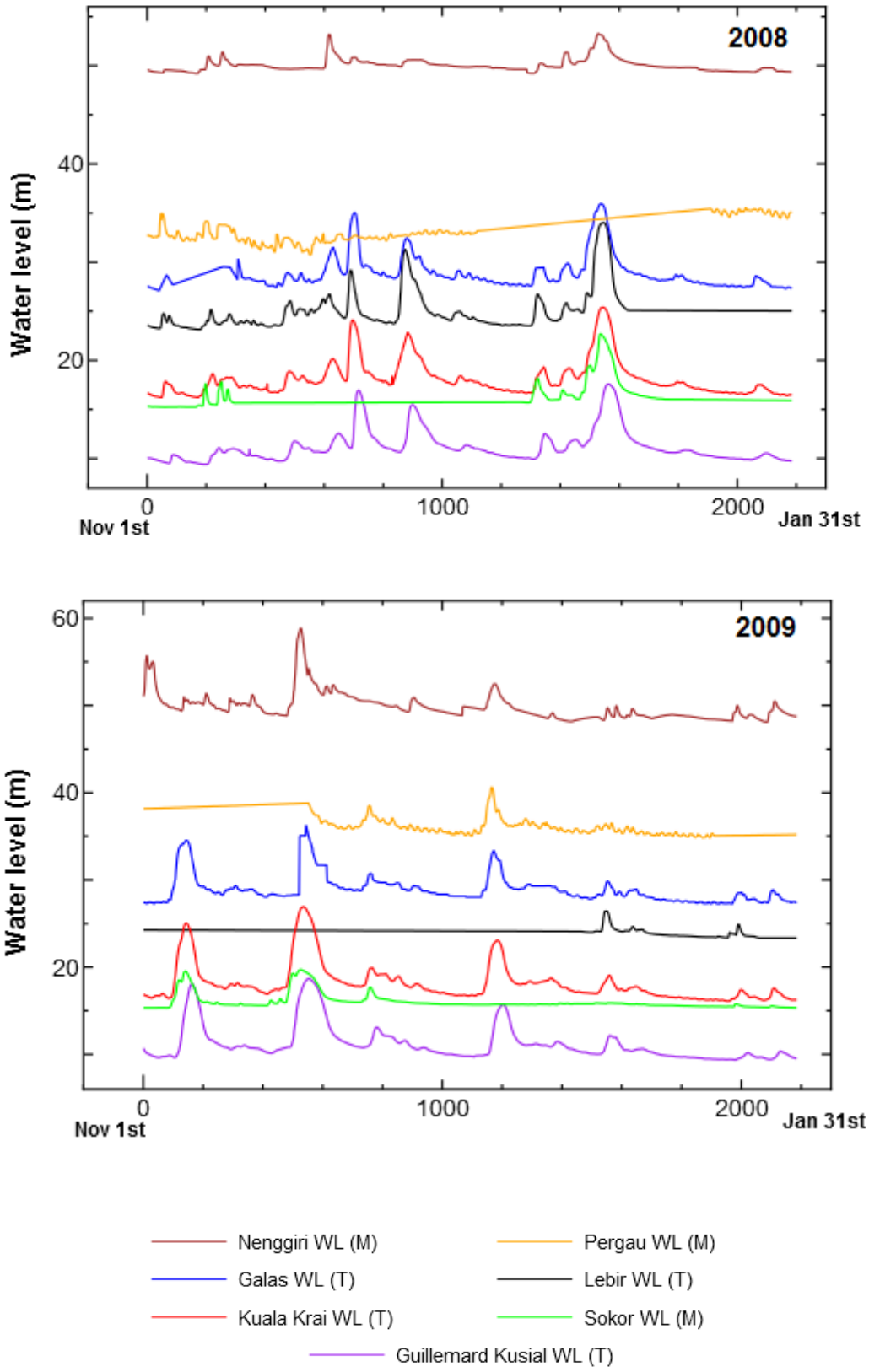
2008
Water level (m)
40
20
0
1000
2000
Nov 1st
Jan 31st
2009
Water level (m)
60
40
20
0
1000
2000
Nov 1st
Jan 31st
Nenggiri WL (M)
Pergau WL (M)
Galas WL (T)
Lebir WL (T)
Kuala Krai WL (T)
Sokor WL (M)
Guillemard Kusial WL (T)

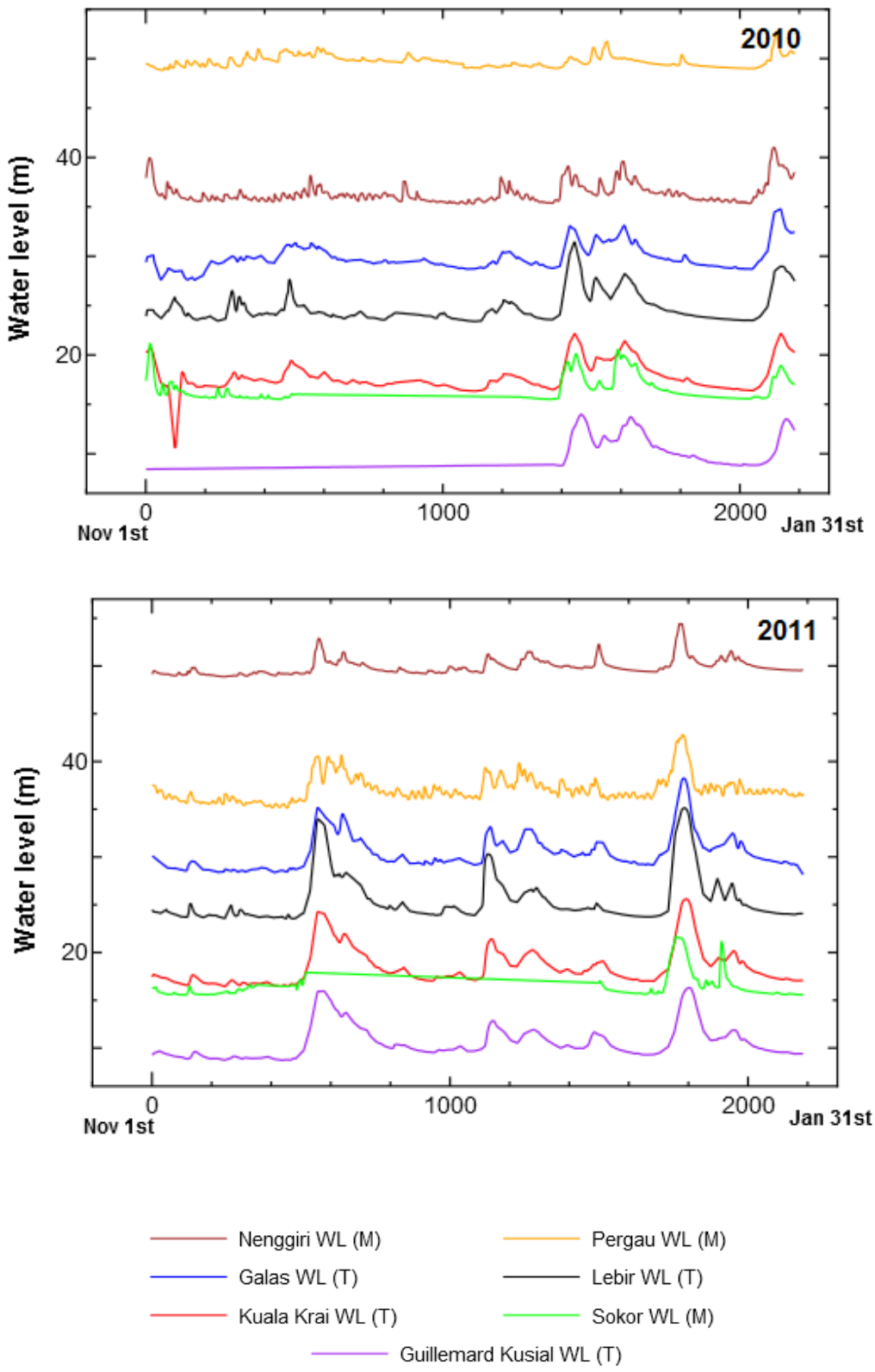
2010
Water level (m)
40
20
0
1000
2000
Nov 1st
Jan 31st
2011
Water level (m)
40
20
0
1000
2000
Nov 1st
Jan 31st
Nenggiri WL (M)
Pergau WL (M)
Galas WL (T)
Lebir WL (T)
Kuala Krai WL (T)
Sokor WL (M)
Guillemard Kusial WL (T)

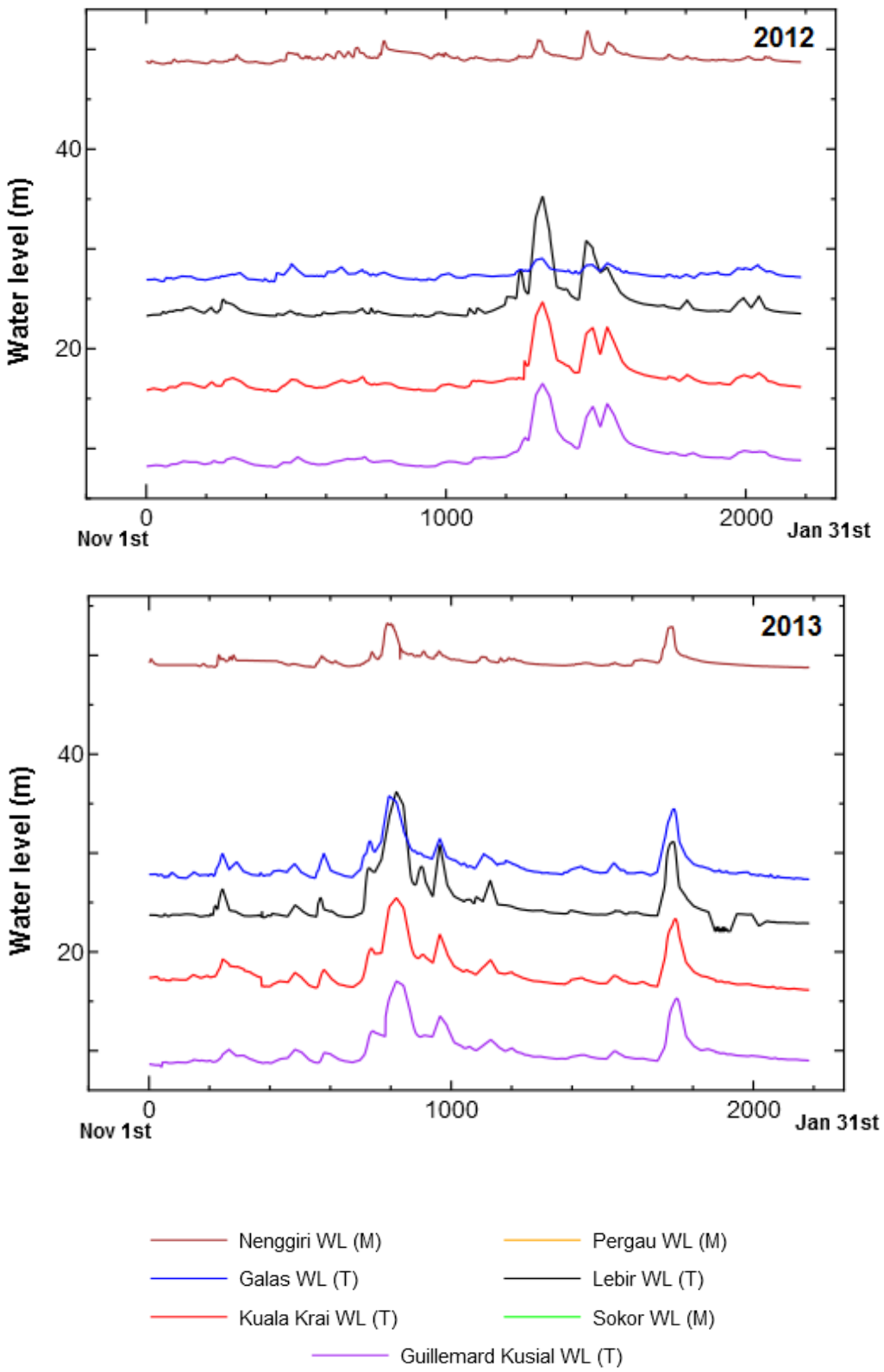
2012
Water level (m)
40
20
0
1000
2000
Nov 1st
Jan 31st
2013
Water level (m)
40
20
0
1000
2000
Nov 1st
Jan 31st
Nenggiri WL (M)
Pergau WL (M)
Galas WL (T)
Lebir WL (T)
Kuala Krai WL (T)
Sokor WL (M)
Guillemard Kusial WL (T)

A-2) Water level- rainfall at Galas station for year 2007 – 2011

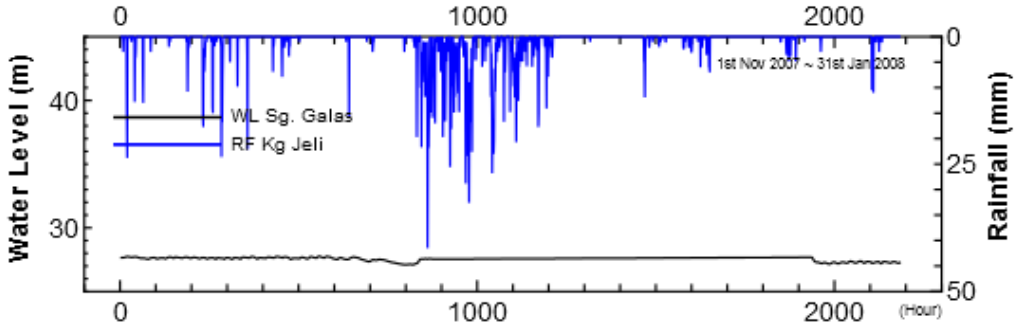

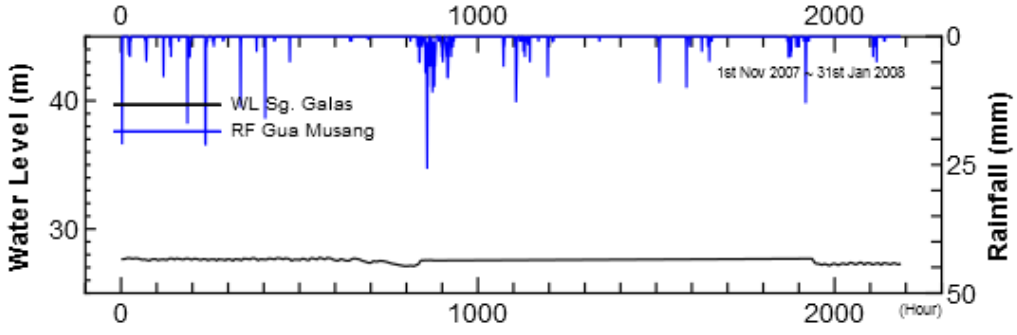

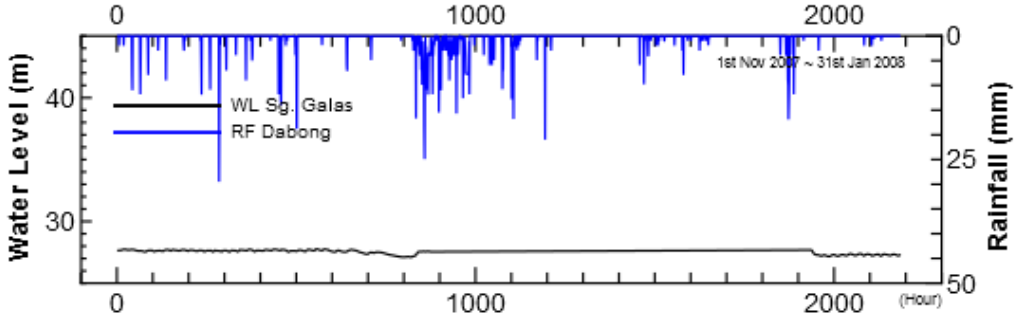

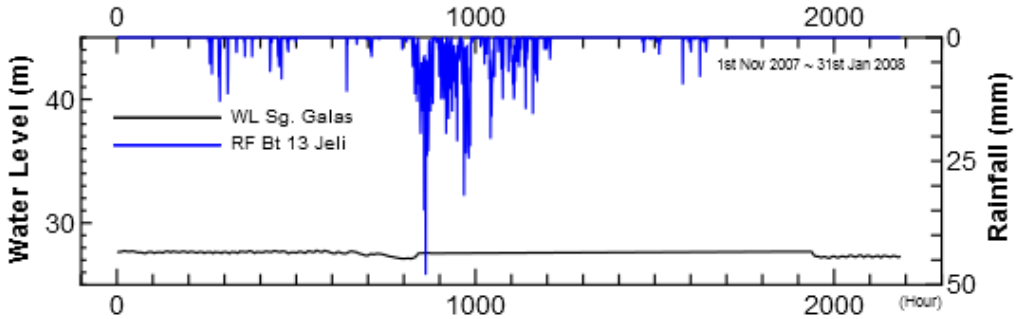

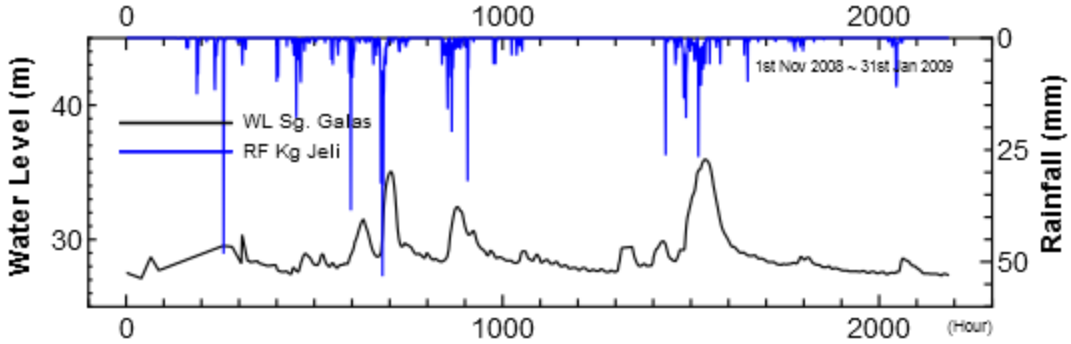
0
1000
2000
1st Nov 2008 ~ 31st Jan 2009
WL Sg. Galas
RF Kg Jeli
Water Level (m)
40
30
0
25
50
Rainfall (mm)
(Hour)

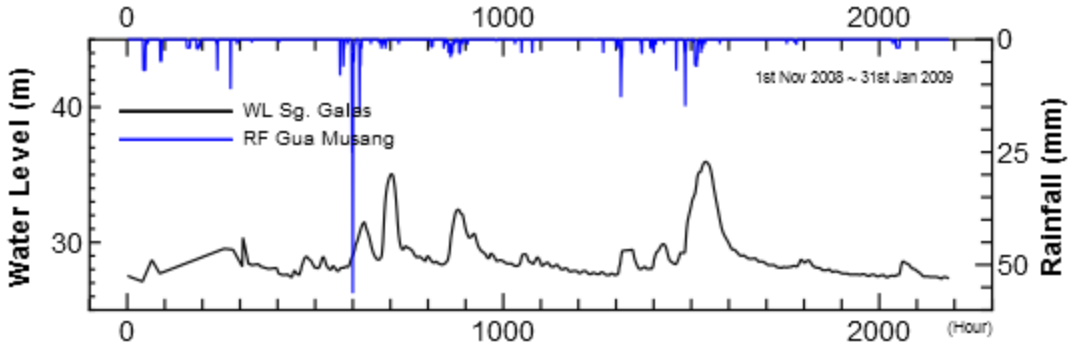
0
1000
2000
1st Nov 2008 ~ 31st Jan 2009
WL Sg. Galas
RF Gua Musang
Water Level (m)
40
30
0
25
50
Rainfall (mm)
(Hour)

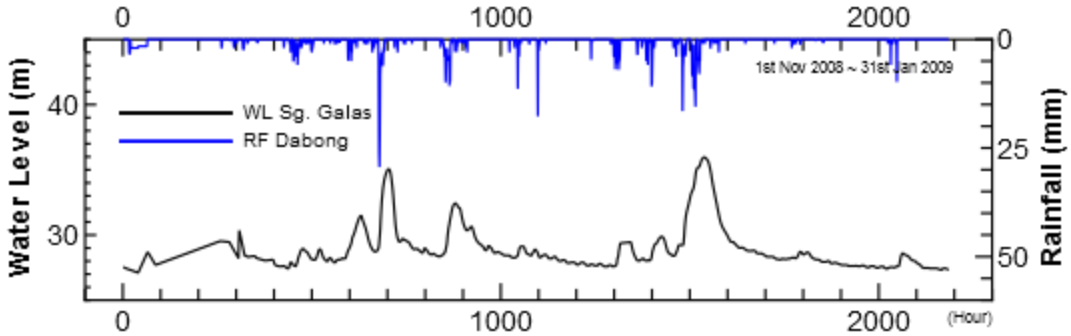
0
1000
2000
1st Nov 2008 ~ 31st Jan 2009
WL Sg. Galas
RF Dabong
Water Level (m)
40
30
0
25
50
Rainfall (mm)
(Hour)

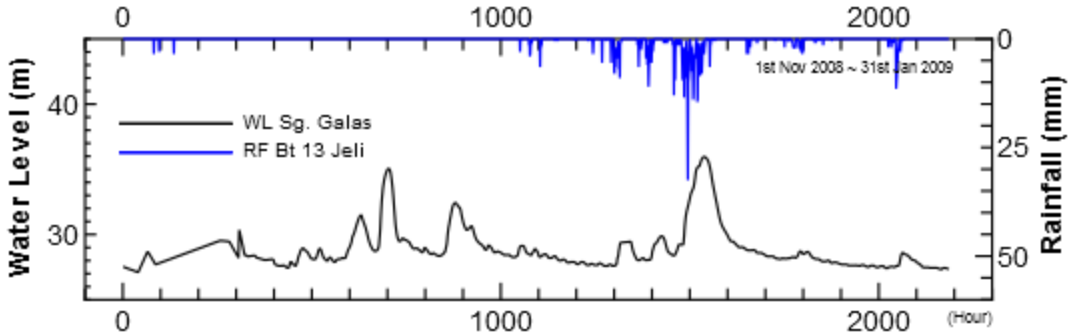
0
1000
2000
1st Nov 2008 ~ 31st Jan 2009
WL Sg. Galas
RF Bt 13 Jeli
Water Level (m)
40
30
0
25
50
Rainfall (mm)
(Hour)

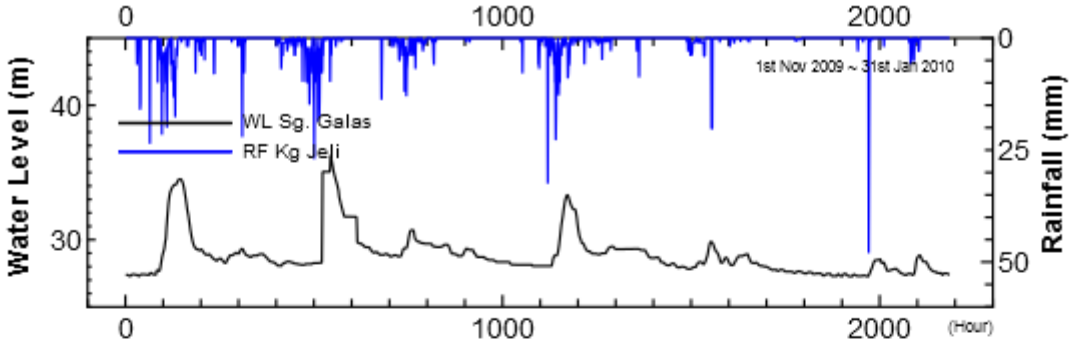
0
1000
2000
1st Nov 2009 ~ 31st Jan 2010
WL Sg. Galas
RF Kg Jeli
Water Level (m)
40
30
0
25
50
Rainfall (mm)
(Hour)

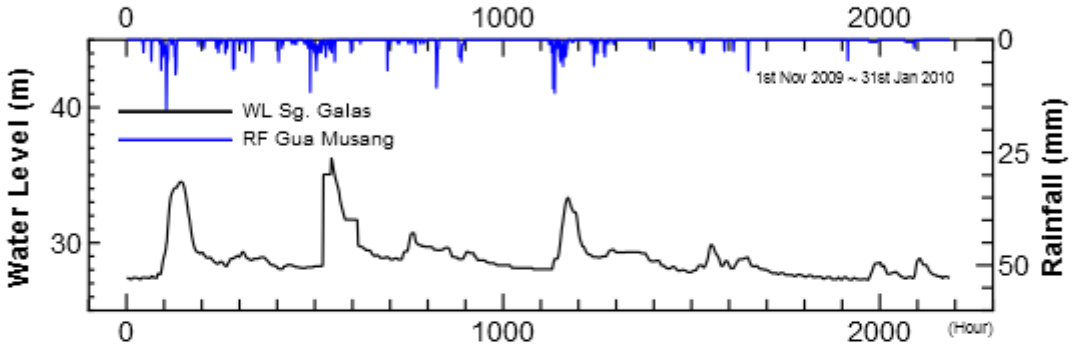
0
1000
2000
1st Nov 2009 ~ 31st Jan 2010
WL Sg. Galas
RF Gua Musang
Water Level (m)
40
30
0
25
50
Rainfall (mm)
(Hour)

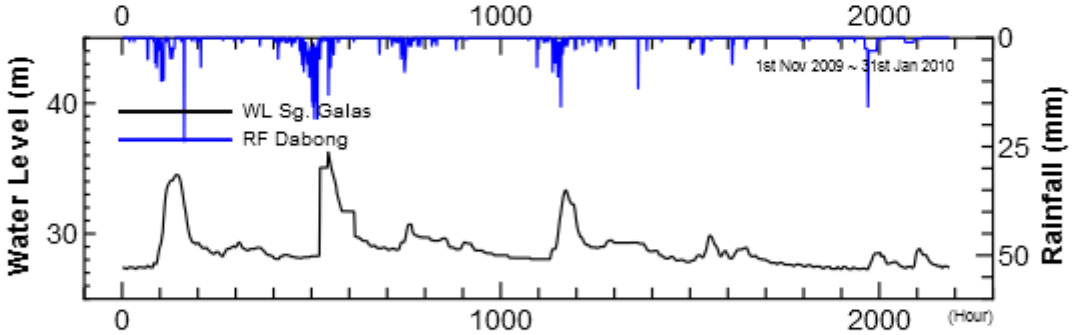
0
1000
2000
1st Nov 2009 ~ 31st Jan 2010
WL Sg. Galas
RF Dabong
Water Level (m)
40
30
0
25
50
Rainfall (mm)
(Hour)

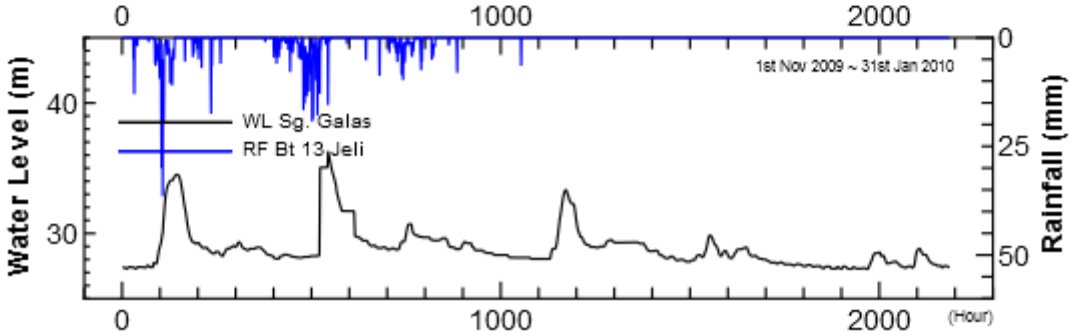
0
1000
2000
1st Nov 2009 ~ 31st Jan 2010
WL Sg. Galas
RF Bt 13 Jeli
Water Level (m)
40
30
0
25
50
Rainfall (mm)
(Hour)

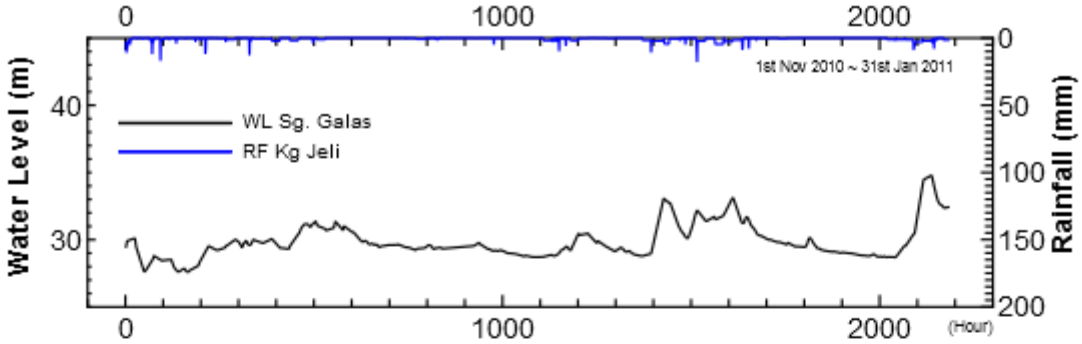
0
1000
2000
1st Nov 2010 ~ 31st Jan 2011
WL Sg. Galas
RF Kg Jeli
Water Level (m)
40
30
Rainfall (mm)
0
50
100
150
200
(Hour)

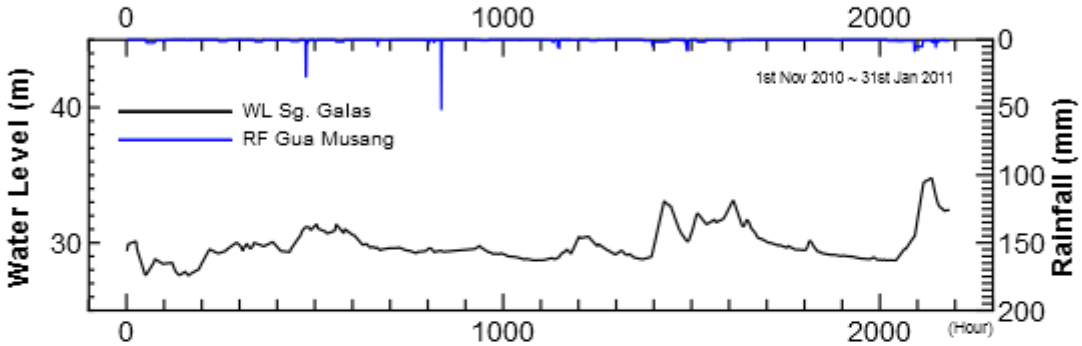
0
1000
2000
1st Nov 2010 ~ 31st Jan 2011
WL Sg. Galas
RF Gua Musang
Water Level (m)
40
30
Rainfall (mm)
0
50
100
150
200
(Hour)

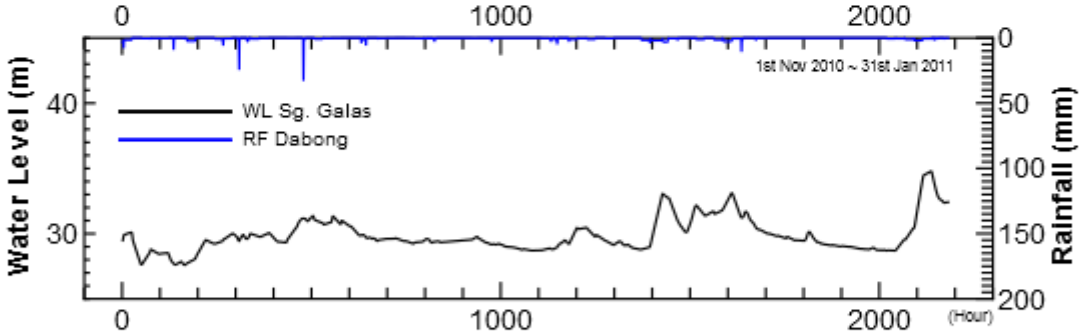
0
1000
2000
1st Nov 2010 ~ 31st Jan 2011
WL Sg. Galas
RF Dabong
Water Level (m)
40
30
Rainfall (mm)
0
50
100
150
200
(Hour)

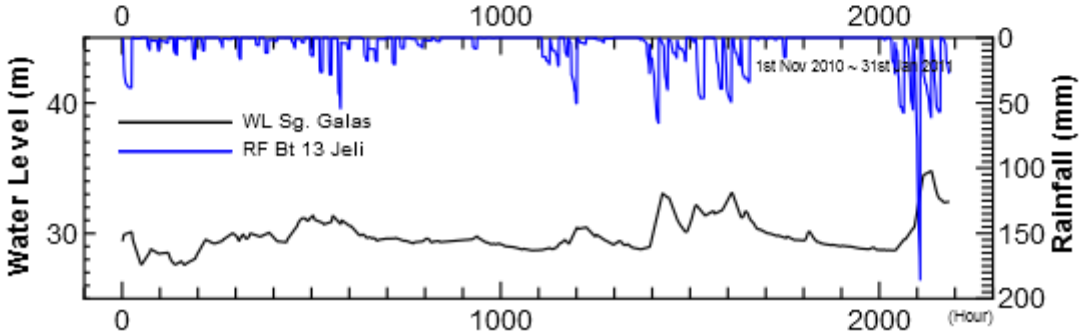
0
1000
2000
WL Sg. Galas
RF Bt 13 Jeli
Water Level (m)
40
30
Rainfall (mm)
0
50
100
150
200
(Hour)

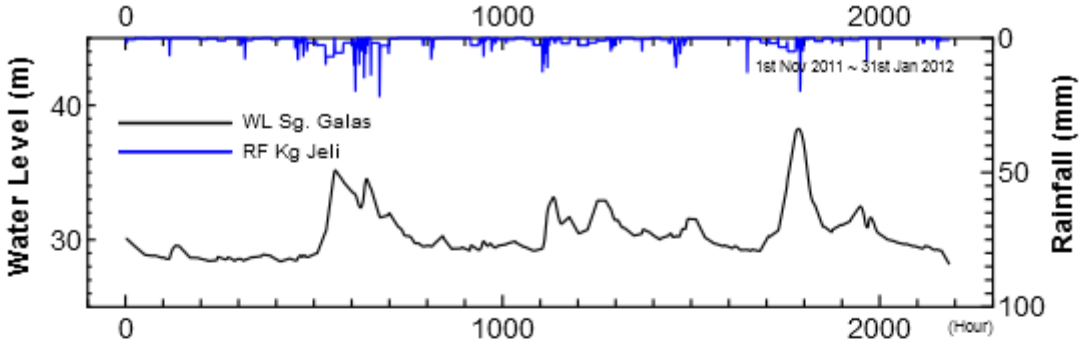
0
1000
2000
1st Nov 2011 ~ 31st Jan 2012
WL Sg. Galas
RF Kg Jeli
Water Level (m)
40
30
Rainfall (mm)
0
50
100
(Hour)

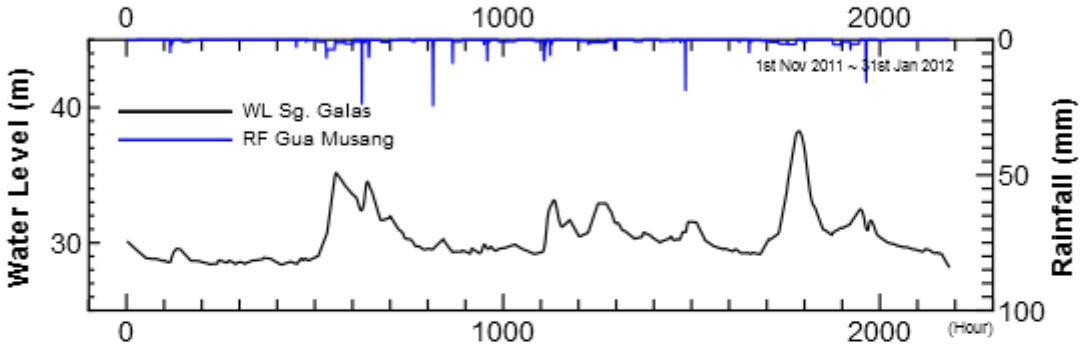
0
1000
2000
1st Nov 2011 ~ 31st Jan 2012
WL Sg. Galas
RF Gua Musang
Water Level (m)
40
30
Rainfall (mm)
0
50
100
(Hour)

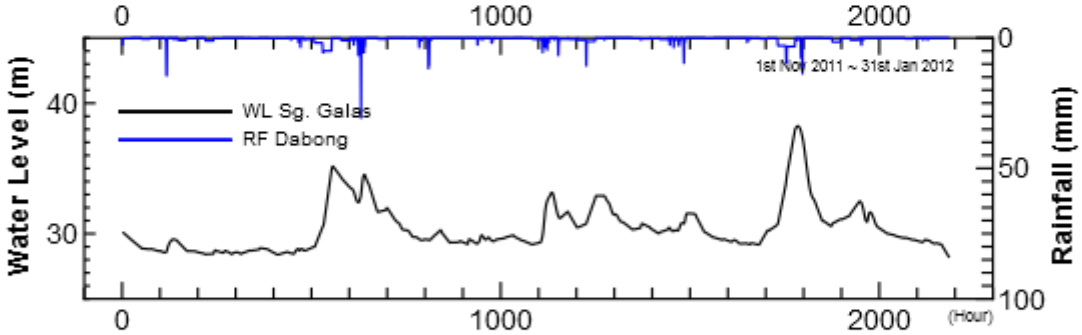
0
1000
2000
1st Nov 2011 ~ 31st Jan 2012
WL Sg. Galas
RF Dabong
Water Level (m)
40
30
Rainfall (mm)
0
50
100
(Hour)

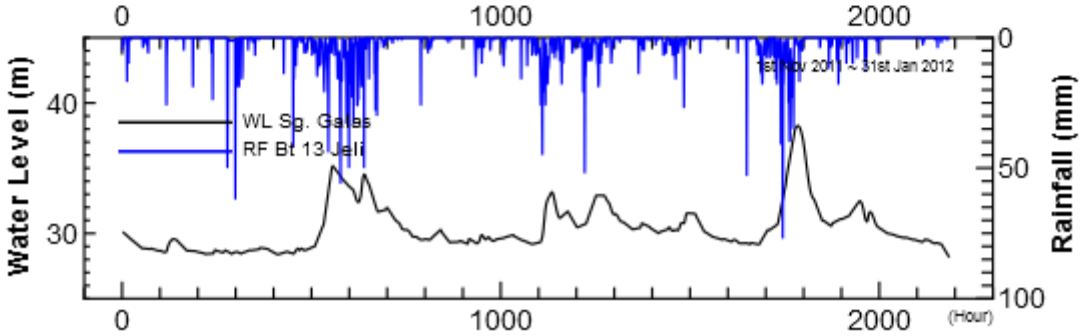
0
1000
2000
1st Nov 2011 ~ 31st Jan 2012
WL Sg. Galas
RF Bt 13 Jeli
Water Level (m)
40
30
Rainfall (mm)
0
50
100
(Hour)

A-3) Water level- rainfall at Lebir station for year 2007 – 2011

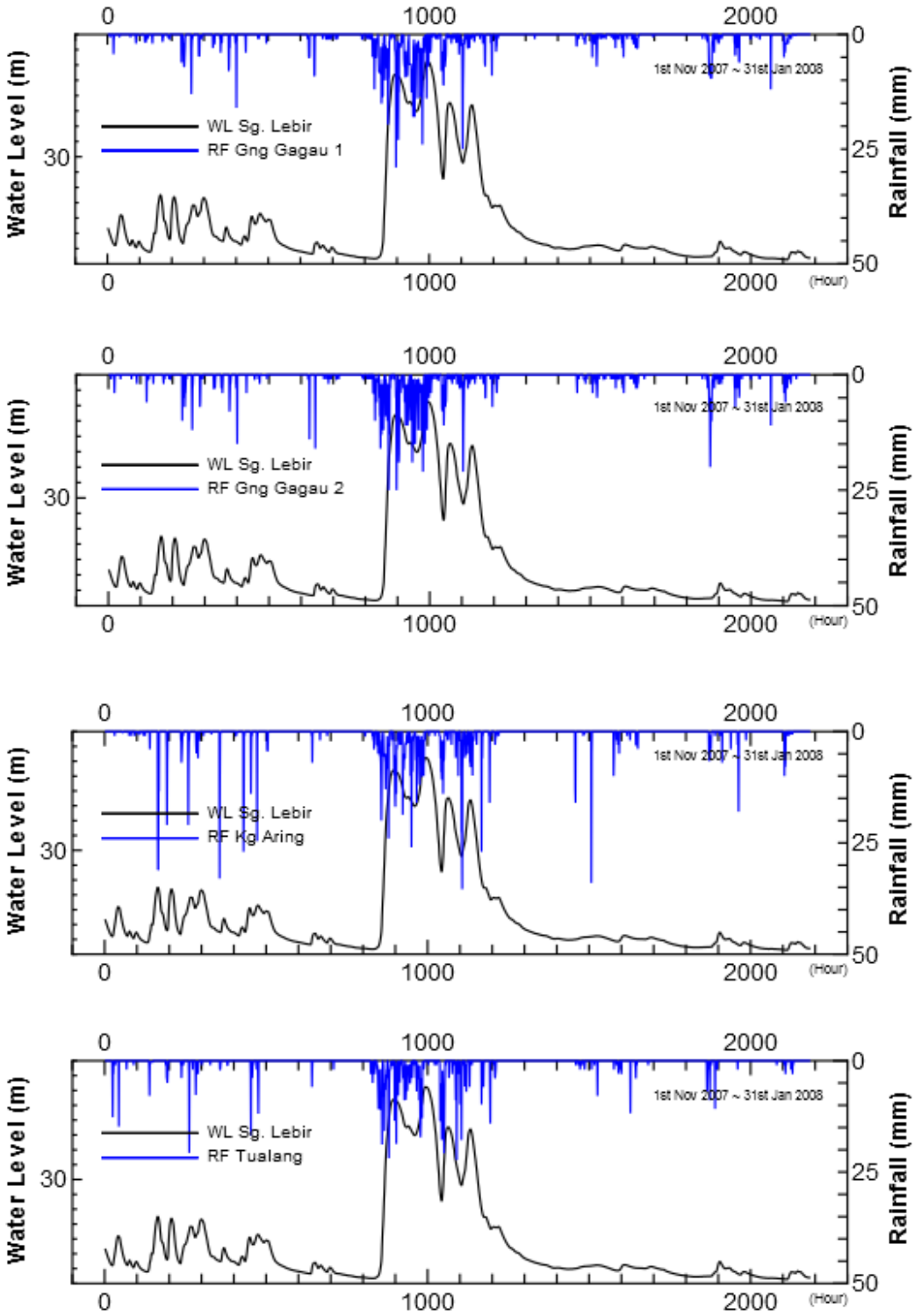

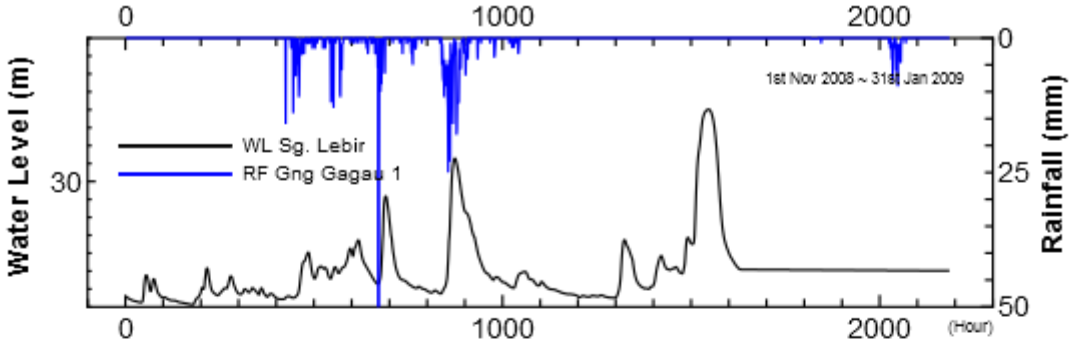
0
1000
2000
1st Nov 2008 ~ 31st Jan 2009
WL Sg. Lebir
RF Gng Gagau 1
Water Level (m)
30
Rainfall (mm)
0
25
50
(Hour)

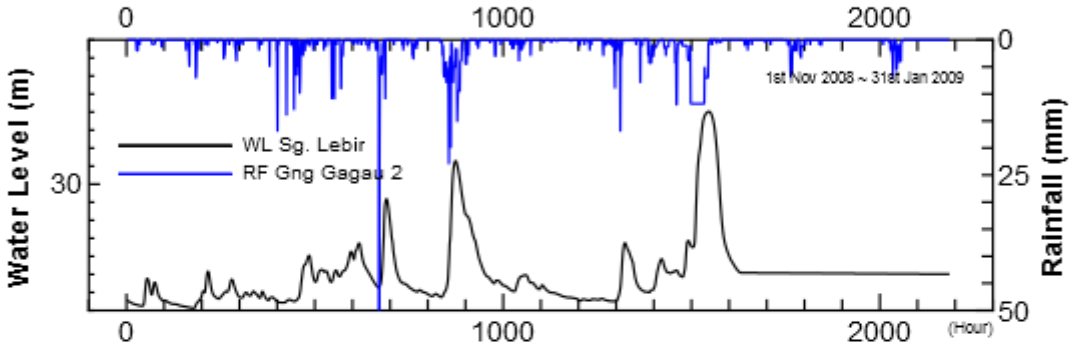
0
1000
2000
1st Nov 2008 ~ 31st Jan 2009
WL Sg. Lebir
RF Gng Gagau 2
Water Level (m)
30
Rainfall (mm)
0
25
50
(Hour)

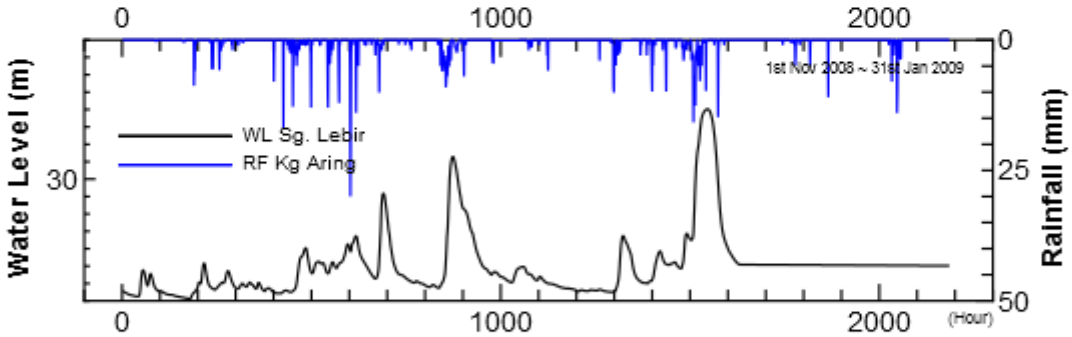
0
1000
2000
1st Nov 2008 ~ 31st Jan 2009
WL Sg. Lebir
RF Kg Aring
Water Level (m)
30
Rainfall (mm)
0
25
50
(Hour)

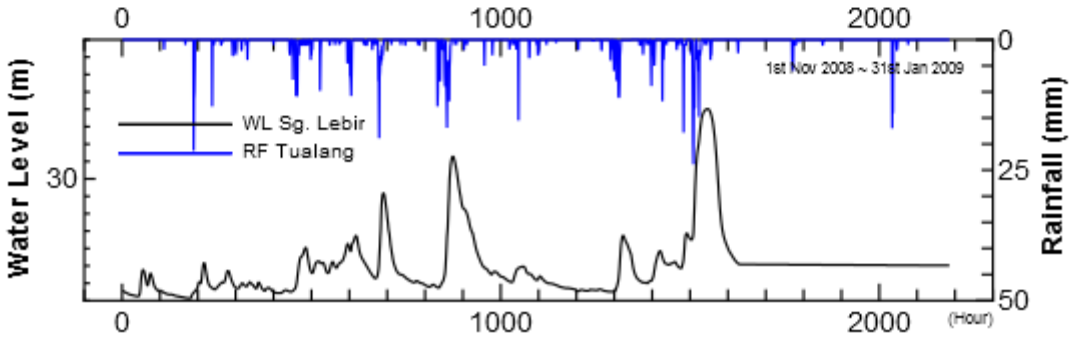
0
1000
2000
1st Nov 2008 ~ 31st Jan 2009
WL Sg. Lebir
RF Tualang
Water Level (m)
30
Rainfall (mm)
0
25
50
(Hour)

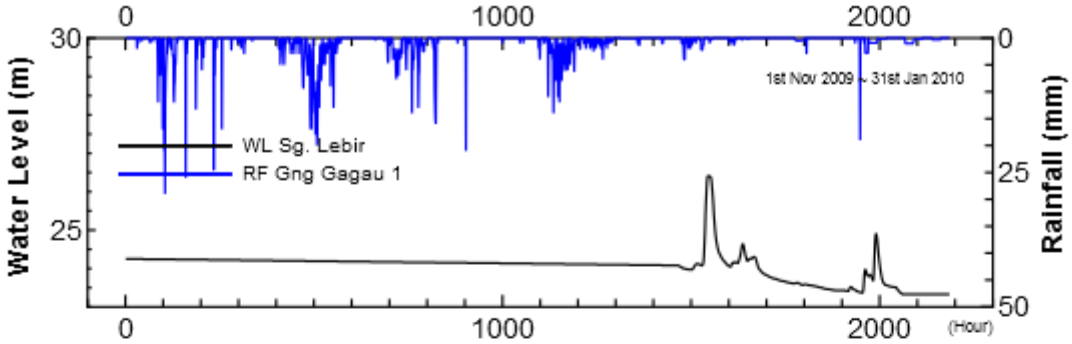
0
1000
2000
30
25
0
25
50
Water Level (m)
Rainfall (mm)
1st Nov 2009 ~ 31st Jan 2010
WL Sg. Lebir
RF Gng Gagau 1
(Hour)

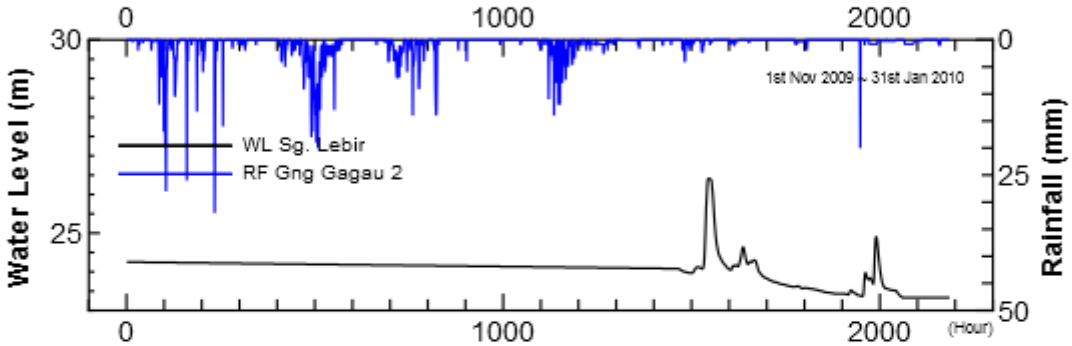
0
1000
2000
30
25
0
25
50
Water Level (m)
Rainfall (mm)
1st Nov 2009 ~ 31st Jan 2010
WL Sg. Lebir
RF Gng Gagau 2
(Hour)

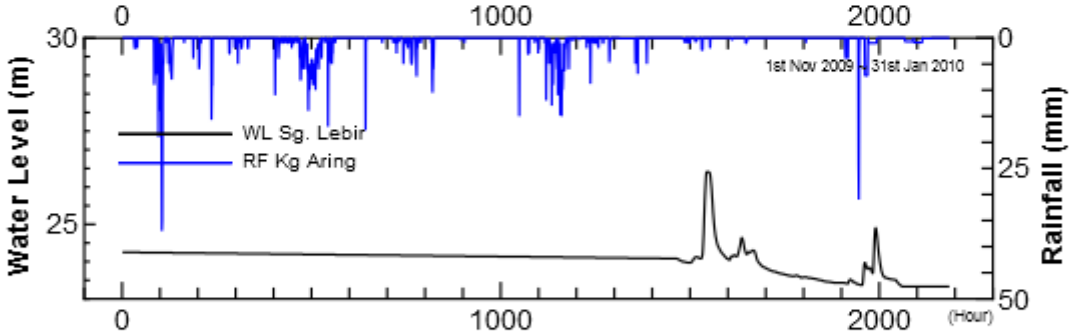
0
1000
2000
30
25
0
25
50
Water Level (m)
Rainfall (mm)
1st Nov 2009 ~ 31st Jan 2010
WL Sg. Lebir
RF Kg Aring
(Hour)

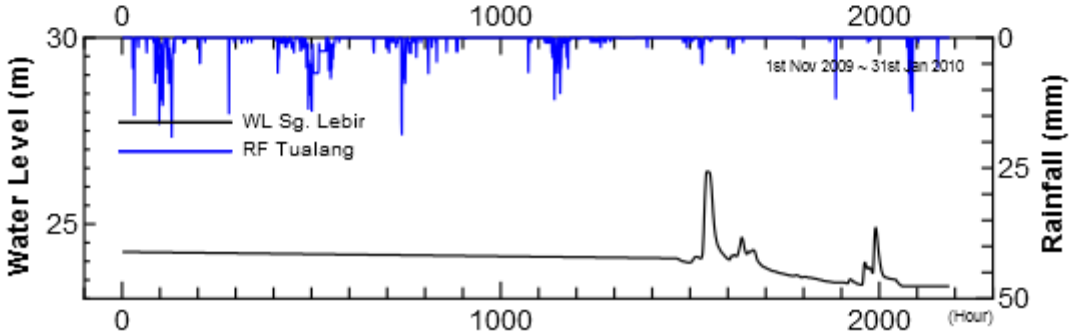
0
1000
2000
30
25
0
25
50
Water Level (m)
Rainfall (mm)
1st Nov 2009 ~ 31st Jan 2010
WL Sg. Lebir
RF Tualang
(Hour)

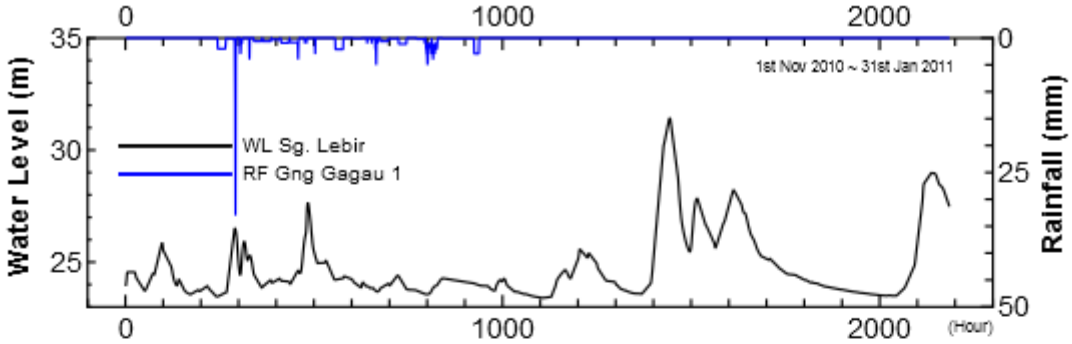
1st Nov 2010 ~ 31st Jan 2011
WL Sg. Lebir
RF Gng Gagau 1
Water Level (m)
Rainfall (mm)
(Hour)

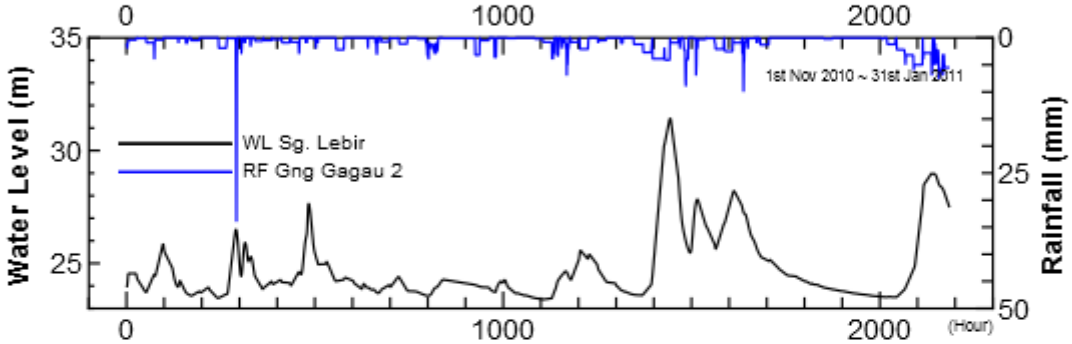
1st Nov 2010 ~ 31st Jan 2011
WL Sg. Lebir
RF Gng Gagau 2
Water Level (m)
Rainfall (mm)
(Hour)

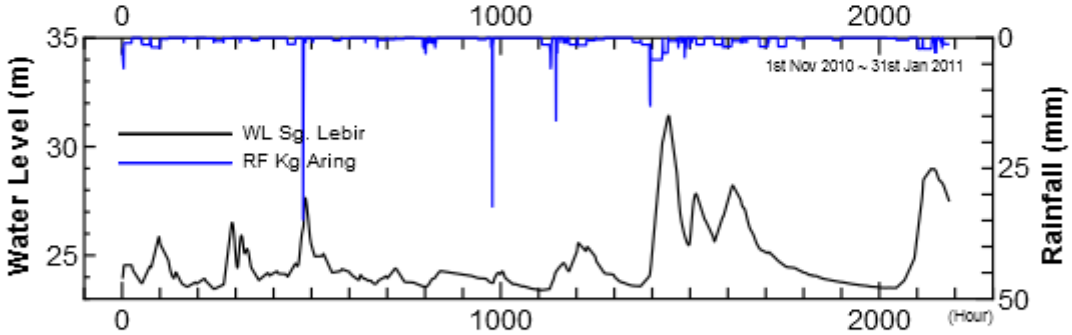
1st Nov 2010 ~ 31st Jan 2011
WL Sg. Lebir
RF Kg Aring
Water Level (m)
Rainfall (mm)
(Hour)

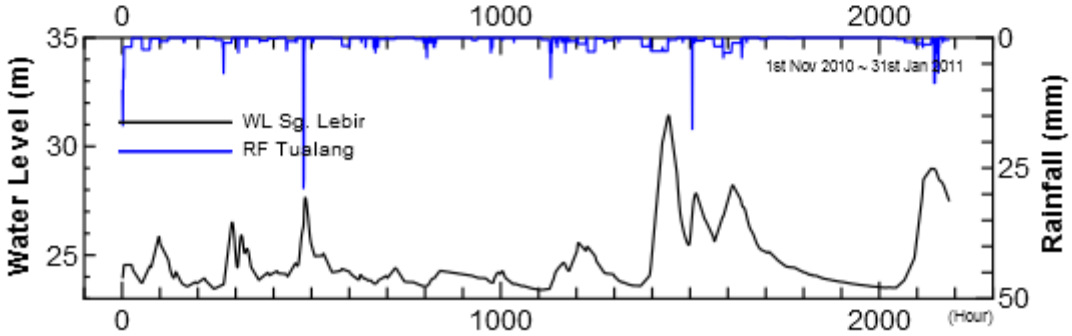
1st Nov 2010 ~ 31st Jan 2011
WL Sg. Lebir
RF Tualang
Water Level (m)
Rainfall (mm)
(Hour)

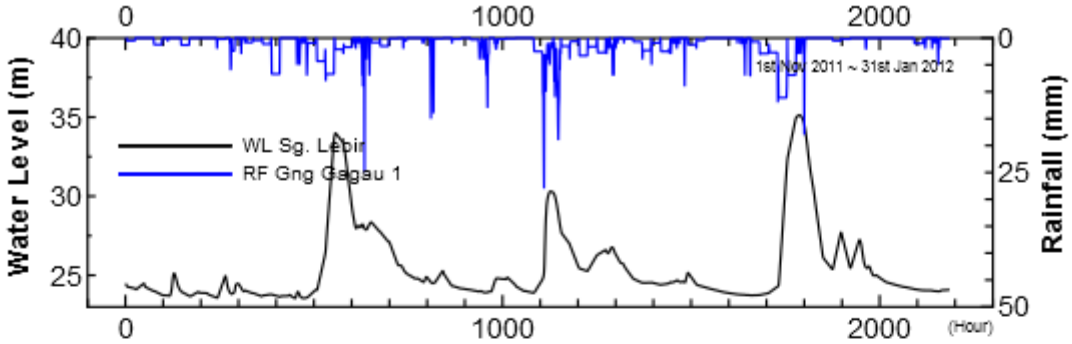
Water Level (m)
Rainfall (mm)
1st Nov 2011 ~ 31st Jan 2012
WL Sg. Lebir
RF Gng Gagau 1
(Hour)

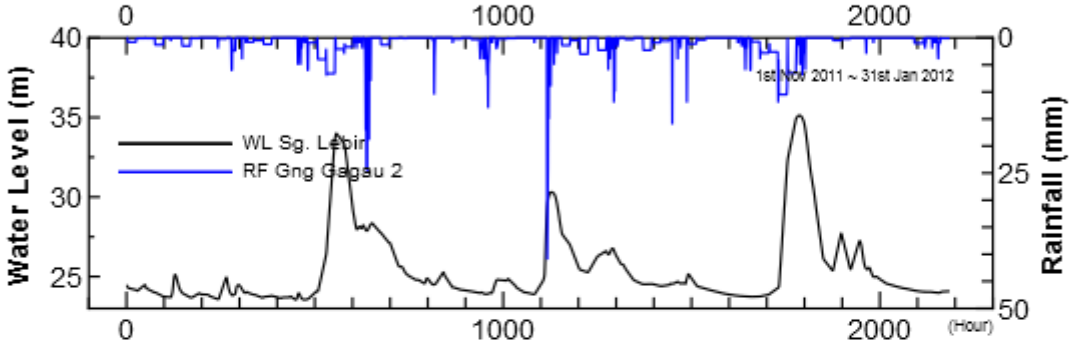
Water Level (m)
Rainfall (mm)
1st Nov 2011 ~ 31st Jan 2012
WL Sg. Lebir
RF Gng Gagau 2
(Hour)

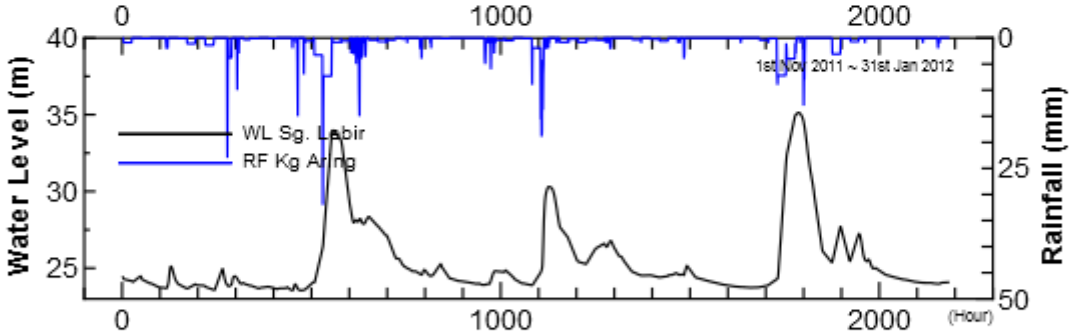
Water Level (m)
Rainfall (mm)
1st Nov 2011 ~ 31st Jan 2012
WL Sg. Lebir
RF Kg Aring
(Hour)

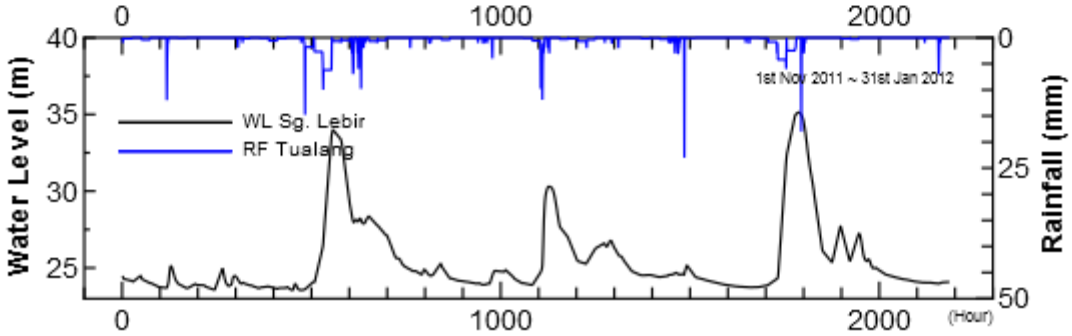
Water Level (m)
Rainfall (mm)
1st Nov 2011 ~ 31st Jan 2012
WL Sg. Lebir
RF Tualang
(Hour)

A-4) Water level- rainfall at Kuala Krai station for year 2007 – 2011

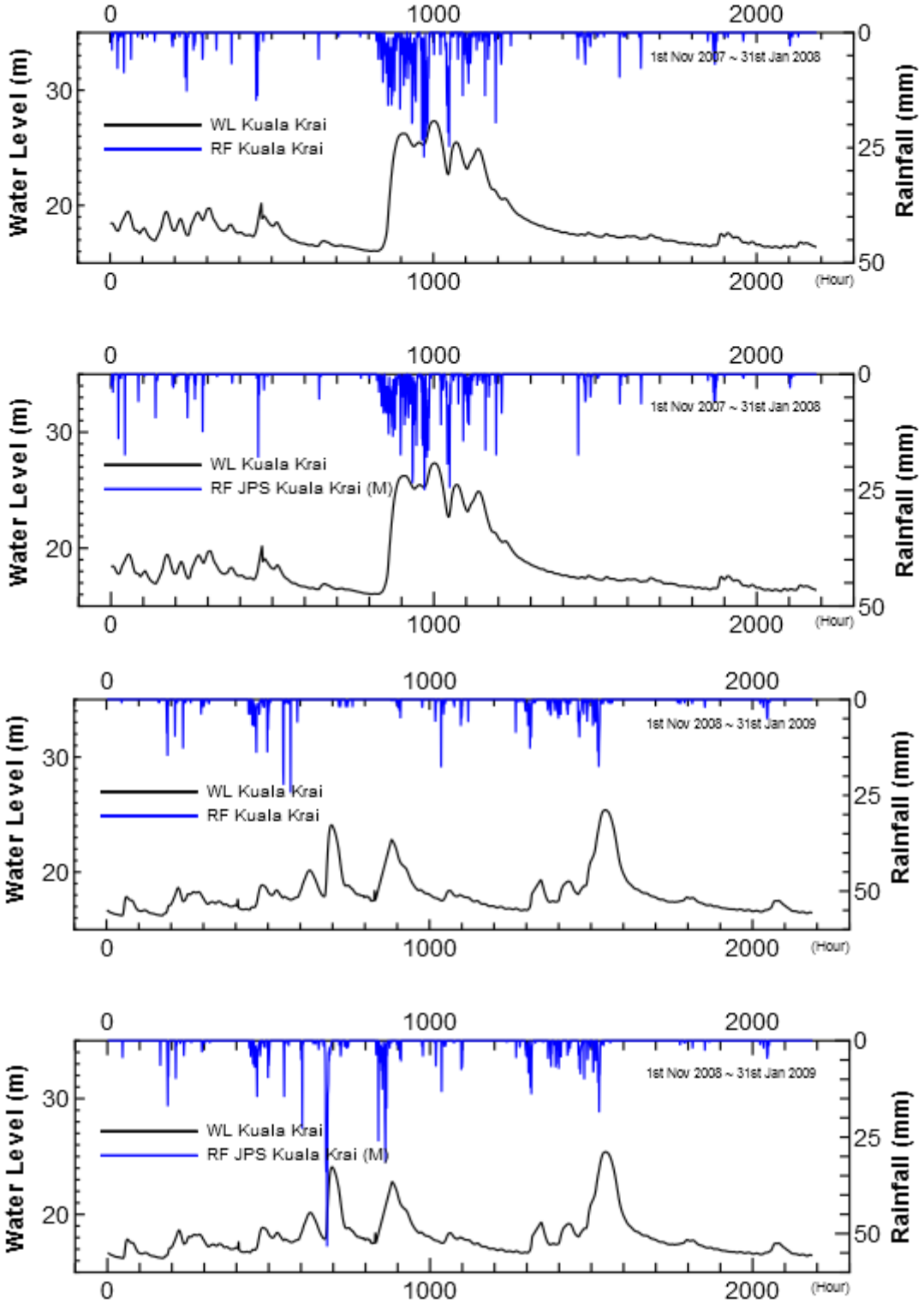

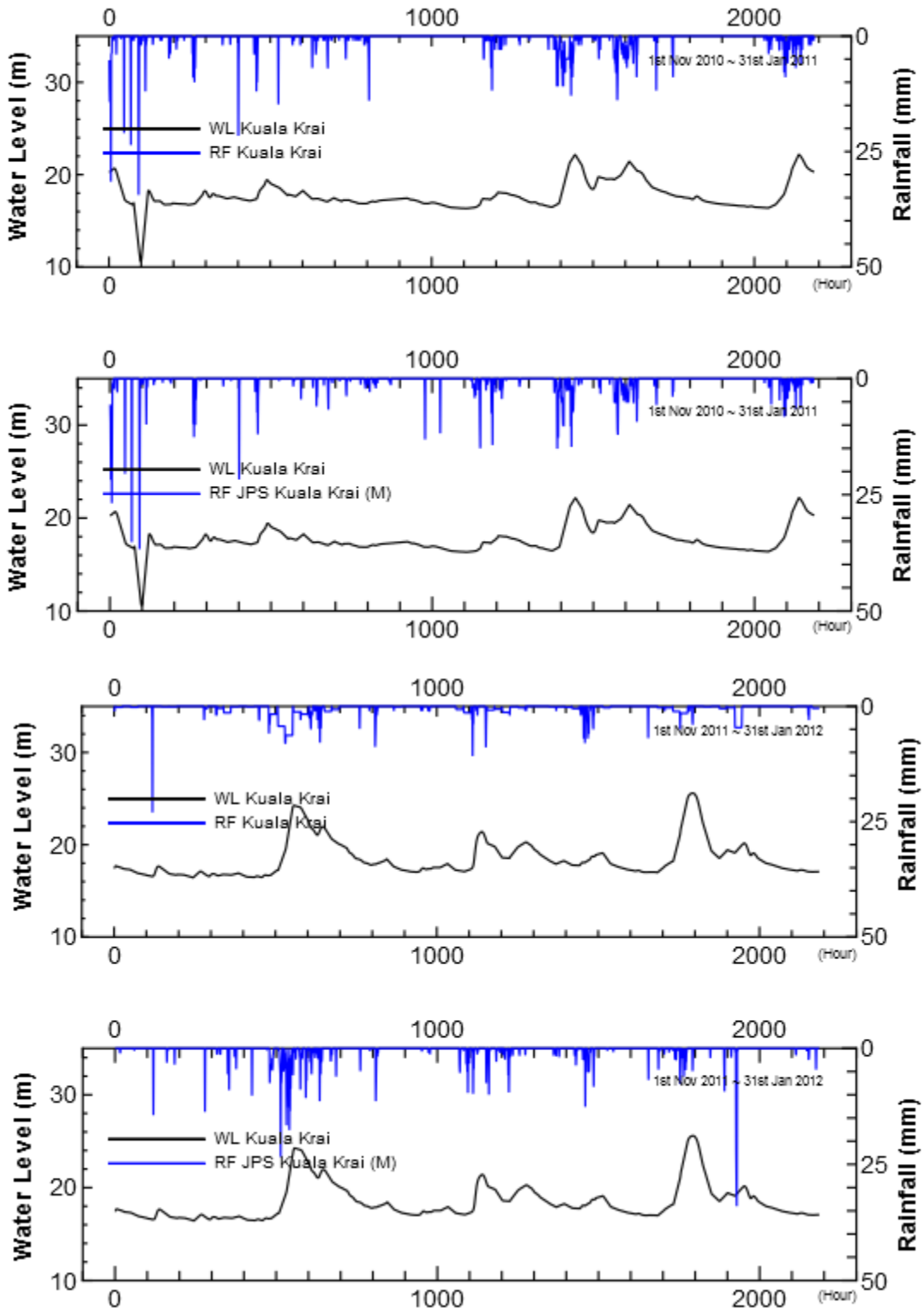
Water Level (m)
Rainfall (mm)
1st Nov 2010 ~ 31st Jan 2011
WL Kuala Krai
RF Kuala Krai
RF JPS Kuala Krai (M)
1st Nov 2011 ~ 31st Jan 2012
(Hour)

A-5) Water level- rainfall at Guillemard Bridge for year 2007 – 2011

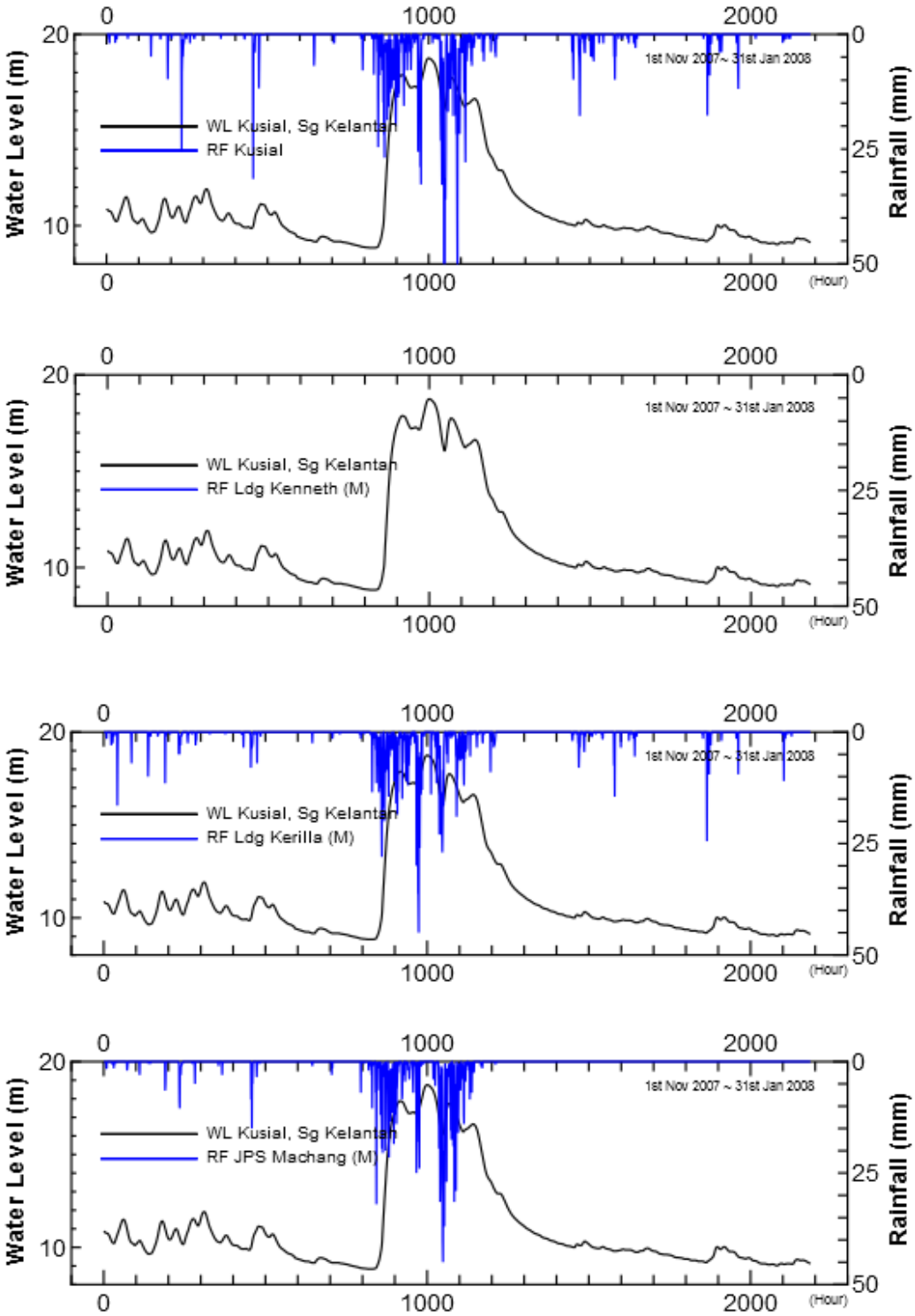

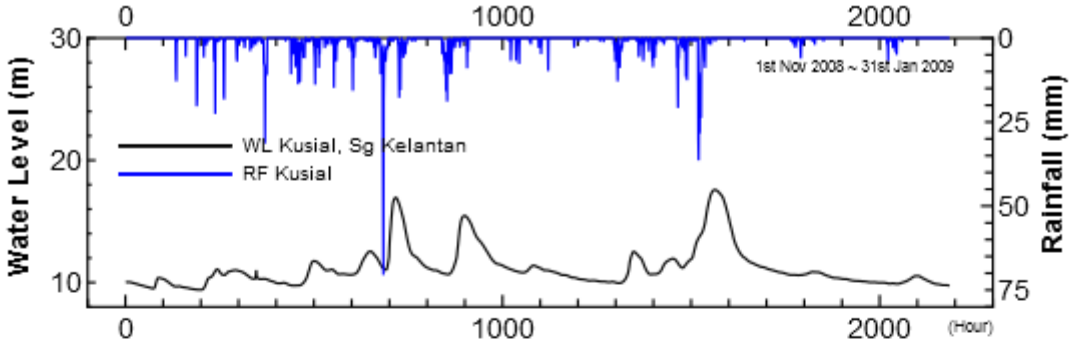
1st Nov 2008 ~ 31st Jan 2009
WL Kusial, Sg Kelantan
RF Kusial
Water Level (m)
Rainfall (mm)
(Hour)

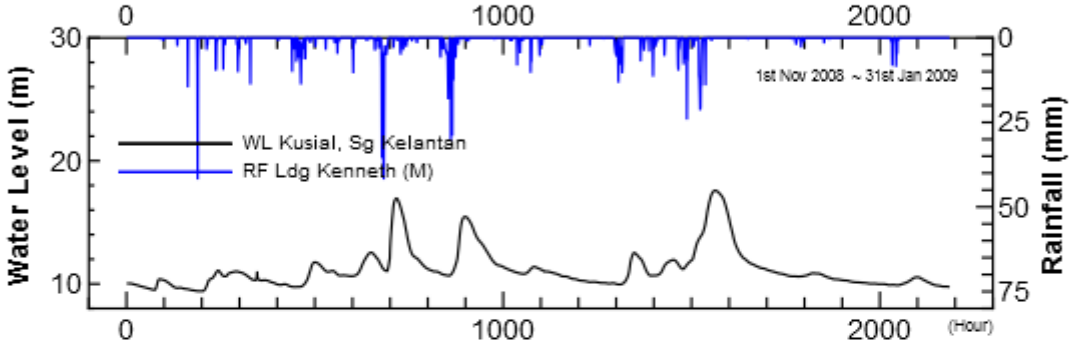
1st Nov 2008 ~ 31st Jan 2009
WL Kusial, Sg Kelantan
RF Ldg Kenneth (M)
Water Level (m)
Rainfall (mm)
(Hour)

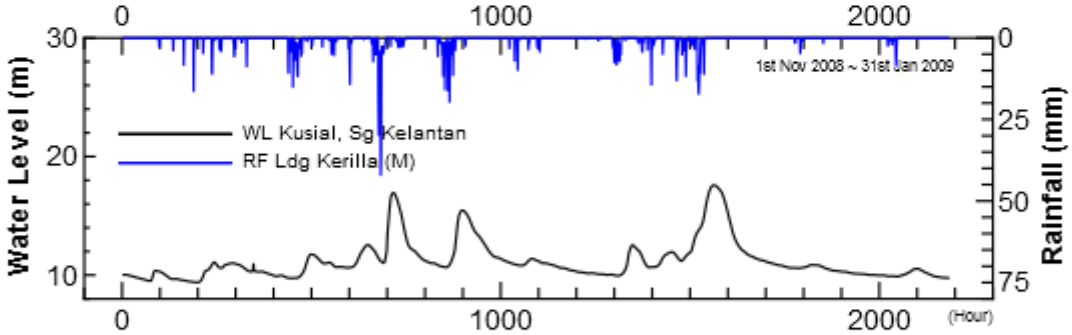
1st Nov 2008 ~ 31st Jan 2009
WL Kusial, Sg Kelantan
RF Ldg Kerilla (M)
Water Level (m)
Rainfall (mm)
(Hour)

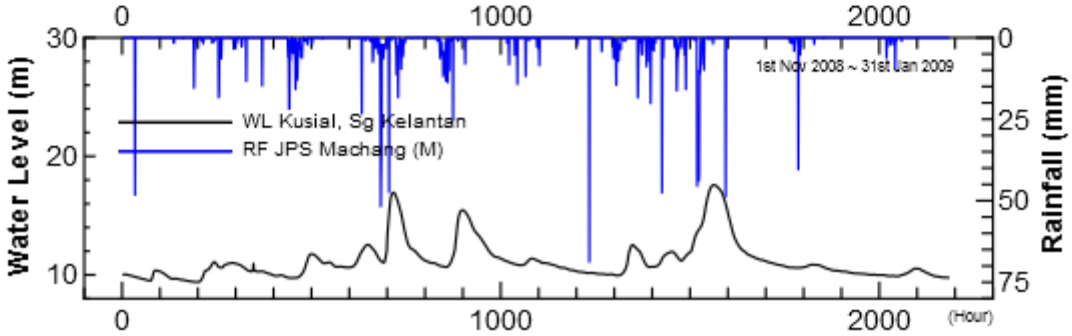
1st Nov 2008 ~ 31st Jan 2009
WL Kusial, Sg Kelantan
RF JPS Machang (M)
Water Level (m)
Rainfall (mm)
(Hour)

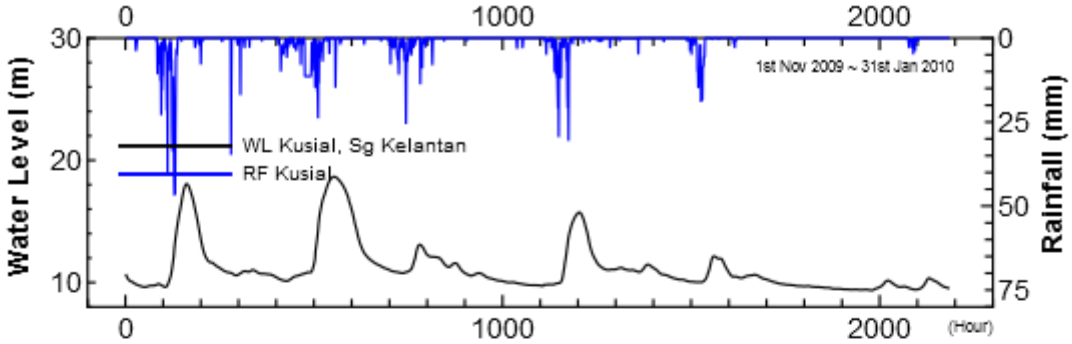
1st Nov 2009 ~ 31st Jan 2010
WL Kusial, Sg Kelantan
RF Kusial
Water Level (m)
Rainfall (mm)
(Hour)

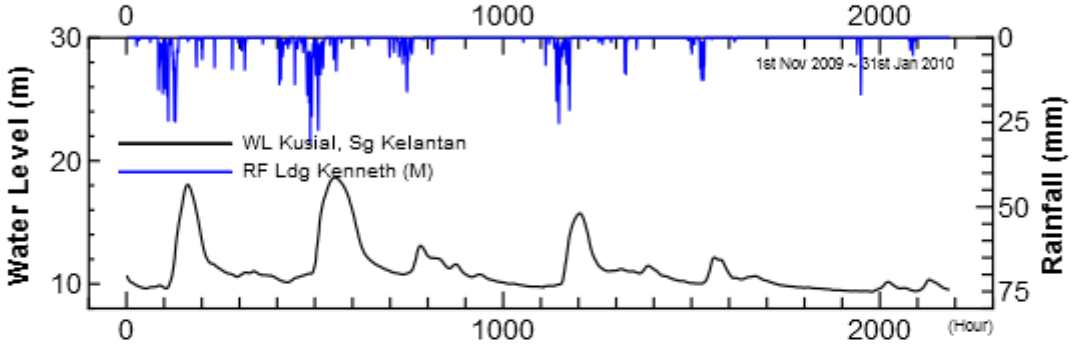
1st Nov 2009 ~ 31st Jan 2010
WL Kusial, Sg Kelantan
RF Ldg Kenneth (M)
Water Level (m)
Rainfall (mm)
(Hour)

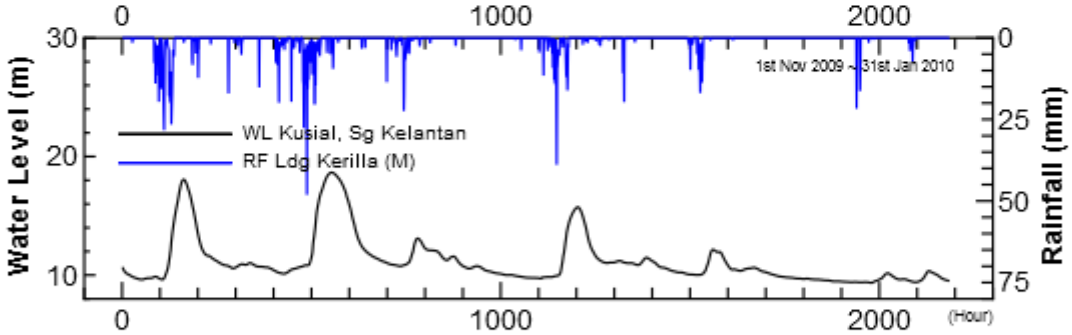
1st Nov 2009 ~ 31st Jan 2010
WL Kusial, Sg Kelantan
RF Ldg Kerilla (M)
Water Level (m)
Rainfall (mm)
(Hour)

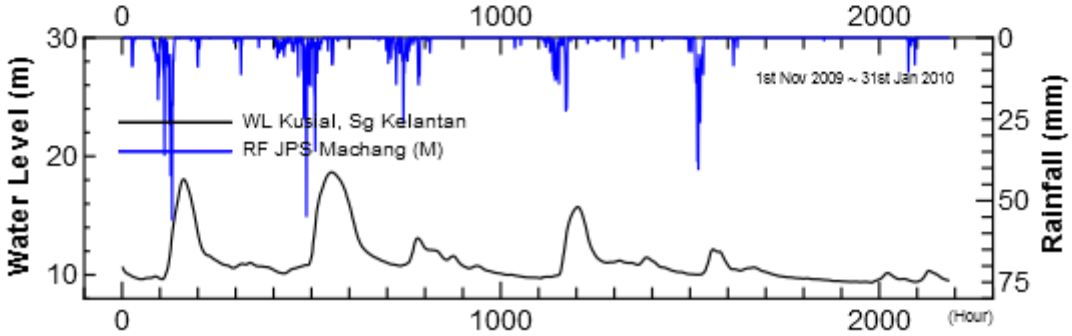
1st Nov 2009 ~ 31st Jan 2010
WL Kusial, Sg Kelantan
RF JPS Machang (M)
Water Level (m)
Rainfall (mm)
(Hour)

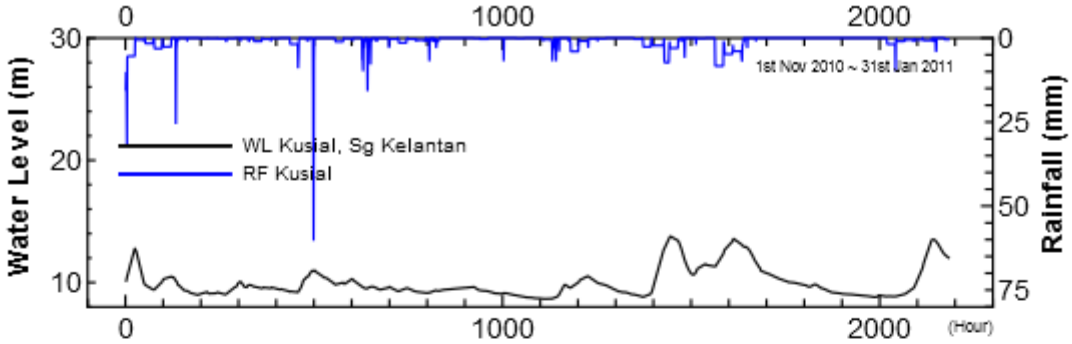
0
1000
2000
30
20
10
Water Level (m)
0
25
50
75
Rainfall (mm)
1st Nov 2010 ~ 31st Jan 2011
WL Kusial, Sg Kelantan
RF Kusial
(Hour)

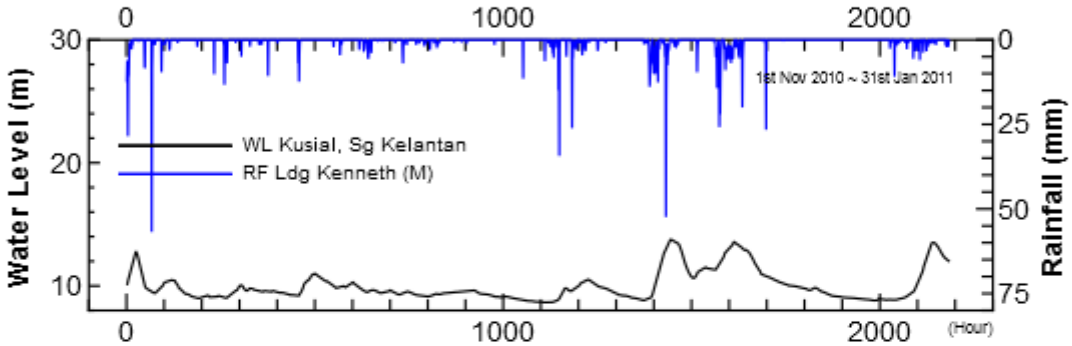
0
1000
2000
30
20
10
Water Level (m)
0
25
50
75
Rainfall (mm)
1st Nov 2010 ~ 31st Jan 2011
WL Kusial, Sg Kelantan
RF Ldg Kenneth (M)
(Hour)

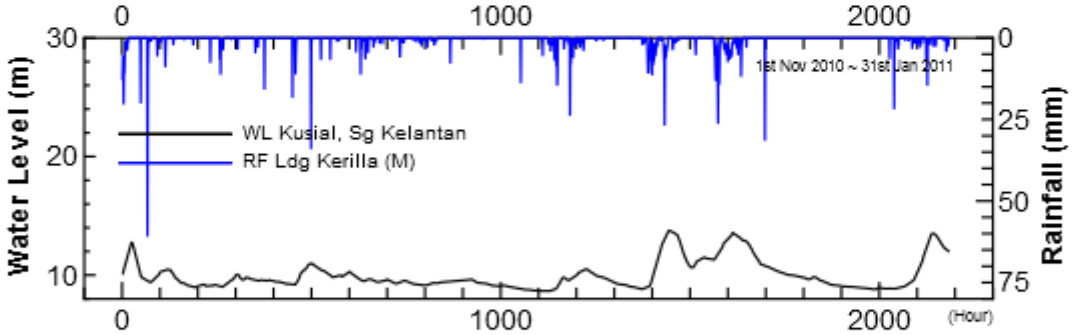
0
1000
2000
30
20
10
Water Level (m)
0
25
50
75
Rainfall (mm)
1st Nov 2010 ~ 31st Jan 2011
WL Kusial, Sg Kelantan
RF Ldg Kerilla (M)
(Hour)

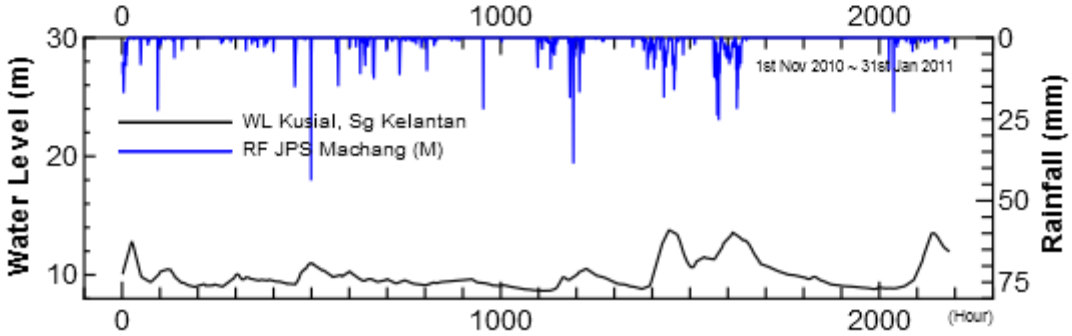
0
1000
2000
30
20
10
Water Level (m)
0
25
50
75
Rainfall (mm)
1st Nov 2010 ~ 31st Jan 2011
WL Kusial, Sg Kelantan
RF JPS Machang (M)
(Hour)

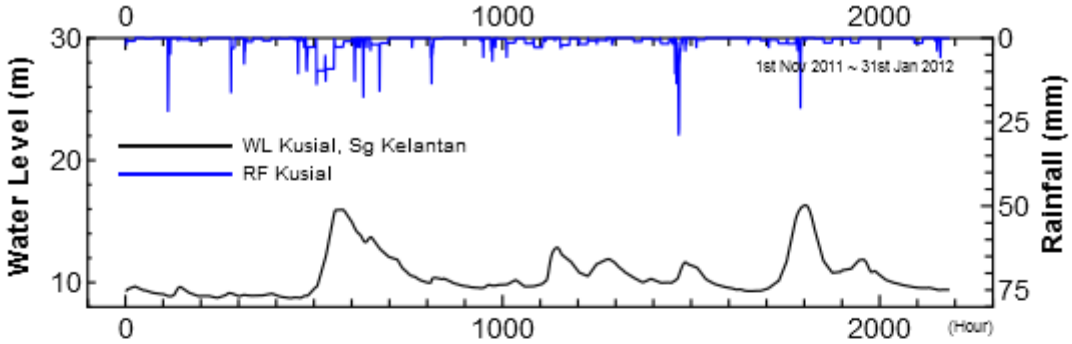
1st Nov 2011 ~ 31st Jan 2012
WL Kusial, Sg Kelantan
RF Kusial
Water Level (m)
Rainfall (mm)
(Hour)

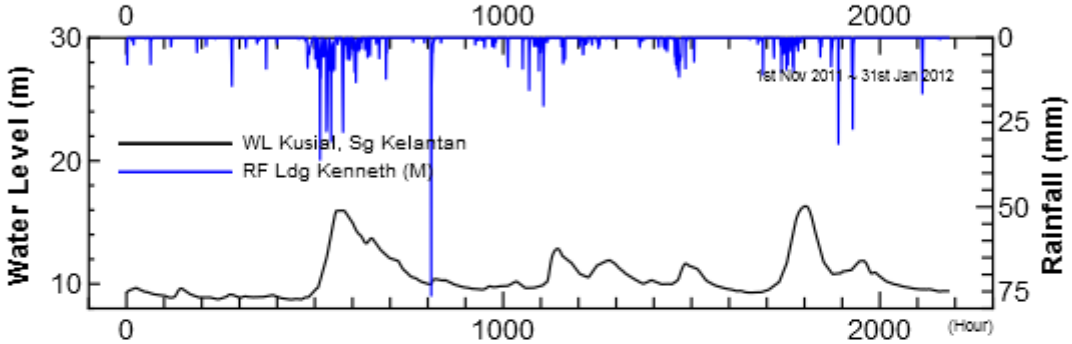
1st Nov 2011 ~ 31st Jan 2012
WL Kusial, Sg Kelantan
RF Ldg Kenneth (M)
Water Level (m)
Rainfall (mm)
(Hour)

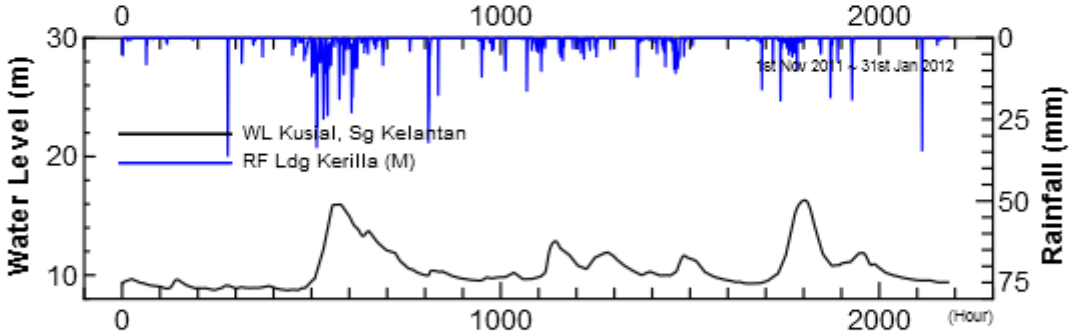
1st Nov 2011 ~ 31st Jan 2012
WL Kusial, Sg Kelantan
RF Ldg Kerilla (M)
Water Level (m)
Rainfall (mm)
(Hour)

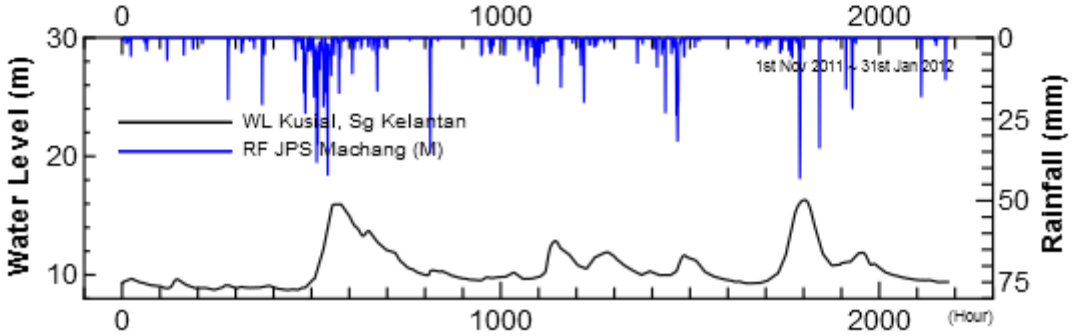
1st Nov 2011 ~ 31st Jan 2012
WL Kusial, Sg Kelantan
RF JPS Machang (M)
Water Level (m)
Rainfall (mm)
(Hour)

A-6) Rainfall distribution (selected days during NEM in 2007)

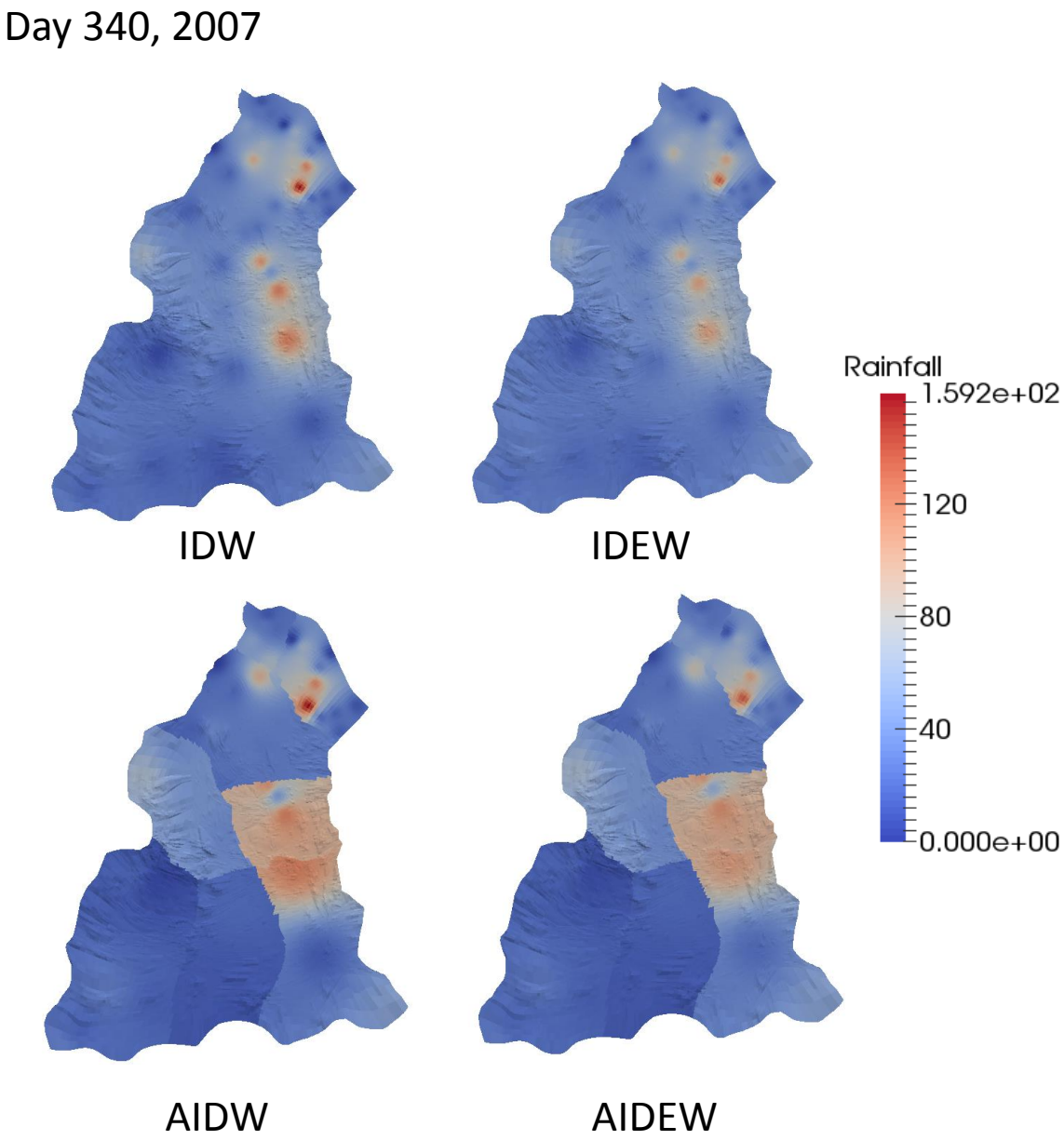

Day 341, 2007

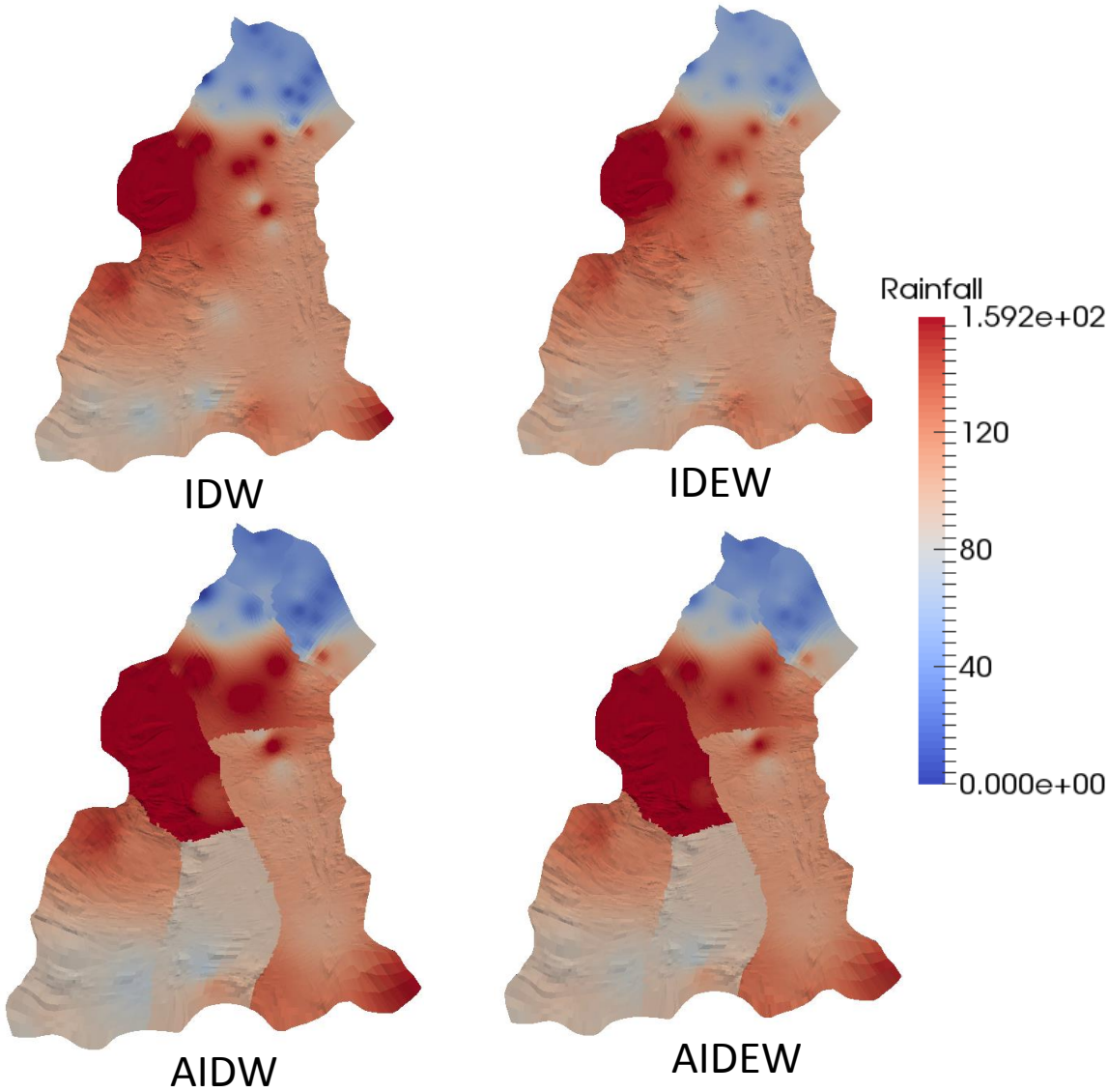

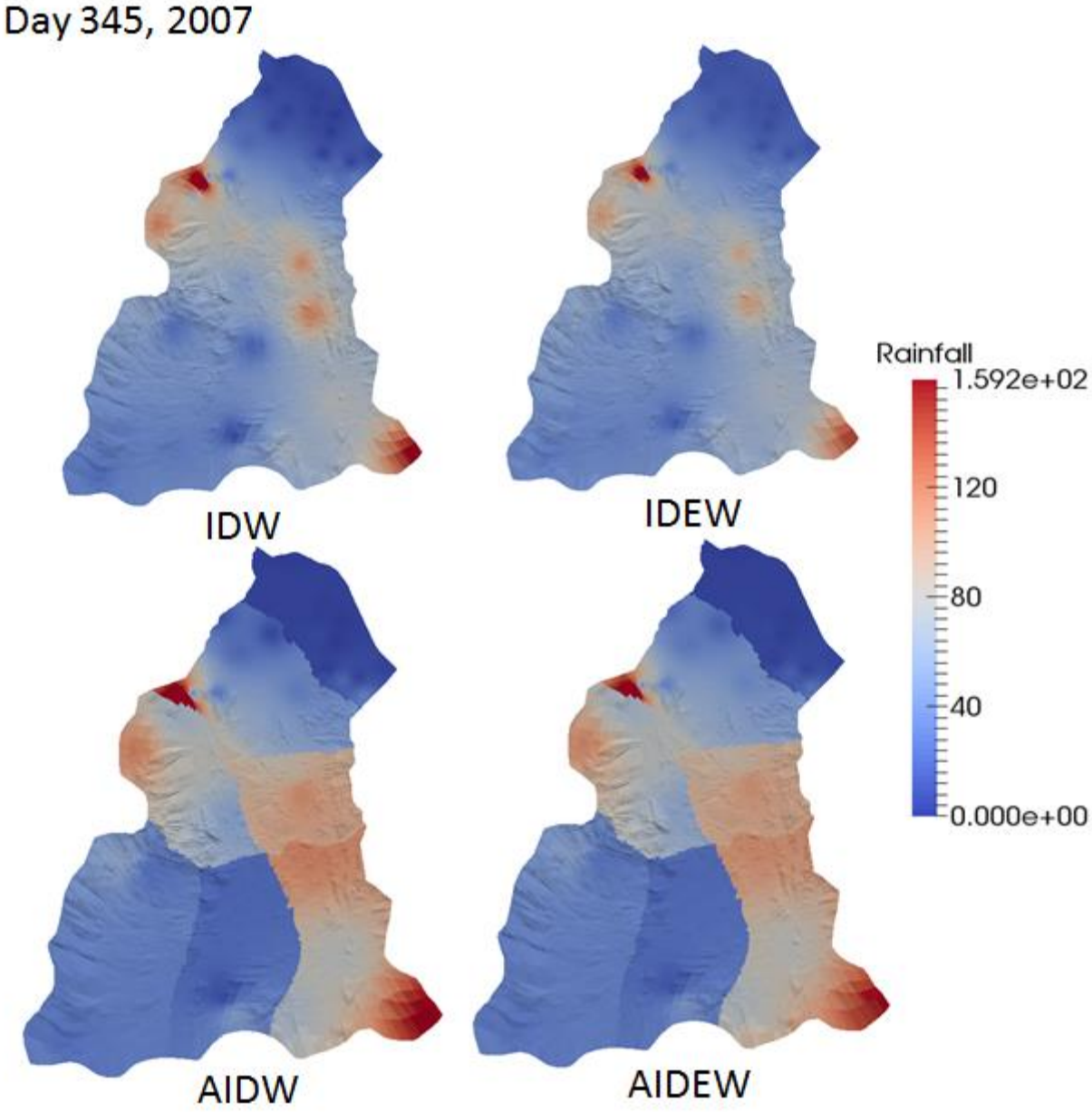
Day 345, 2007
IDW
IDEW
AIDW
AIDEW
Rainfall
1.592e+02
120
80
40
0.000e+00

Day 346, 2007